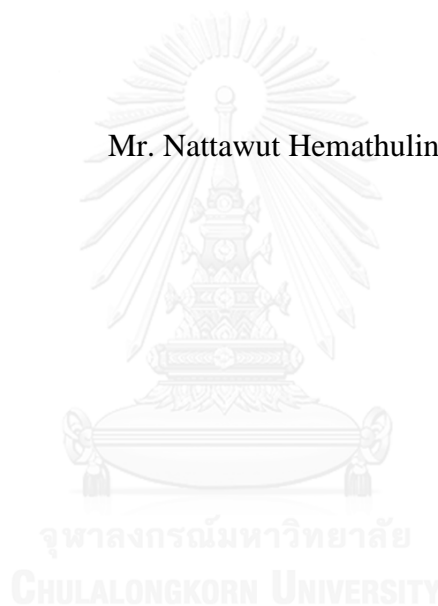


**GROUND VIBRATION INDUCED BY MAN-  
MADE ACTIVITIES IN THAILAND**

**Mr. Nattawut Hemathulin**



บทคัดย่อและแฟ้มข้อมูลฉบับเต็มของวิทยานิพนธ์ตั้งแต่ปีการศึกษา 2554 ที่ให้บริการในคลังปัญญาจุฬาฯ (CUIR)  
เป็นแฟ้มข้อมูลของนิสิตเจ้าของวิทยานิพนธ์ ที่ส่งผ่านทางบัณฑิตวิทยาลัย

The abstract and full text of theses from the academic year 2011 in Chulalongkorn University Intellectual Repository (CUIR)  
are the thesis authors' files submitted through the University Graduate School.

**A Dissertation Submitted in Partial Fulfillment of the Requirements  
for the Degree of Doctor of Philosophy Program in Civil Engineering**

**Department of Civil Engineering**

**Faculty of Engineering**

**Chulalongkorn University**

**Academic Year 2014**

**Copyright of Chulalongkorn University**

การสิ้นสะท้อนของพื้นดินเนื่องจากกิจกรรมของมนุษย์ในประเทศไทย



วิทยานิพนธ์นี้เป็นส่วนหนึ่งของการศึกษาตามหลักสูตรปริญญาวิศวกรรมศาสตรดุษฎีบัณฑิต

สาขาวิชาวิศวกรรมโยธา ภาควิชาวิศวกรรมโยธา

คณะวิศวกรรมศาสตร์ จุฬาลงกรณ์มหาวิทยาลัย

ปีการศึกษา 2557

ลิขสิทธิ์ของจุฬาลงกรณ์มหาวิทยาลัย











## CONTENTS

	Page
THAI ABSTRACT .....	iv
ENGLISH ABSTRACT.....	v
ACKNOWLEDGEMENTS .....	vi
CONTENTS.....	vii
LIST OF TABLES .....	13
LIST OF FIGURES .....	16
LIST OF ABBREVIATIONS.....	20
Greek Symbols.....	20
Roman Symbols.....	20
Roman Symbols (Continued) .....	21
CHAPTER I.....	22
INTRODUCTION .....	22
1. Research Background and Motivation .....	22
2. Research Objectives .....	23
3. Scope of Study.....	23
CHAPTER II.....	24
LITERATURE REVIEWS .....	24
1. Introduction .....	24
2. Fundamentals of ground vibrations .....	24
3. Basics of dynamics for vibrating systems .....	24
3.1. Vibratory motion .....	24
3.1.1. Harmonic motion.....	24
3.1.2. Transient motion.....	25
3.2. Types of seismic waves.....	25
3.2.1. Surface waves .....	26
3.2.2. Body waves .....	26
4. Vibration sources.....	27
4.1. Pile driving .....	27

	Page
4.2. Blasting.....	29
4.3. Vibratory rollers .....	30
5. Vibration propagation.....	31
5.1. Peak Particle Velocity, PPV .....	31
5.2. Frequency of vibrations.....	31
5.3. Attenuation of ground vibration .....	32
6. Prediction models .....	36
6.1. Pile driving .....	36
6.2. Blasting.....	37
6.3. Vibratory rollers .....	38
6.4. Allowable values of ground borne vibration .....	38
CHAPTER III .....	41
METHODOLOGY .....	41
1. Introduction .....	41
2. Vibration sources.....	41
2.1. Pile driving .....	41
2.2. Blasting.....	41
2.3. Vibratory rollers .....	43
3. Instruments and measurement setup.....	45
3.1 Pile driving and vibratory rollers.....	45
3.2. Blasting.....	45
4. Ground conditions of studied areas .....	49
4.1. Pile driving .....	49
4.2. Blasting.....	51
4.3. Vibratory rollers .....	56
5. Measurement results .....	58
5.1. Peak particle velocity and dominant frequency .....	58
5.2. Attenuation characteristics of each ground type .....	59
5.2.1. General form of vibration prediction model.....	59

	Page
5.2.2. Piecewise model .....	60
5.3. Comparisons between prediction methods and measured results .....	60
CHAPTER IV .....	61
RESULTS AND DISCUSSIONS .....	61
1. Pile driving .....	61
1.1. Clayey ground .....	61
1.1.1. Ground vibrations when piles were penetrating through the 2 <sup>nd</sup> strata.....	61
1.1.1.1. Ground vibrations due to pile driving in each direction ..	61
1.1.1.2. Attenuation of vibration due to pile driving in clayey grounds .....	61
1.1.1.3. Discussion on the first attenuation pattern observed in site no. 4 .....	66
1.1.1.4. Comparison between prediction models.....	66
1.1.1.5. Discussion on the second attenuation pattern observed in site no. 7 .....	70
1.1.1.6. Attenuation characteristic .....	72
1.1.1.7. Variation of dominant frequency and the beginning of b-zone.....	73
1.1.1.8. Comparison with other prediction models.....	75
1.1.1.9. Discussion on the third attenuation pattern observed in site no. 1 .....	76
1.1.1.10. Attenuation characteristic .....	79
1.1.1.11. Attenuation in each sites .....	80
1.1.1.12. Variation of dominant frequency.....	83
1.1.1.13. Comparison between prediction models.....	85
1.1.2. Ground vibrations when piles were penetrating through the 3 <sup>rd</sup> soil strata.....	86
1.1.2.1. Vibration in each direction .....	86
1.1.2.2. Attenuation characteristic .....	88

	Page
1.1.2.3. Attenuation in each sites.....	91
1.1.2.4. Comparison between prediction models.....	93
1.2. Sandy ground.....	94
1.2.1. Ground vibrations when piles were penetrating through the 1 <sup>st</sup> strata.....	95
1.2.1.1. Ground vibrations due to pile driving in each direction ..	95
1.2.1.2. Attenuation of vibration due to pile driving in sandy ground .....	95
1.2.1.3. Discussion on the first attenuation pattern observed in site no. 2-1, 2-2.....	100
1.2.1.4. Comparison between prediction models.....	100
1.2.1.5. Ground vibrations when piles were penetrating through the 2 <sup>nd</sup> strata of sandy ground .....	105
1.2.1.6. Ground vibrations due to pile driving in each direction	105
1.2.1.7. Attenuation of vibration due to pile driving in sandy ground .....	105
1.2.1.8. Discussion on the first attenuation pattern observed in site no. 3 .....	107
1.2.1.9. Comparison with other prediction models.....	108
1.2.1.10. Discussion on the second attenuation pattern observed in site no. 2-1 .....	110
1.2.1.11. Attenuation characteristic .....	111
1.2.1.12. Variation of dominant frequency and the beginning of B-zone .....	111
1.2.1.13. Comparison with other prediction models.....	112
1.3. The influence of input energy and parameter n.....	113
1.4. The influence of body wave .....	114
1.5. Normalizing by using input energy and $N_{SPT}$ .....	114
1.6. Frequency content and comparison with DIN 4150's guideline .....	117
1.7. Summarized results .....	120
2. Blasting.....	123

	Page
2.1. Vibration in each direction .....	123
2.2. Attenuation of vibration in each ground type.....	124
2.2.1. Clayey ground .....	124
2.2.2. Sandy ground.....	126
2.2.3. Rocky ground .....	130
2.3. The influence of explosive weight and ground type .....	130
2.4. Variation of dominant frequency .....	132
2.5. Comparison with other prediction models .....	138
2.5.1. Clayey ground .....	138
2.5.2. Sandy ground.....	139
2.5.3. Rocky ground .....	141
3. Vibratory rollers .....	143
3.1. Comparison of vibrations in radial, transverse and vertical directions ..	143
3.2. Attenuation characteristics in each ground type.....	143
3.2.1. Results from test pattern R .....	143
3.2.2. Results from test pattern T .....	145
3.3. Variation of dominant frequency .....	147
3.4. Comparison with other prediction models .....	148
3.5. The influence of roller weight .....	149
3.6. Frequency content and comparison with DIN 4150's guideline.....	150
3.7. Result summary .....	152
CHAPTER V .....	154
CONCLUSIONS.....	154
Pile driving.....	154
Blasting .....	155
Vibratory rollers.....	156
REFERENCES .....	158
APPENDIX A.....	162
APPENDIX B .....	165

	Page
APPENDIX C .....	175
VITA .....	229



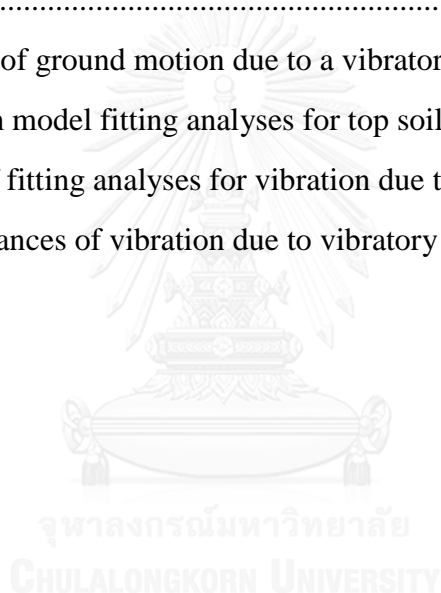


## LIST OF TABLES

Table 1 Geometric attenuation coefficients (Amick and Gendreau, 2000) .....	32
Table 2 Empirical attenuation parameters ( $n$ ) for each soil class, (Woods et al., 1997) .....	33
Table 3 Summary of material damping coefficients (Amick and Gendreau, 2000)....	35
Table 4 Material damping attenuation coefficient (Woods et al., 1997) .....	35
Table 5 Hammer and pile properties.....	42
Table 6 Basic properties of explosives used in this study .....	43
Table 7 Site conditions of blasting studies .....	43
Table 8 Properties of vibratory rollers used in this study .....	44
Table 9 Site conditions of vibratory rollers studies .....	44
Table 10 Properties of sandy grounds in the studies of pile driving .....	51
Table 11 Properties of clayey grounds in the studies of pile driving .....	51
Table 12 Properties of clayey grounds in the studies of blasting .....	54
Table 13 Properties of rocky grounds in the studies of blasting.....	55
Table 14 Properties of sandy grounds in the studies of blasting.....	55
Table 15 Ground properties in the studies of vibratory rollers.....	57
Table 16 Results from fitting analyses.....	68
Table 17 Results from model fitting analyses for the measured data of the 20-22 m pile penetrated depth in site no. 4 .....	69
Table 18 Fitting analyses for the 2 <sup>nd</sup> attenuation patterns (site no. 7 and no. 8).....	72
Table 19 Statistics of dominant frequency in each site.....	75
Table 20 The beginning of B-zone from ground vibration source in each site .....	75
Table 21 Fitting analyses with prediction models in literatures (site no. 7 and no. 8) .....	75
Table 22 Results from fitting analyses for the data of 18-19 m of pile penetrated depth in site no. 6.....	79
Table 23 Results from fitting analyses for the data of 18-19 m of pile penetrated depth in site no. 6.....	81

Table 24 fitting analyses for 16-23 m of pile penetrated depth in site no. 1 .....	83
Table 25 Statistics of dominant frequency in each site.....	85
Table 26 The beginning of B-zone from ground vibration source in each site .....	85
Table 27 Results from model fitting analyses for the 2nd stratum of site no. 6 .....	85
Table 28 Results from model fitting analyses for the measured data of the 24.0-25.0 m pile penetrated depth in site no. 7 .....	90
Table 29 Results from model fitting analyses of site no. 1, 4 and 5 .....	91
Table 30 Results from model fitting analyses of site no. 6 and 8.....	92
Table 31 Statistics of dominant frequency in each sites .....	93
Table 32 The beginning of B-zone from ground vibration source in each sites.....	93
Table 33 Results from model fitting analyses for the measured data of the 25.0 m pile penetrated depth in site no. 7 .....	94
Table 34 Results from fitting analyses.....	101
Table 35 Statistics of dominant frequency in each ground type.....	104
Table 36 Results from model fitting analyses for top soil of sandy ground .....	104
Table 37 Results from fitting analyses for the 2 <sup>nd</sup> strata.....	108
Table 38 Statistics of dominant frequency in each ground type.....	109
Table 39 Results from model fitting analyses for the measured data of the 2.4-8.4 m pile penetrated depth in site no. 3-3.....	110
Table 40 Results from model fitting analyses.....	111
Table 41 Statistics of dominant frequency in each site.....	112
Table 42 The beginning of B-zone from ground vibration source in each site .....	112
Table 43 Results from model fitting analyses for the measured data of the 2.4-3.9 m pile penetrated depth in site no. 2-1 .....	112
Table 44 the results of sandy ground .....	115
Table 45 the results of clayey ground .....	116
Table 46 the results of 80% upper bound limit of sandy ground.....	119
Table 47 the results of 80% upper bound limit of clayey ground.....	120
Table 48 the summarized results for pile driving .....	122
Table 49 Fitting analysis results for blasting in clayey ground .....	125

Table 50 Fitting analysis results for blasting in sandy ground .....	128
Table 51 Results from fitting analyses considering explosive weight.....	131
Table 52 Statistics of dominant frequency in each ground type.....	138
Table 53 Comparison of prediction models for blasting in clayey ground.....	139
Table 54 Comparison of prediction models for blasting in sandy ground.....	140
Table 55 Comparison of prediction models for blasting in rocky ground.....	142
Table 56 Results from fitting analyses for the measured data of layout R from site 1.....	145
Table 57 Results from fitting analyses for the measured data of layout T from site 1.....	146
Table 58 Trajectories of ground motion due to a vibratory roller .....	147
Table 59 Results from model fitting analyses for top soil of sandy ground .....	149
Table 60 Summary of fitting analyses for vibration due to vibratory rollers .....	151
Table 61 Setback distances of vibration due to vibratory rollers.....	152



## LIST OF FIGURES

Figure 1 Quantities describing harmonic motion (Woods et al., 1997).....	25
Figure 2 Typical wave motions generated by vibration sources focused in this study.....	25
Figure 3 Three types of waves traveling in a continuum media:.....	27
Figure 4 Schematic of vibrational wave fronts radiating from a percussive driven pile. (Attewell and Farmer, 1973).....	28
Figure 5 Transfer of vibrations from the hammer, through the pile, into surrounding soil, under and into adjacent buildings (Massarsch, 2004).....	29
Figure 6 Geometrical diagrams of branch blasting: (a) top view; (b) side view; (c) decked hole .....	30
Figure 7 Dependency of n on source geometry, vibration type and wave type (German Standard).....	33
Figure 8 Blasting vibration criterion for residential houses (Siskind et al., 1980) .....	39
Figure 9 Comparison of various threshold vibration criteria for structural damage. (Athanasopoulos and Pelekis, 2000).....	40
Figure 10 Field measurement locations .....	45
Figure 11 Measuring equipments.....	46
Figure 12 2.0-Hz triaxial geophone .....	47
Figure 13 4.5-Hz geophones .....	47
Figure 14 Geophone arrangement for pile driving .....	47
Figure 15 Geophone arrangement for vibratory roller.....	48
Figure 16 Layout of geophone array in 2D and 3D seismic surveys.....	48
Figure 17 Axis transformation of measured signal .....	48
Figure 18 Clayey ground profile (site no. 1, pile driving).....	49
Figure 19 Sandy ground profile (site no. 2, pile driving) .....	50
Figure 20 Photos taken from clayey and sandy sites of pile driving studies .....	50
Figure 21 Soil profiles in pile driving studies.....	51
Figure 22 Blasting sites no. 1 (Supan Buri province).....	52
Figure 23 Blasting sites no. 3 (Burirum province) .....	53

Figure 24 Blasting sites no. 5 (Kalasin province).....	54
Figure 25 Soil profiles in blasting studies.....	55
Figure 26 Sandy ground profile (site no. 1, Sakon Nakorn province, vibratory rollers).....	56
Figure 27 Sandy ground profile (site no. 2, Nong Khai province, vibratory rollers) ..	57
Figure 28 Soil profiles in vibratory roller studies .....	58
Figure 29 Examples of signals measured from each vibration source.....	59
Figure 30 Vibration of each direction of site no. 1 .....	63
Figure 31 Vibration of each direction of site no. 4 .....	64
Figure 32 Vibration of each direction of site no. 7 .....	65
Figure 33 Ground vibration with pile penetrated depth of site no. 4.....	67
Figure 34 The peak particle velocities versus horizontal distance with log –log scale in site no.4.....	68
Figure 35 Variation of dominant frequency with distance in each ground type.....	69
Figure 36 The prediction models fitting for the 2 <sup>nd</sup> stratum of site no. 4 .....	70
Figure 37 two peak of vibration over distance.....	70
Figure 38 the peak particle velocities versus horizontal distance at different pile penetrated depths in site no. 7.....	71
Figure 39 the peak particle velocities versus horizontal distance with log –log scale at 17.0-23.0 m of pile penetrated depth. ....	72
Figure 40 Variation of dominant frequency with distance in each sites.....	74
Figure 41 the prediction models fitting for the measured data from the 24.0-25.0 m pile penetrated depth in site no. 7 .....	76
Figure 42 the vibration over distance of pattern 3 .....	77
Figure 43 Vibration of each direction of 2 <sup>nd</sup> strata in site no. 6.....	77
Figure 44 the peak particle velocities versus horizontal distance at different pile penetrated depths of site no. 6.....	78
Figure 45 the attenuation of measured data from 17-19 m of pile penetrated depth in site no.6.....	80
Figure 46 The attenuation of measured data from 18-19 m of pile penetrated depth in site no.6.....	82

Figure 47 Piecewise fitting of measured data from 17-19 m of pile penetrated depth in site no.6. ....	82
Figure 48 Variation of dominant frequency with distance in each sites.....	84
Figure 49 the prediction models fitting for the measured data of 18-19 m depth in the 2 <sup>nd</sup> stratum of site no. 6 .....	86
Figure 50 Vibration of each direction of site no. 7 .....	87
Figure 51 Two peak of vibration over distance .....	88
Figure 52 the peak particle velocities versus horizontal distance at different pile penetrated depths. ....	89
Figure 53 the peak particle velocities versus horizontal distance with log –log scale at 24-25.0 m of pile penetrated depth. ....	90
Figure 54 Variation of dominant frequency with distance in each sites.....	92
Figure 55 the prediction models fitting for the measured data of the 25.0 m pile penetrated depth in site no. 7 .....	94
Figure 56 Vibration in each direction .....	96
Figure 57 the peak particle velocities versus horizontal distance at different pile penetration depths. ....	97
Figure 58 Vibration of each direction of site no. 2-1.....	98
Figure 59 Vibration of each direction of site no. 2-2.....	99
Figure 60 the peak particle velocities versus horizontal distance with log –log scale of 0.9-1.2 m penetration depth of site no. 2-1.....	102
Figure 59 inclining of pile while driving due to body wave traveling along the free surface .....	102
Figure 60 the effect of pile driving in site no. 2-2. ....	103
Figure 63 Variation of dominant frequency with distance in each ground type.....	103
Figure 62 the prediction models fitting for top soil of sandy ground .....	105
Figure 65 Vibration in each direction .....	106
Figure 65 Vibration in each direction .....	107
Figure 67 Variation of dominant frequency with distance in each ground type.....	109
Figure 68 the prediction models fitting for the 2 <sup>nd</sup> stratum of site No. 3-3 .....	110
Figure 65 the prediction models fitting for the measured data from the 2.4-3.9 m pile penetrated depth in site no. 2-1 .....	113

Figure 66 The influence of input energy and parameter n.....	114
Figure 67 Guideline values at building foundations for short-term vibration (after DIN 4150) .....	117
Figure 68 Comparisons between blasting vibration in each direction.....	124
Figure 69 Attenuation of blasting vibration in clayey ground.....	126
Figure 70 Fitting results of piecewise models for blasting vibration in clayey ground .....	126
Figure 71 Attenuation of blasting vibration in sandy ground.....	129
Figure 72 Attenuation of vibrations in rocky ground .....	130
Figure 73 The influence of explosive weight in sandy ground.....	131
Figure 74 Normalized PPVs based on measurement in sandy ground .....	132
Figure 75 Variations of dominant frequency in clayey ground .....	133
Figure 76 Variations of dominant frequency in sandy ground (2 kg explosives).....	134
Figure 77 Variations of dominant frequency in sandy ground (3 kg explosives).....	135
Figure 78 Variations of dominant frequency in sandy ground (4 kg explosives).....	136
Figure 79 Variations of dominant frequency in rocky ground .....	137
Figure 80 Comparison of prediction models for blasting in clayey ground .....	139
Figure 81 Comparison of prediction models for blasting in sandy ground .....	141
Figure 82 Comparison of prediction models for blasting in rocky ground.....	142
Figure 83 Test patterns for the study of vibrations due to vibratory rollers .....	143
Figure 84 Comparisons between vibrations due to vibratory rollers in each direction .....	144
Figure 85 Attenuation of vibration of the layout R.....	145
Figure 86 Attenuation of vibration of the layout T.....	146
Figure 87 Dominant frequency of vibration due to rollers .....	148
Figure 88 the prediction models fitting for layout T.....	149

## LIST OF ABBREVIATIONS

Key symbols used in the text are listed below

### Greek Symbols

Symbol	Represents	Unit
$\omega$	Circular frequency	rad/sec
$\alpha$	Material damping coefficient	$m^{-1}$
$\alpha^*$	Estimated material damping coefficient	$m^{-1}$
$\alpha 1$	A known value at frequency $f_1$	$m^{-1}$
$\alpha 2$	An unknown value at frequency $f_2$	$m^{-1}$

### Roman Symbols

Symbol	Represents	Unit
$A$	Vertical displacement	mm
$A_1$	Amplitude of motion at distance $r_1$ from source	mm/s
$A_2$	Amplitude of motion at distance $r_2$ from source	mm/s
$A_m$	The nominal amplitude of the vibrating drums	mm
$A_P$	Amplitude of motion	mm
$b$	Non-negative fitting parameter	-
$c$	Velocity of wave propagation	m/s
$c_R$	Surface wave velocity	m/s
$D_M$	Material damping	$\text{Hz} \cdot \text{s}^{-1}$
$f$	Vibration frequency	Hz
$G$	The operating weight of the vibrating machine	tons
$g$	Acceleration of earth's gravity	$\text{m/s}^2$
$k$	Non-negative fitting parameter	-
$k_f$	Coefficient	-
$k_{RC}$	Empirical constants	-



**Roman Symbols (Continued)**

Symbol	Represents	Unit
$L$	Pile length	m
$N_{VD}$	Number of vibrating drums (i.e. 1 or 2)	-
$N_{SPT}$	Standard penetration test result	Blows/ft
$n$	Geometric attenuation coefficient	-
$PPV$	Peak particle velocity	mm/s
$r_1, r_2$	Distances from vibration source	m
$r_c$	Distance between the center of the explosive charge and measuring	m
$SD$	Scaled distance	-
$T$	Time	s
$V_{s,t}$	The amplitude of a vibration vector at time $t$	mm/s
$V_{r,t}$	Particle velocity in radial direction at time $t$	mm/s
$V_{t,t}$	Particle velocity in transverse direction at time $t$	mm/s
$V_{z,t}$	Particle velocity in vertical direction at time $t$	mm/s
$W_{vd}$	The width of the roller's drum	m
$w$	Energy of vibration source	-
$x_1, x_2, x_3$	Constants of proportionality	-
$Z$	pile impedance	

## CHAPTER I

### INTRODUCTION

#### 1. Research Background and Motivation

The controversies between contractors and house owners frequently occur because of damage caused by man-made activities. Ground vibration is one of the effects from such activities which can cause damages in a building from light damages such as loosening of paints, cracks in plaster walls, stucco and tiles to severe structural damages such as cracks in beams or columns. The sources of vibration focused in this study are pile driving, vibratory rollers used in road constructions and blasting used in seismic reflection surveys.

Pile driving is a construction activity that scatters over Thailand. The process of driving a pile usually generates impulsive waves in the ground. The magnitude of such vibrations can be estimated by empirical formulas which were reported in literatures. However, a good degree of accuracy might not be achieved because the condition of a site can be different from the reported ones.

Vibratory rollers differ from pile drivers and explosives because they generate harmonic vibrations at some fixed frequencies instead of impulsive waves. A strong response can occur when the natural frequency of a building component matches with the operational frequency of a roller.

Explosives are widely used in mining industries. They are also one of the most convenient sources for seismic reflection surveys. When an explosive is used, setback distances to existing structures are usually required for limiting damages caused by vibration. For each exploration area in Thailand, a concessionaire shall submit an environmental impact assessment report that commits minimum distances, or setback distances, between an explosive and various types of structures to the Department of Mineral Fuels (DMF). The current practice in Thailand is to provide setback distances of about 100-200 m for residential buildings and 500-2,000 m for industrial and historic buildings. These distances accompany explosive weights of 1.0, 1.5, and 2.0 kg for sand, clay, and rocky ground, respectively. Since the basis for determining the setback distances were neither explained nor based on measurements from seismic reflection surveys, it is not uncommon for a local authority to request wider separation distances than the ones submitted to the DMF.

The response of ground and structures to a vibration can be described by the magnitude of particle motion and its frequency. The most commonly used parameters for vibration evaluation are the peak particle velocity (PPV) and the dominant frequency (DF). During propagating from a vibration source, the PPV of a wave decreases along with distance because of geometric damping and material damping.

The influence of geometric damping depends on the type and the location of vibration source (Woods and Jedele, 1985), whereas the influence of material damping depends on the properties of ground and vibration amplitude. By providing separation distances between a vibration source and buildings to be protected, it is possible to reduce or avoid the damages due to vibration.

Many researchers proposed empirical equations for predicting the PPV at an arbitrary distance for different types of vibration source (Bornitz (1931); Wiss (1981); Woods and Jedele (1985); Massarsch et al. (1995); Kim and Lee (2000). These equations were calibrated for the areas of their studies but might not be applicable to other areas. Since few studies on the effect of vibration had been made in Thailand (Tangchawal (2006), Rachpech et al. (2014), Brenner and Viranuvut (1977), this study is an attempt to validate and propose equations for estimating vibrations due to man-made activities based on field measurements. The result from this study should reflect domestic ground conditions and work practices and should be useful for preparing vibration mitigation and monitoring plans in Thailand.

## **2. Research Objectives**

- 2.1. To determine the attenuation characteristics of vibration due to pile driving, blasting and vibratory rollers in Thailand.
- 2.2. To propose new prediction models for ground vibration induced by pile driving, blasting and vibration rollers in Thailand.
- 2.3. To propose set back distances for ground vibration induced by pile driving, blasting and vibration rollers in Thailand.

## **3. Scope of Study**

- 3.1. Vibration sources in this study were pile driving, vibratory rollers, and blasting in seismic reflection surveys. The areas of studied consisted of 7 sites for blasting, 8 sites for pile driving, 2 sites for vibratory compactions. All measurements were carried out in Thailand.
- 3.2. The ground conditions were grouped into three types which are sandy, clayey and rocky ground.

## CHAPTER II

### LITERATURE REVIEWS

#### 1. Introduction

A summary of literature studies is presented here. The chapter begins with fundamentals of ground vibrations followed by discussions on vibration sources, methods for estimation of ground vibrations and relevant standards for determining allowable ground vibrations.

#### 2. Fundamentals of ground vibrations

In this section, concepts of geodynamics and dynamic of vibration systems which are necessary for understanding problems caused by ground vibrations will be explained.

#### 3. Basics of dynamics for vibrating systems

##### 3.1. Vibratory motion

A vibration is an oscillatory movement around a state of equilibrium. The vibratory motion can be described by displacement, velocity or acceleration. There are different types of vibratory motion as described below.

##### 3.1.1. Harmonic motion

The simplest form of vibratory motion is represented by a sinusoidal or harmonic motion which can be expressed mathematically as shown by Eq. (1) and Figure 1.

$$A_p = A_m \sin(\omega t) \quad (1)$$

where $A_p$	=	particle displacement (mm)
$A_m$	=	displacement amplitude (mm)
$\omega$	=	circular frequency (rad/s)
$t$	=	time (s)

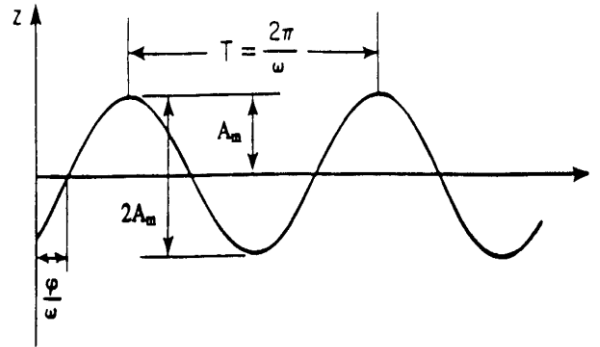


Figure 1 Quantities describing harmonic motion (Woods et al., 1997)

### 3.1.2. Transient motion

A transient motion is an irregular motion that starts with a high intensity and gradually decreases over a period of time. Examples of wave motions generated by man-made activities that are the focus of this study are shown in Figure 2.

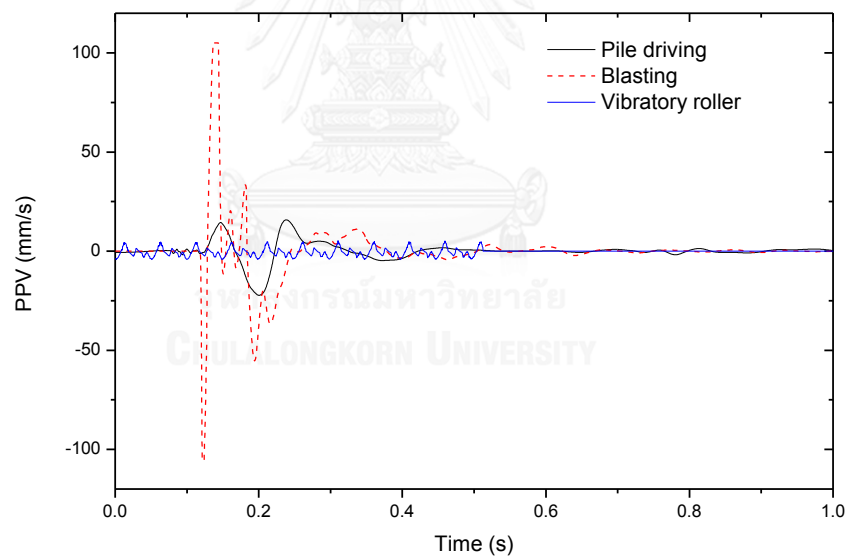


Figure 2 Typical wave motions generated by vibration sources focused in this study

### 3.2. Types of seismic waves

A seismic wave can be considered as the travelling of energy through a medium. Two seismic wave types that are important for this study are body wave and surface wave. Body waves travel through the interior (or body) of the ground whereas surface waves travel only along the ground surface.

### 3.2.1. Surface waves

Surface waves only travel along the ground surface. Two common types of surface waves are Love and Rayleigh waves. The motion of ground when excited by a Rayleigh wave is show in Figure 3a. Surface waves usually have large amplitude and low frequency.

### 3.2.2. Body waves

Body waves can be divided into two types which are primary waves and secondary waves.

Primary waves are also known as longitudinal or compression waves. The motion of ground when excited by a compression wave is show in Figure 3b. The typical speeds of primary waves are 330 m/s in air, 1450 m/s in water, 400-1,700 m/s in clay, 500-2,000 m/s in sand and 2,400-5,000 m/s in granite (Dowding (1985). Compression waves move at nearly twice the speed of surface waves and can travel through all types of material.

Secondary waves are also known as shear waves. Secondary waves can travel only through solid materials. The motion of ground when excited by a secondary wave is show in Figure 3c. The propagation velocities of secondary waves are typically around 60% of primary waves.

For a seismic event, the energy transmitted by Rayleigh waves, secondary waves and primary waves are 67%, 26% and 7%, respectively. Since primary and secondary waves decay more rapidly than Rayleigh waves, Rayleigh waves are the most significant disturbance along the ground surface and may be the only clearly distinguishable waves at a large distance from a vibration source, (Richart et al., 1970).

The ground responses to a vibration source are different under near field and far field conditions. The response is complicate in the near field due to plastic deformation in the ground. Both of body waves and surface waves can be observed in this zone. On the contrary, the ground behaves in elastic manner in the far field and dominated by surface waves (Massarsch, 2004).

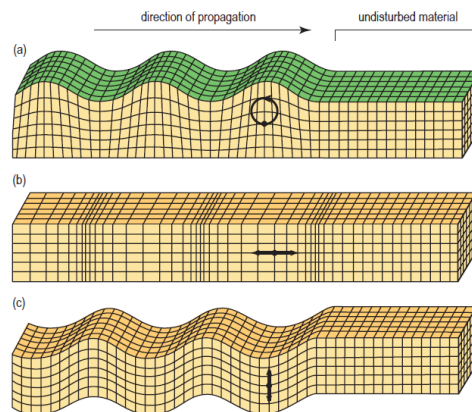


Figure 3 Three types of waves traveling in a continuum media:

(a) Rayleigh wave (b) Primary wave (c) Secondary wave (Peterie et al. (2014))

#### 4. Vibration sources

The most common sources of man-made vibrations in Thailand are pile driving, vibratory compaction and blasting. The duration and amplitude of vibrations generated by these activities vary widely. For vibration mitigation planning, it is useful to categorize ground vibrations into transient or steady-state vibrations. The transient vibrations include a single event or a sequence of short term vibrations. The steady-state or long-term vibrations occur in a continuous manner, over a period of time. The steady-state vibrations can be generated by vibratory pile drivers, vibratory compaction equipment, vibratory rollers, etc.

##### 4.1. Pile driving

The impact energy during pile driving can transfer to the ground through the skin friction and end bearing resistance of a pile. These mechanisms directly related with the generation of shear waves and compression waves as shown in Figure 4. The amplitude of ground vibration depends on many factors such as hammer weight, drop height, pile type, pile cushion and strength of soil. In addition to shear and compression waves, Rayleigh waves also occur near to the ground surface due to the interaction of the former two wave types.

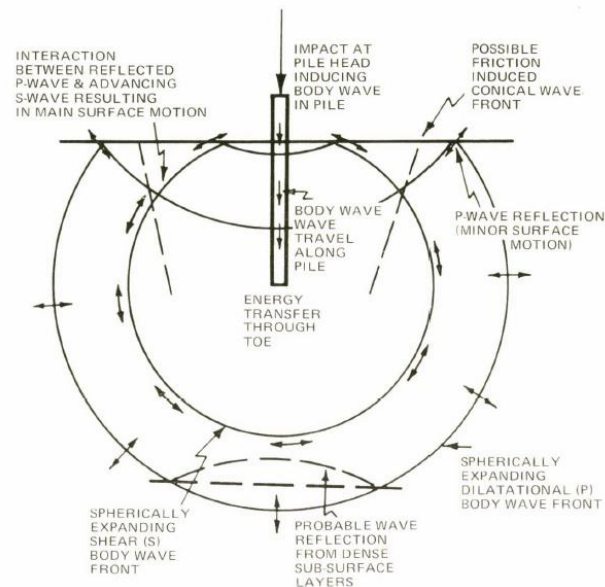


Figure 4 Schematic of vibrational wave fronts radiating from a percussive driven pile.  
(Attewell and Farmer, 1973)

Intensive discussions of ground vibrations due to pile driving and impacts on nearby buildings were made by Massarsch et al. (1995) and Massarsch (2002). They proposed that the process of wave transmission to buildings consists of four main stages as shown by letters A, B, C, D in Figure 5.

A. Wave propagation in the pile: energy generated by the impact of the hammer (1) at the pile cap, pile cushion and pile head (2) which is transmitted through the pile (3).

B. Pile-soil interaction: along the pile shaft (4) and at the pile toe (5).

C. Wave propagation in the ground: transmission of vibrations through the medium (soil).

D. Dynamic soil-structure interaction: dynamic response of foundations and vibration amplification in structures.

When assessing vibrations caused by pile driving, most investigations focus on the generation of energy by the impacting hammer (A) and the propagation of vibrations in the ground (C). In some cases, the soil-structure interaction and dynamic response of buildings subjected to vibrations (D) are addressed without considering the important aspect of transfer of stresses and vibrations through the entire system: including vibrations transmitted from the hammer to the pile and the dynamic properties of the soil (B). Even though, this is the most important part in the vibration transmission chain.



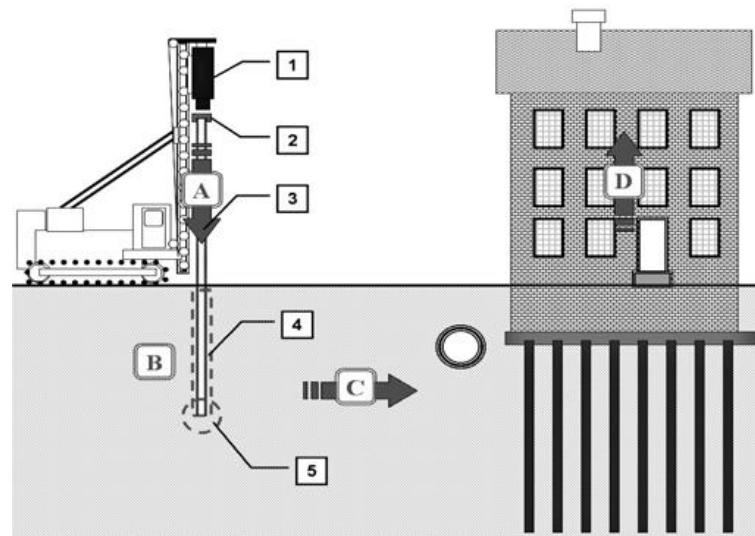


Figure 5 Transfer of vibrations from the hammer, through the pile, into surrounding soil, under and into adjacent buildings (Massarsch, 2004).

Martin (1980) found that pile shape may affect ground vibrations around the driven pile and when driving of sheet piles do not generate large horizontal vibrations in perpendicular direction to the line of the sheet piles.

Heckman and Hagerty (1978) reported that a reduction of pile impedance can increase the amplitude of ground vibration.

Woods et al. (1997), Svinkin et al. (2000) had been proposed effects of varied on pile type, cross-section of pile, and soil conditions. There are pronounced effects of penetration of piles on ground vibrations occur predominantly at distances less than 10 m from pile driving.

Svinkin (1999) found that dominant frequency of propagating waves from short term sources ranged between 3 Hz and 60 Hz.

Brenner Brenner and Viranuvut (1977) measured vibrations during pile driving in north of Bangkok and correlated with cone penetration test results. The results showed that vibration velocity varied according to the cone resistance.

#### 4.2. Blasting

Blasting is used in constructions and mining industries, e.g., tunnel excavations in rock, rock slope cutting and seismic reflection surveys. The magnitude of ground vibrations due to blasting depends on many factors including explosive type and weight, delay-timing variations, size and number of holes, distance between holes and rows, method and direction of blast initiation, geology and overburden (Nicholls et al. (1971); Ghosh and Daemen (1983); Dowding (1996) ; Rai and Singh (2004). When there is geologic complexity, behaviors of waves might vary with propagating directions. The high-frequency components of vibrations were affected by overburden (Svinkin, 1999).

Explosive weight influences the magnitude and the attenuation rate of vibration (Dowding, 1996). For instance, the attenuation rate seemed to be higher when less weight of explosive was used (Tripathy and Gupta, 2002).

Dowding (1996) found that vibration became stronger when the distance from a charge to free surface (burden) increased. On the other hand, Uysal et al. (2007) reported that vibration was lowered by the increase burden distance.

Ground motion is proportional to the detonation velocity of an explosive and the square root of its weight. The peak particle velocity can be reduced by providing appropriated microsecond-delay time between each blast (which is connected to a parameter called the maximum charge weight per delay). For open pit mines, blasts are usually done by delayed detonating to reduce PPV values (Kopp and Siskind, 1986), (Dowding, 1996). Delay blasting caps are used to provide delay times between bore holes as shown in Figure 6 (b) and also between each depth in the same borehole (separation of charge, decking) as shown in Figure 6 (c).

Based on measurements from surface mining in Thailand, Tangchawal (2000) recommended safe distances to be in a range of 150-300 m. The explosive weight used in his study was in a range of 64-643kg per delay. Rachpech et al. (2014) proposed equations for vibration prediction in three ground types in Mae Moh lignite mine, in the northern part of Thailand. They also observed that the propagation of waves was affected by geological structures in the site.

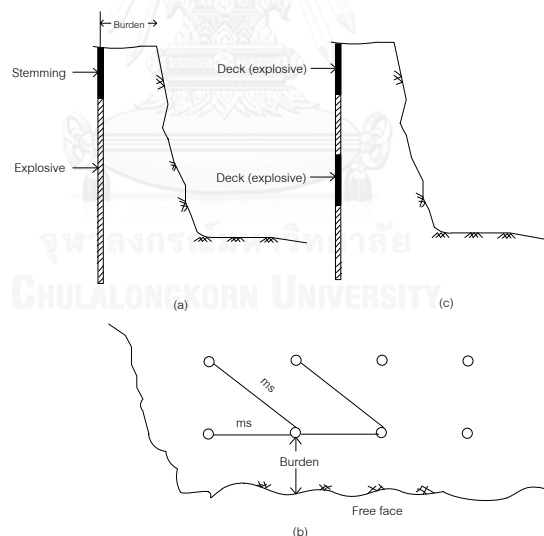


Figure 6 Geometrical diagrams of branch blasting: (a) top view; (b) side view; (c) decked hole

#### 4.3. Vibratory rollers

A vibratory roller causes continuous ground vibration or long-term vibration. Since dynamic roller compaction is based on a near surface dynamical excitation of ground, the wave propagation is dominated by Rayleigh waves (Verruijt, 2010).

Pistrol et al. (2013) found that primary waves and secondary waves were less importance for near surface wave propagation.

The vibration energy is proportional to the vibration amplitude of the roller which is specified by the manufacturer and can be verified when required. The frequency of vibrations due to vibratory rollers ranges between 0 and 53 Hz and can be approximated as a point source (Hiller and Crabb, 2000). The amplitude of vibrations also increases as the compaction speed decreases.

## 5. Vibration propagation

The response of ground and structures to a vibration can be described by the magnitude of particle motion and its frequency. The most commonly used parameters for vibration evaluation are the peak particle velocity (PPV) and the dominant frequency (DF). During propagating from a vibration source, the PPV of a wave decreases along with distance because of geometric damping and material damping. The influence of geometric damping depends on the type and the location of vibration source (Woods and Jedele, 1985), whereas the influence of material damping depends on the properties of ground and vibration amplitude. On the contrary to attenuation, the amplification of waves can occur at some locations due to the contrast of ground impedance or due to the resonance in the ground.

Ground conditions are important for the propagation of vibrations through the soil. Deckner (2013) stated that stiff and dense soils transmit vibrations more readily than compressible materials. Therefore, the presence of any harder layers in the soil profile enables vibrations to transmit more easily, potentially resulting in higher vibration levels. Heckman and Hagerty (1978) (as cited in Deckner (2013)) stated that stiff layers in the ground may lead to the vibrations being transmitted over greater distances. Auersch and Said (2010) found that soft soils generally have larger vibration amplitudes than stiffer soils in near field areas.

### 5.1. Peak Particle Velocity, PPV

The peak particle velocity is the maximum velocity of particle motion during a seismic event. A commonly used unit of the PPV is millimeters per second (mm/s). The PPV can be the maximum of velocity in either of three orthogonal directions (radial, transverse and vertical) or the maximum amplitude of resultant vector built from the former three velocities.

### 5.2. Frequency of vibrations

Structural responses depend on the frequency of ground vibrations (Dowding, 1996). By applying the fast Fourier transform, a record of ground vibration can be decomposed into a group of sinusoidal waveforms. Among these decomposed waves, the most influential wave is the one that has the largest amplitude. The frequency of this wave is an important parameter for vibration evaluation and is called as the dominant frequency. The dominant frequency of propagating waves from impact sources ranges mostly between 3 and 60 Hz, but for some cases lower and upper values could be between 1 and 100 Hz, respectively (Svinkin, 2004).

### 5.3. Attenuation of ground vibration

A general equation for modeling the attenuation of ground vibration over distance is written as

$$A_2 = A_1 \cdot \left(\frac{r_2}{r_1}\right)^{-n} \cdot e^{-\alpha \cdot (r_2 - r_1)} \quad (2)$$

where  $A_1$  = amplitude of motion at distance  $r_1$   
 $A_2$  = amplitude of motion at distance  $r_2$   
 $r_1$  = distance from source to point of known amplitude  
 $r_2$  = distance from source to point of unknown amplitude  
 $n$  = geometric attenuation coefficient  
 $\alpha$  = material damping coefficient.

Another popular form of prediction model is as shown by Eq. (3) where the influence from geometric damping and material damping are lumped together into an empirical parameter ( $\hat{n}$ ).

$$A_2 = A_1 \cdot \left(\frac{r_2}{r_1}\right)^{-\hat{n}} \quad (3)$$

The geometric attenuation coefficient depends on the wave type and propagation path. Table 1 and Figure 7 show the summary of geometric attenuation coefficient derived from theoretical basis. For the empirical attenuation parameter ( $\hat{n}$ ), the values as shown in Table 2 were reported by Woods and Jedele (1985).

Table 1 Geometric attenuation coefficients (Amick and Gendreau, 2000)

Source	Wave type	Measurement point	$n$
Point on surface	R	Surface	0.5
Point on surface	Body (P or S)	Surface	2.0
Point at depth	Body (P or S)	Surface	1.0
Point at depth	Body (P or S)	Depth	1.0

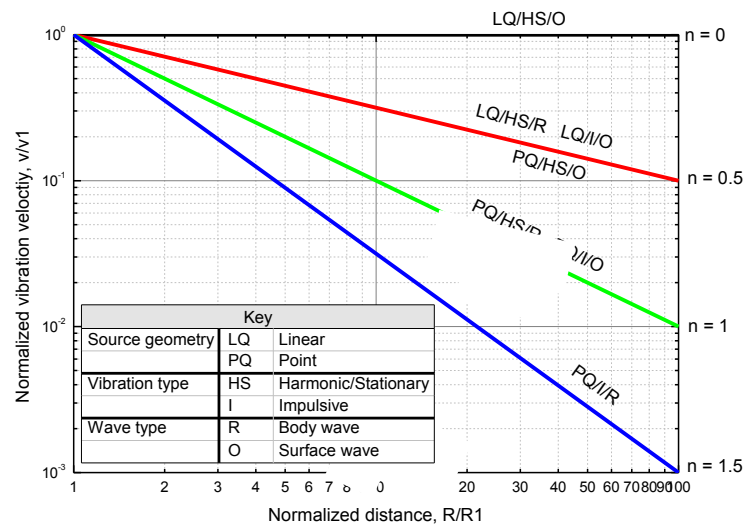


Figure 7 Dependency of  $n$  on source geometry, vibration type and wave type (German Standard)

Table 2 Empirical attenuation parameters ( $\hat{n}$ ) for each soil class, (Woods et al., 1997)

Soil Class	Soil Type	$n$
Class I	Weak or soft soils: lossy soils, dry or partially saturated peat and muck, mud, loose beach sand, dune sand, recently plowed ground, soft spongy forest or jungle floor, organic soils, topsoil (shovel penetrates easily), $N < 5$	Not identified
Class II	Competent soils: most sands, sandy clays, silty clays, gravel, silts, weathered rock (can dig with a shovel), $5 < N < 15$	1.5
Class III	Hard soils: dense compacted sand, dry consolidated clay, consolidated glacial till, some exposed rock (cannot dig with a shovel, need a pick to break up), $15 < N < 50$	1.1
Class IV	Hard, competent rock: bedrock, freshly exposed hard rock (difficult to break with a hammer), $N > 50$	Not identified

For material damping, it is effected by many factors including soil types, temperature, moisture content, and frequency of vibration (Woods et al., 1997). Softer materials generally have greater  $\alpha$  values whereas harder materials have smaller  $\alpha$  values. Clays tend to exhibit higher material damping than sandy soil (Wiss, 1967). Richart et al. (1970) found that propagation of R waves is moderately affected by presence or absence of water. Clough and Chameau (1980) reported that the material damping coefficients,  $\alpha$ , were 1.3-2.5 times greater for hard driving than those for normal driving. A summary of material damping coefficients for various soil types is show in Table 3. The material damping coefficient,  $\alpha$ , might be estimated from Eq. (4) (Massarsch, 1993).

$$\alpha^* = 2\pi D_m f / c_R \quad (4)$$

where  $\alpha^*$  = material damping coefficient ( $\text{m}^{-1}$ ) estimated from Eq.(4)

$D_M$  = material damping ( $\text{Hz}\cdot\text{s}$ )-1

$f$  = vibration frequency (Hz)

$c_R$  = surface wave velocity (m/s)

Table 3 Summary of material damping coefficients (Amick and Gendreau, 2000)

Investigator	Soil Type	$\alpha$ ( $m^{-1}$ )
Forssblad	Silty gravelly sand	0.13
Richart	4-in. concrete slab over compact granular fill	0.02
Woods	Silty fine sand	0.26
Barkan	Saturated fine grain sand	0.01
	Saturated fine grain sand in frozen state	0.06
	Saturated sand with laminate of peat and organic silt	0.04
	Clayey sand, clay with some sand, and silt above water level	0.04
	Marly chalk	0.1
	Loess and loessial soil	0.1
	Saturated clay with sand and silt	0.0–0.12
Dalmatov	Sand and silt	0.026–0.36
Clough, Chameau	Sand fill over bay mud	0.05–0.2
	Dune sand	0.025–0.65
Peng	Soft Bangkok clay	0.026–0.44
Hendriks	Sand-silt, clayey silt, silty sand	0.021

Table 4 Material damping attenuation coefficient (Woods et al., 1997)

Class	Material damping coefficient, $\alpha$ ( $m^{-1}$ )		Description of material
	5 Hz	50 Hz	
I	0.01-0.03	0.1-0.3	Weak or soft soils ( $N < 5$ )†
II	0.003-0.01	0.03-0.1	Competent soils ( $5 < N < 15$ )†
III	0.0003-0.003	0.003-0.03	Hard soils ( $15 < N < 50$ ).
IV	$< 0.0003$	$< 0.003$	Hard, competent rock ( $NSPT > 50$ )†

## 6. Prediction models

### 6.1. Pile driving

Prediction models in literatures could be categorized into 3 groups as follows

1) models that consider the energy of driving equipment, i.e., Attewell and Farmer (1973), Wiss (1981) and Attewell et al. (1992)

2) models that consider the energy of driving equipment and the properties of piles, i.e., Svinkin (2008)

3) models that consider the energy of driving equipment, the properties of piles and soils, i.e., Massarsch and Fellenius (2008).

Attewell and Farmer (1973);

$$v = k \cdot \left( \frac{\sqrt{w}}{r} \right) \quad (5)$$

where  $k$  = empirically determined constant of proportionality ( $\text{m}^2/\text{sJ}$ ).

$w$  = input energy (hammer energy), J

$r$  = horizontal distance between pile and monitoring point, m

Wiss (1981);

$$v = k \cdot \left( \frac{r}{\sqrt{w}} \right)^n \quad (6)$$

where  $n$  = empirically determined values

Attewell et al. (1992)

$$\log v = x_1 + x_2 \cdot \log\left(\frac{\sqrt{w}}{r}\right) + x_3 \cdot \log^2 \cdot \left(\frac{\sqrt{w}}{r}\right) \quad (7)$$

where  $x_1, x_2, x_3$  = constants of proportionality

Svinkin (2008)

$$v = 0.00039 \cdot \frac{w}{r} \cdot \sqrt{\frac{c}{Z \cdot L}} \quad (8)$$

where  $c$  = velocity of wave propagation in pile

$Z$  =  $ES/c$  = pile impedance



E	= modulus of elasticity of pile material
S	= pile cross-sectional area
L	= pile length
w	= energy of source
r	= distance from source

## 6.2. Blasting

To evaluate the influence of vibrations to nearby structures, a number of equations had been proposed for predicting the PPV at a distance, for a variety of vibration sources and soil types.

Hendron (1978) (As cited in Dowding, 1985) proposed that the PPV can be estimated by Eq. (9) which uses the scaled distance instead of using the distance directly. The scaled distance can be obtained by dividing the distance by the explosive weight as shown in Eq. (10).

$$v = k * SD^{n_e} \quad (9)$$

$$SD = \frac{D}{\sqrt{w}} \quad (10)$$

where $SD$	=	scaled distance
$w$	=	the maximum weight of explosive (in pound per delay)
$D$	=	distances from a vibration source
$k, n_e$	=	empirical fitting parameters

USBM (1959), Ambraseys and Hendron (1968) and Ghosh and Daemen (1983) proposed prediction models with a consideration of explosive weight as shown in Eq. (11), (12), and (13), respectively.

USBM (1959);

$$v = k \cdot \left( \frac{r}{\sqrt{w}} \right)^x \quad (11)$$

Ambraseys and Hendron (1968)

$$v = k \cdot \left( \frac{r}{\sqrt[3]{w}} \right)^x \quad (12)$$

Ghosh and Daemen (1983)

$$v = k \cdot \left(\frac{r}{\sqrt{w}}\right)^x \cdot e^{-\alpha r} \quad (13)$$

### 6.3. Vibratory rollers

The prediction models for ground vibration due to vibratory rollers were proposed by Hiller and Crabb (2000), Achmus et al. (2004) and Philipps G (2010) as shown in Eq. (14), (15), and (16), respectively.

Hiller and Crabb (2000)

$$v = k_{VR} \cdot N_{VD}^{0.5} \cdot \left(\frac{A_m}{(r+l)}\right)^{1.5} \quad (14)$$

where  $k_{VR}$  = empirical constants

$N_{VD}$  = number of vibrating drums (i.e. 1 or 2)

$A_m$  = the nominal amplitude of the vibrating drums, (mm)

$l$  = the width of the vibrating drum, (m)

$r$  = the distance from the roller to the measuring point, (m)

Achmus et al. (2004)

$$v = k_{VR} \cdot \frac{\sqrt{G}}{r} \quad (15)$$

where  $G$  = the weight of vibrating machine, (tons)

Philipps G (2010)

$$v = 1.1 \cdot \frac{\sqrt{G}}{r^{0.7}} \quad (16)$$

### 6.4. Allowable values of ground borne vibration

Three levels of cracking may be classified according to Dowding (1996):

- Cosmetic cracking, for example, threshold damage such as opening of old cracks and formation of new plaster cracks and dislodging of loose structural particles.
- Architectural cracking or minor damage, for example, fallen plaster and hairline cracks, not affecting the strength of the structure.

- Structural cracking or major damage that results in serious weakening of the building (large cracks, shifting of foundations or bearing walls, major settlement resulting in distortion or weakening of the structure, wall put out of plump).

Specifications, guidelines, regulations and code provisions (at the international, regional and national level) had been issued by various agencies. Richart et al. (1970) presented allowable values in graphical form for limiting damages to structures and the operations of machines. The allowable values for human perception were also given in the same work. It was found that structural damages were well correlated with the PPV of structure vibrations. Nicholls et al. (1971) proposed the criterion for structural damage of residential buildings by limiting the PPV at 50 mm/s for the frequency range of 3-100 Hz. Wiss (1967) suggested the PPV to be less than 100 mm/s for limiting damages in commercial structures. Studies by U.S. Bureau of Mines and Siskind et al. (1980) resulted in a criterion for limiting structural damages in residential buildings as show in Figure 8.

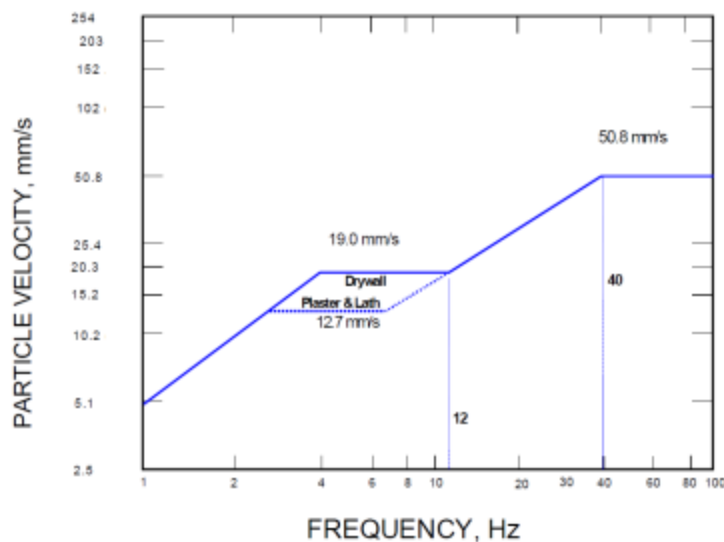


Figure 8 Blasting vibration criterion for residential houses (Siskind et al., 1980)

Figure 9 shows provisions from four national codes. It may be seen from the plots of Figure 9 that the allowable values increase with the frequency of vibration and depend on the type and the construction quality of the building. It should be noted that the low allowable limits specified by DIN and SN are not based on scientific observation of cracking but they are, rather, administrative guidelines to control annoyance.

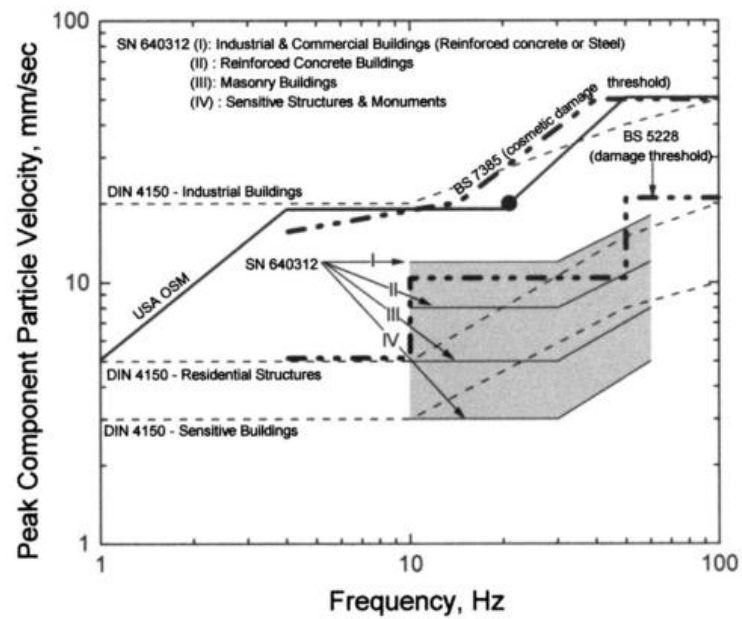


Figure 9 Comparison of various threshold vibration criteria for structural damage.

(Athanasopoulos and Pelekis, 2000)

## CHAPTER III

### METHODOLOGY

#### 1. Introduction

In this study, ground vibrations generated by pile driving, blasting and vibratory compactors were measured and used in later analyses. The studied areas were selected to cover three common ground types namely sandy ground, clayey ground, and rocky ground. The analyses were focused on the attenuation of vibrations in each ground type, the energy of each vibration sources and the validity of formula in the literatures. The details of the study are explained as follows;

#### 2. Vibration sources

##### 2.1. Pile driving

Two types of pile driving hammers, which are hydraulic hammers and drop hammers, were used in this study. The variations of hammer weight, drop height, pile cushion types and ground condition were observed and considered in later analyses. Vibrations were measured from the driving of 6 piles in sandy ground and 8 piles in clayey ground which corresponding to 1,000 and 500 seismic events, respectively. The areas of studies are shown in Figure 10 whereas the driving conditions are shown in Table 5.

##### 2.2. Blasting

Blasting vibrations were collected from on-land seismic reflection surveys using emulsion explosives (Emulex® 700) of weights 1, 1.5, 2, 3 and 4 kilograms. The properties of this explosive type are shown in Table 5, Table 6 and appendix A. The studied areas comprised sandy, clayey and rocky ground across Thailand. The site conditions and locations are shown in Table 7 and Figure 10, respectively.

Table 5 Hammer and pile properties

No.	Soil type	No. of Piles	Pile Type	Dimension (m)	wall thickness (m)	Perimeter (m)	Length (m)	Pile tip (m)	Ram weight (t)	Helmet weight (t)	Hammer type	Cushion type	Thickness (cm)		Drop height (m)		Pile weight (t)	Pile weight (t)	Ram weight (t)	
													Pile cushion	Hammer cushion						
1	Clay	1	spur pile	0.8	0.11	2.51	26	-27.00	12.0	0.500	Hydraulics	plywood	8.0	8.0	0.5		0.7	17.3	0.7	
2	Sand	1	square pile	0.4x0.4	-	1.60	15	-6.50	6.6	0.220	Drop	plywood	20.0	20.0	0.6		0.4	5.8	1.1	
	Sand	1	square pile	0.65x0.65	-	2.60	15	-4.50	6.6	0.440	Drop	plywood	20.0	20.0	0.8		1.0	15.2	0.4	
3	Sand	3	square pile	0.35x0.35	-	1.40	16	-16.00	7.0	0.084	Drop	plywood.sag	2.5	2.5	0.3		0.3	4.7	1.5	
4	Clay	1	I-pile	I-26	-	1.31	27	-24.10	4.6	0.040	Drop	plywood.sag	2.5	2.5	0.3		0.1	3.1	1.5	
5	Clay	1	square pile	0.4x0.4	-	1.60	25	-22.50	8.7	0.220	Drop	plywood	20.0	25.0	0.3	0.5	0.7	0.4	8.8	1.0
6	Clay	1	I-pile	I-35	-	1.73	24	-22.00	4.5	0.105	Drop	plywood.sag	8.0	8.0	0.6		0.2	5.1	0.9	
7	Clay	1	spur pile	0.8	0.11	2.51	32	-26.75	12.0	0.500	Drop	plywood	4.5	15.0	0.6		0.7	21.3	0.6	
8	Clay	1	I-pile	I-22	-	1.05	21	-20.50	3.5	0.040	Drop	sag	5.0	5.0	0.3		0.1	1.8	1.9	

Table 6 Basic properties of explosives used in this study

Weight (kg)	Diameter (mm)	Length (mm)	L/D	Explosion energy (MJ/kg)
1.0	60	360	6	3
1.5	60	540	9	4.5
2.0	60	720	12	6
3.0	60	1080	18	9
4.0	60	1440	24	12

Table 7 Ground and blasting conditions

No.	Study area	Soil type	Buried depth (m)	Explosive weight (kg)	Number of data	Seismic survey
1	Suphan Buri	Saturate, Clayey	19-21	1	56	3D
2	Udon Thani	Dry, Rocky	5-9	1.5	20	2D
		Dry, Sandy	9.6	2.0	9	2D
3	Kalasin	Dry, Rocky	9	1.5	10	3D
4	Ubon Rachathani	Dry, Rocky	5-12	1.5	17	3D
5	Surat Thani	Saturate, Sandy	15-19	2	63	2D
6	Maha Sarakham	Dry, Sandy	13	3	7	2D
7	Buriram	Dry, Sandy	13	3	26	2D
8	Surin	Dry, Sandy	13	4	35	2D

### 2.3. Vibratory rollers

Two vibratory rollers with weight of 10.7 and 19.2 tons were used in this study. The vibration energy of each roller can be adjusted to two fixed levels which operate on different frequencies. Properties of the rollers are shown in Table 8 and Appendix A. The locations of studied areas are shown in Figure 10.

Table 8 Properties of vibratory rollers used in this study

Model	Surface type	Size (WxD) (m)	Operation weight (tons)	Vibration mode 1			Vibration mode 2		
				Frequency	Nominal Amplitude (mm)	Centrifugal forces (kN)	Frequency	Nominal Amplitude (mm)	Centrifugal forces (kN)
Sakai, SV505D1	Smooth	2.13x1.53	10.67	37	0.93	172	28	2.0	226
Bomag, BW 219	Smooth	2.13x1.6	19.20	31	1.20	240	26	2.1	326

Table 9 Site conditions of vibratory rollers studies

No	Location	Soil type	Roller compactor models	Vibration frequency (Hz)	Number of data
1	Sakon Nakorn	Sandy	Bomag BW 219	31/26	100
2	Nong Kai	Sandy	Sakai, SV505D1	28	60



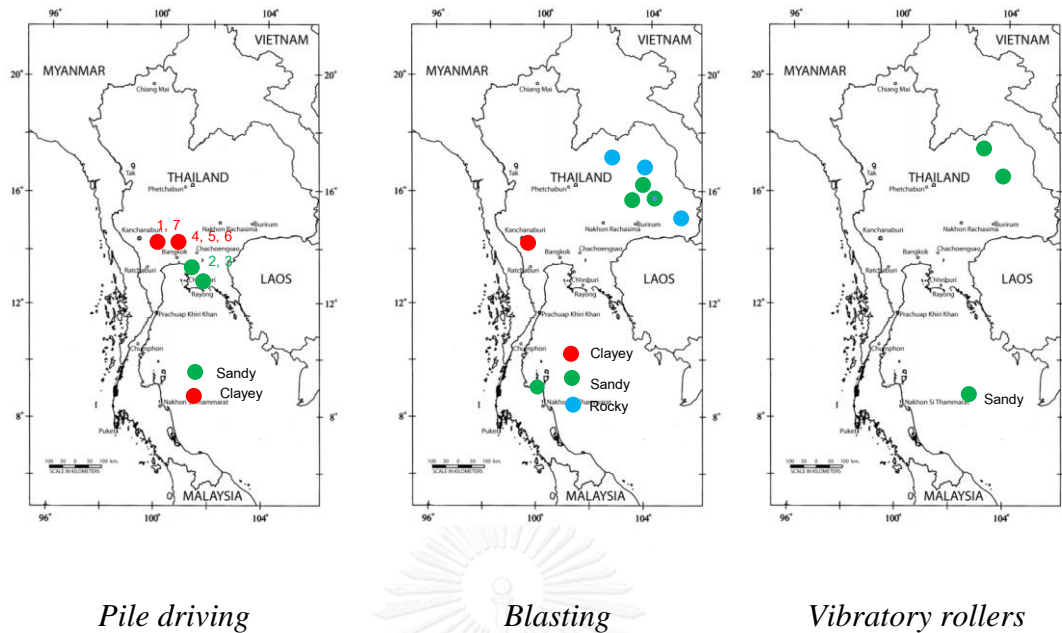


Figure 10 Field measurement locations

### 3. Instruments and measurement setup

Ground vibrations were measured by the equipments listed below. They are also shown in Figure 11.

- four 2.0-Hz triaxial geophones and sixteen 4.5-Hz vertical geophones
- two seismometers (servo type, maker IMV corp. model VM-5112)
- a data logger (computer) and a digitizer (NI compact DAQ USB chassis with analog input module)
- a measuring tape and a survey-grade GPS receiver

#### 3.1. Pile driving and vibratory rollers

Ground vibrations were collected by four 2-Hz and sixteen 4.5-Hz geophones at various distances ( $r$ ) from the sources of vibration. For pile driving, the depth of pile penetration ( $t$ ) during driving was also recorded. The signal in each seismic event was recorded at a sampling rate of 2000 Hz over a period of 1 second. The arrangements of geophones for pile driving and vibratory rollers are shown in Figure 14, Figure 15 and Table 15, respectively. The geophones were installed at 5-70 meters from the sources of vibration.

#### 3.2. Blasting

For 2D seismic reflection surveys, geophones and explosives used for the exploration were installed along the same line. For 3D surveys, geophones were

installed along lines that run in parallels and explosives were installed along lines perpendicular to the geophone lines as shown in Figure 16.

In each study area, the geophones used for this study were installed on the ground surface at a regular interval (20 m for 4.5Hz geophones and 25 m for 2.0Hz geophones) and used to record vibrations from detonation points in nearby areas. The source-to-receiver distance in this study ranged between 10~1,000 m. The locations of instrument geophones and explosives were recorded by surveyor-grade GPS. They were used to transform measured signals into radial, transverse and vertical directions as well as to determine source-to-receiver distance, based on geometric relations shown in Figure 17.



Data logger and digitizer



Measuring tape and survey-grade GPS receiver



Vertical geophone and Triaxial geophone

Figure 11 Measuring equipments



Figure 12 2.0-Hz triaxial geophone



Figure 13 4.5-Hz geophones

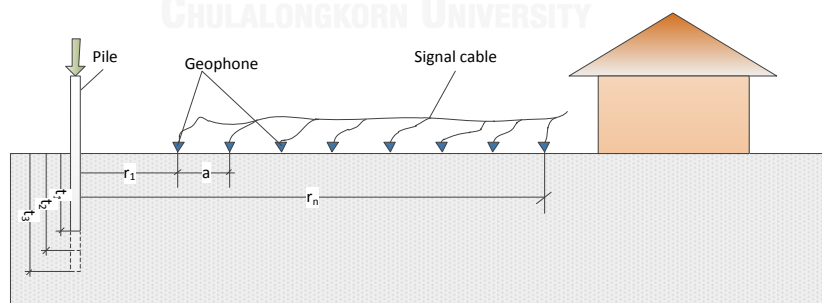


Figure 14 Geophone arrangement for pile driving

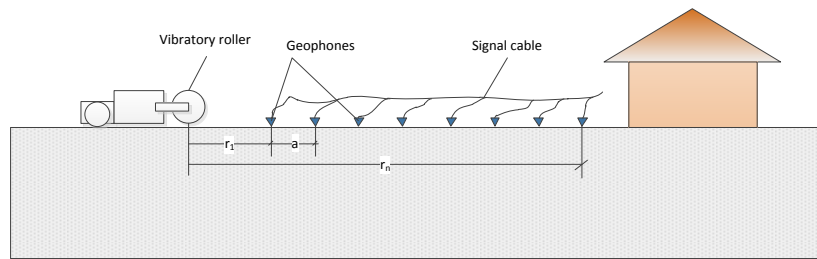
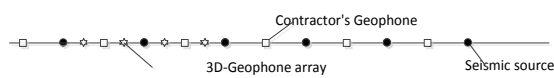
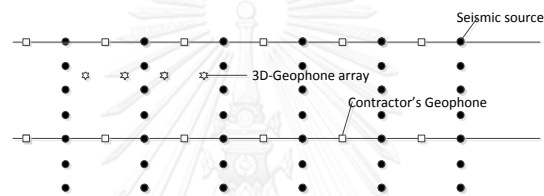


Figure 15 Geophone arrangement for vibratory roller.



(a) 2D



(b) 3D

Figure 16 Layout of geophone array in 2D and 3D seismic surveys

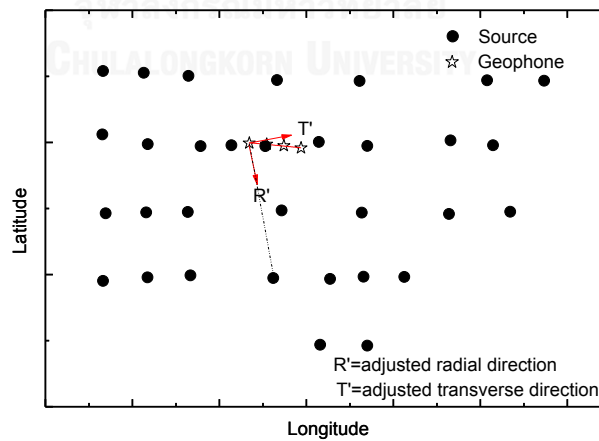


Figure 17 Axis transformation of measured signal

#### 4. Ground conditions of studied areas

##### 4.1. Pile driving

The ground conditions in the studies of pile driving were grouped into two types based on the majority of soil in the upper 30 meters. Ground profiles of site no. 1 and no. 2 are shown in Figure 18 and Figure 19 as examples for clayey and sandy ground types. Photos taken from these sites are shown in Figure 20. The ground conditions of all sites can be seen in Appendix B. The ranges of thickness, depth and SPT N values are summarized in Table 10, Table 11 and Figure 21.

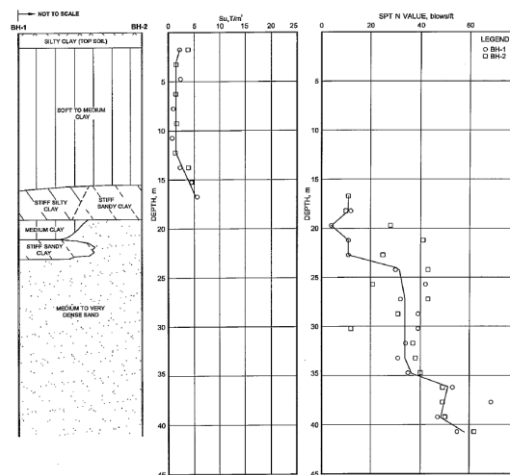


Figure 18 Clayey ground profile (site no. 1, pile driving)

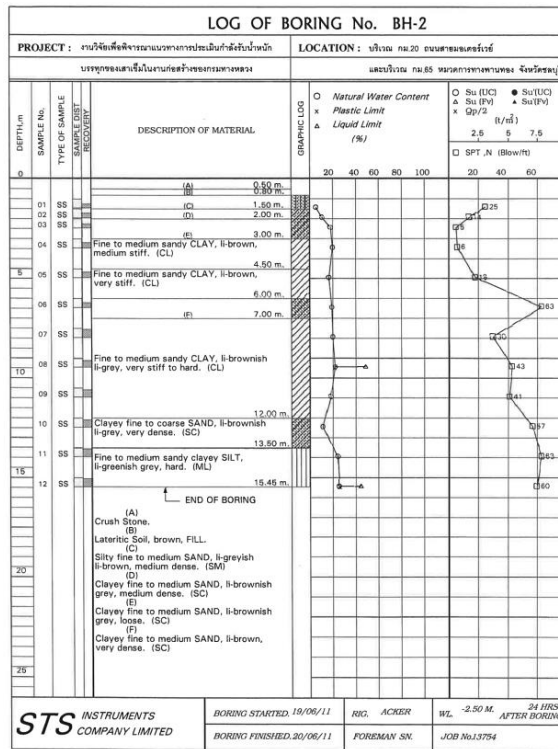


Figure 19 Sandy ground profile (site no. 2, pile driving)



Clayey ground (site no.1)



Sandy ground (site no.2)

Figure 20 Photos taken from clayey and sandy sites of pile driving studies

Table 10 Properties of sandy grounds in the studies of pile driving

Layer	Soil condition	Thickness (m)			Depth (m)			N <sub>SPT</sub>		
		min	aver	max	min	aver	max	min	aver	max
1	First strata	1.8	2.0	2.2	1.8	2.0	2.2	14.5	17.0	19.5
2	Second strata	4.6	11.9	16.0	4.6	13.2	18.2	7.8	12.9	21.1
3	Third strata	1.5	4.5	9.0	9.0	16.2	19.8	49.5	55.3	65.3

Table 11 Properties of clayey grounds in the studies of pile driving

Layer	Soil condition	Thickness (m)			Depth (m)			N <sub>SPT</sub>		
		min	aver	max	min	aver	max	min	aver	max
1	First strata	1.5	1.5	1.5	1.5	1.5	1.5	N/A	N/A	N/A
2	Second strata	15.5	18.0	23.0	15.5	19.3	24.5	4.9	6.2	8.3
3	Third strata	10.5	16.0	30.0	18.0	33.1	49.8	36.6	42.2	49.6

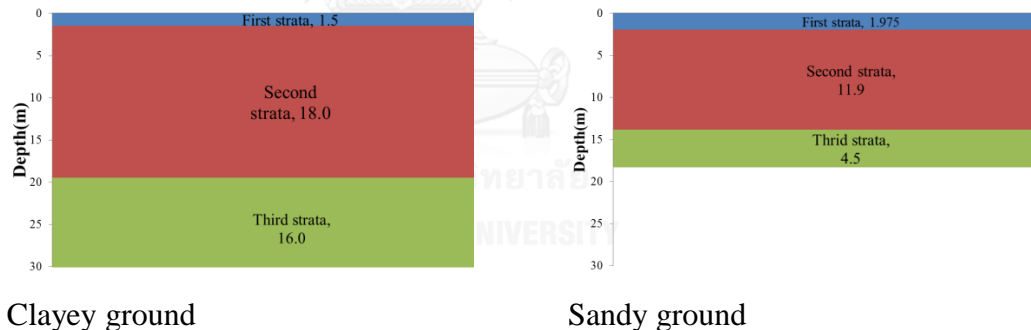


Figure 21 Soil profiles in pile driving studies

#### 4.2. Blasting

The ground conditions in the studies of blasting were grouped into sandy ground, clayey ground or rocky ground based on the majority of soil in the upper 30 meters. Ground profiles of site no. 1, 3 and 5 are shown in Figure 18 and Figure 19 as examples. The ground conditions of all sites can be seen in Appendix B. The ranges of thickness, depth and SPT N values are summarized in Table 12 to Table 14 and Figure 25.

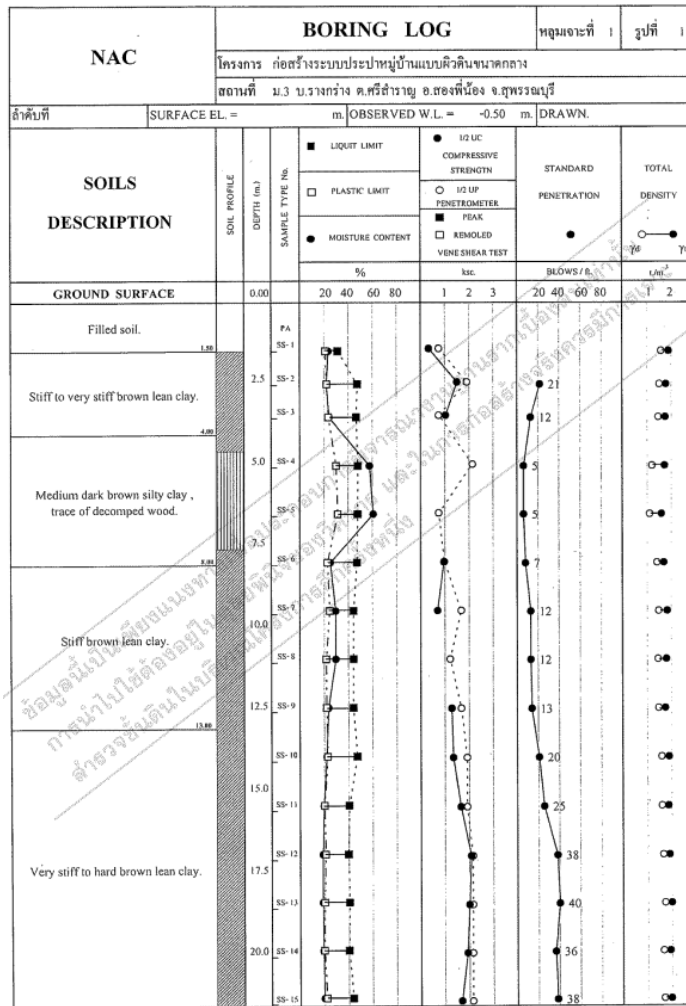


Figure 22 Blasting sites no. 1 (Supan Buri province)



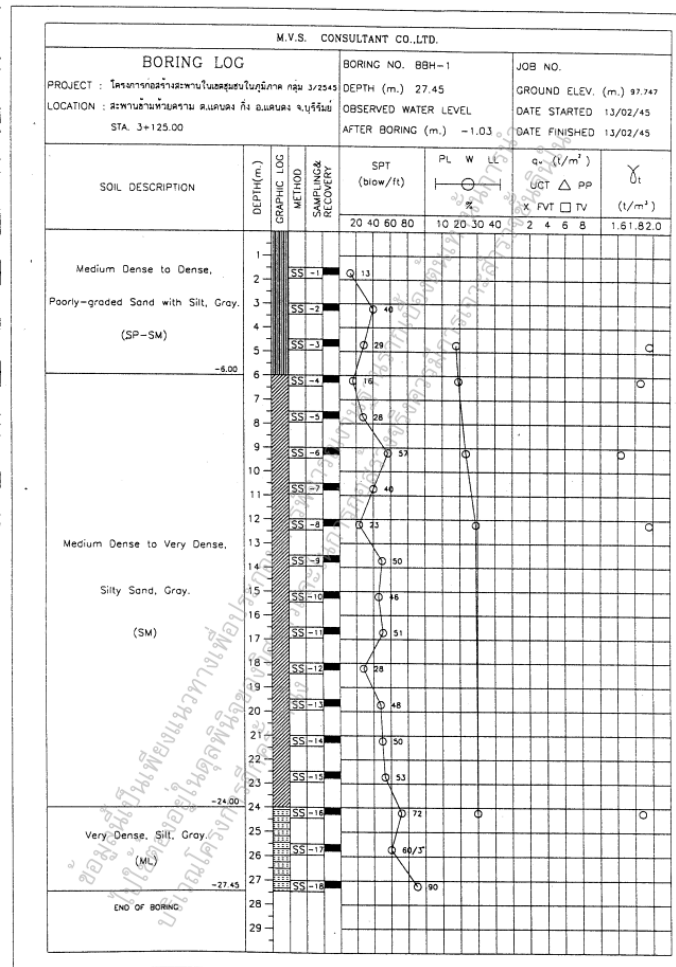


Figure 23 Blasting sites no. 3 (Burirum province)

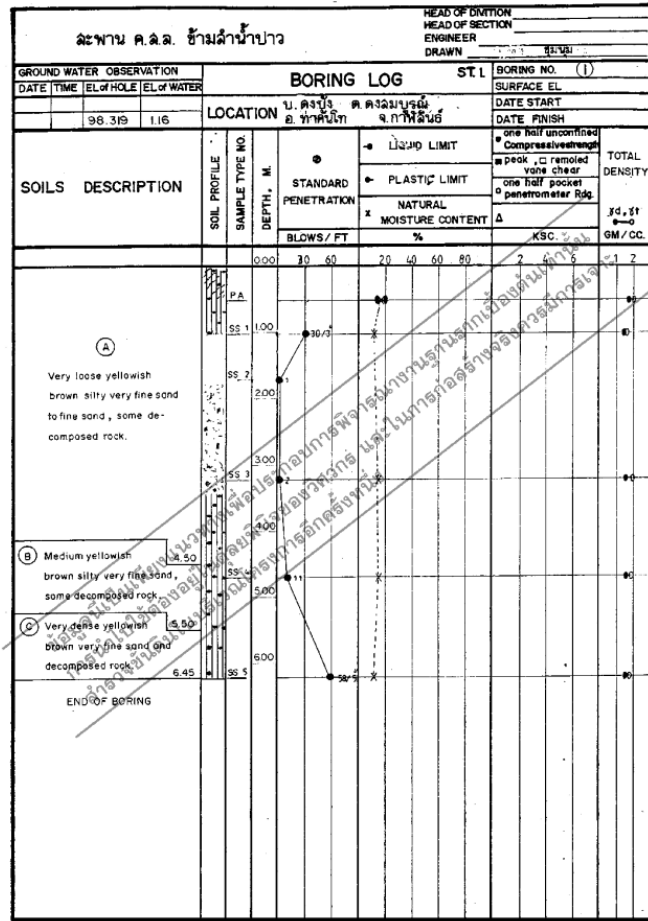


Figure 24 Blasting sites no. 5 (Kalasin province)

Table 12 Properties of clayey grounds in the studies of blasting

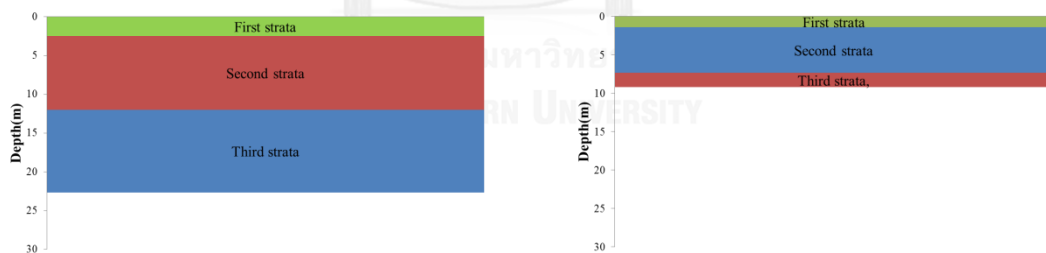
Layer	Soil condition	Thickness (m)			Depth (m)			N <sub>SPT</sub>		
		min	aver	max	min	aver	max	min	aver	max
1	First strata	2.5	2.5	2.5	2.5	2.5	2.5	21	21	21
2	Second strata	9.5	9.5	9.5	12	12	12	9.4	9.4	9.4
3	Third strata	10.7	10.7	10.7	22.7	22.7	22.7	34.4	34.4	34.4

Table 13 Properties of rocky grounds in the studies of blasting

Layer	Soil condition	Thickness (m)			Depth (m)			N <sub>SPT</sub>		
		min	aver	max	min	aver	max	min	aver	max
1	First strata	0.5	1.4	2.0	0.5	1.4	2.0	47.3	53.6	60
2	Second strata	1.5	6.0	10.0	2.0	7.3	11.5	1.0	22.7	126
3	Third strata	1.0	1.9	3.0	3.9	9.1	12.5	35.5	54.1	60.

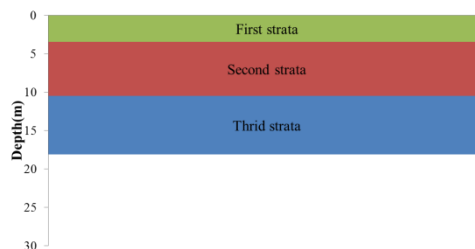
Table 14 Properties of sandy grounds in the studies of blasting

Layer	Soil condition	Thickness (m)			Depth (m)			SPT-N		
		min	aver	max	min	aver	max	min	aver	max
1	First strata	2.0	3.5	6.5	2.0	3.4	6.4	5.0	18.5	38.7
2	Second strata	3.0	7.0	10.5	5.0	9.5	15.4	10.6	17.6	24.8
3	Third strata	1.5	7.6	16.4	11.0	17.4	27.4	41.8	52.3	71.5



Clayey ground

Rocky ground



Sandy ground

Figure 25 Soil profiles in blasting studies

4.3. Vibratory rollers

The studies of vibratory rollers were only made in sandy ground. Ground profiles of site no. 1 and no. 2 are shown in Figure 26 and Figure 27. The ranges of thickness, depth and SPT N values are summarized in Table 15 and Figure 28.

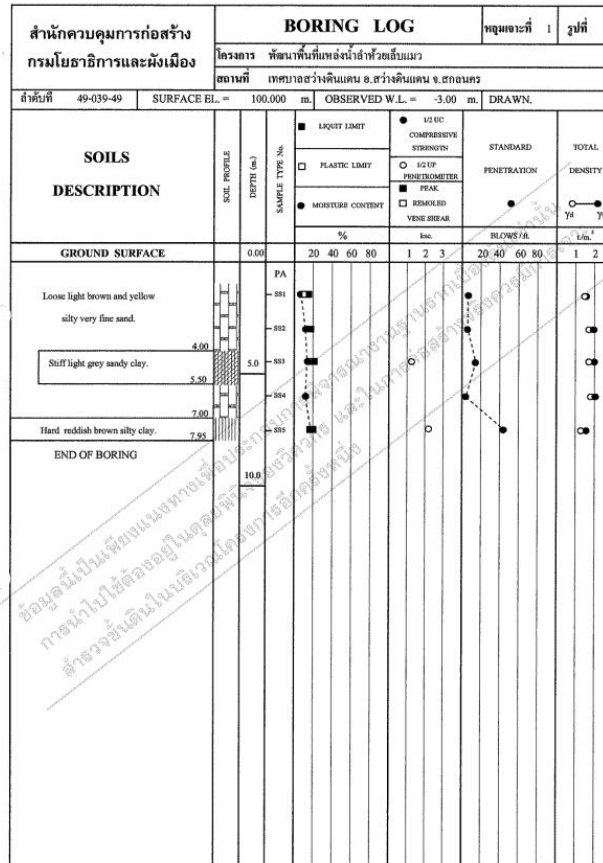


Figure 26 Sandy ground profile (site no. 1, Sakon Nakorn province, vibratory rollers)

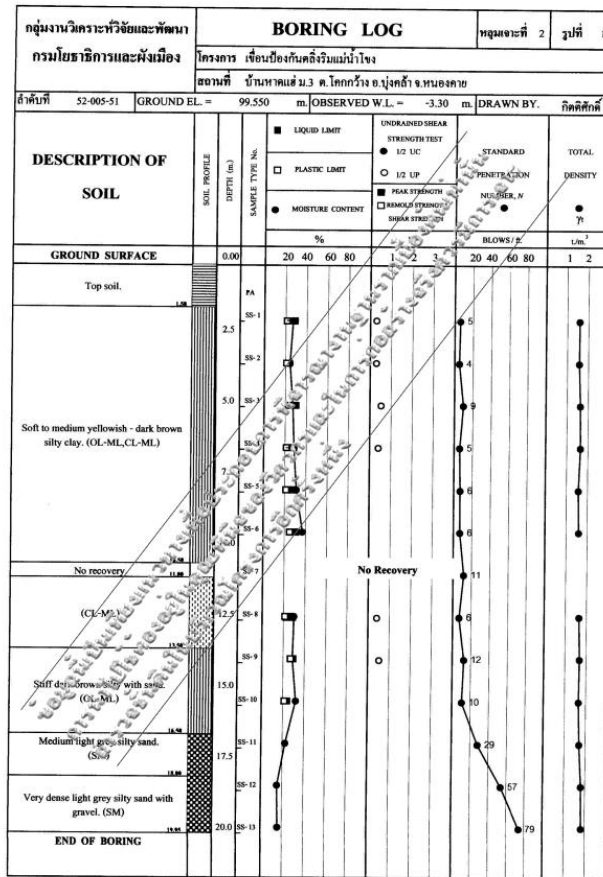


Figure 27 Sandy ground profile (site no. 2, Nong Khai province, vibratory rollers)

Table 15 Ground properties in the studies of vibratory rollers

Layer	Soil condition	Thickness (m)			Depth (m)			N <sub>SPT</sub>		
		min	aver	max	min	aver	max	min	aver	max
1	First strata	1.5	1.5	1.5	1.5	1.5	1.5	N/A	N/A	N/A
2	Second strata	3.3	8.5	13.8	4.8	10.0	15.3	7.8	8.4	9.0
3	Third strata	1.5	3.0	4.5	6.3	13.0	19.8	44.0	54.7	65.3

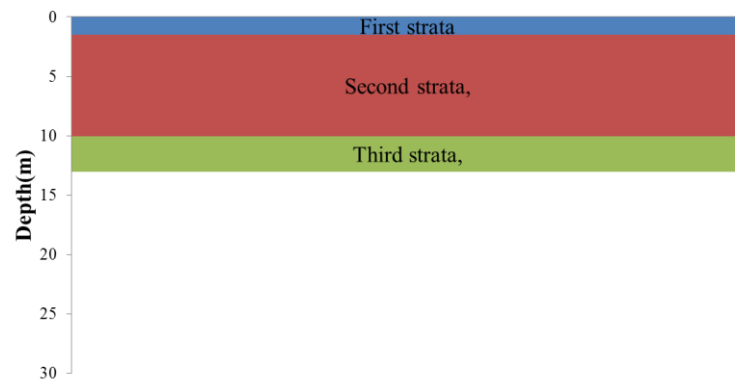


Figure 28 Soil profiles in vibratory roller studies

## 5. Measurement results

Peak particle velocities (PPV) and dominant frequencies of ground motions at various distances were calculated from measured data. They were used to determine the coefficients of geometric and material attenuation and to construct prediction models which are suitable for work practices and ground conditions in Thailand. The formulas obtained by this study were compared with the field data and other models in literatures.

### 5.1. Peak particle velocity and dominant frequency

Examples of recorded signals in time domain are shown in Figure 29. Due to the limitation of measuring devices, the vibrations in this study ranged between 0.5 to 120 mm/s. The peak particle velocities (PPV) were determined from the maximum values of these graphs. Then, the signals were transformed into frequency domain by fast Fourier transform for determining the dominant frequencies where the maximum amplitudes occurred.

In addition to peak particle velocities in radial, transverse and vertical directions, the maximum amplitude of the vibration vector was also considered. The amplitude of a vibration vector at time  $t$  ( $v_{s,t}$ ) is calculated by

$$v_{s,t} = \sqrt{v_{r,t}^2 + v_{t,t}^2 + v_{z,t}^2} \quad (17)$$

where  $v_{r,t}$ ,  $v_{t,t}$ ,  $v_{z,t}$  are particle velocities in radial, transverse, and vertical directions at time  $t$ , respectively.

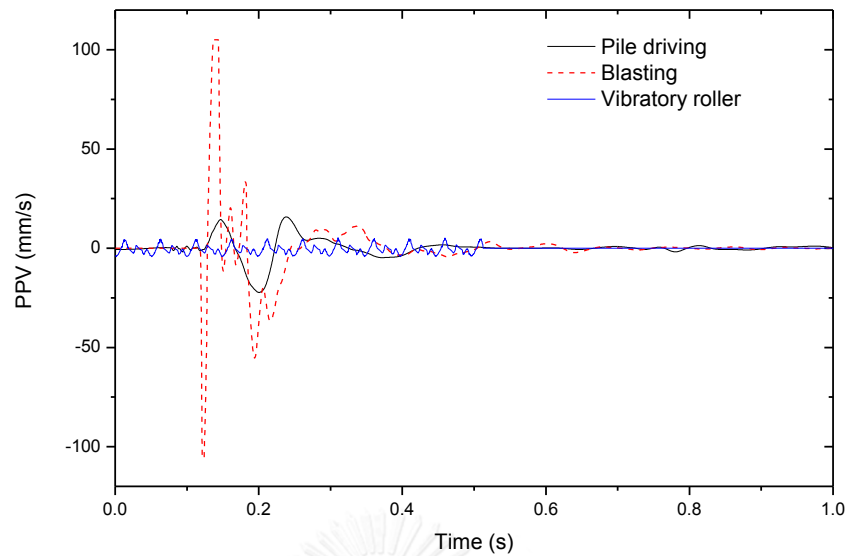


Figure 29 Examples of signals measured from each vibration source

## 5.2. Attenuation characteristics of each ground type

### 5.2.1. General form of vibration prediction model

A general form of ground vibration prediction model can be written as

$$v = k \cdot w^b \cdot r^{-n} \cdot e^{-\alpha r} \quad (18)$$

where  $v$  = peak particle velocity at an interested point

$k, b, n, \alpha$  = non-negative fitting parameters

$w$  = energy of the vibration source

$r$  = distance from the vibration source

When the influence from the energy of vibration source is not considered, the first two components in Eq. (18) can be lumped together for obtaining a simplified form as shown by Eq. (19). By assuming that the effect of the material attenuation is negligible, a more simplified model as shown by Eq. (20) can be obtained.

$$v = \hat{k} \cdot r^{-n} \cdot e^{-\alpha r} \quad (19)$$

$$v = \hat{k} \cdot r^{-n} \quad (20)$$

### 5.2.2. Piecewise model

It was observed in this study that ground vibrations near and far from vibration sources behaved differently. Vibrations near to a vibration source were dominated by body waves whereas vibrations in far zone were dominated by surface waves. Consequently, a piecewise function shown in Eq. (21) was proposed and used in this study.

$$v = \begin{cases} k_1 r^{-n_1} & , \text{ if } r < r_c \\ k_2 r^{-n_2} & , \text{ if } r > r_c \end{cases} \quad \text{subject to } k_1 r_c^{-n_1} = k_2 r_c^{-n_2} \quad (21)$$

where  $r_c$  is the distance at the boundary between near and far zones.

### 5.3. Comparisons between prediction methods and measured results

Non-linear regression analyses by curve fitting of Eq. (19), (20) and (21) were carried out. The optimum values of geometric and material damping coefficients were justified by the highest coefficient of determination ( $R^2$ ). When comparing between each prediction models, the most appropriate one was selected based on the Akaike information criterion (AIC). The selected model is the one that has the smallest AIC score.



## CHAPTER IV

### RESULTS AND DISCUSSIONS

#### 1. Pile driving

Vibrations due to pile driving were measured from 8 locations. The grounds were grouped by the properties in the upper 30 m into sandy and clayey ground types. The ground type of each study area is shown in Table 10. Clayey ground types were encountered at sites no. 1, 4, 5, 6, 7 and 8 while sandy ground types were encountered at site no.2 and 3. For each area, the ground was divided, from the top to the bottom, into three layers namely the 1<sup>st</sup> strata, the 2<sup>nd</sup> strata and the 3<sup>rd</sup> strata respectively. The 1<sup>st</sup> strata, or the top soils, were moderately stiff and usually made of backfill materials. The 2<sup>nd</sup> strata were the layers which piles should be penetrated through. They were usually made of soft clays or loose sands. The 3<sup>rd</sup> strata were stiff clays or dense sands where the tips of piles rested on.

In the following sections, the ground vibrations which were measured during pile driving will be explained and discussed.

##### 1.1. Clayey ground

Data to be discussed were taken from site no. 1, 4, 5, 6, 7, and 8. Since piles penetrated through the 1<sup>st</sup> strata over short durations, the measured results were only available during the penetration through the 2<sup>nd</sup> and 3<sup>rd</sup> strata.

##### *1.1.1. Ground vibrations when piles were penetrating through the 2<sup>nd</sup> strata*

In the following sections, the measurements from site no. 1, 4 and 7 were chosen for discussion. The complete data from all sites are shown in Appendix C.

##### *1.1.1.1. Ground vibrations due to pile driving in each direction*

The PPV in each direction and the PPV of velocity vectors of all measurements were plotted against distance in Figure 30 to Figure 32. When close to the piles, the PPVs in vertical direction were almost equal to the values from velocity vectors and higher than the other components. However, the vertical vibrations decreased at a faster rate than the horizontal components when moving away from the piles. At the farthest measuring points, the vibrations in three directions were in the same range. Since the vibrations were almost governed by the vertical components, further analyses were based on the data from 4.5Hz vertical geophones for the interest of more data points.

#### 1.1.1.2. Attenuation of vibration due to pile driving in clayey grounds

Three attenuation patterns were observed in this study.

For the first attenuation pattern, the PPV decreases monotonically with the distance as shown in Figure 31 and Figure 33. This attenuation pattern was observed in site no. 4.

For the second attenuation pattern, the PPV decreases in the same way as the 1<sup>st</sup> pattern. However when the distance increases to a certain point the PPV jumps to a higher value before starts decreasing again. This attenuation pattern was observed in site no. 7 and no. 8.

For the third attenuation pattern, the variation of the PPV is similar to the 2<sup>nd</sup> pattern. However the attenuation of vibration over distance in the second stage is much slower than the 2<sup>nd</sup> case. This attenuation pattern was observed in site no. 1.



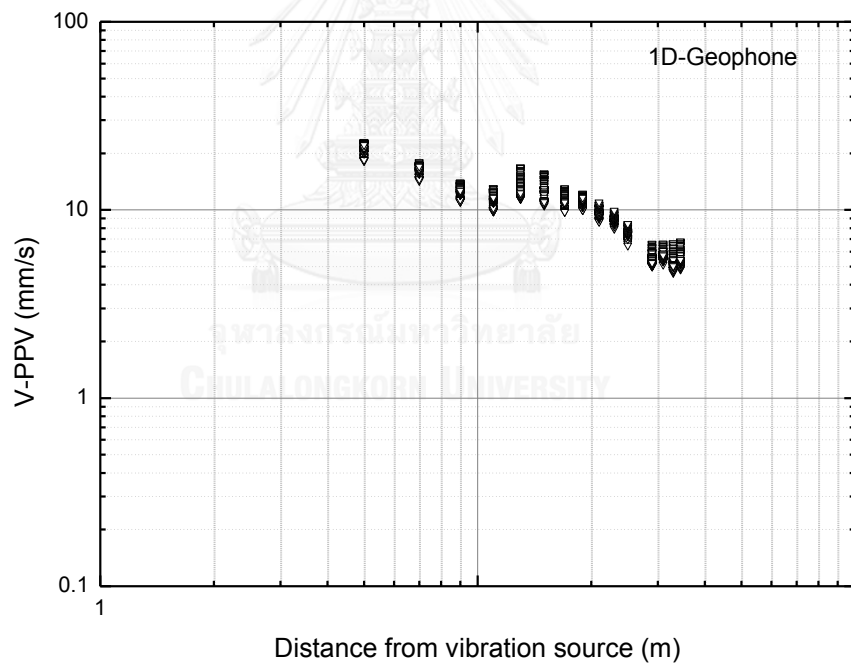
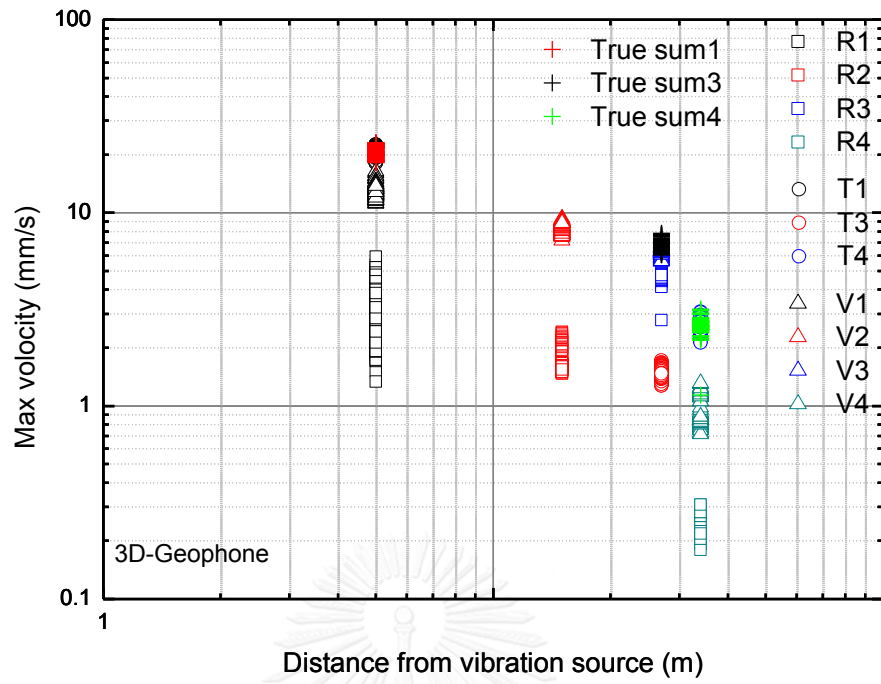


Figure 30 Vibration of each direction of site no. 1

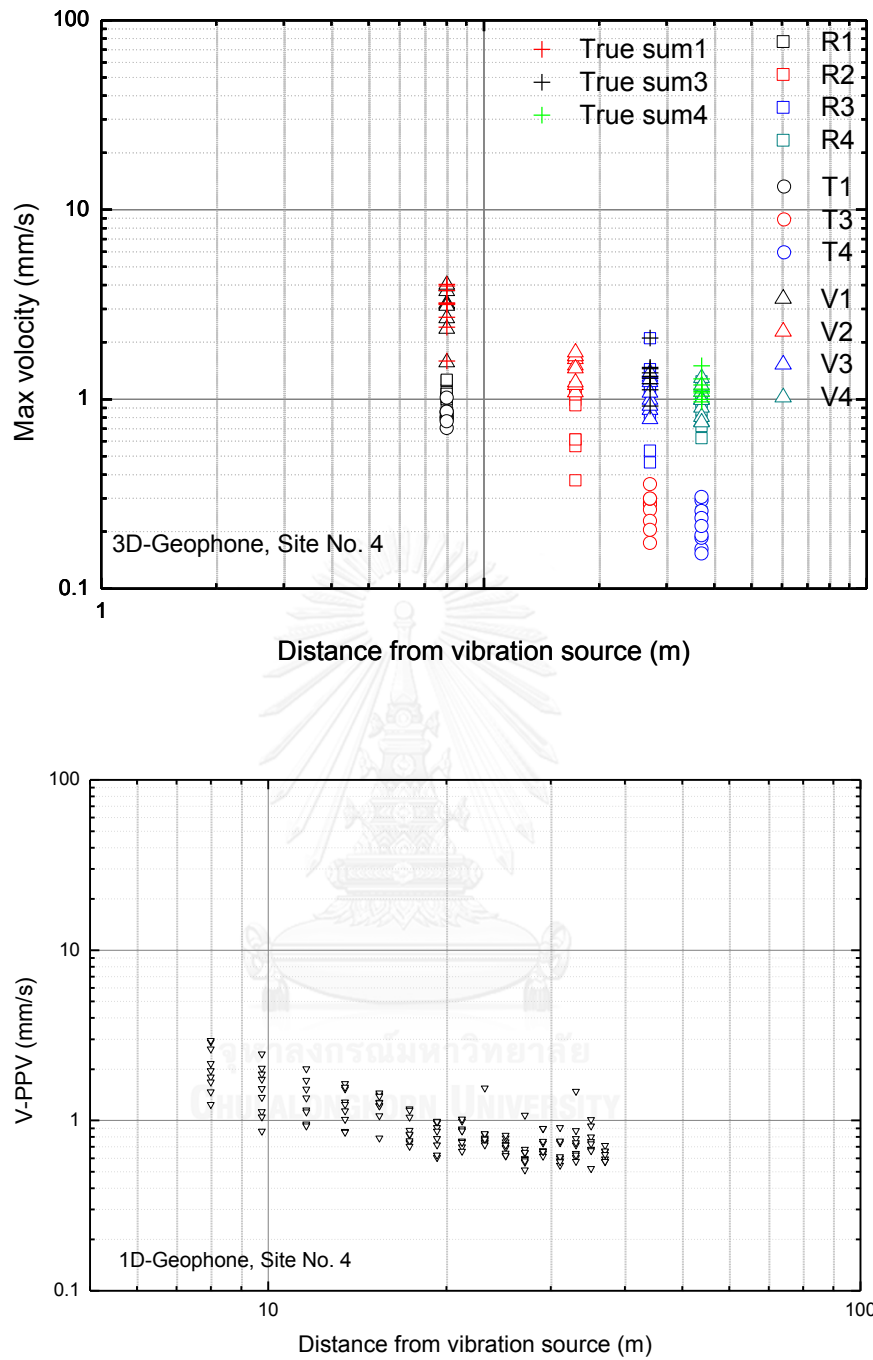


Figure 31 Vibration of each direction of site no. 4

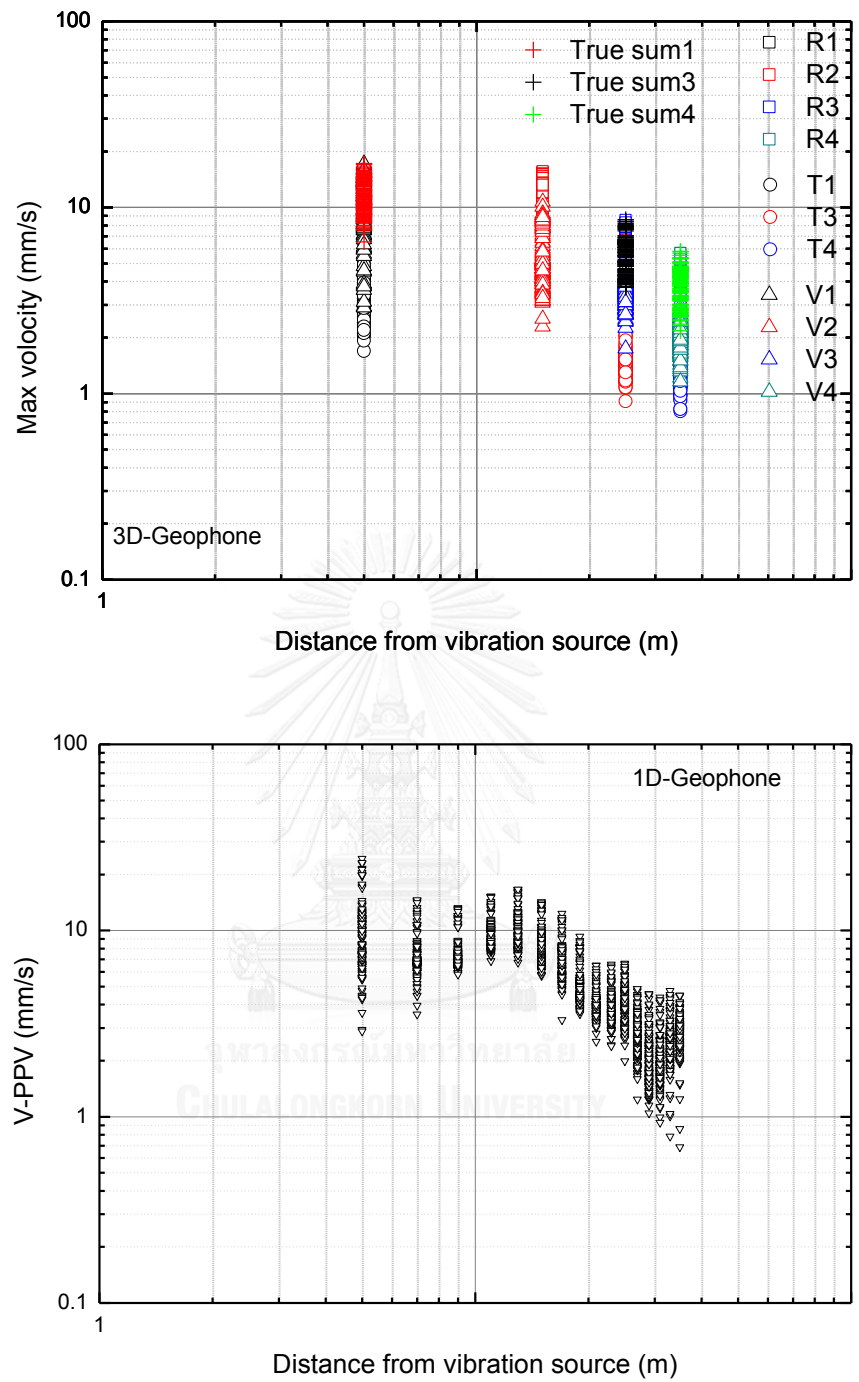


Figure 32 Vibration of each direction of site no. 7

#### 1.1.1.3. Discussion on the first attenuation pattern observed in site no. 4

Results from fitting analyses of site no. 4 using Eq. (20) are shown in Table 16. The highest  $R^2$  obtained from the 2<sup>nd</sup> model implies that the vibrations were governed by body waves (cf. PQ/HS/R, PQ/I/O, and LQ/I/R lines in Figure 7). Based on the data shown in Figure 35, the dominant frequency and distance seemed to be independent of each other. The average value and the standard deviation of dominant frequency of this site were 4 and 1 Hz, respectively.

#### 1.1.1.4. Comparison between prediction models

Fitting results from selected prediction models are shown in Table 17 and Figure 36. Acceptable coefficients of determination ( $R^2$ ) can be obtained from the first three models. It is noted that the negative  $R^2$  in the 5<sup>th</sup> model can occur when performing non-linear curve fitting. In cases where negative values arise, the mean of the data provides a better fit than do the fitted function values.



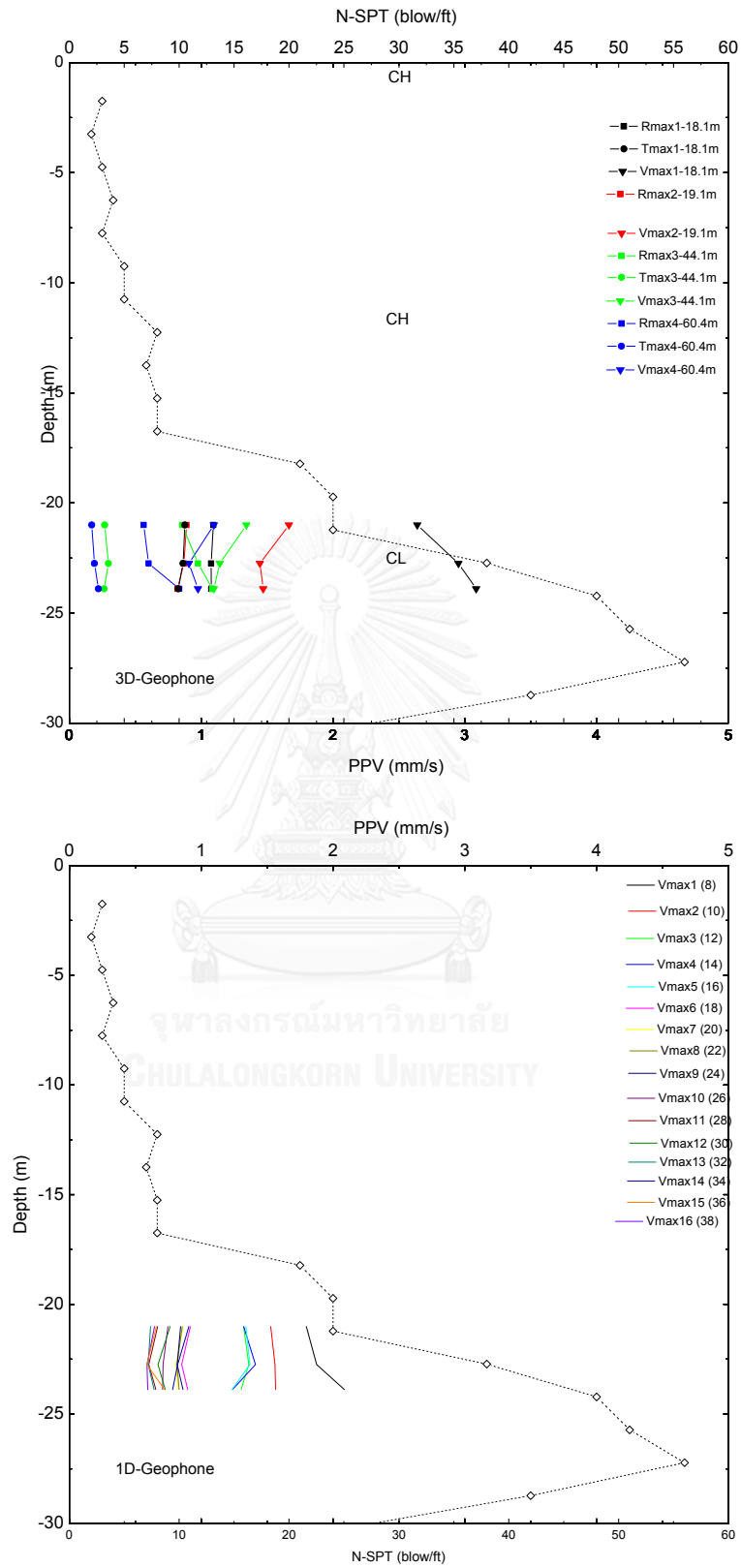


Figure 33 Ground vibration with pile penetrated depth of site no. 4

Table 16 Results from fitting analyses

Site No.	Depth (m)	Fitting models		Fitting parameters		$R^2$	Remarks
				$k$	$n$		
		Conventional models					
4	20.0-22.0 (N=23)	1	$v = k \cdot r^{-n}$	11	0.7	0.896	
		2	$v = k \cdot r^{-0.5}$	4		0.742	
		3	$v = k \cdot r^{-1.0}$	17		0.865	
		4	$v = k \cdot r^{-1.5}$	56		0.451	
		5	$v = k \cdot r^{-2.0}$	171		-0.171	

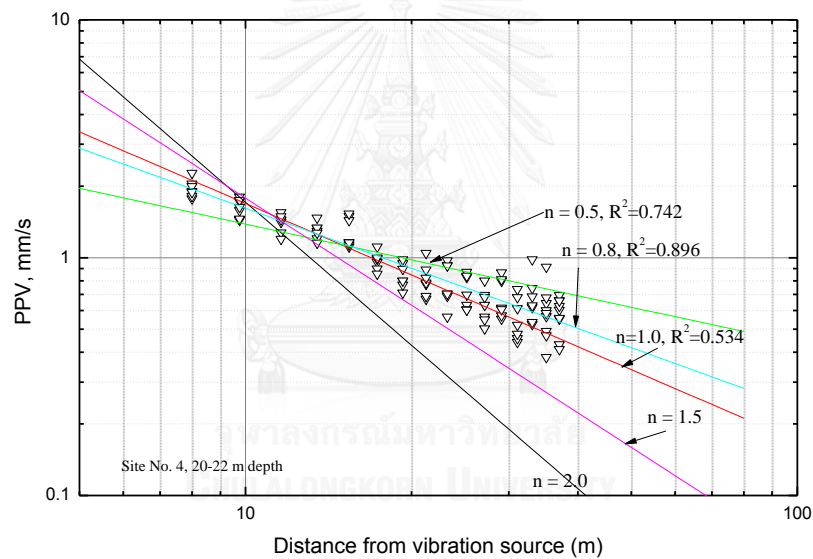


Figure 34 The peak particle velocities versus horizontal distance with log –log scale in site no.4.



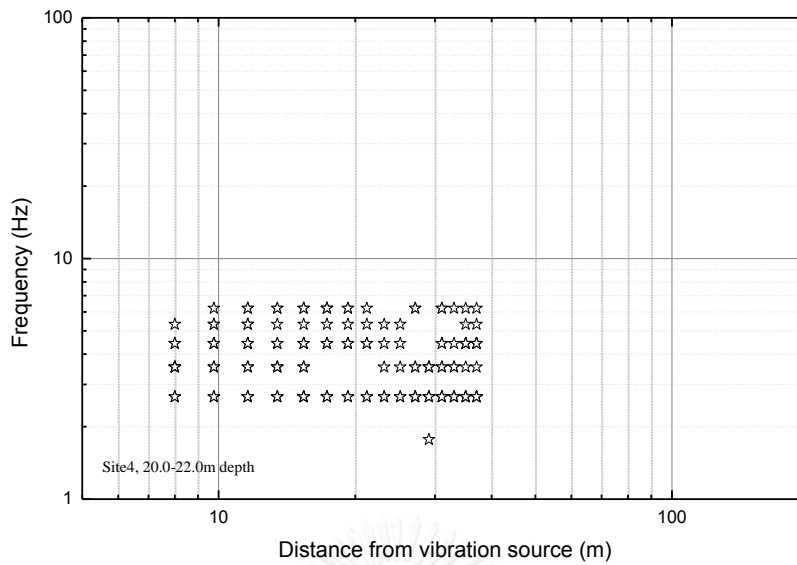


Figure 35 Variation of dominant frequency with distance in each ground type

Table 17 Results from model fitting analyses for the measured data of the 20-22 m pile penetrated depth in site no. 4

Fitting models		Fitting parameters		$R^2$	Remarks
		$k$	$n$		
Prediction models					
1	Attewell and Farmer (1973); $v = k \cdot (w^{0.5} / r)$	5		0.864	
2	Wiss (1981); $v = k \cdot (r / w^{0.5})^n$	5	1.0	0.864	
3	Svinkin (2008), $v = 0.00037 \cdot (w / r) \cdot (c / Z \cdot L)^{0.5}$	18			$r = 1$

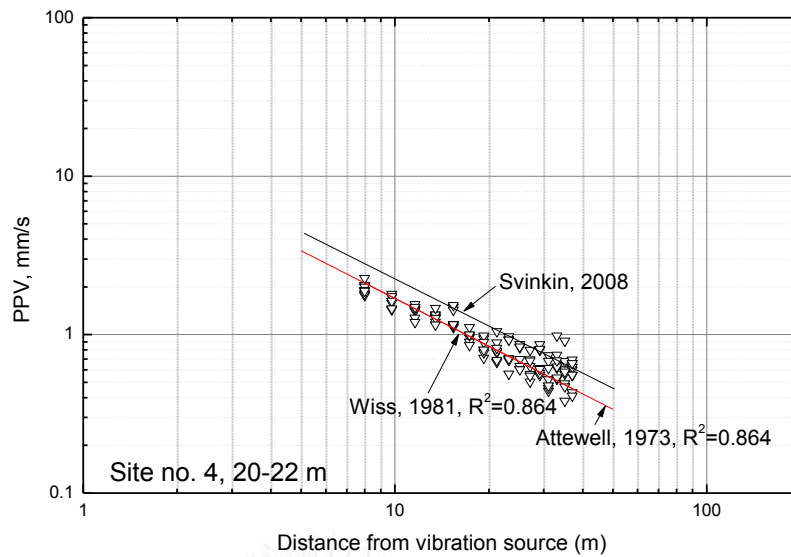


Figure 36 The prediction models fitting for the 2<sup>nd</sup> stratum of site no. 4

#### 1.1.1.5. Discussion on the second attenuation pattern observed in site no. 7

For the second attenuation pattern, the PPV decreases in the same way as the 1<sup>st</sup> pattern. However when the distance increases to a certain point the PPV jumps to a higher value before starts decreasing again. As shown in Figure 37, the variation of vibrations can be separated at the second peak into zone T (Turbulence) and zone B. The beginning of B-zone from ground vibration source in each site was shown in Table 22. In this study, only the behavior in zone B was considered.

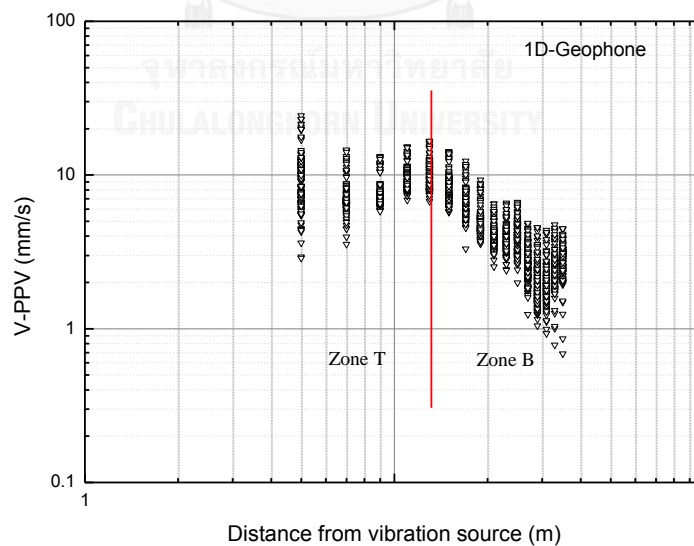


Figure 37 two peak of vibration over distance

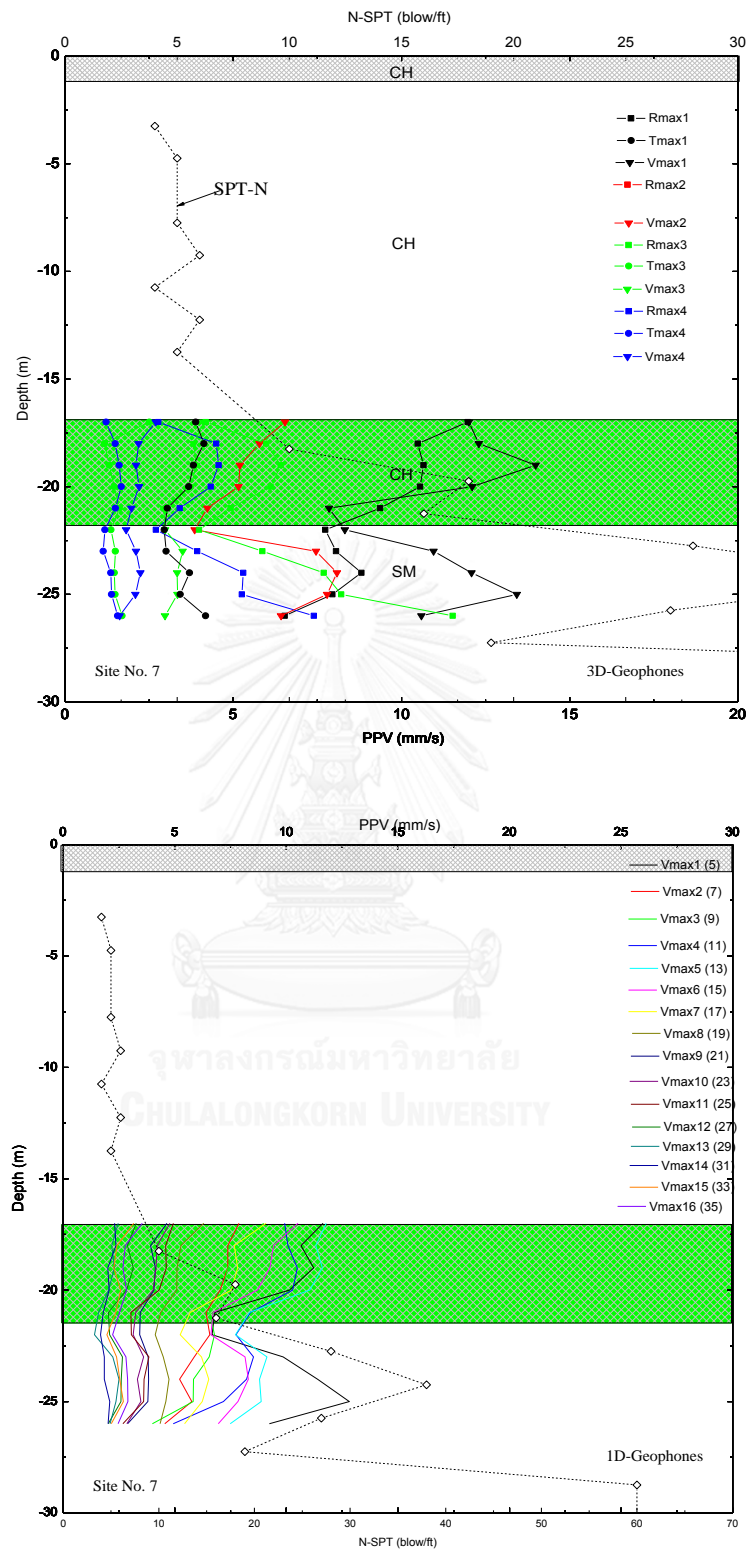


Figure 38 the peak particle velocities versus horizontal distance at different pile penetrated depths in site no. 7.

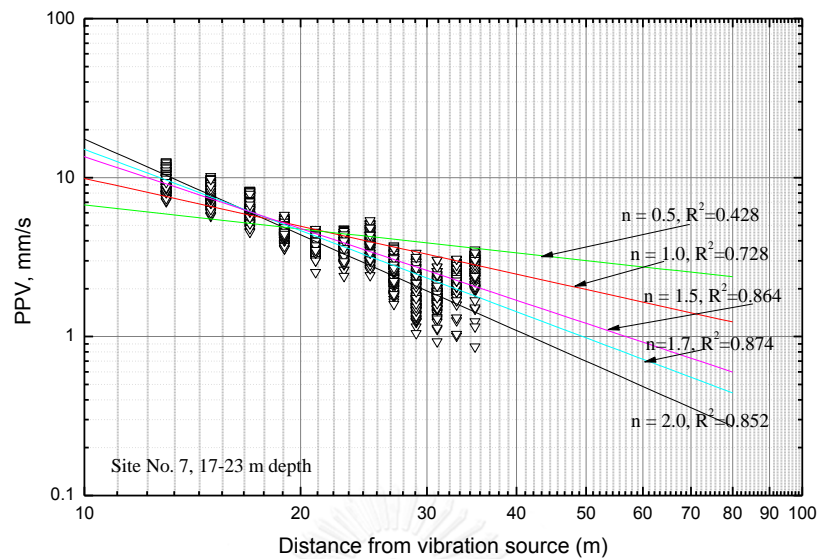


Figure 39 the peak particle velocities versus horizontal distance with log –log scale at 17.0-23.0 m of pile penetrated depth.

#### 1.1.1.6. Attenuation characteristic

Fitting analyses using Eq. (20) are shown in Table 18 and Figure 39. The highest  $R^2$  obtained from the 3<sup>rd</sup> model imply that the vibrations were governed by point load impulsive body wave with  $n = 1.5$  (cf. PQ/I/R lines in Figure 7).

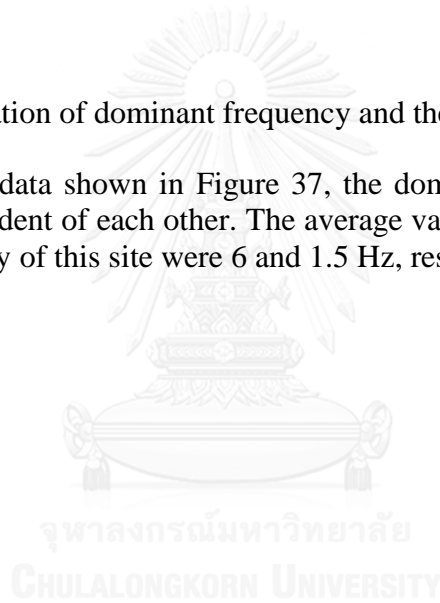
Table 18 Fitting analyses for the 2<sup>nd</sup> attenuation patterns (site no. 7 and no. 8)

Site No.	Depth (m)	Fitting models		Fitting parameters		$R^2$	Remarks
				$k$	$n$		
		Conventional models					
7	17.0-23.0 (N=24)	1	$v = k \cdot r^{-n}$	749	1.7	0.874	
		2	$v = k \cdot r^{-0.5}$	21		0.428	
		3	$v = k \cdot r^{-1.0}$	99		0.728	
		4	$v = k \cdot r^{-1.5}$	428		0.864	
		5	$v = k \cdot r^{-2.0}$	1747		0.852	

Site No.	Depth (m)	Fitting models		Fitting parameters		$R^2$	Remarks
				$k$	$n$		
		Conventional models					
8	12.0-18.0 (N=24)	1	$v = k \cdot r^{-n}$	180	1.5	0.729	
		2	$v = k \cdot r^{-0.5}$	12		0.423	
		3	$v = k \cdot r^{-1.0}$	51		0.664	
		4	$v = k \cdot r^{-1.5}$	199		0.730	
		5	$v = k \cdot r^{-2.0}$	746		0.660	

#### 1.1.1.7. Variation of dominant frequency and the beginning of b-zone

Based on the data shown in Figure 37, the dominant frequency and distance seemed to be independent of each other. The average value and the standard deviation of dominant frequency of this site were 6 and 1.5 Hz, respectively.



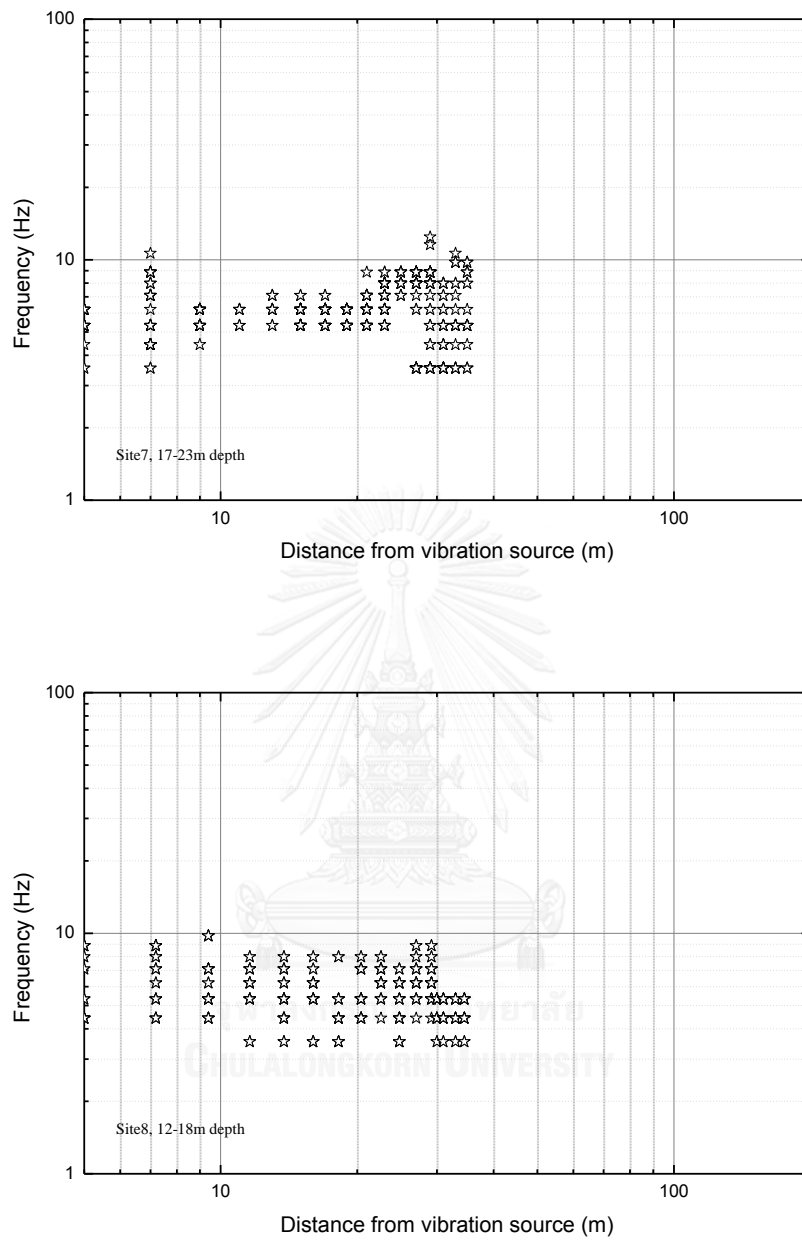


Figure 40 Variation of dominant frequency with distance in each sites

Table 19 Statistics of dominant frequency in each site

Sites	Sample size	Mean, $\mu$ (Hz)	S.D., $\sigma$ (Hz)	$\mu - 2\sigma$ (Hz)
No. 7 (17.0-23.0 m)	1632	6	2	2
No. 8 (12.0-18 m)	225	6	1	4

Table 20 The beginning of B-zone from ground vibration source in each site

Site	Depth (m)		N- SPT	The beginning of B zone form source of ground vibration (m)	Distance of B Zone/Depth		Remarks
	From	To			From	To	
7	17.0	23.0	25	13	0.8	0.6	
8	12.0	18.0	24	11.3	0.9	0.6	

#### 1.1.1.8. Comparison with other prediction models

Fitting results from selected prediction models are shown in Table 21 and Figure 41. The coefficients of determinations ( $R^2$ ) of models in the literatures were less than 0.6 while the best  $R^2$  of 0.546 was obtained from the 1<sup>st</sup> model

Table 21 Fitting analyses with prediction models in literatures (site no. 7 and no. 8)

Fitting models		Fitting parameters		$R^2$	Remark
		$k$	$n$		
Prediction models					
1	Attewell and Farmer (1973); $v = k \cdot (w^{0.5} / r)$	25		0.546	
2	Wiss (1981) ; $v = k \cdot (r / w^{0.5})^n$	7	1.5	0.097	
3	Svinkin (2008), $v = 0.00037 \cdot (w/r) \cdot (c/Z \cdot L)^{0.5}$	130			$r = 1$

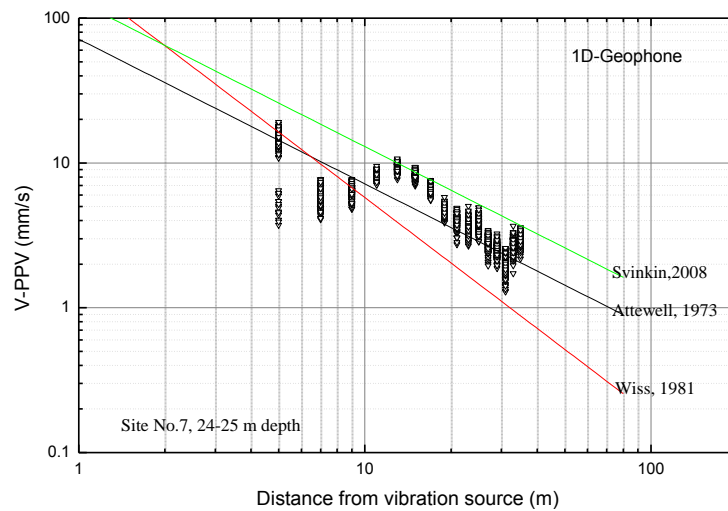


Figure 41 the prediction models fitting for the measured data from the 24.0-25.0 m pile penetrated depth in site no. 7

#### 1.1.1.9. Discussion on the third attenuation pattern observed in site no. 1

For the third attenuation pattern, the variation of the PPV is similar to the 2<sup>nd</sup> pattern. However the attenuation of vibration over distance in the second stage is much slower than the 2<sup>nd</sup> case. This attenuation pattern was observed in site no. 1 and no. 6. As shown in Figure 42, the variation of vibrations can be separated at the second peak into zone T (Turbulence) and zone B. The variation in zone B can be divided further into zone B and zone R based on the slope of the fitted curve.



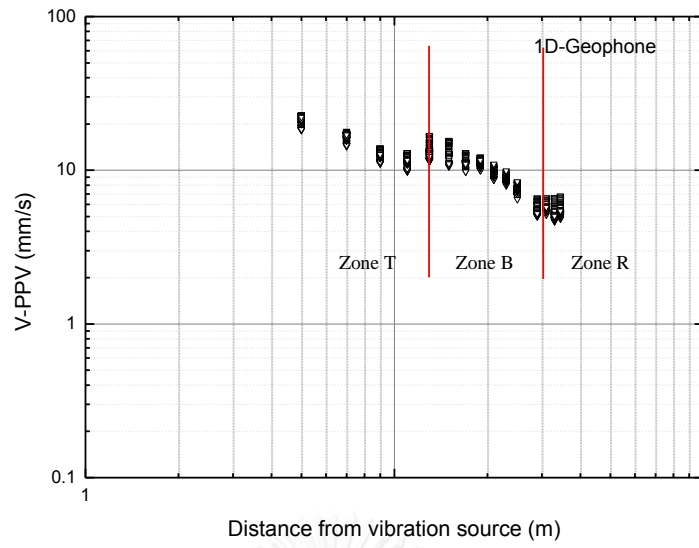


Figure 42 the vibration over distance of pattern 3

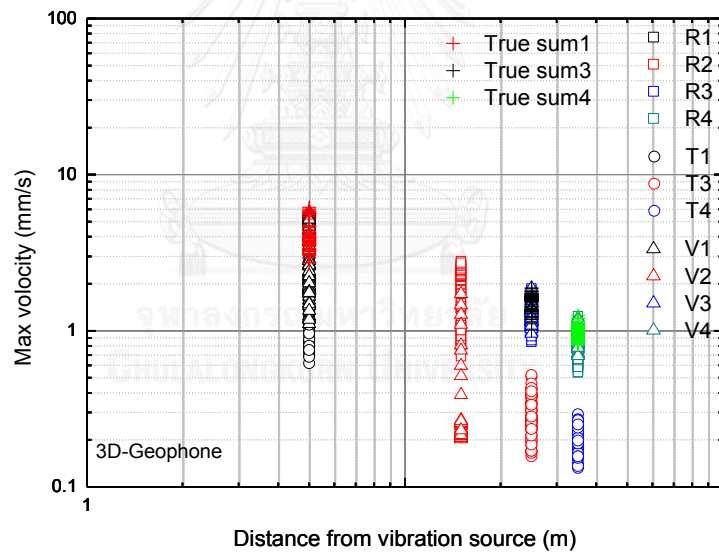


Figure 43 Vibration of each direction of 2<sup>nd</sup> strata in site no. 6

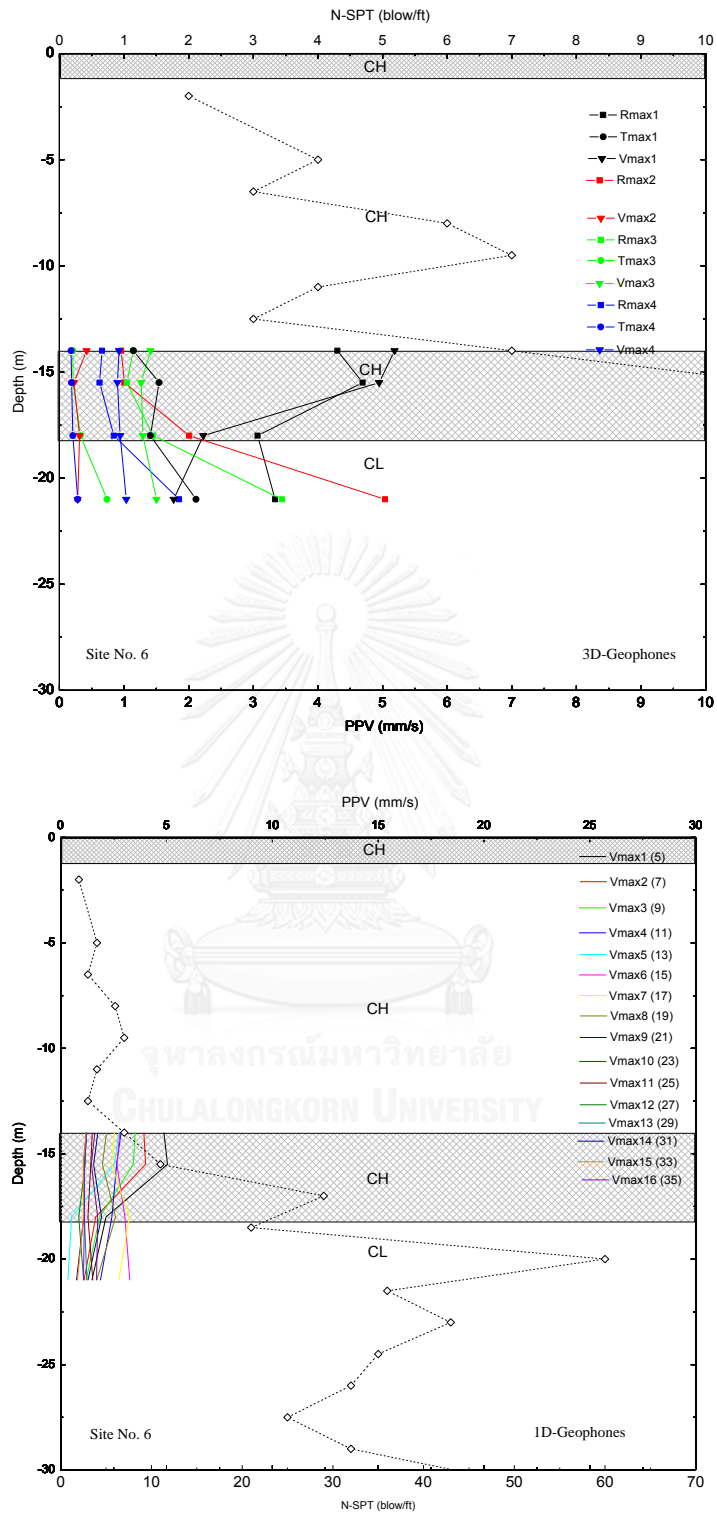


Figure 44 the peak particle velocities versus horizontal distance at different pile penetrated depths of site no. 6.

### 1.1.1.10. Attenuation characteristic

Fitting analyses using Eq. (20) are shown in Table 22. It was noticed from Figure 45 that the data were well aligned with the  $n = 2.0$  line when the distance was less than 30 meter. The vibration tended to decrease in the same rate as the  $n = 0.5$  line when the distance was larger than 30 m. Therefore it was assumed based on this observation that the vibration in the near zone was dominated by body waves whereas the vibration in the far zone was dominated by surface waves (Ghosh and Daemen, 1983).

Table 22 Results from fitting analyses for the data of 18-19 m of pile penetrated depth in site no. 6

Fitting models		Fitting parameters		$R^2$	Remarks
		$k$	$n$		
Conventional models					
1	$v = k \cdot r^{-n}$	796	1.95	0.870	
2	$v = k \cdot r^{-0.5}$	8		0.382	
3	$v = k \cdot r^{-1.0}$	41		0.665	
4	$v = k \cdot r^{-1.5}$	198		0.826	
5	$v = k \cdot r^{-2.0}$	914		0.870	

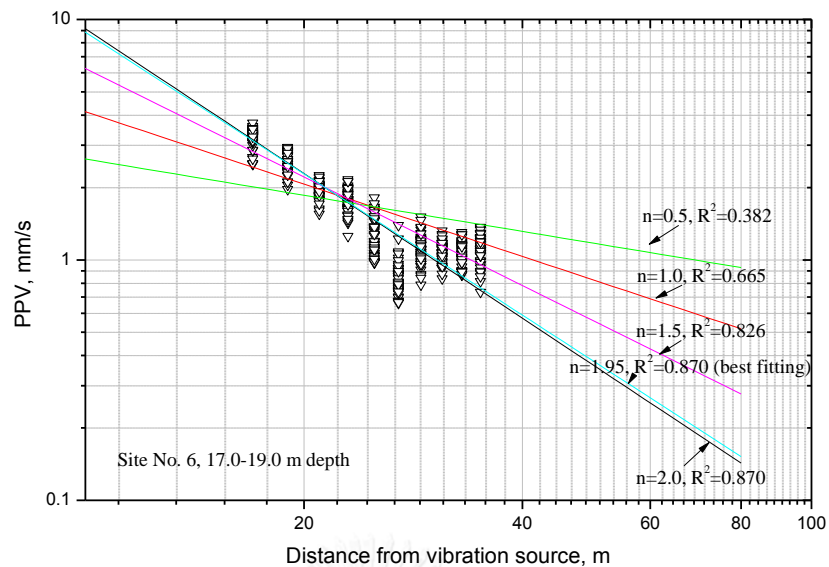


Figure 45 the attenuation of measured data from 17-19 m of pile penetrated depth in site no.6.

According to Figure 46, to validate this assumption, the data was fitted by a piecewise function shown in Eq. (21) which is the 6<sup>th</sup> model in Table 23. Further studies were also made by setting the  $n_1$  and  $n_2$  to some characteristic values which are the 7<sup>th</sup> and 8<sup>th</sup> models in Table 23. The 8<sup>th</sup> model is recommended for the interest of generalization and theoretical study.

#### 1.1.1.11. Attenuation in each sites

Fitting analyses were carried out for determining the attenuation of PPV over distance in the top soil of sandy ground in site no. 1. Due to the reason mentioned earlier, the further studies were carried out by comparing the Eq. (21) which derives the value  $n$  from theoretical basis. The geometric attenuation parameter  $n_1$  was fixed to 1, 1.5 and 2, while  $n_2$  was fixed to 0.5 as shown in Table 24. According to Table 23 and Table 24, site no. 6 and no. 1 the highest  $R^2$  were obtained from the 6<sup>th</sup> model, the majority of waves were likely to be body wave traveling along the free surface with  $n = 2.0$  and 1.0 respectively.

Table 23 Results from fitting analyses for the data of 18-19 m of pile penetrated depth in site no. 6

Fitting models		Fitting parameters			$R^2$	Remarks
		$k$	$n$	$r_c$		
Conventional models						
1	$v = k \cdot r^{-n}$	796	1.95		0.870	
2	$v = k \cdot r^{-0.5}$	8			0.383	
3	$v = k \cdot r^{-1.0}$	41			0.665	
4	$v = k \cdot r^{-1.5}$	198			0.826	
5	$v = k \cdot r^{-2.0}$	915			0.870	
Piecewise models						
6	$v = k_1 \cdot r^{-n_1}, r < r_c$	3988	2.50	26.0	0.921	
	$v = k_2 \cdot r^{-n_2}, r > r_c$	2.5	0.23	26.0		
7	$v = k_1 \cdot r^{-1.8}, r < r_c$	4092	2.51	25.5	0.917	
	$v = k_2 \cdot r^{-0.5}, r > r_c$	5	0.43	25.5		
8	$v = k_1 \cdot r^{-2.0}, r < r_c$	884	2	27	0.900	
	$v = k_2 \cdot r^{-0.5}, r > r_c$	6	0.5	27		

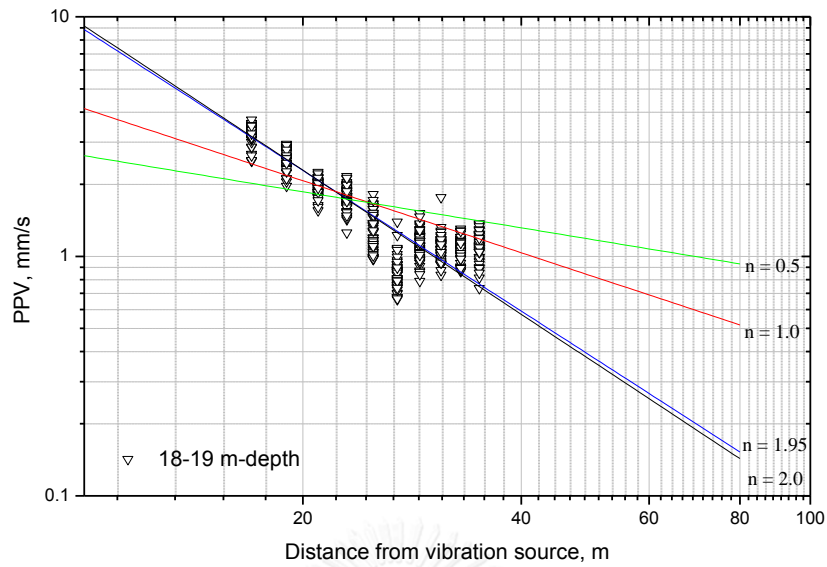


Figure 46 The attenuation of measured data from 18-19 m of pile penetrated depth in site no.6.

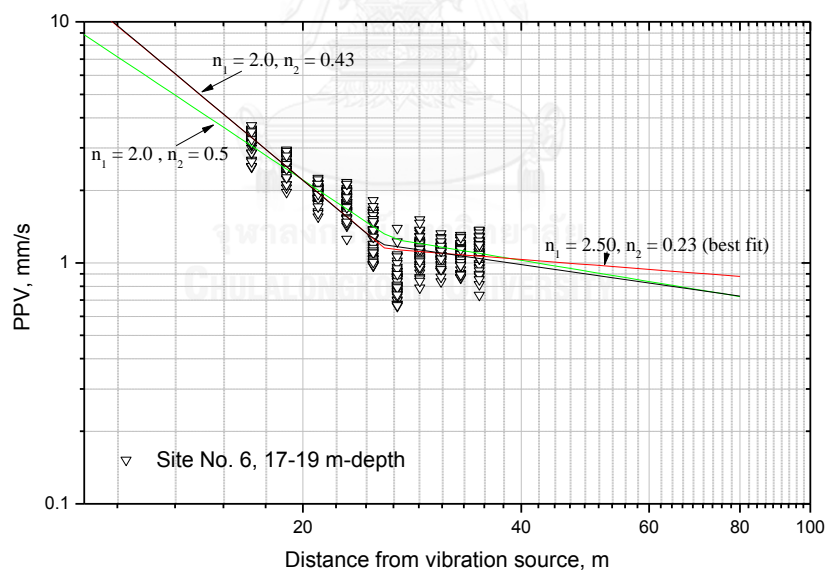


Figure 47 Piecewise fitting of measured data from 17-19 m of pile penetrated depth in site no.6.

Table 24 fitting analyses for 16-23 m of pile penetrated depth in site no. 1

Fitting models		Fitting parameters			$R^2$	Remarks
		$k$	$n$	$r_c$		
Conventional models						
1	$v = k \cdot r^{-n}$	193	1.0		0.913	
2	$v = k \cdot r^{-0.5}$	42			0.680	
3	$v = k \cdot r^{-1.0}$	189			0.912	
4	$v = k \cdot r^{-1.5}$	789			0.722	
5	$v = k \cdot r^{-2.0}$	3122			0.237	
Piecewise models						
6	$v = k_1 \cdot r^{-1.0}, r < r_c$	189		31	0.913	
	$v = k_2 \cdot r^{-0.5}, r > r_c$	30		31		
7	$v = k_1 \cdot r^{-1.5}, r < r_c$	788		31.5	0.736	
	$v = k_2 \cdot r^{-0.5}, r > r_c$	25		31.5		
8	$v = k_1 \cdot r^{-2.0}, r < r_c$	3121		31.5	0.227	
	$v = k_2 \cdot r^{-0.5}, r > r_c$	18		31.5		

## 1.1.1.12. Variation of dominant frequency

Based on the data shown in Figure 48, the dominant frequency and distance seemed to be independent of each other. The average value and the standard deviation of dominant frequency of this site were 6.5 and 2 Hz, respectively.

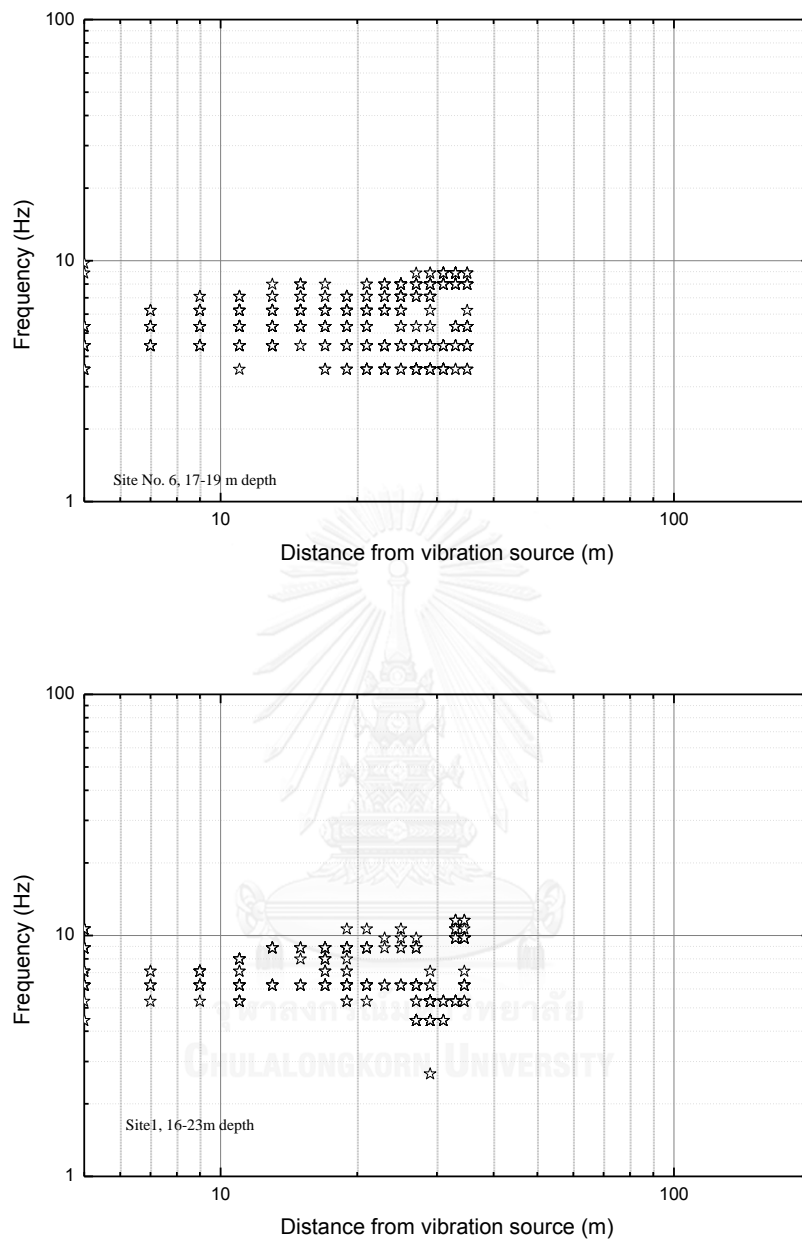


Figure 48 Variation of dominant frequency with distance in each sites



Table 25 Statistics of dominant frequency in each site

Sites	Sample size	Mean, $\mu$ (Hz)	S.D., $\sigma$ (Hz)	$\mu - 2\sigma$ (Hz)
No. 6 (17-19 m)	570	6	2	2
No. 1 (16-23 m)	1243	7	2	3

Table 26 The beginning of B-zone from ground vibration source in each site

Site	Depth (m)		$N_{SPT}$	Beginning of B zone (m)	Ending of B zone (m)	Beginning/Depth		Ending/Depth	
	From	To				From	To	From	To
6	17	19	25	17	26	1.0	0.9	1.5	1.4
1	16	23	11	13	31	0.8	0.6	1.9	1.3

#### 1.1.1.13. Comparison between prediction models

Fitting results from selected prediction models are shown in Table 27 and Figure 49. A good fitting result cannot be obtained from these models

Table 27 Results from model fitting analyses for the 2nd stratum of site no. 6

Fitting models		Fitting parameters		$R^2$	Remark
		$k$	$n$		
Prediction models					
1	Attewell and Farmer (1973); $v = k \cdot (w^{0.5} / r)$	7		-1.10	
2	Wiss (1981); $v = k \cdot (r / w^{0.5})^n$	3	2.0	-3.33	
3	Svinkin (2008); $v = 0.00037 \cdot (w/r) \cdot (c/Z \cdot L)^{0.5}$	130			$r = 1$

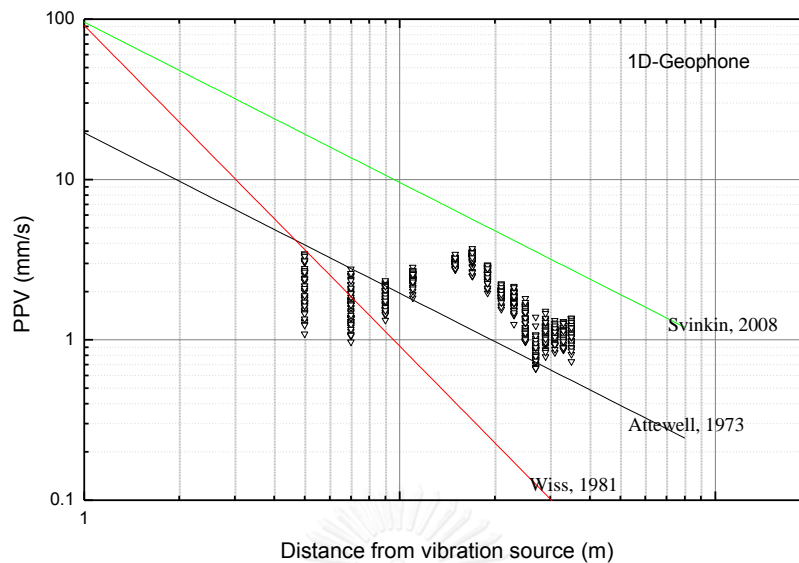


Figure 49 the prediction models fitting for the measured data of 18-19 m depth in the 2<sup>nd</sup> stratum of site no. 6

### 1.1.2. Ground vibrations when piles were penetrating through the 3<sup>rd</sup> soil strata

The measured data that caused by pile driving at this stratum were collected from clayey ground, site no. 1, 4, 5, 6, 7 and 8. Further studies were accorded to measured data of the 3<sup>rd</sup> soil stratum in site no 7 on clayey ground.

#### 1.1.2.1. Vibration in each direction

The maximum values were picked up from the recorded signals and plotted against the separation distance in to Figure 50. For other sites, the peak particle velocities and frequencies are shown in the Appendix C. In this study, the maximum value of vibrations in each direction as well as the maximum value of the vibration vectors was considered.

According to Figure 50 , the ground vibrations from 3D geophone decrease gradually with distance and it can be seen that the values of vertical component were almost closely to the values from true velocity vectors as higher than other two components at near the vibration source. The horizontal component, radial and transverse, were almost equally to the values from true velocity vectors at long distance but hardly distinguished. Therefore, it can be concluded that the vibrations were dominated by the vertical component. Based on this evidence, further analyses for these ground types were based on the data from 4.5 Hz vertical geophones for the interest of more data points. From measured data of six sites show that, the ground

vibration over distance were seem to be similar to pattern 1 and 2 of 2<sup>nd</sup> strata. For next study, the recorded data of site no. 7 were chosen for discussion.

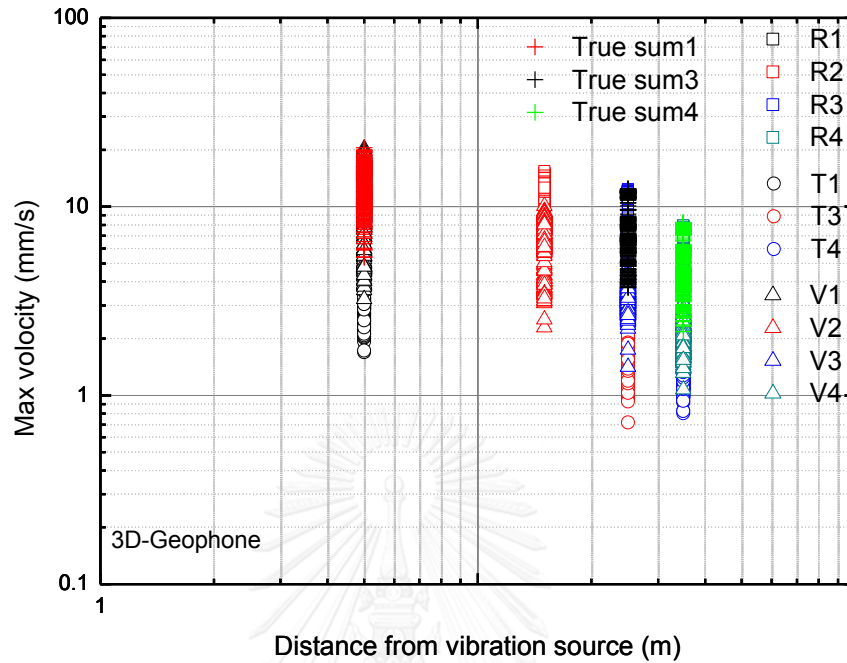


Figure 50 Vibration of each direction of site no. 7

According to Figure 50, the recorded signals of 4.5 Hz geophone were plotted over distance. The results show the pattern of vibration similar with the 2<sup>nd</sup> pattern of stratum 2, two peaks over distance.

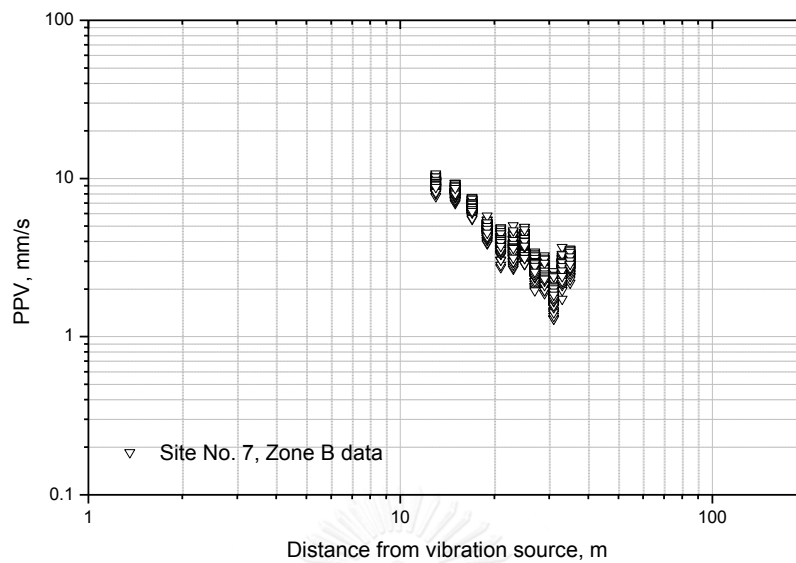


Figure 51 Two peak of vibration over distance

#### 1.1.2.2. Attenuation characteristic

Studies were carried out by using data from the 24.0-25.0 m of pile penetrated depth in site no.7. Fitting analysis were carried out by using Eq. (20) as shown in Table 28 and Figure 53 which derive the value  $n$  from theoretical basis. The geometric attenuation parameter ( $n$ ) was fixed to 0.5, 1.0, 1.5 and 2.0 as shown in Table 50. The results show that, the coefficients of determination ( $R^2$ ) by using Eq. (20) were greater than 0.49.

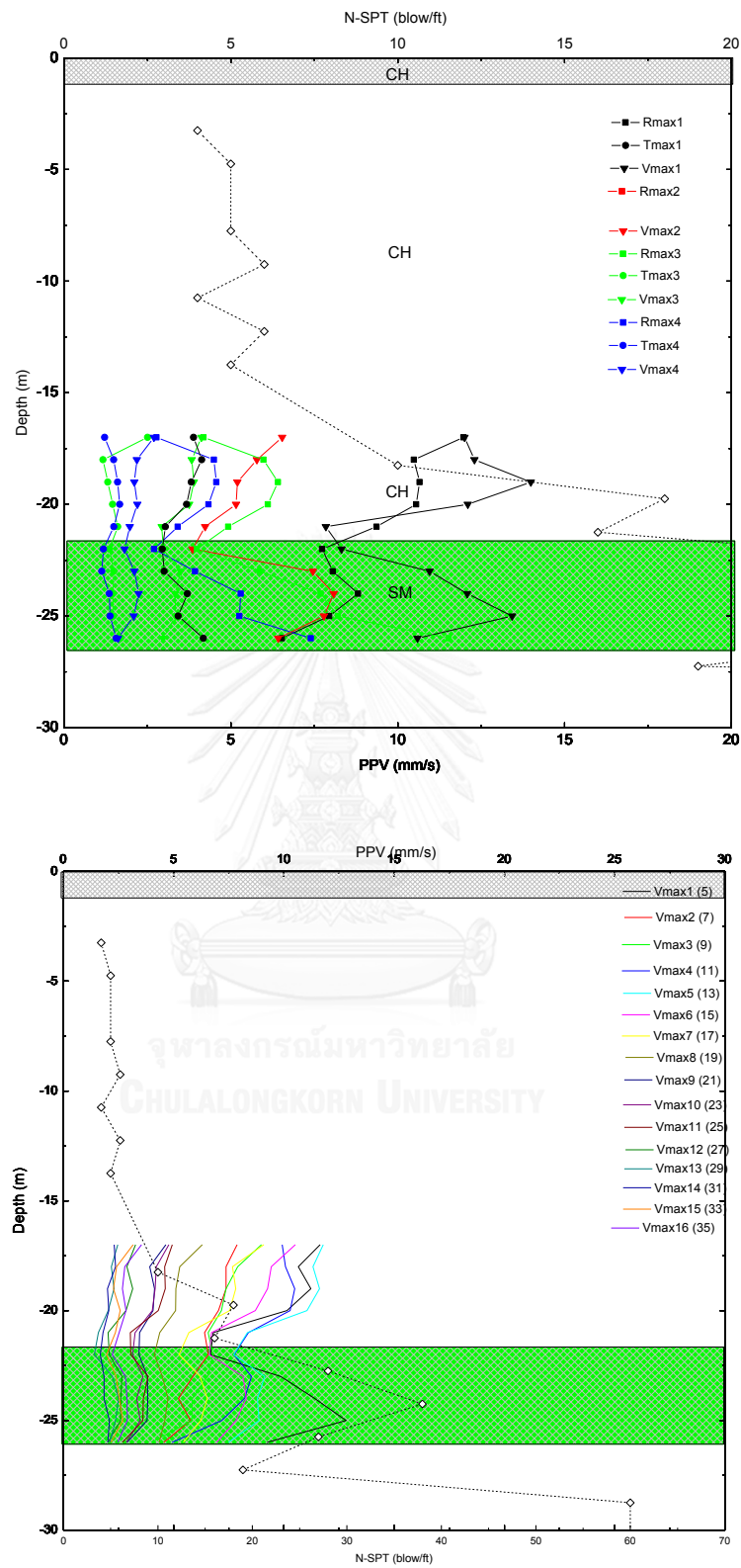


Figure 52 the peak particle velocities versus horizontal distance at different pile penetrated depths.

Table 28 Results from model fitting analyses for the measured data of the 24.0-25.0 m pile penetrated depth in site no. 7

Site No.	Depth (m)	Fitting models		Fitting parameters		$R^2$	Remarks
				$k$	$n$		
		Conventional models					
7	24.0-25.0 ( $N_{SPT} = 35$ )	1	$v = k \cdot r^{-n}$	493	1.5	0.924	
		2	$v = k \cdot r^{-0.5}$	22		0.490	
		3	$v = k \cdot r^{-1.0}$	101		0.810	
		4	$v = k \cdot r^{-1.5}$	434		0.923	
		5	$v = k \cdot r^{-2.0}$	1761		0.859	

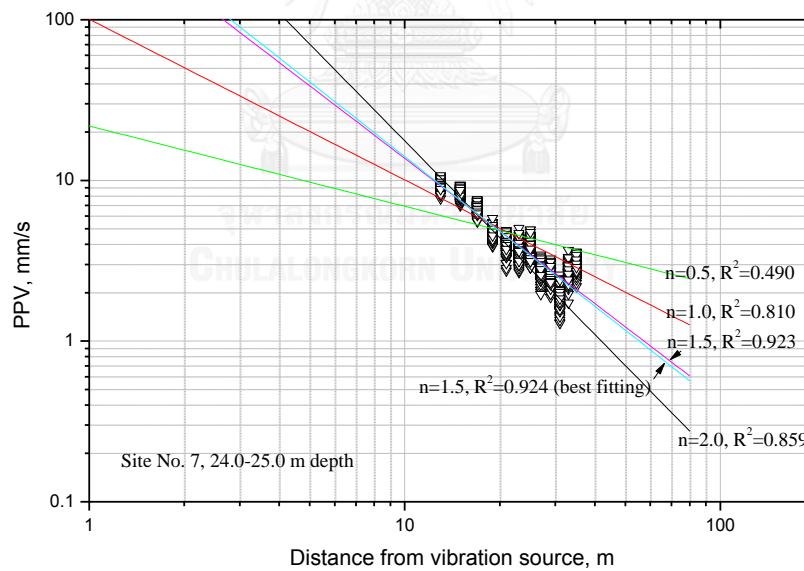


Figure 53 the peak particle velocities versus horizontal distance with log –log scale at 24-25.0 m of pile penetrated depth.

### 1.1.2.3. Attenuation in each sites

Fitting analyses were carried out for determining the attenuation of PPV over distance in 3<sup>rd</sup> stratum in site no. 1, 4, 5, 6, 7 and 8 and shown in Table 29 and Table 30. According to Figure 43 and Figure 44, the highest  $R^2$  for site no. 7 and no. 8 were obtained from the 4<sup>th</sup> model, the majority of waves were likely be the point load impulsive body waves with  $n = 1.5$  (cf. PQ/I/R lines in Figure 7). While, as the highest  $R^2$  for Site No 1 and 4 and 5 were obtained from the 3<sup>rd</sup> model, the majority of waves were likely to be body waves with  $n = 1$ . Based on the data shown in Figure 54, the dominant frequency and distance seemed to be independent of each other.

Table 29 Results from model fitting analyses of site no. 1, 4 and 5

Site No.	Depth (m)	Fitting models		Fitting parameters		$R^2$	Remarks
				$k$	$n$		
		Conventional models					
1	24.5-25.0 ( $N_{SPT}=36$ )	1	$v = k \cdot r^{-n}$	84	0.8	0.887	
		2	$v = k \cdot r^{-0.5}$	43		0.764	
		3	$v = k \cdot r^{-1.0}$	138		0.815	
		4	$v = k \cdot r^{-1.5}$	354		0.330	
		5	$v = k \cdot r^{-2.0}$	819		-0.236	
4	24.0-24.3 ( $N_{SPT}=48$ )	1	$v = k \cdot r^{-n}$	10	0.7	0.650	
		2	$v = k \cdot r^{-0.5}$	4		0.553	
		3	$v = k \cdot r^{-1.0}$	17		0.618	
		4	$v = k \cdot r^{-1.5}$	55		0.274	
		5	$v = k \cdot r^{-2.0}$	168		-0.223	
5	23.0 ( $N_{SPT}=34$ )	1	$v = k \cdot r^{-n}$	46	0.8	0.804	
		2	$v = k \cdot r^{-0.5}$	15		0.675	
		3	$v = k \cdot r^{-1.0}$	76		0.781	
		4	$v = k \cdot r^{-1.5}$	361		0.406	
		5	$v = k \cdot r^{-2.0}$	1619		-0.230	

Table 30 Results from model fitting analyses of site no. 6 and 8

Site No.	Depth (m)	Fitting models		Fitting parameters		$R^2$	Remarks
				$k$	$n$		
		Conventional models					
6	20.0-23.0 ( $N_{SPT}=46$ )	1	$v = k \cdot r^{-n}$	305	1.7	0.810	
		2	$v = k \cdot r^{-0.5}$	8		0.403	
		3	$v = k \cdot r^{-1.0}$	38		0.677	
		4	$v = k \cdot r^{-1.5}$	173		0.801	
		5	$v = k \cdot r^{-2.0}$	753		0.788	
8	20.5-22.0 ( $N_{SPT}=40$ )	1	$v = k \cdot r^{-n}$	210	1.5	0.923	
		2	$v = k \cdot r^{-0.5}$	13		0.527	
		3	$v = k \cdot r^{-1.0}$	54		0.830	
		4	$v = k \cdot r^{-1.5}$	209		0.924	
		5	$v = k \cdot r^{-2.0}$	780		0.848	

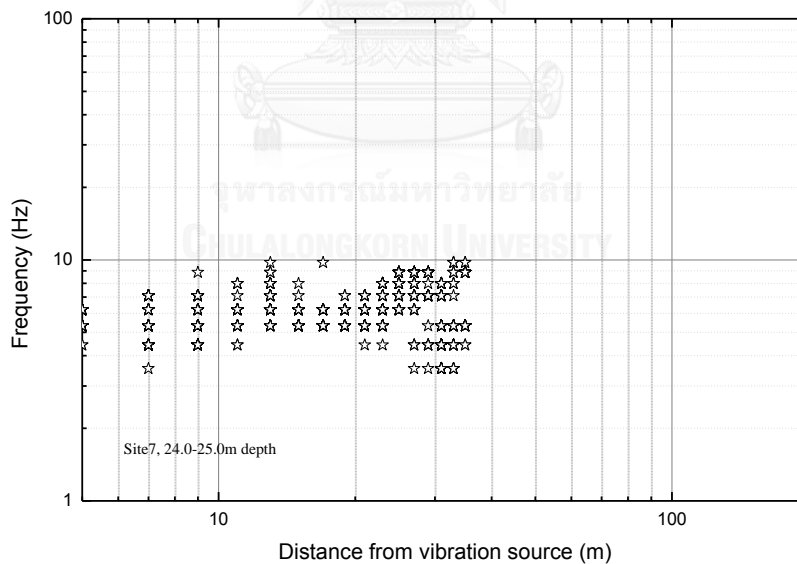


Figure 54 Variation of dominant frequency with distance in each sites



Table 31 Statistics of dominant frequency in each sites

Sites	Sample size	Mean, $\mu$ (Hz)	S.D., $\sigma$ (Hz)	$\mu - 2\sigma$ (Hz)
No. 1 (24.5-25.0 m)	1328	12	3	6
No. 4 (24.0-24.3 m)	112	4	1	2
No.5 (23.0 m)	42	5	1	3
No. 6 (20.0-23.0 m)	1308	6	3	<1
No. 7 (24.0-25.0 m)	1776	6	2	2
No. 8 (19.0-20.5 m)	570	7	1	5

Table 32 The beginning of B-zone from ground vibration source in each sites

Site	Depth (m)		$N_{SPT}$	The beginning of B zone form source of ground vibration (m)	Distance of B Zone/Depth		Remark
	From	To			From	To	
6	20.0	23.0	46	15	0.75	0.65	
7	24.0	25.0	35	13	0.54	0.52	
8	19.0	20.5	40	11.6	0.61	0.57	

#### 1.1.2.4. Comparison between prediction models

The data and fitting results are shown in Table 46 and Figure 68. From the fitting models in Table 46, the coefficients of determinations ( $R^2$ ) are less than 0.6. The model 1<sup>st</sup> shows the highest  $R^2$  of 0.546.

Table 33 Results from model fitting analyses for the measured data of the 25.0 m pile penetrated depth in site no. 7

Fitting models		Fitting parameters		$R^2$	Remark
		$k$	$n$		
Prediction models					
1	Attewell and Farmer (1973); $v = k \cdot (w^{0.5} / r)$	25		0.546	
2	Wiss (1981); $v = k \cdot (r / w^{0.5})^n$	7	1.5	0.01	
3	Svinkin (2008); $v = 0.00037 \cdot (w / r) \cdot (c / Z \cdot L)^{0.5}$	130			$r = 1$

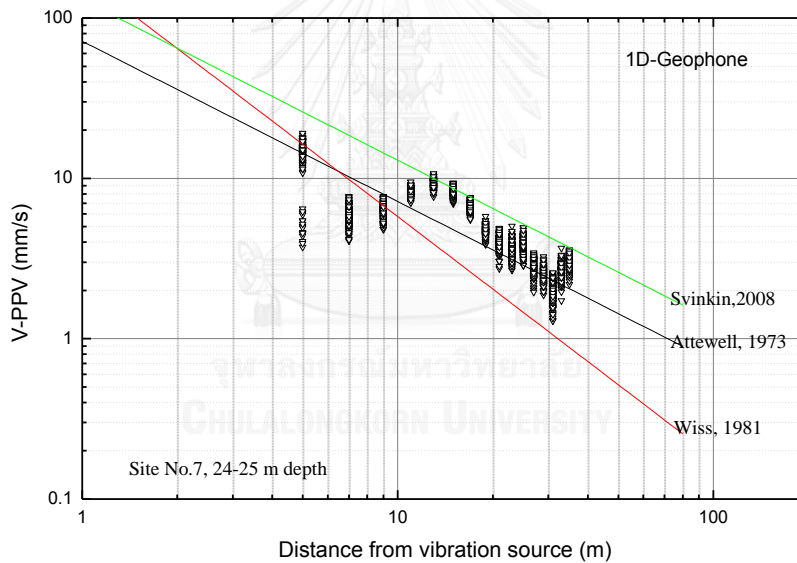


Figure 55 the prediction models fitting for the measured data of the 25.0 m pile penetrated depth in site no. 7

## 1.2. Sandy ground

Field measurements from site no. 2 and 3 were used in this study. The driving of piles on these sites stopped in the 2<sup>nd</sup> strata. Therefore, only vibrations when pile tips were in the 1<sup>st</sup> and 2<sup>nd</sup> layers will be discussed here.

### *1.2.1. Ground vibrations when piles were penetrating through the 1<sup>st</sup> strata*

In the following sections, the measurements from site no. 2-1, 2 and site no. 3-3 were chosen for discussion. The complete data from all sites are shown in Appendix C.

#### 1.2.1.1. Ground vibrations due to pile driving in each direction

The PPV in each direction and the PPV of velocity vectors of all measurements were plotted against distance in Figure 56. When close to the piles, the PPVs in vertical direction were almost equal to the values from velocity vectors and higher than the other components. However, the vertical vibrations decreased at a faster rate than the horizontal components when moving away from the piles. At the farthest measuring points, the vibrations in three directions were in the same range. Since the vibrations were almost governed by the vertical components, further analyses were based on the data from 4.5Hz vertical geophones.

#### 1.2.1.2. Attenuation of vibration due to pile driving in sandy ground

Two attenuation patterns were observed in this study.

For the first attenuation pattern, the PPV decreases monotonically with the distance as shown in and. This attenuation pattern was observed in site no. 2.

For the second attenuation pattern, the PPV decreases in the same way as the 1st pattern. However when the distance increases to a certain point the PPV jumps to a higher value before starts decreasing again. This attenuation pattern was observed in site no. 2 and no. 3, when pile penetrated through 2<sup>nd</sup> strata.

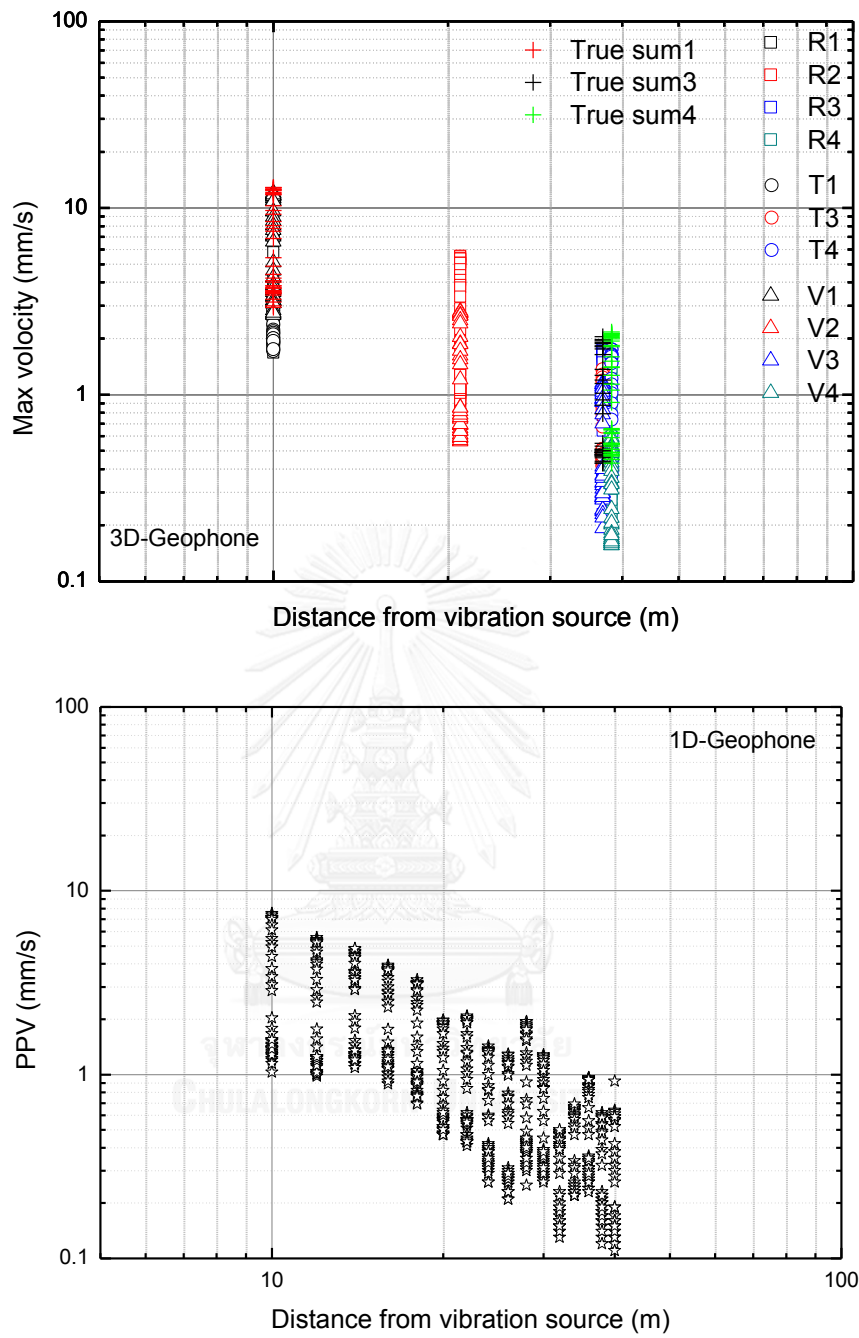
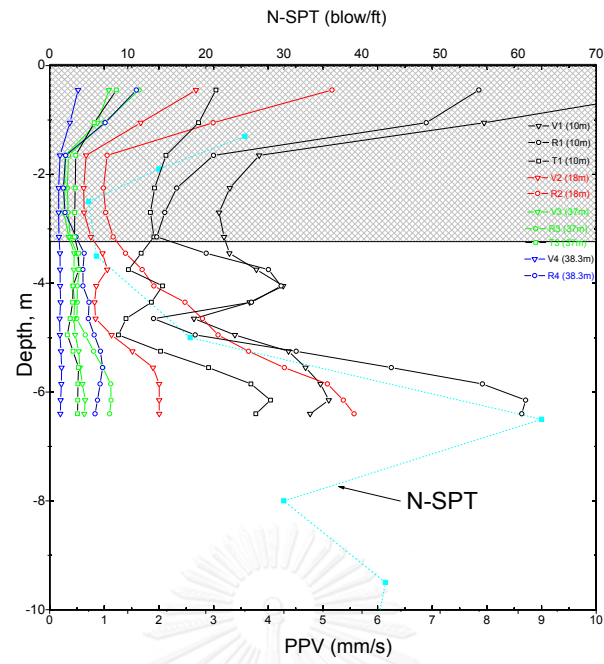
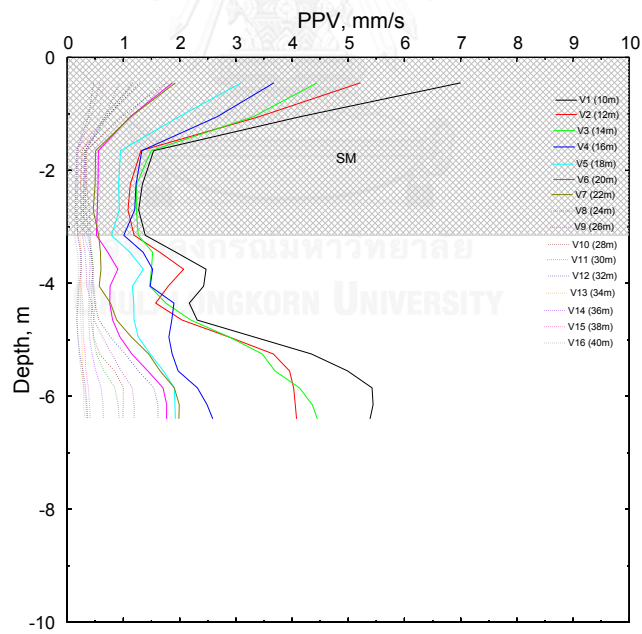


Figure 56 Vibration in each direction



3 D-Geophone



1 D-Geophone

Figure 57 the peak particle velocities versus horizontal distance at different pile penetration depths.

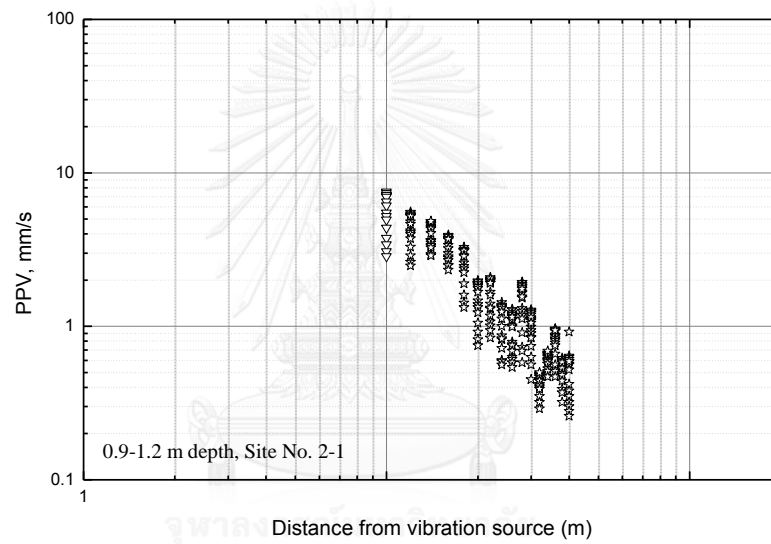
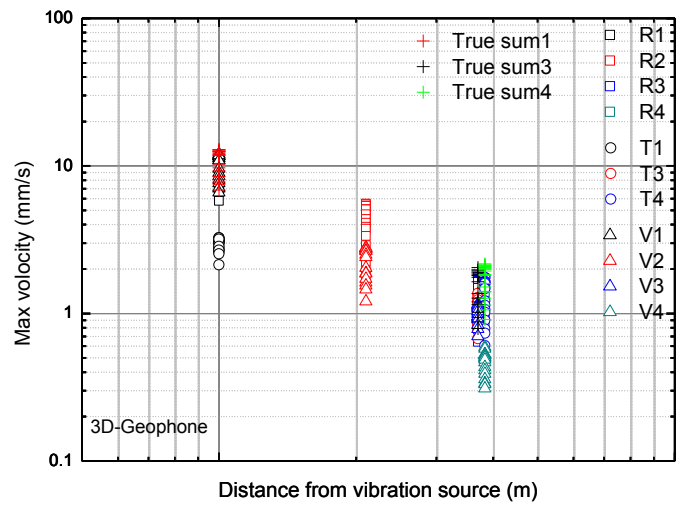


Figure 58 Vibration of each direction of site no. 2-1

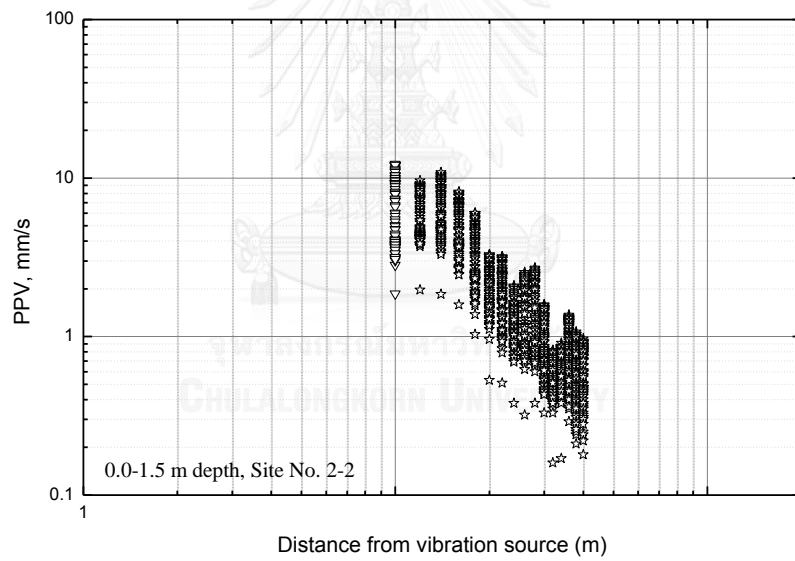
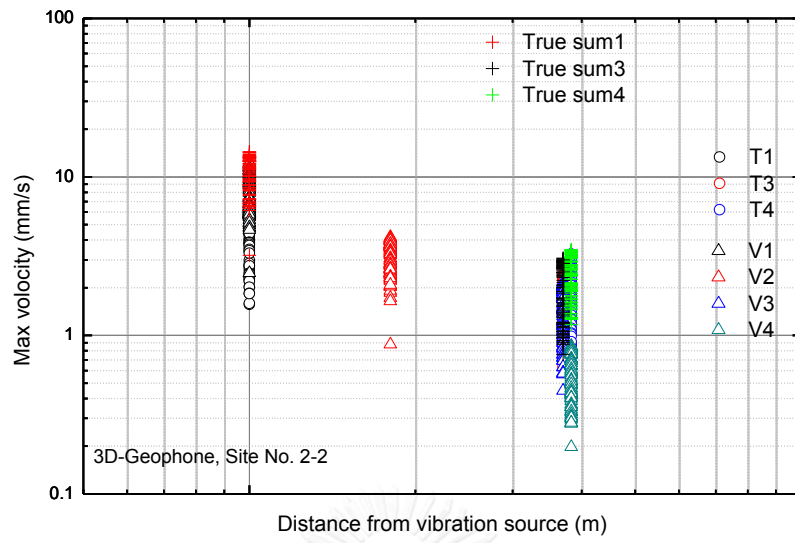


Figure 59 Vibration of each direction of site no. 2-2

### 1.2.1.3. Discussion on the first attenuation pattern observed in site no. 2-1, 2-

2

Results from fitting analyses of site no. 2-1 using Eq. (20) are shown in Table 34. The highest  $R^2$  obtained from the 4<sup>th</sup> model implies that the vibrations were governed by body waves (cf. PQ/I/R lines in Figure 7). Based on the data shown in Figure 67, the dominant frequency and distance seemed to be independent of each other. The average value and the standard deviation of dominant frequency of this site were 19 and 7 Hz, respectively.

Results from fitting analyses of site no. 2-2 using Eq. (20) are shown in Table 34. The highest  $R^2$  obtained from the 5<sup>nd</sup> model implies that the vibrations were governed by body waves traveling along the free surface with  $n = 2$  (Ghosh and Daemen, 1983). It seemed to be that the incline of pile occurred while driving as shown in Figure 61 and Figure 64 .

Based on the data shown in Figure 67, the dominant frequency and distance seemed to be independent of each other. The average value and the standard deviation of dominant frequency of this site were 19 and 4 Hz, respectively.

### 1.2.1.4. Comparison between prediction models

Fitting results from selected prediction models are shown in Table 36 and Figure 64. Acceptable coefficients of determination ( $R^2$ ) can be obtained from the first three models. It is noted that the negative  $R^2$  in the 5<sup>th</sup> model can occur when performing non-linear curve fitting. In cases where negative values arise, the mean of the data provides a better fit than do the fitted function values.



Table 34 Results from fitting analyses

Site No.	Depth (m)	Fitting models		Fitting parameters		$R^2$	Remarks
				$k$	$n$		
		Conventional models					
2-1	0.9-1.2 ( $N_{SPT} = 25$ )	1	$v = k \cdot r^{-n}$	253	1.6	0.839	
		2	$v = k \cdot r^{-0.5}$	11		0.424	
		3	$v = k \cdot r^{-1.0}$	47		0.719	
		4	$v = k \cdot r^{-1.5}$	184		0.835	
		5	$v = k \cdot r^{-2.0}$	660		0.807	
2-2	0.0-1.5 ( $N_{SPT} = 25$ )	1	$v = k \cdot r^{-n}$	6626	2.6	0.809	
		2	$v = k \cdot r^{-0.5}$	12		0.273	
		3	$v = k \cdot r^{-1.0}$	62		0.512	
		4	$v = k \cdot r^{-1.5}$	291		0.682	
		5	$v = k \cdot r^{-2.0}$	1272		0.777	
3-3	0-2.4 ( $N_{SPT} = 15$ )	1	$v = k \cdot r^{-n}$	105	1.0	0.747	
		2	$v = k \cdot r^{-0.5}$	24		0.557	
		3	$v = k \cdot r^{-1.0}$	109		0.748	
		4	$v = k \cdot r^{-1.5}$	448		0.572	
		5	$v = k \cdot r^{-2.0}$	1712		0.172	

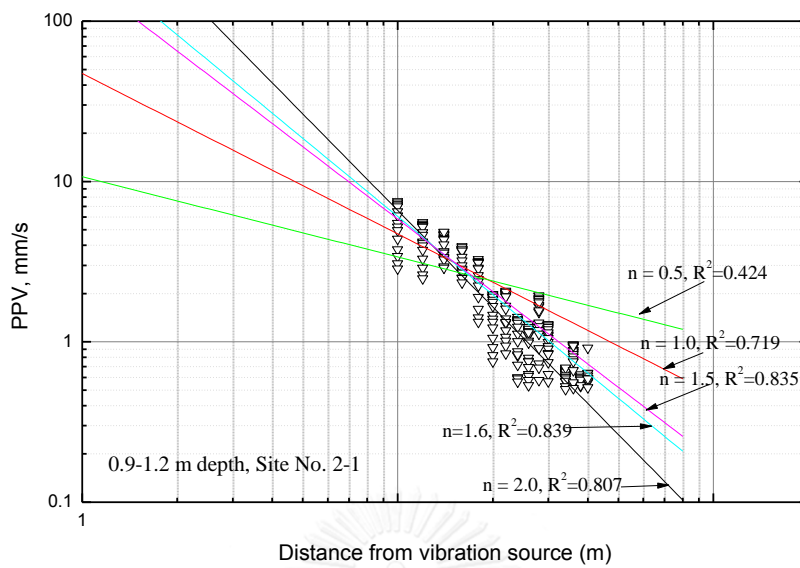


Figure 60 the peak particle velocities versus horizontal distance with log –log scale of 0.9-1.2 m penetration depth of site no. 2-1.

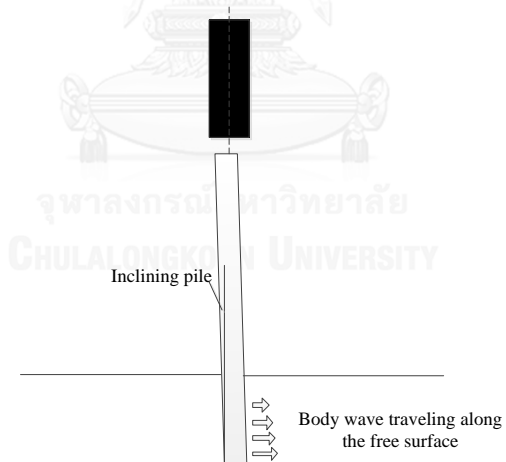


Figure 61 inclining of pile while driving due to body wave traveling along the free surface



Figure 62 the effect of pile driving in site no. 2-2.

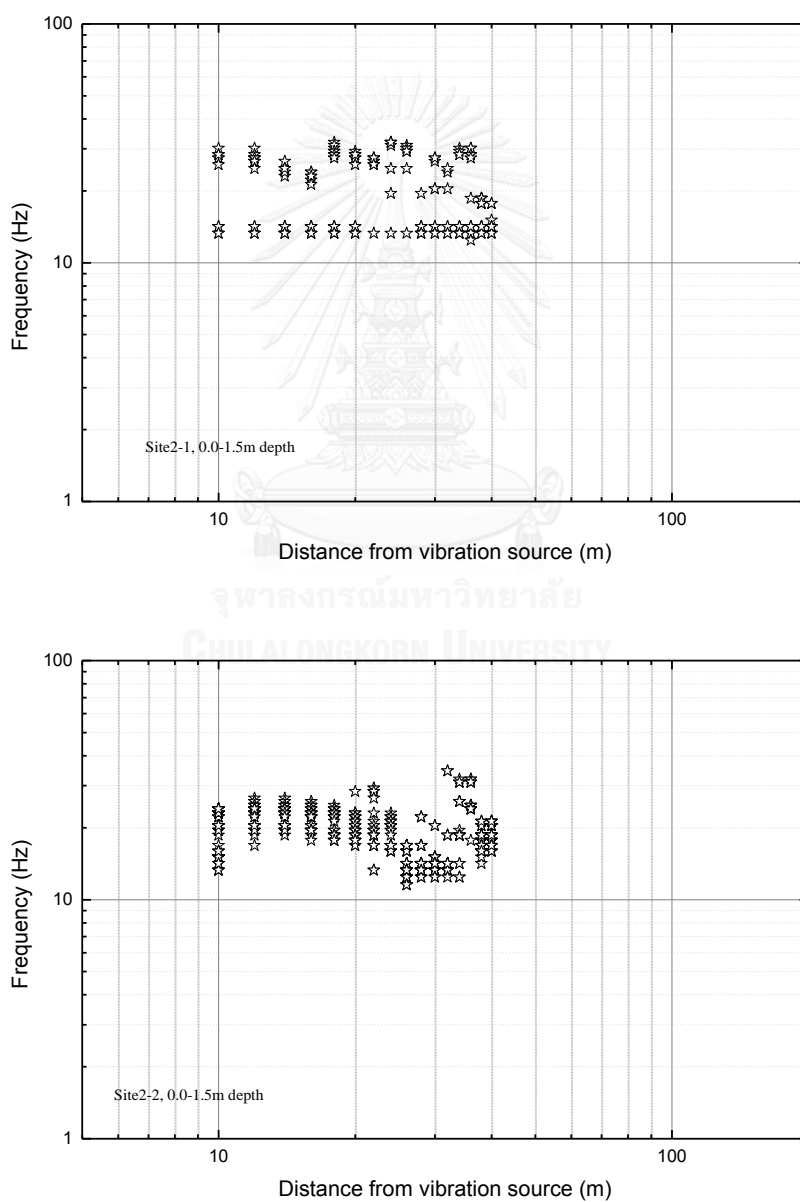


Figure 63 Variation of dominant frequency with distance in each ground type

Table 35 Statistics of dominant frequency in each ground type

Sites	Sample size	Mean, $\mu$ (Hz)	S.D., $\sigma$ (Hz)	$\mu - 2\sigma$ (Hz)
No. 2-1 (0.0-1.5 m)	1162	19	7	5
No.2-2 (0.0-1.5 m)	1162	19	4	11
No. 3-3 (0.0-2.4 m)	368	6	1	4

Table 36 Results from model fitting analyses for top soil of sandy ground

Fitting models		Fitting parameters		$R^2$	Remarks
		$k$	$n$		
Prediction models					
1	Attewell and Farmer (1973); $v = k \cdot (w^{0.5} / r)$	51		0.747	
2	Wiss (1981); $v = k \cdot (r / w^{0.5})^n$	24	0.5	0.747	
3	Svinkin (2008), $v = 0.00037 \cdot (w / r) \cdot (c / Z \cdot L)^{0.5}$	77			$r = 1$

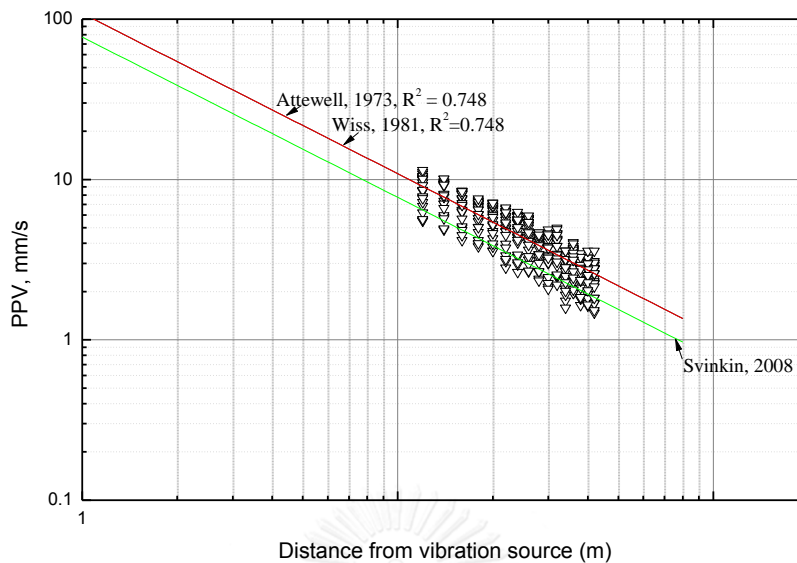


Figure 64 the prediction models fitting for top soil of sandy ground

#### 1.2.1.5. Ground vibrations when piles were penetrating through the 2<sup>nd</sup> strata of sandy ground

In the following sections, the measurements from site no. 2 and site no. 3 were chosen for discussion. The complete data from all sites are shown in Appendix C.

#### 1.2.1.6. Ground vibrations due to pile driving in each direction

The PPV in each direction and the PPV of velocity vectors of all measurements were plotted against distance in Figure 69 and Figure 70. When close to the piles, the PPVs in vertical direction were almost equal to the values from velocity vectors and higher than the other components. However, the vertical vibrations decreased at a faster rate than the horizontal components when moving away from the piles. At the farthest measuring points, the vibrations in three directions were in the same range. Since the vibrations were almost governed by the vertical components, further analyses were based on the data from 4.5Hz vertical geophones.

#### 1.2.1.7. Attenuation of vibration due to pile driving in sandy ground

Two attenuation patterns were observed in this study.

For the first attenuation pattern, the PPV decreases monotonically with the distance as shown in and. This attenuation pattern was observed in site no. 3.

For the second attenuation pattern, the PPV decreases in the same way as the 1st pattern. However when the distance increases to a certain point the PPV jumps to

a higher value before starts decreasing again. This attenuation pattern was observed in site no. 2.

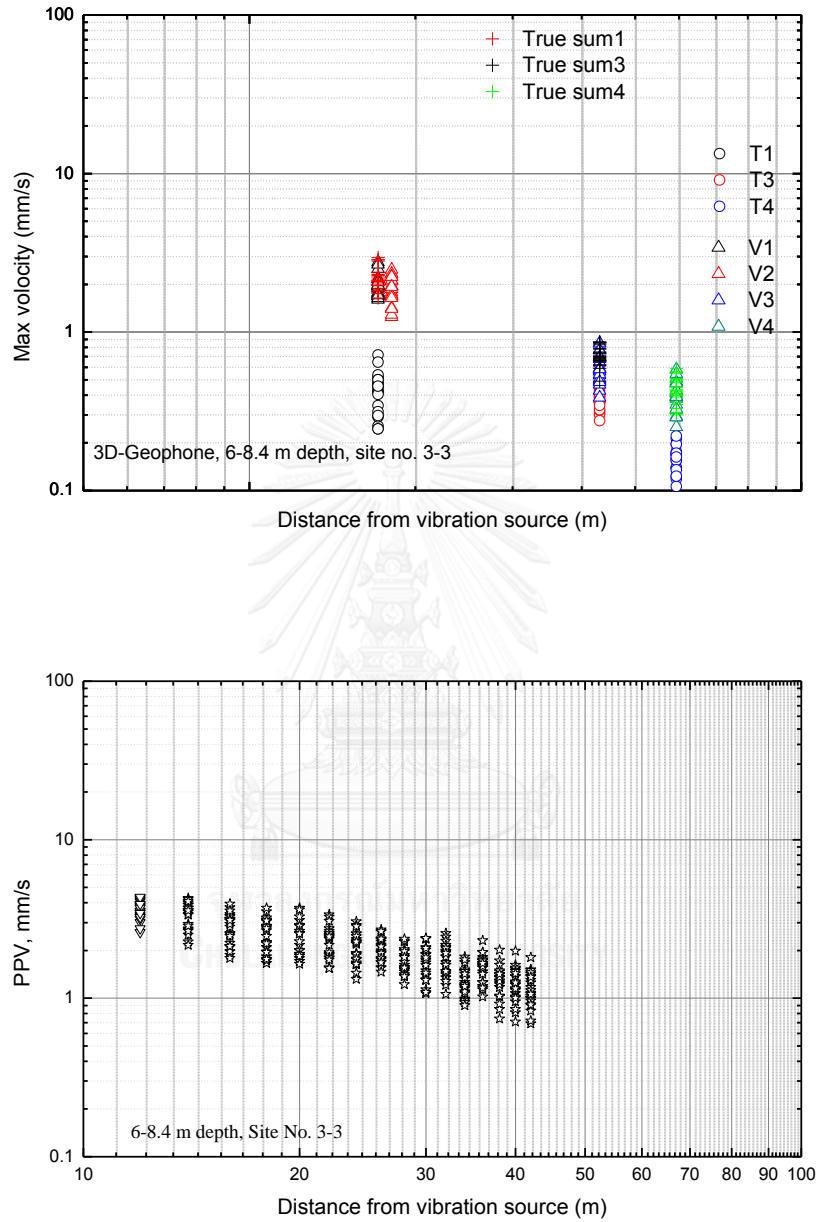


Figure 65 Vibration in each direction

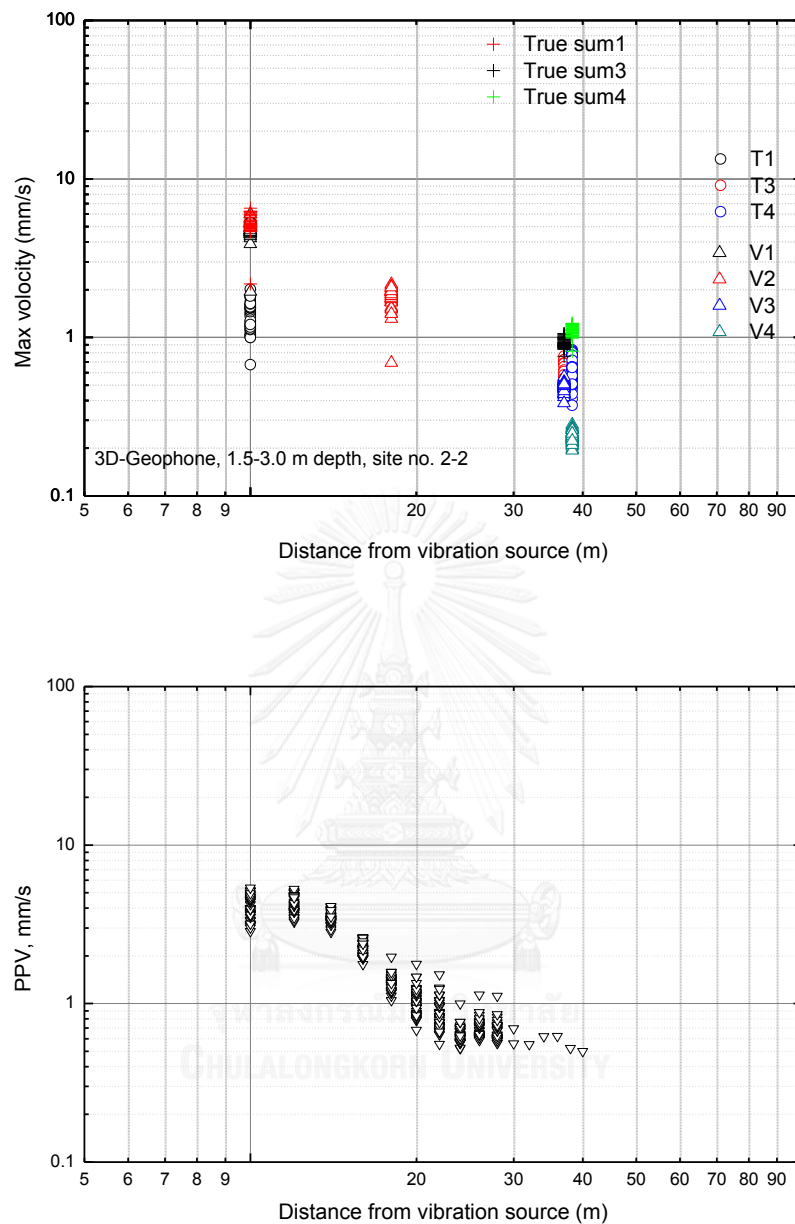


Figure 66 Vibration in each direction

#### 1.2.1.8. Discussion on the first attenuation pattern observed in site no. 3

Results from fitting analyses of site no. 3-3 using Eq. (20) are shown in Table 37. The highest  $R^2$  obtained from the 3<sup>rd</sup> model implies that the vibrations were governed by body waves (cf. PQ/HS/R, PQ/I/O and LQ/I/R lines in Figure 7). Based on the data shown in Table 38 and Figure 67, the dominant frequency and distance seemed to be independent of each other. The average value and the standard deviation of dominant frequency of this site were 6 and 1 Hz, respectively.

## 1.2.1.9. Comparison with other prediction models

Fitting results from selected prediction models are shown in Table 39 and Figure 68. The coefficients of determinations ( $R^2$ ) of models in the literatures were less than 0.65 while the best  $R^2$  of 0.639 was obtained from the 1<sup>st</sup> model.

Table 37 Results from fitting analyses for the 2<sup>nd</sup> strata

Site No.	Depth (m)	Fitting models		Fitting parameters		$R^2$	Remark
				$k$	$n$		
		Conventional models					
3-1	10.6-14.5 ( $N_{SPT} = 19$ )	1	$v = k \cdot r^{-n}$	14	0.7	0.449	
		2	$v = k \cdot r^{-0.5}$	7		0.411	
		3	$v = k \cdot r^{-1.0}$	36		0.367	
		4	$v = k \cdot r^{-1.5}$	168		-0.083	
		5	$v = k \cdot r^{-2.0}$	749		-0.784	
3-2	9.5-15.0 ( $N_{SPT} = 33$ )	1	$v = k \cdot r^{-n}$	29	0.9	0.587	
		2	$v = k \cdot r^{-0.5}$	9		0.472	
		3	$v = k \cdot r^{-1.0}$	41		0.585	
		4	$v = k \cdot r^{-1.5}$	173		0.339	
		5	$v = k \cdot r^{-2.0}$	678		-0.102	
3-3	6.0-8.4 ( $N_{SPT} = 35$ )	1	$v = k \cdot r^{-n}$	30	0.8	0.691	
		2	$v = k \cdot r^{-0.5}$	10		0.572	
		3	$v = k \cdot r^{-1.0}$	47		0.668	
		4	$v = k \cdot r^{-1.5}$	192		0.323	
		5	$v = k \cdot r^{-2.0}$	728		-0.262	



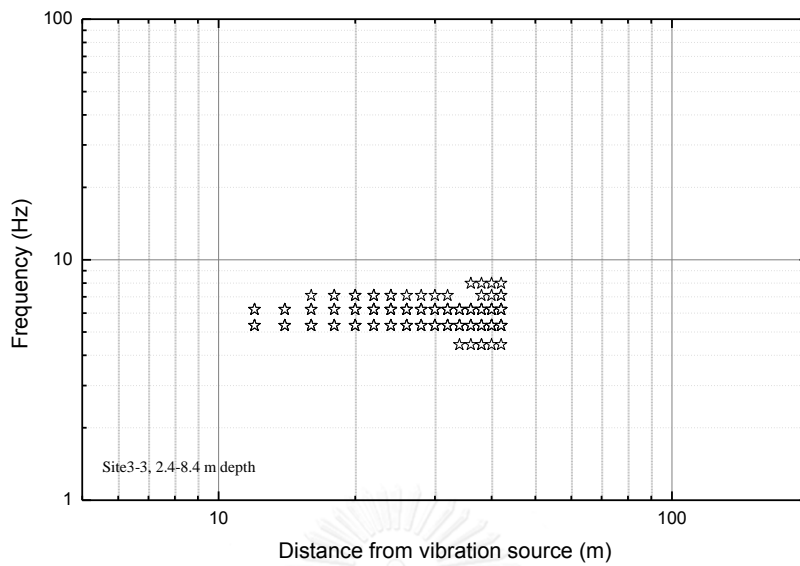


Figure 67 Variation of dominant frequency with distance in each ground type

Table 38 Statistics of dominant frequency in each ground type

Sites	Sample size	Mean, $\mu$ (Hz)	S.D., $\sigma$ (Hz)	$\mu - 2\sigma$ (Hz)
No. 3-1 (10.6-14.5 m)	2272	6	1	4
No. 3-2 (9.5-15.0 m)	2928	6	1	4
No. 3-3 (2.4-8.4 m)	496	6	1	4

Table 39 Results from model fitting analyses for the measured data of the 2.4-8.4 m pile penetrated depth in site no. 3-3

Fitting models		Fitting parameters		$R^2$	Remark
		$k$	$n$		
Prediction models					
1	Attewell and Farmer (1973); $v = k \cdot (w^{0.5} / r)$	24		0.639	
2	Wiss (1981); $v = k \cdot (r / w^{0.5})^n$	11	1.0	0.639	
3	Svinkin (2008), $v = 0.00037 \cdot (w/r) \cdot (c/Z \cdot L)^{0.5}$	77			$r = 1$

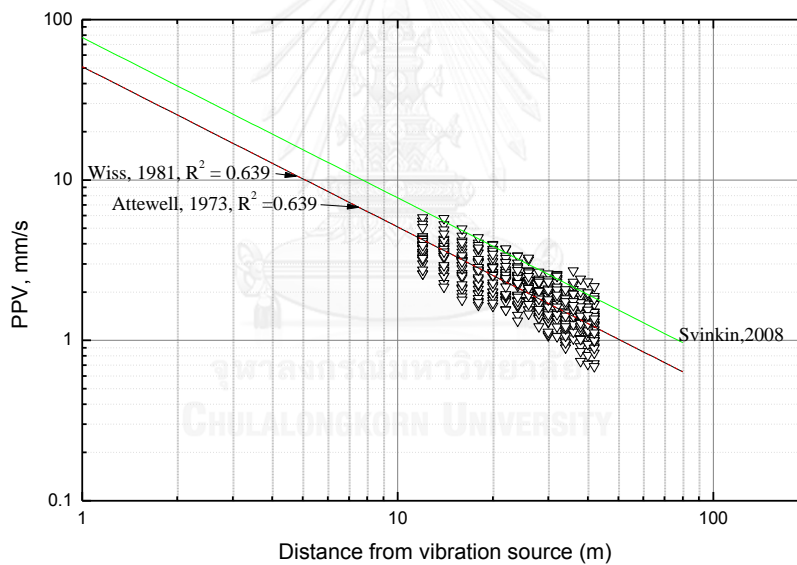


Figure 68 the prediction models fitting for the 2<sup>nd</sup> stratum of site No. 3-3

#### 1.2.1.10. Discussion on the second attenuation pattern observed in site no. 2-1

For the second attenuation pattern, the PPV decreases in the same way as the 1st pattern. However when the distance increases to a certain point the PPV jumps to a higher value before starts decreasing again as shown in Figure 66.

## 1.2.1.11. Attenuation characteristic

Fitting analyses using Eq. (20) are shown in Table 40 and Figure 69. The highest  $R^2$  obtained from the 5<sup>th</sup> model imply that the vibrations were governed by body wave traveling along the free surface with  $n = 2$ .

## 1.2.1.12. Variation of dominant frequency and the beginning of B-zone

Based on the data shown in Table 41, the dominant frequency and distance seemed to be independent of each other. The average value and the standard deviation of dominant frequency of this site were 25 and 6 Hz, respectively. The beginning of B-zone from ground vibration source in each site were shown in Table 42

Table 40 Results from model fitting analyses

Site No.	Depth (m)	Fitting models		Fitting parameters		$R^2$	Remarks
				$k$	$n$		
		Conventional models					
2-1	2.4-3.9 ( $N_{SPT}=6$ )	1	$v = k \cdot r^{-n}$	1252	2.5	0.688	
		2	$v = k \cdot r^{-0.5}$	4		0.260	
		3	$v = k \cdot r^{-1.0}$	18		0.457	
		4	$v = k \cdot r^{-1.5}$	76		0.592	
		5	$v = k \cdot r^{-2.0}$	322		0.668	
2-2	1.8-3.0 ( $N_{SPT}=10$ )	1	$v = k \cdot r^{-n}$	2437	2.5	0.934	
		2	$v = k \cdot r^{-0.5}$	8		0.321	
		3	$v = k \cdot r^{-1.0}$	35		0.594	
		4	$v = k \cdot r^{-1.5}$	145		0.789	
		5	$v = k \cdot r^{-2.0}$	574		0.899	

Table 41 Statistics of dominant frequency in each site

Sites	Sample size	Mean, $\mu$ (Hz)	S.D., $\sigma$ (Hz)	$\mu - 2\sigma$ (Hz)
No. 2-1 (2.1-3.9 m)	153	25	6	13
No. 2-2 (1.5-3 m)	401	17	5	7

Table 42 The beginning of B-zone from ground vibration source in each site

Site	Depth (m)		$N_{SPT}$	The beginning of B zone form source of ground vibration (m)	Distance of B Zone/Depth		Remark
	From m	To			From	To	
2-1	2.4	3.9	6	16	6.7	4.1	
2-2	1.8	3.0	10	16	8.9	5.3	

#### 1.2.1.13. Comparison with other prediction models

Fitting results from selected prediction models are shown in Table 43 and Figure 69. The coefficients of determinations ( $R^2$ ) of models in the literatures were less than 0.67 while the best  $R^2$  of 0.667 was obtained from the 2<sup>nd</sup> model.

Table 43 Results from model fitting analyses for the measured data of the 2.4-3.9 m pile penetrated depth in site no. 2-1

Fitting models		Fitting parameters		$R^2$	Remark
		$k$	$n$		
Prediction models					
1	Attewell and Farmer (1973); $v = k \cdot (w^{0.5} / r)$	7		0.457	
2	Wiss (1981) ; $v = k \cdot (r / w^{0.5})^n$	2	1.5	0.667	

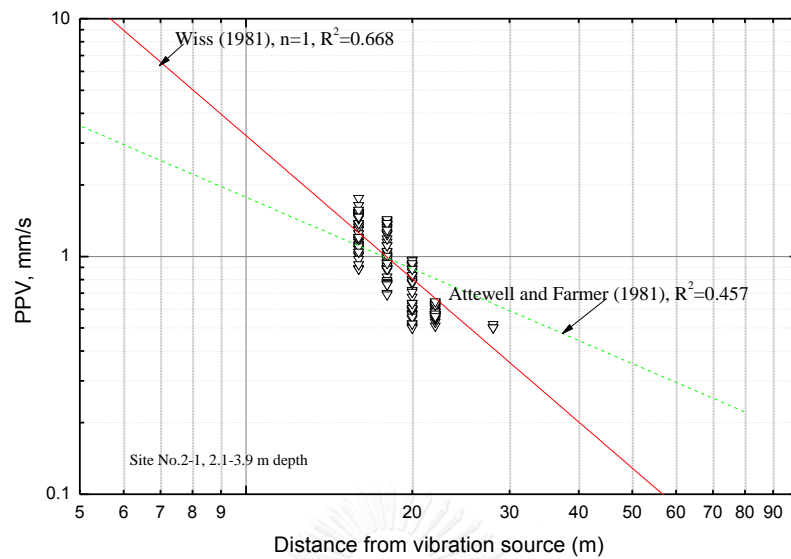


Figure 69 the prediction models fitting for the measured data from the 2.4-3.9 m pile penetrated depth in site no. 2-1

### 1.3. The influence of input energy and parameter $n$

The influence of input energy on vibration level was studied from the measurements in clay ground of site no. 5 where the drop height varied between 0.3, 0.5, 0.7 m. Based on the Eq. (19), when the parameter  $n$  was fixed to either of 1.0, 1.5 the values of  $k$  properly vary with the drop height and the parameter  $n$  as shown in Figure 70

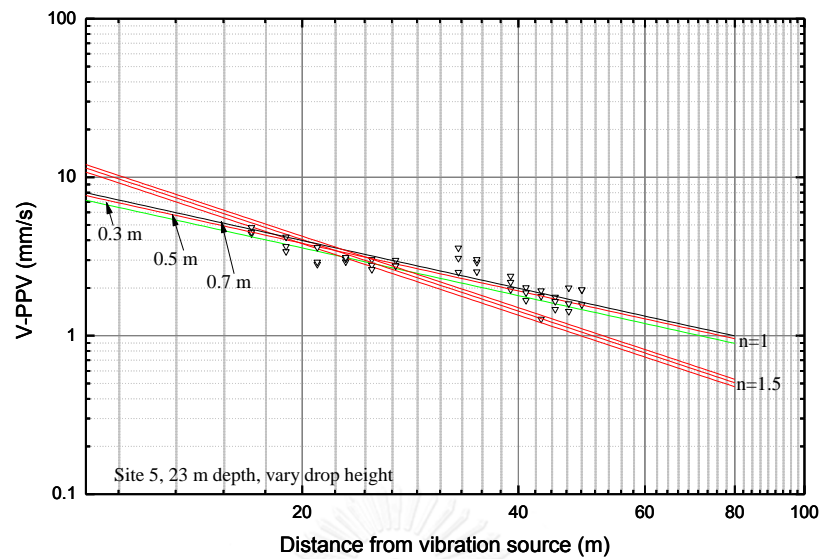


Figure 70 The influence of input energy and parameter n

#### 1.4. The influence of body wave

In generally, ground vibration gradually decrease over distance but the measured data from site no. 1 and 6 show that the decreasing of ground vibration seem to be divided in three zone as shown in Figure 30. From the recorded data show that, particle velocities in horizontal direction were greater than vertical direction. In this studies, the evident was clearly show that the influence of body wave was started at 0.5-1.0 time of the pile penetrated depth. It was also noticed that the value of  $r_c$ , or the boundary where the attenuation characteristic changed from  $n_1$  to  $n_2$ , in between 1.3-1.9 times of pile penetrated. Therefore, the influence of body wave can be seen in range of 0.6-1.9 time of pile penetrated depth.

#### 1.5. Normalizing by using input energy and $N_{SPT}$

Input energy of pile driving was force of gravity and drop height of hammer as shown in Eq. (22). The results of this study show that ground vibration seemed to be proportional to the stiffness of ground. According to power law and Eq. (18), new prediction model could evaluated as shown in Eq. (24). The results of each site show in Table 44 and Table 45.

$$w = mgh \quad (22)$$

where  $m$  = weight of hammer (kg)

$g$  = gravity of earth, 9.807 (m/s<sup>2</sup>)

$h$  = drop height of hammer (m)

$$k^* = \frac{\hat{k}}{\sqrt{\frac{w}{N-SPT}}} \quad (23)$$

Proposed equation;

$$v = \sqrt{\frac{w}{N-SPT}} \cdot k^* \cdot r^{-n} \quad (24)$$

Table 44 the results of sandy ground

Site No.	Depth (m)	Fitting models	Fitting parameters		$R^2$	Hammer weight, (kg)	$N_{SPT}$	Drop height (m)	$w$	$k^*$
			$k$	$n$						
2-1	0.9-1.2	$v = k \cdot r^{-n}$	253	1.5	0.835	6600	25	0.6	38848	6
	2.4-3.9	$v = k \cdot r^{-n}$	322	2	0.668	6600	6	0.6	38848	4.0
2-2	0.0-1.5	$v = k \cdot r^{-n}$	1272	2	0.777	6600	25	0.6	38848	32
	1.8-3.0	$v = k \cdot r^{-n}$	574	2	0.899	6600	10	0.6	38848	9.2
3-1	10.6-14.5	$v = k \cdot r^{-n}$	7	0.5	0.411	7000	19	0.6	41202	0.2
3-2	9.5-15.0	$v = k \cdot r^{-n}$	41	1	0.585	7000	33	0.6	41202	1.2
3-3	0.0-2.4	$v = k \cdot r^{-n}$	109	1	0.748	7000	15	0.3	20601	3
	6.0-8.4	$v = k \cdot r^{-n}$	47	1	0.668	7000	35	0.6	41202	1.4

Table 45 the results of clayey ground

Site No.	Depth (m)	Fitting models	Fitting parameters		$R^2$	Hammer weight (kg)	$N_{SPT}$	Drop height(m)	$w$	$k^*$
			$k$	$n$						
		Conventional models								
1	16-23	$v = k_1 \cdot r_c^{-n_1}$	189	1	0.913	12000	11	0.5	58860	2.6
		$v = k_2 \cdot r_c^{-n_2}$	30	0.5					58860	0.4
	24.5-25.0	$v = k \cdot r^{-n}$	138	1	0.815	12000	36	0.5	58860	3.4
4	20.0-22.0	$v = k \cdot r^{-n}$	17	1	0.865	4600	23	0.3	13538	0.7
	24.0-24.3	$v = k \cdot r^{-n}$	17	1	0.618	4600	48	0.3	13538	1.0
5	23	$v = k \cdot r^{-n}$	76	1	0.781	8700	34	0.3	25604	2.8
6	17-19	$v = k_1 \cdot r_c^{-n_1}$	884	2	0.9	4500	25	0.6	26487	27.2
		$v = k_2 \cdot r_c^{-n_2}$	6	0.5					26487	0.2
	20.0-23.0	$v = k \cdot r^{-n}$	173	1.5	0.801	4500	46	0.6	26487	7.2
7	17.0-23.0	$v = k \cdot r^{-n}$	428	1.5	0.864	12000	24	0.6	70632	7.9
	24.0-25.0	$v = k \cdot r^{-n}$	434	1.5	0.923	12000	24	0.6	70632	8.0
8	12.0-18.0	$v = k \cdot r^{-n}$	199	1.5	0.73	3500	24	0.3	10301	9.6
	20.5-22.0	$v = k \cdot r^{-n}$	209	1.5	0.923	3500	40	0.3	10301	13.0



### 1.6. Frequency content and comparison with DIN 4150's guideline

DIN-4150 suggests that the effects of a vibration event on structures can be evaluated from its maximum velocity accompanied with the main vibration frequency (usually referred to as the dominant frequency). The guideline in DIN-4150 can be explained by three lines in Figure 71. For instance, significant damage will not occur on buildings under preservation order when a point, representing dominant frequency-maximum velocity pair, is lower than the L3 line.

To adopt the aforementioned guideline, it was interesting to know the variation of dominant frequency over distance such as the ones shown in Figure 72. Based on the same figure, the dominant frequency was not correlated with the distance, but rather depends on the ground condition. Statistics in Table 46 Statistics of dominant frequency in each site Table 46 showed that the dominant frequency of saturated sandy ground were higher than the clayey ground.

It can be seen from Figure 71 that less vibration velocity is permitted when the dominant frequency decreases. Therefore the dominant frequency at  $\mu - 2\sigma$ , which is approximately lower than 98% of the population, will be assumed in further analyses for the conservative sake. Since the limit values of L1, L2, L3 lines stop decreasing when the dominant frequency is lower than 10 Hz, the frequency of 10 Hz will be assumed when a  $\mu - 2\sigma$  is less than 10 Hz.

The measured data of each strata were compared to DIN 4150's guideline for residential building. The results show that the setback distance were less than 29 m and 10 m from the vibration source when pile penetrated of hard clay and dense sand respectively. In addition to the setback distance compared to pile penetrated depth, the results were 1.6 and 1.0 for dense sand and hard clay respectively when hammer weight/pile weight more than 1.0, while hammer weight/pile weight less than 1.0, the setback distances were less than 20 m from vibration source for hard clay as shown in Table 49. Because of the lack of data and incline of pile, the results from stiff clay and top soil were not proposed in this study.

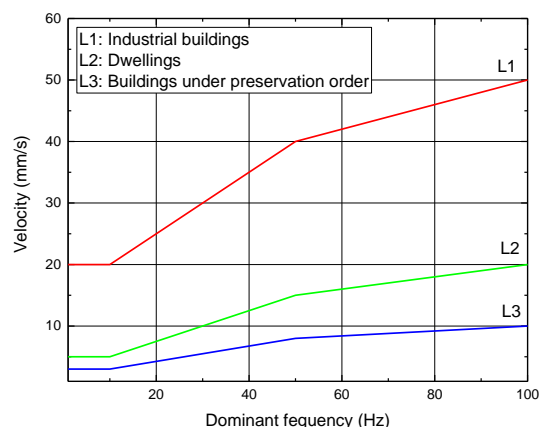


Figure 71 Guideline values at building foundations for short-term vibration (after DIN 4150)

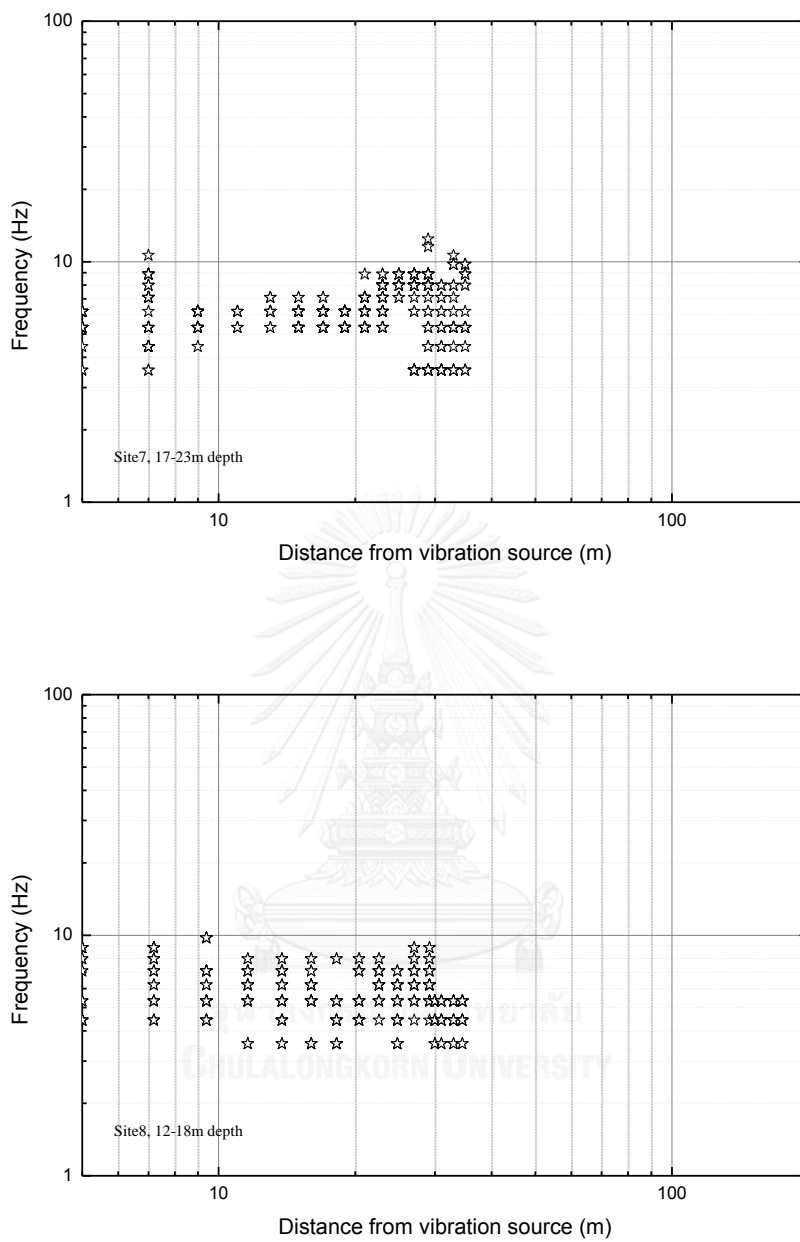


Figure 72 Variation of dominant frequency with distance in each sites

Table 46 Statistics of dominant frequency in each site

Sites	Sample size	Mean, $\mu$ (Hz)	S.D., $\sigma$ (Hz)	$\mu - 2\sigma$ (Hz)
No. 7 (17.0-23.0 m)	1632	6	2	2
No. 8 (12.0-18 m)	225	6	1	4

Table 47 the results of 80% upper bound limit of sandy ground

Site No.	Soil type	Depth h (m)	Fitting models	Fitting parameters		Hammer/Pile weight	DIN 4150's guideline (mm)	Setback distances	Setback distances / Depth
			Conventional models	$k$	$n$				
2-1	Medium	0.9	$v = k \cdot r^{-n}$	253	1.5	1.1	5	14	15.2
	Loose sand	2.4	$v = k \cdot r^{-n}$	322	2			8	3.3
2-2	Medium	1.5	$v = k \cdot r^{-n}$	1272	2	0.4	5	16	10.6
	Loose sand	1.8	$v = k \cdot r^{-n}$	574	2			11	6.0
3-1	Medium sand	10.6	$v = k \cdot r^{-n}$	8	0.5	1.5	5	2	0.2
3-2	Dense sand	9.5	$v = k \cdot r^{-n}$	42	1	1.5		8	0.9
3-3	Medium	2.4	$v = k \cdot r^{-n}$	114	1	1.5	5	23	9.5
	Dense sand	6	$v = k \cdot r^{-n}$	48	1			10	1.6

Table 48 the results of 80% upper bound limit of clayey ground

Site No.	Soil type	Depth (m)	Fitting models	Fitting parameters		Ram/Pile weight	DIN 4150's guideline (mm)	Setback distances	Setback distances / Depth
			Conventional models	$k$	$n$				
1	Stiff clay	16	$v = k_1 \cdot r_c^{-n_1}$	192	1	0.7	5	38	2.4
		16	$v = k_2 \cdot r_c^{-n_2}$	42	0.5			70	4.4
	Hard clay	24.5	$v = k \cdot r^{-n}$	143	1			29	1.2
4	Hard clay	24	$v = k \cdot r^{-n}$	18	1	1.5		4	0.1
5	Hard clay	23	$v = k \cdot r^{-n}$	79	1	1		16	0.7
6	Very stiff clay	17	$v = k_1 \cdot r_c^{-n_1}$	901	2	0.9		13	0.8
		17	$v = k_2 \cdot r_c^{-n_2}$	6	0.5			2	0.1
	Hard clay	20	$v = k \cdot r^{-n}$	175	1.5			11	0.5
7	Very stiff clay	17	$v = k \cdot r^{-n}$	432	1.5	0.6		20	1.1
	Hard clay	24	$v = k \cdot r^{-n}$	436	1.5			20	0.8
8	Very stiff clay	12	$v = k \cdot r^{-n}$	215	1.5	1.9	12	1.0	
	Hard clay	20.5	$v = k \cdot r^{-n}$	211	1.5		12	0.6	

### 1.7. Summarized results

Based on the results in this study, the results can be summarized as shown in Table 49 and made as follows;

1. For near field, the attenuation of vibration can be described by setting the geometric damping parameter to 2.0 when the vibration in vertical component

compared to horizontal component was less than 60 % . This characteristic conformed to the condition of body waves traveling along the surface. Geometric damping parameters were 1.5 and 1.0 when the vibration in vertical component compared to horizontal component was more than 110 % , 75% , respectively. This characteristic conformed to the condition of body waves generated by an impulsive point source. Parameter  $n = 2.0$  and 1.5 seem to be occurred when the hammer/pile weight ratio less than 1. For far field, Geometric damping parameter was 0.5. This characteristic conformed to the condition of surface waves generated by harmonic point source.

2. For near field, vibration in clayey and sandy ground were dominated by the vertical component when the ratio of ram weight over pile weight more than 1, while horizontal component were dominated when the pile was penetrated in very stiff clay or dense sand with the ratio of ram weight over pile weight less than 1. For far zone, vibration in clayey and sandy ground were dominated by the vertical component.
3. Pile driving generated two wave type when the vibration in vertical component compared to horizontal component was less than 75% and hammer/pile weight ratio seem to be less than 1. According to the studies, hammer/pile weight ratio more than 1. Those two waves could not be found but it does not mean that it was there because the lack of data over distance.
4. Observed data shows no significant correlation between the dominant frequency and distance. On the contrary, the dominant frequency seemed to be related with ground condition. The dominant frequencies of vibration were around 4 ~12 Hz in clayey ground and 17~ 25 Hz in loose sandy ground.
5. The results of this study show that prediction model could not be replied the high accurately of ground vibration from vibration source over distance.

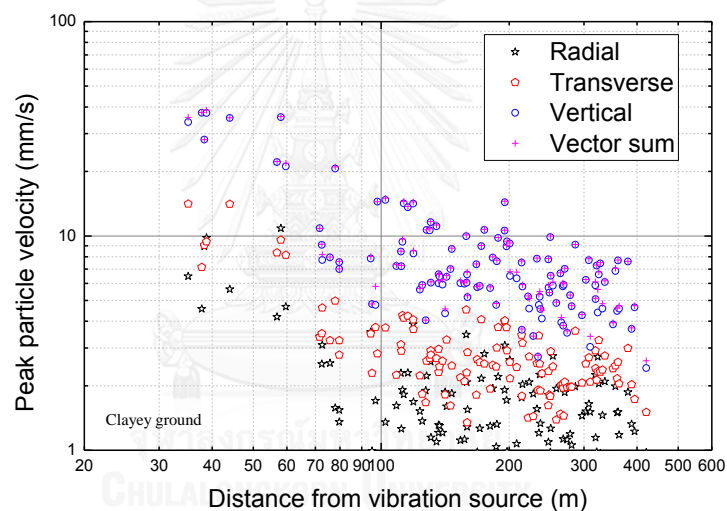
Table 49 the summarized results for pile driving

Site	Soil type	Depth (m)	N-SPT	Ram/Pile weight	Starting point of measurement (m)	$n_1$	$n_2$	Beginning of body wave/penetrated depth	Ending of body wave/penetrated depth	Mean of dominant frequency (Hz)	Vertical/Horizontal
2-1	Loose sand	2.4-3.9	6	1.1	10	2				25	0.6
2-2	Loose sand	1.8-3.0	10	0.4	10	2				17	0.6
3-1	Medium sand	10.6-14.5	19	1.5	16.6	0.5				6	1.4
3-2	Dense sand	9.5-15.0	33	1.5	12.8	1				6	1.4
	Medium sand	0-2.4	15			1				6	
3-3	Dense sand	6.0-8.4	35	1.5	12	1				6	1.4
1	Stiff clay	16.0-23.0	11	0.7	5	1	0.5	0.6-0.8	1.5-1.9	6	0.75
	Hard clay	24.5-25.0	36			1				12	0.75
4	Very stiff clay	20.0-22.0	23	1.5	8	1				4	1.1
	Hard clay	24.0-24.3	48			1				4	1.1
5	Hard clay	23.0	34	1	17	1				5	N/A
6	Very stiff clay	18.0-19.0	21	0.9	5	2	0.5	0.9-1.0	1.4-1.5	6	0.2
	Hard clay	20.0-23.0	46			1.5		0.7-0.8		6	1.1
7	Very stiff clay	17.0-23.0	24	0.6	5	1.5		0.6-0.8		6	1.1
	Hard clay	24.0-25.0	35			1.5				6	1.1
8	Very stiff clay	12.0-18.0	24	1.9	5	1.5		0.6-0.9		6	N/A
	Hard clay	19.0-20.5	40			1.5		0.57-0.6		7	N/A

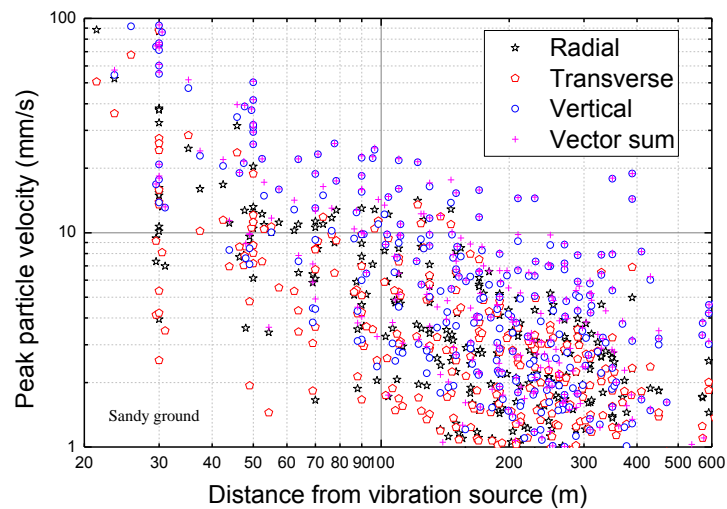
## 2. Blasting

### 2.1. Vibration in each direction

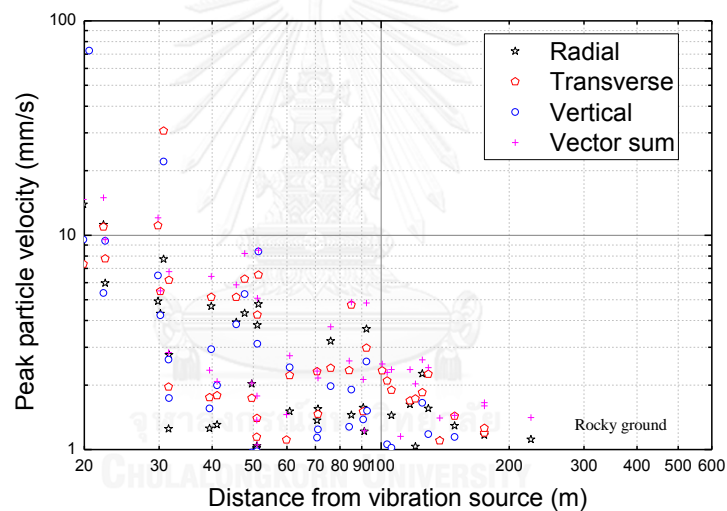
The PPV in each direction and the PPV of velocity vectors of all measurements were plotted against distance in Figure 73. The plot for each individual site is provided in Appendix C. For clayey and sandy grounds, the PPVs in vertical direction were almost equal to the values from velocity vectors and higher than the other components. Therefore, it was concluded that the vibrations were dominated by the vertical component. Further analyses for these ground types were based on the data from 4.5Hz vertical geophones for the interest of more data points. On the contrary, no consistent relationship was found between the PPVs of true velocity vectors and the PPVs of each direction in rocky ground. Vibrations in this ground type seemed to propagate through a number of reflections before arrive at instrument geophones in random directions. The PPVs of velocity vectors were used for further analyses in this ground type.



a) Clayey ground



b) Sandy ground



c) Rocky ground

Figure 73 Comparisons between blasting vibration in each direction

## 2.2. Attenuation of vibration in each ground type

### 2.2.1. Clayey ground

Since only 1.0 kg explosives were used in this ground type, the influence from explosive weight was not considered. Fitting analyses were performed by Eq. (19) and Eq. (20) for determining the attenuation of PPV over distance. The fitting results are shown in Figure 74 and Table 50. From the first model in Table 50, the optimum result occurred when the parameter  $\alpha$  (which subject to a condition of non-negative value) was zero. Therefore, it was concluded that the influence of material damping is negligible.



Further studies were carried out by comparing the first model with the 2<sup>nd</sup> to 4<sup>th</sup> models in Table 50 which derive the value of  $n$  from theoretical basis. When the geometric attenuation parameter ( $n$ ) was fixed to 1.0 and 1.5, the coefficients of determination ( $R^2$ ) decreased from the optimum values but still be higher than 0.8.

It was noticed from Figure 74 that the data were well aligned with the  $n = 1.5$  line when the distance is less than 50 m. Although the data became more scatter when the distance was larger than 50 meter, they tended to decrease over distance in the same rate as the  $n = 0.5$  line. Therefore it was assumed based on this observation that the vibration in near zone was dominated by body waves whereas the vibration in the far zone was dominated by surface waves. To validate this assumption, the data was fitted by a piecewise function shown in Eq. (21) which is the 5<sup>th</sup> model in Table 50. Further studies were also made by setting the  $n_1$  and  $n_2$  to some characteristic values which are the 6<sup>th</sup> and 7<sup>th</sup> models in Table 50. Although the 5<sup>th</sup> model gave the best  $R^2$ , the 6<sup>th</sup> model is recommended for the interest of generalization and theoretical study.

Table 50 Fitting analysis results for blasting in clayey ground

Fitting models		Fitting parameters				$R^2$
		$k$	$n$	$a$	$r_c$	
Conventional models						
1	$v = k \cdot r^{-n} \cdot e^{-ar}$	1598	1.15	0.0		0.819
2	$v = k \cdot r^{-0.5}$	83				0.419
3	$v = k \cdot r^{-1.0}$	879				0.792
4	$v = k \cdot r^{-1.5}$	5443				0.689
Piecewise models						
5	$v = k_1 \cdot r^{-n_1}, r < r_c$	3091	1.33		101	0.888
	$v = k_2 \cdot r^{-n_2}, r > r_c$	40	0.41		101	
6	$v = k_1 \cdot r^{-1.5}, r < r_c$	5008			78	0.876
	$v = k_2 \cdot r^{-0.5}, r > r_c$	64			78	
7	$v = k_1 \cdot r^{-1.5}, r < r_c$	4695			34	0.841
	$v = k_2 \cdot r^{-1.0}, r > r_c$	796			34	

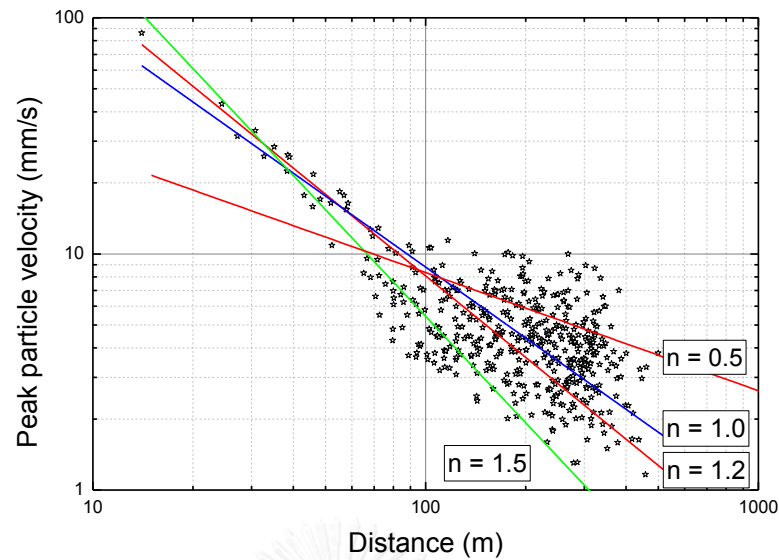


Figure 74 Attenuation of blasting vibration in clayey ground

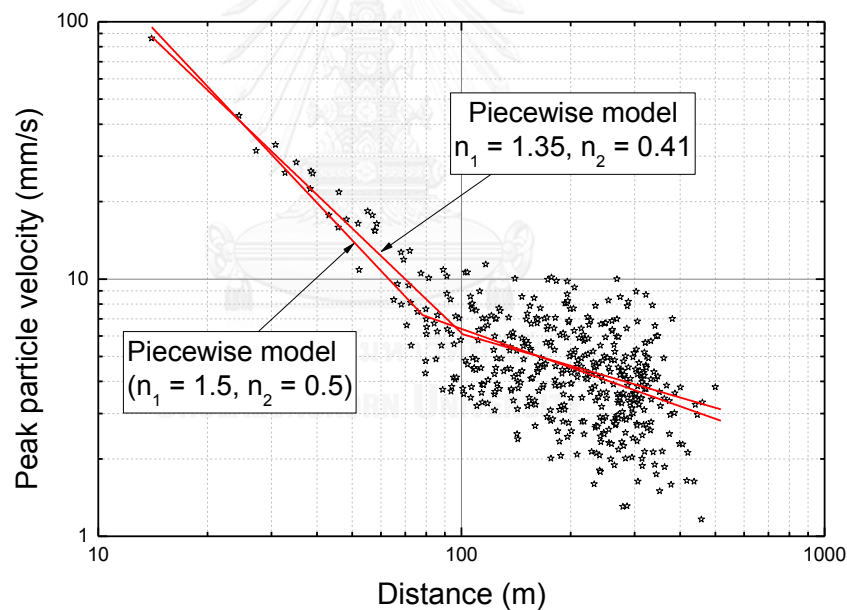


Figure 75 Fitting results of piecewise models for blasting vibration in clayey ground

### 2.2.2. Sandy ground

The procedure used in the previous section was also applied in this section. It was found that the effect of material damping was also negligible in sandy ground. For the interest of brevity, only analyses by Eq. (20) will be presented. The data and fitting results are shown in Figure 75 and Table 51. From the first model in Table 51, the empirical values of  $n$  ranged between 1.19 to 1.40 with the minimum  $R^2$  of 0.601.

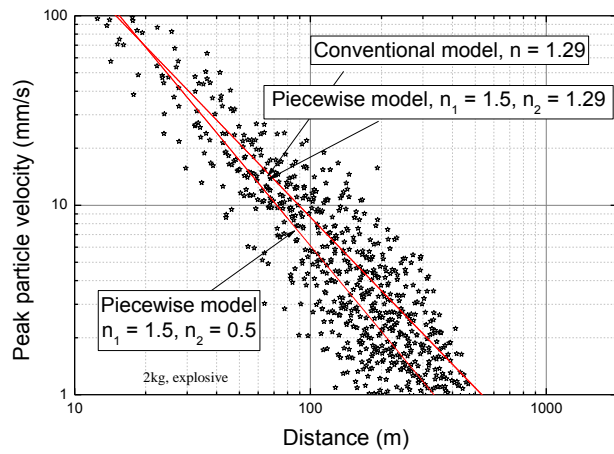
When the geometric attenuation parameter was fixed to 1.0 and 1.5, the coefficients of determination ( $R^2$ ) decreased slightly from the optimum values.

To investigate whether the attenuation rate in near zone is different from the one in far zone or not, piecewise fitting analyses were carried out by assuming the value of  $n_1$  to be 1.5 for the interest of unification with the clayey ground case. The fit results of the 4<sup>th</sup> model in Table 51 showed that the optimum values of  $n_2$  were close to 0.5 for the 3 and 4 kg explosives but not for the case of 2 kg explosives. Since the data were not available after the distance of 500 meter in the latter case, the behavior of  $n = 0.5$  type might not be recognized by the fitting algorithm. Finally, when the  $n_1$  and  $n_2$  were fixed to 1.5 and 0.5 respectively, the coefficients of determination ( $R^2$ ) decreased slightly from the 4<sup>th</sup> model but still better than the 1<sup>st</sup> model except for the case of 2 kg explosives. Again, the fit algorithms decided to use the  $n_1$  which was close to the optimum value (1.29) than the  $n_2$ .

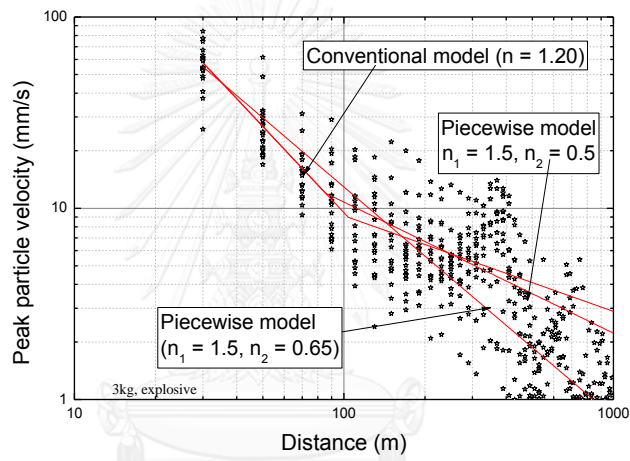


Table 51 Fitting analysis results for blasting in sandy ground

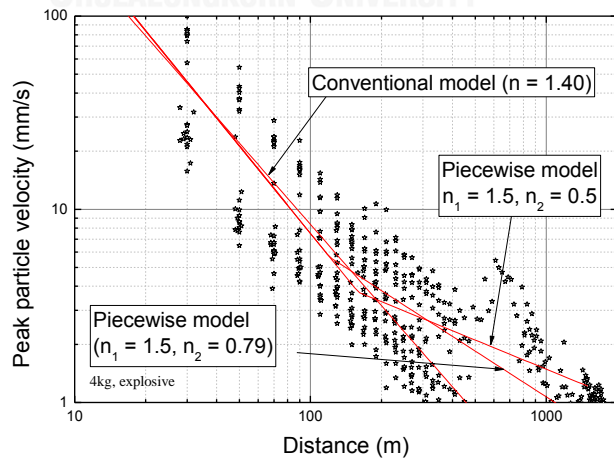
Fitting models		Explosive weight (kg)	Fitting parameters					$R^2$
			$k_1$	$n_1$	$k_2$	$n_2$	$r_c$	
Conventional models								
1	$v = k \cdot r^{-n}$	2	3254	1.29				0.826
		3	3273	1.20				0.830
		4	5177	1.40				0.636
2	$v = k \cdot r^{-1.0}$	2	1276					0.783
		3	1500					0.813
		4	1137					0.599
3	$v = k \cdot r^{-1.5}$	2	6100					0.811
		3	9734					0.808
		4	7552					0.635
Piecewise models								
4	$v = k_1 \cdot r^{-1.5}, r < r_c$ $v = k_2 \cdot r^{-n_2}, r > r_c$	2	4125		3270	1.29	3	0.826
		3	9458		253	0.69	85	0.852
		4	7486		246	0.79	121	0.640
5	$v = k_1 \cdot r^{-1.5}, r < r_c$ $v = k_2 \cdot r^{-0.5}, r > r_c$	2	6100		7		832	0.831
		3	9485		91		104	0.851
		4	7501		47		159	0.639



a) 2 kg explosives



b) 3 kg explosives



c) 4 kg explosives

Figure 76 Attenuation of blasting vibration in sandy ground

### 2.2.3. Rocky ground

Due the reason mentioned earlier, the PPVs from velocity vectors were used instead of the data from vertical geophones. The relationship between the PPV and distance was compared with Eq. (20) as shown in Figure 77. Since the slope of the best fit line was closed to 1.5, it was concluded that the attenuation of  $n = 1.5$  type occurred in rocky ground. It was also observed that vibrations in rocky ground were significantly smaller than those in other ground types.

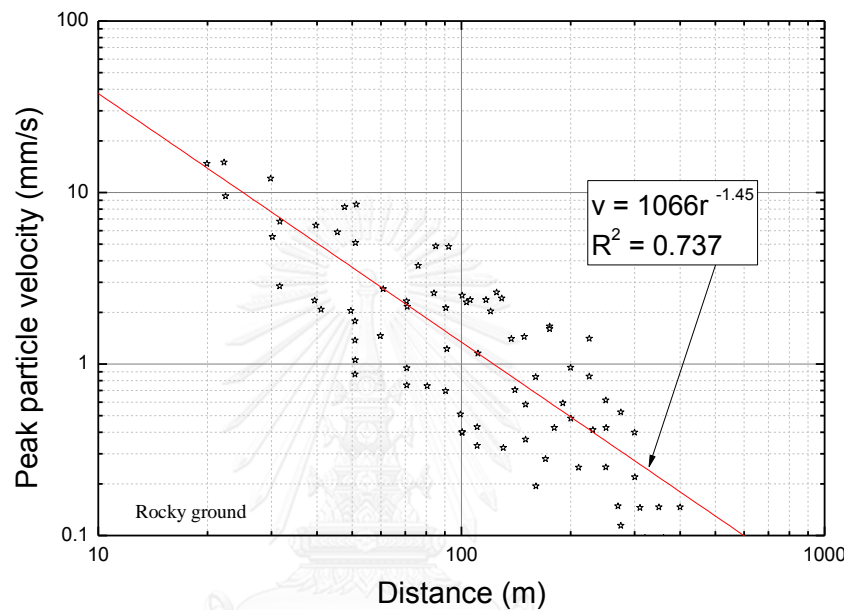


Figure 77 Attenuation of vibrations in rocky ground

### 2.3. The influence of explosive weight and ground type

Based on Eq.(19), the magnitude of vibration near to its source ( $r = 1$  m) is controlled by the parameter  $\hat{k}$ . The influence of explosive weight on vibration level was studied from the measurements in sandy ground where the explosive weight varied between 2 – 4 kg. Based on the first model in Table 51 and Figure 78, the values of  $\hat{k}$  appeared to be proportional with the explosive weight.

From a theoretical point of view, the energy of vibration is proportional to the square of the amplitude of a wave. Since the energy of an explosive is proportional to its weight, the amplitude of a wave could be normalized by the square root of the weight of the explosive. The normalized equations as well as their qualities of fit for all ground types are shown in Table 52. The  $R^2$  of all cases were higher than 0.7 and came out to be sufficient for practical purposes.

The parameter  $k$  reflects the influences from remaining unconsidered factors, such as the energy loss at the detonation point, the stiffness of the ground, and so on. This parameter was empirically linked with ground type in this study. From Table 52 and Figure 79, the  $k_1$  of sandy ground and rocky ground compared to clayey ground

were 87% and 20%, respectively. The corresponding ratios for the  $k_2$  were 65% and 9% for sandy ground and rocky ground, respectively.

It was also noticed that the value of  $r_c$ , or the boundary where the attenuation characteristic changed from  $n = 1.5$  to  $n = 0.5$ , varied in opposite direction with  $k_1$  and  $k_2$ . The values of  $r_c$  increased to 1.79 and 2.06 times when the ground type changed from clayey to sandy and rocky, respectively.

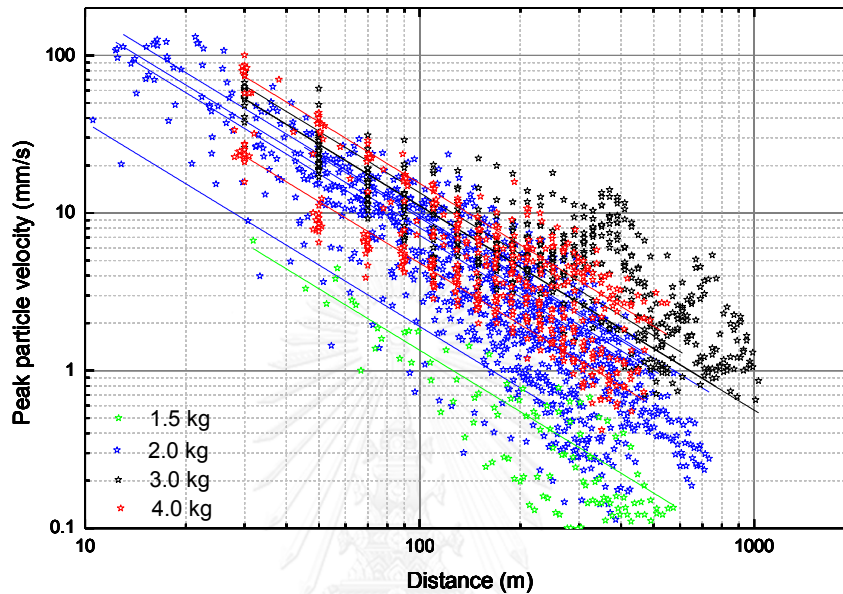


Figure 78 The influence of explosive weight in sandy ground

Table 52 Results from fitting analyses considering explosive weight.

Fitting models		Ground type	Fitting parameters			$R^2$
			$k_1$	$k_2$	$r_c$	
1	$v = k_1 \cdot w^{0.5} \cdot r^{-1.5}, r < r_c$	Clayey	5007	64	78	0.875
	$v = k_2 \cdot w^{0.5} \cdot r^{-0.5}, r > r_c$	Sandy	4355	42	102	0.874
		Rocky	981	6	161	0.743

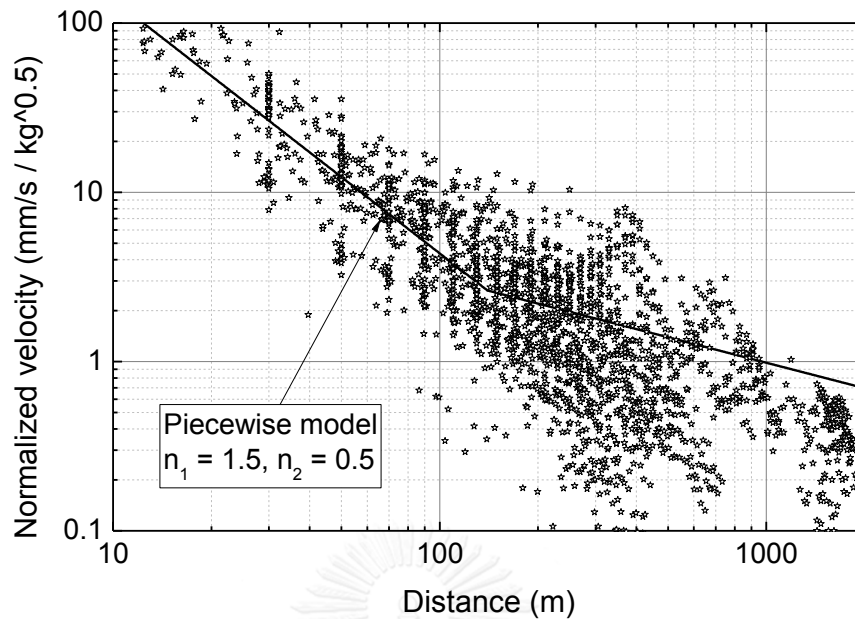


Figure 79 Normalized PPVs based on measurement in sandy ground

#### 2.4. Variation of dominant frequency

The relationships between PPV, dominant frequency and distance are shown in Figure 80 to Figure 84. Statistics of all ground types are shown in Table 53. Based on these figures, the dominant frequency seemed to be uncorrelated with the distance, but rather depends on the ground condition. The dominant frequencies in sandy ground under saturated condition were higher than the corresponding values under dry condition. For rocky ground, the dominant frequency was high and scattered over a wider range. The dominant frequency of clayey ground was also higher and less scattered than other ground types.



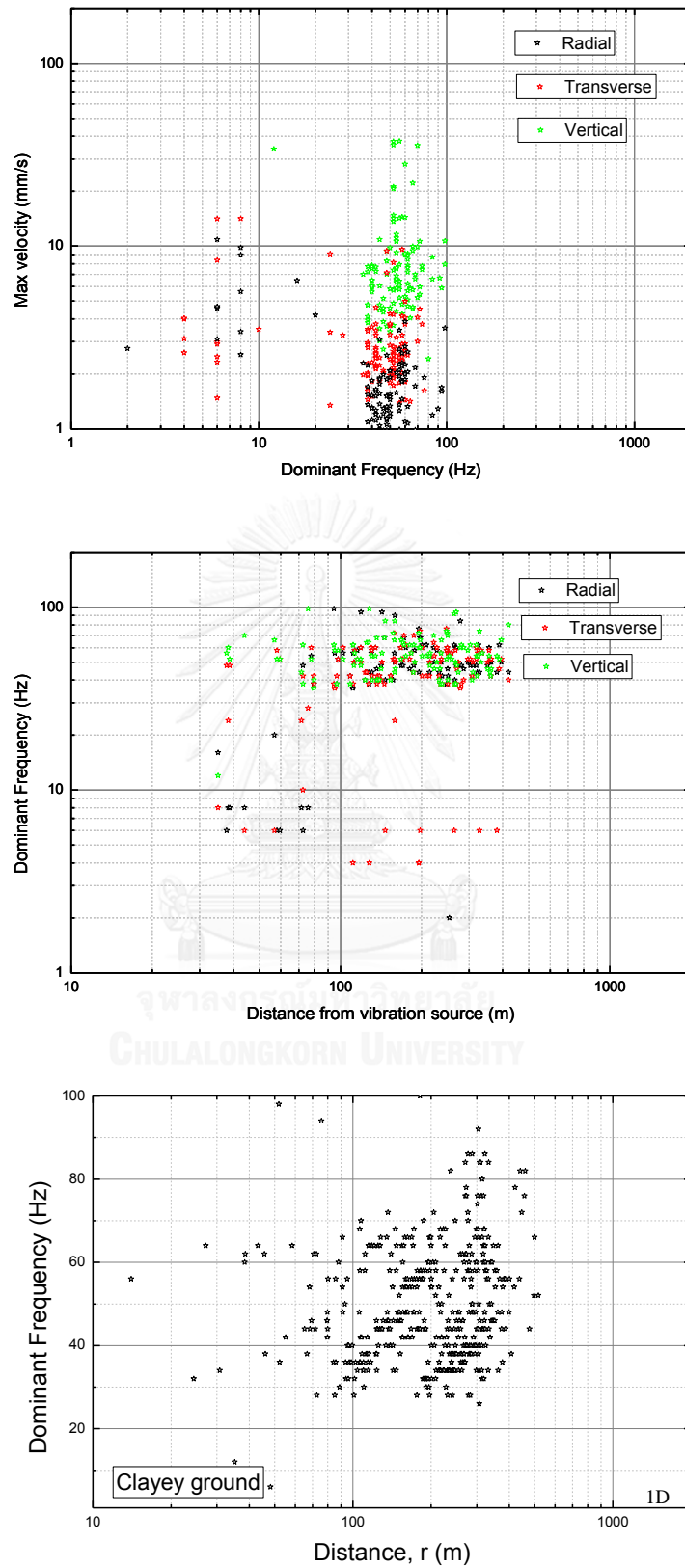


Figure 80 Variations of dominant frequency in clayey ground

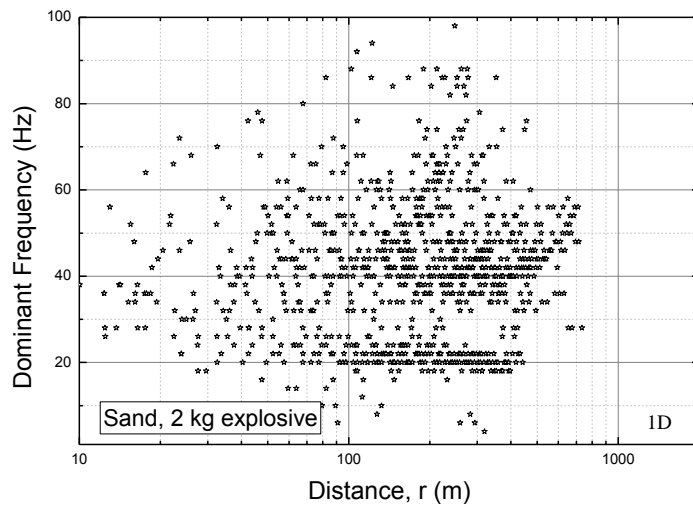
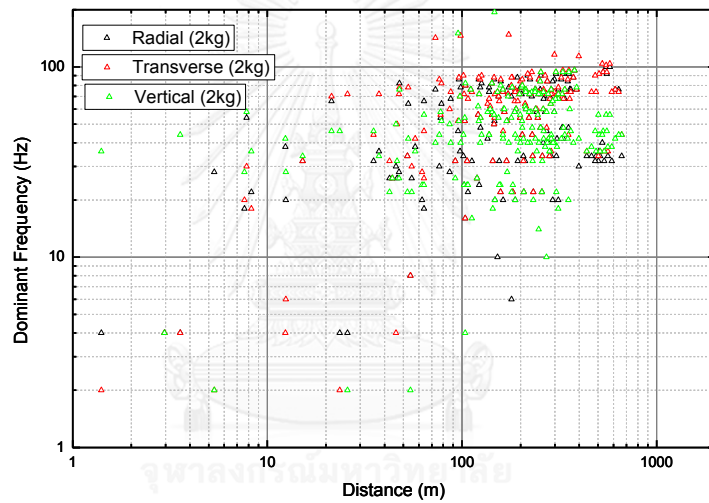
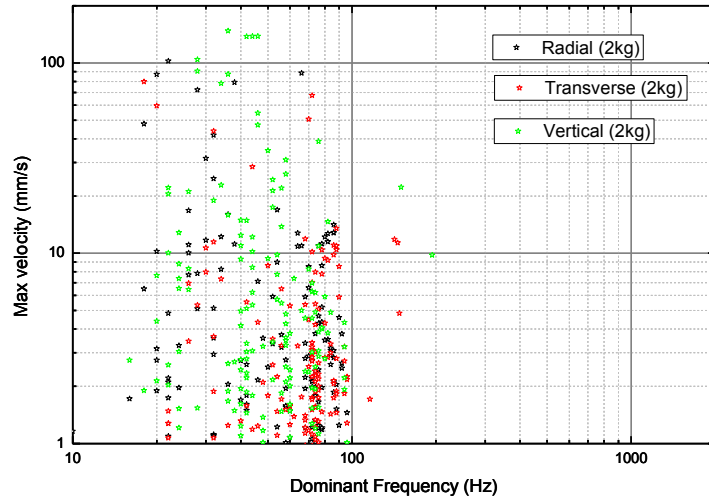


Figure 81 Variations of dominant frequency in sandy ground (2 kg explosives)

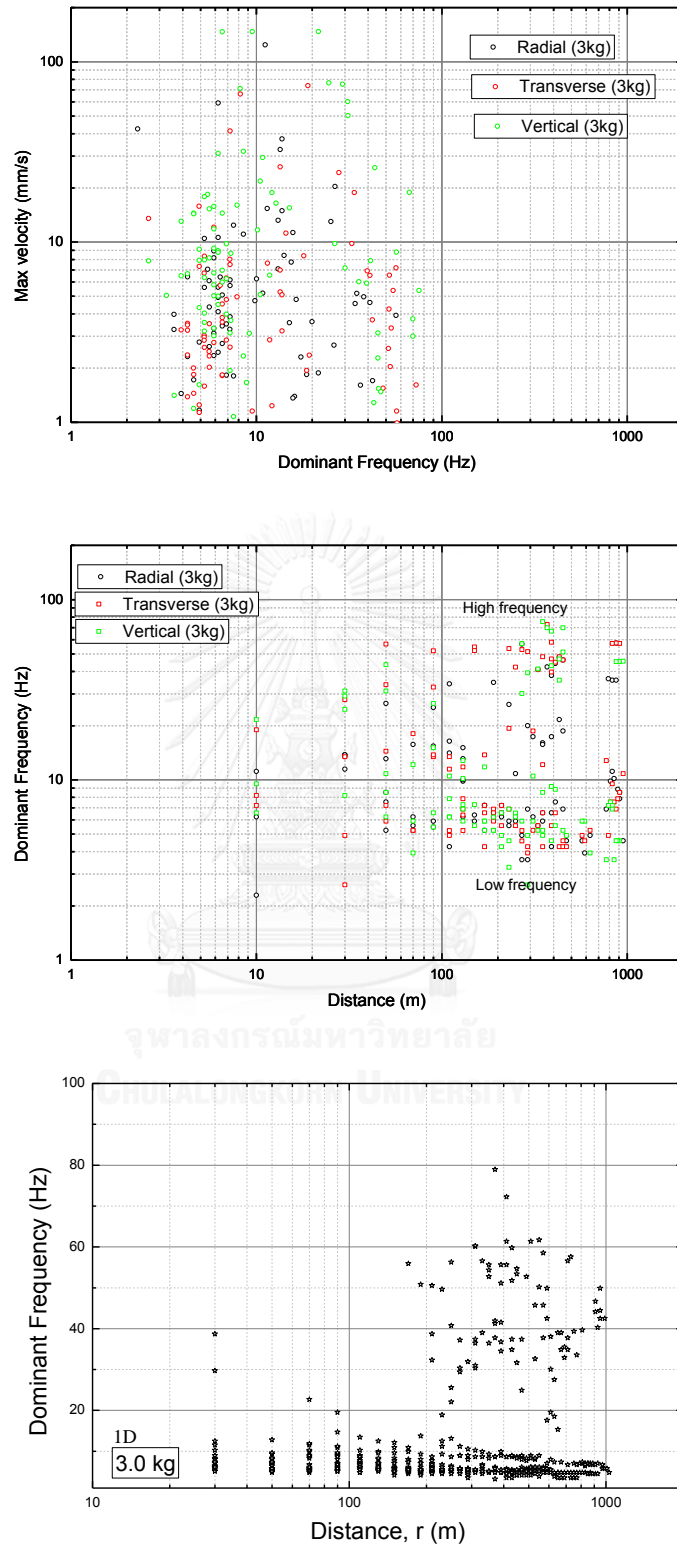


Figure 82 Variations of dominant frequency in sandy ground (3 kg explosives)

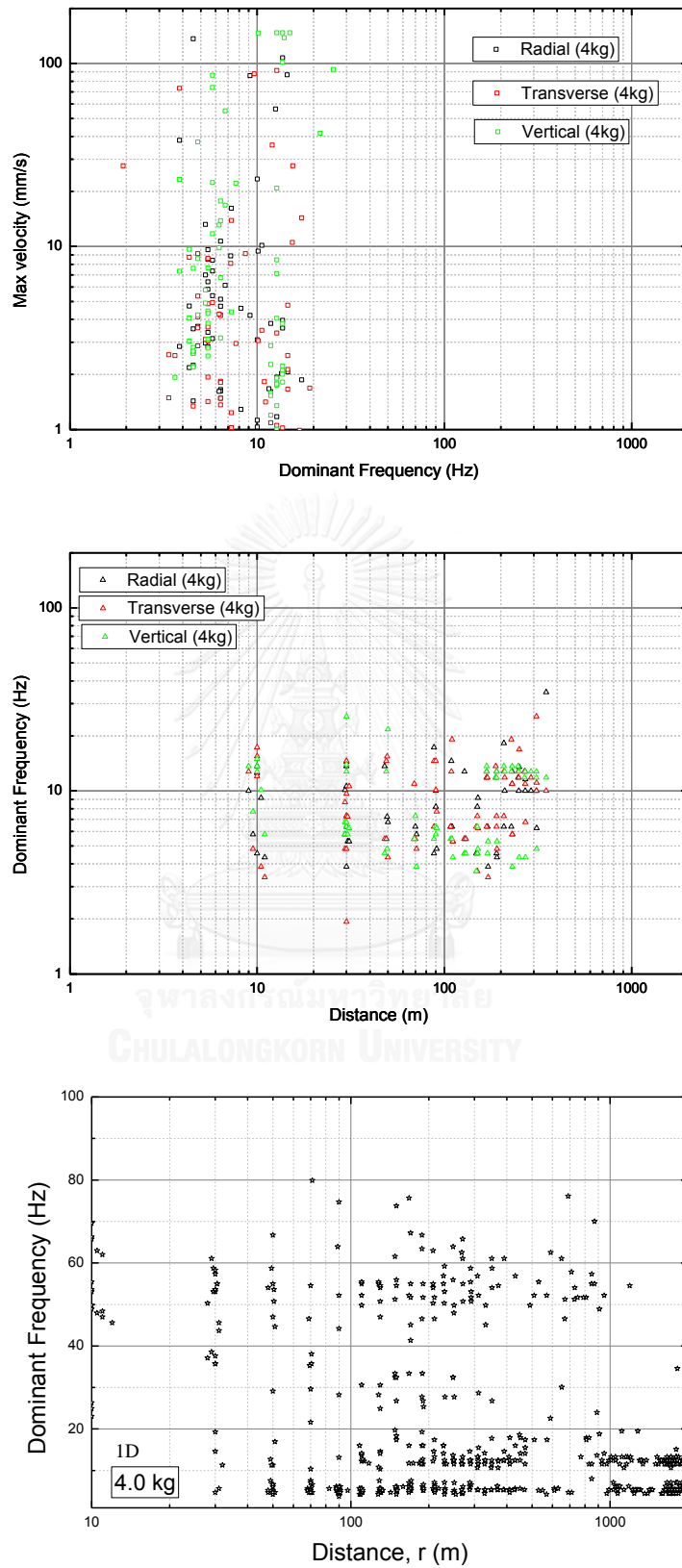


Figure 83 Variations of dominant frequency in sandy ground (4 kg explosives)

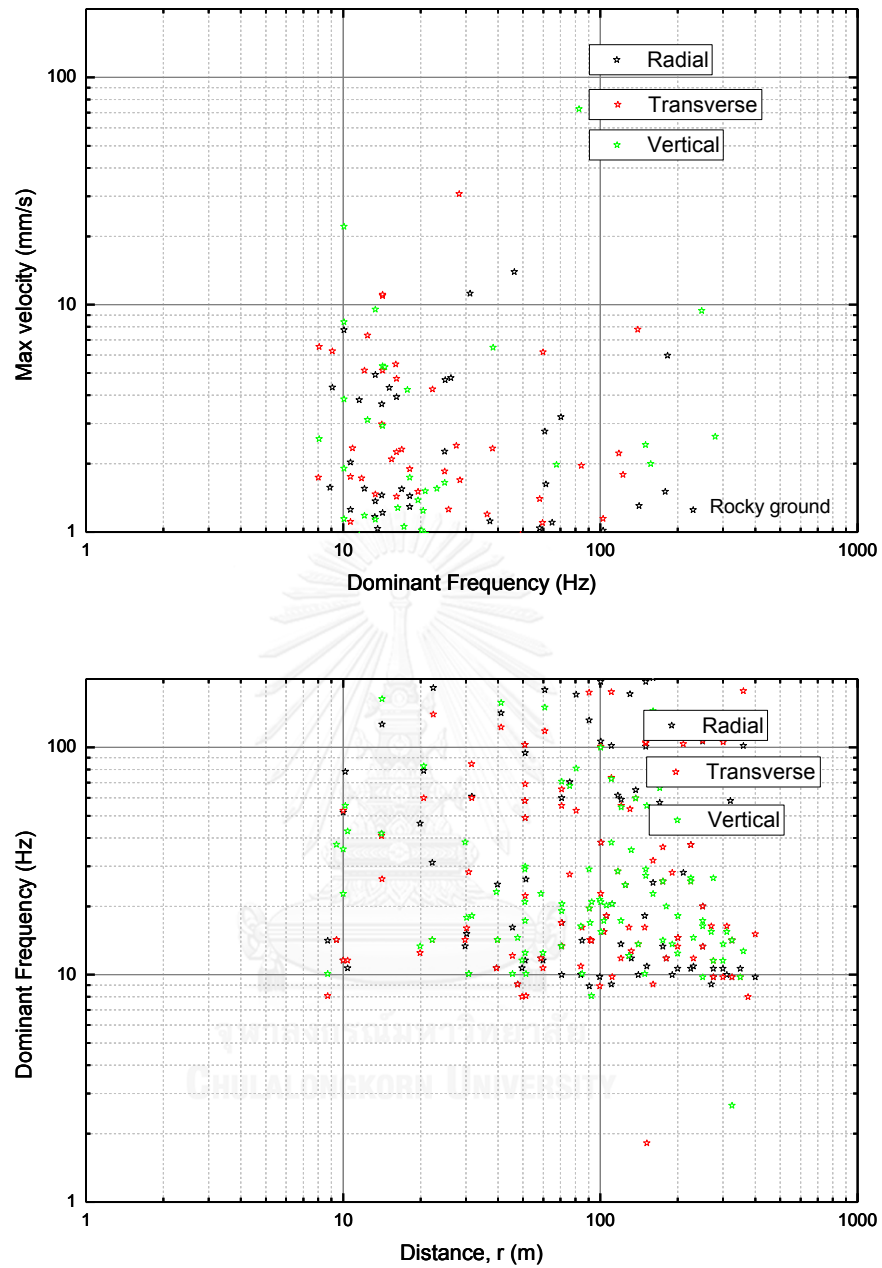


Figure 84 Variations of dominant frequency in rocky ground

Table 53 Statistics of dominant frequency in each ground type

Ground type	Sample size	Mean, $\mu$ (Hz)	S.D., $\sigma$ (Hz)	$\mu - 2\sigma$ (Hz)
Clayey ground (Saturate)	861	49	14	21
Sandy ground (Dry)	1116	17	18	<10
Sandy ground (Saturate)	978	42	21	<10
Sandy ground (all data)	2094	29	23	<10
Rocky ground (Radial direction)	111	45	52	<10
Rocky ground (Transverse direction)	111	36	38	<10
Rocky ground (Vertical direction)	666	32	51	<10

## 2.5. Comparison with other prediction models

### 2.5.1. Clayey ground

Fitting results from selected prediction models are shown in Figure 85 and Table 54. From Table 54, the coefficients of determinations ( $R^2$ ) of models in the literatures are approximately 0.8 while the  $R^2$  of the piecewise model is close to 0.9. Based on AIC scores, the ranking of models from the highest to the lowest are the piecewise model, Ghosh and Daemen (1983), Ambraseys and Hendron (1968) and USBM, respectively.

Table 54 Comparison of prediction models for blasting in clayey ground

Fitting models		Fitting parameters				$R^2$
		$k$	$n$	$a$	$r_c$	
Prediction models						
1	USBM; $v = k \cdot (r/w^{0.5})^n$ ,	5247	-1.5			0.814
2	Ambraseys and Hendron (1968) $v = k \cdot (r/w^{0.33})^n$	5247	-1.5			0.814
3	Ghosh and Daemen (1983) $v = k \cdot (r/w^{0.67})^n \cdot e^{-ar}$	5247	-1.5	0.0		0.814
Piecewise model						
4	$v = k_1 \cdot w^{0.5} \cdot r^{-1.5}, r < r_c$	5016			77	0.905
	$v = k_2 \cdot w^{0.5} \cdot r^{-0.5}, r > r_c$	65			77	

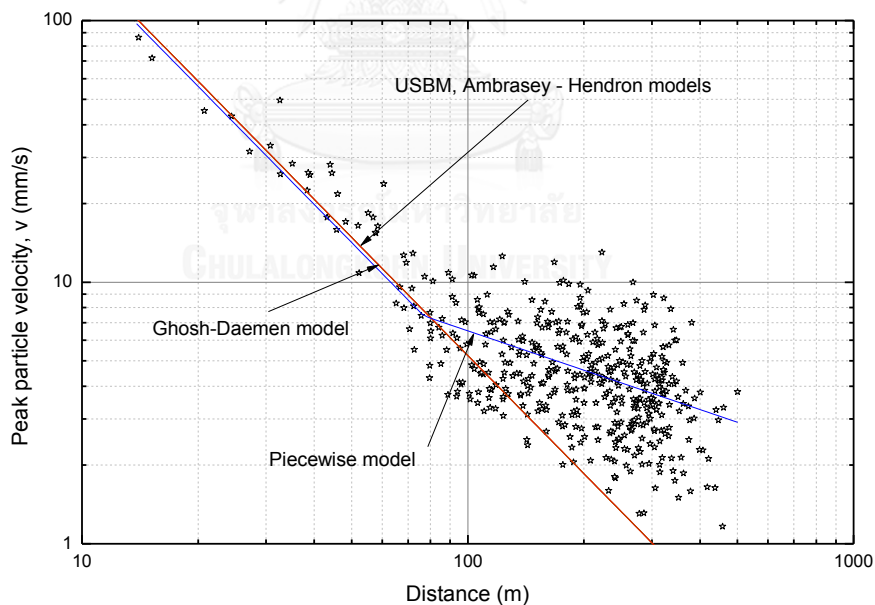


Figure 85 Comparison of prediction models for blasting in clayey ground

### 2.5.2. Sandy ground

Fitting results from selected prediction models are shown in Figure 86 and Table 55. From Table 55, the coefficients of determinations ( $R^2$ ) of models in the literatures are approximately 0.8 while the  $R^2$  of the piecewise model is close to 0.85.

Based on AIC scores, the ranking of models from the highest to the lowest are the piecewise model, Ghosh and Daemen (1983), Ambraseys and Hendron (1968) and USBM, respectively.

Table 55 Comparison of prediction models for blasting in sandy ground

Fitting models		Fitting parameters				$R^2$
		$k$	$n$	$a$	$r_c$	
Prediction models						
1	USBM; $v = k \cdot (r/w^{0.5})^n$ ,	4270	-1.5			0.804
2	Ambraseys and Hendron (1968); $v = k \cdot (r/w^{0.33})^n$	9734	-1.5			0.804
3	Ghosh and Daemen (1983); $v = k \cdot (r/w^{0.67})^n \cdot e^{-ar}$	9734	-1.5	0.0		0.804
Piecewise models						
4	$v = k_1 \cdot w^{0.5} \cdot r^{-1.5}, r < r_c$	5476			102	0.85
	$v = k_2 \cdot w^{0.5} \cdot r^{-0.5}, r > r_c$	54			102	0



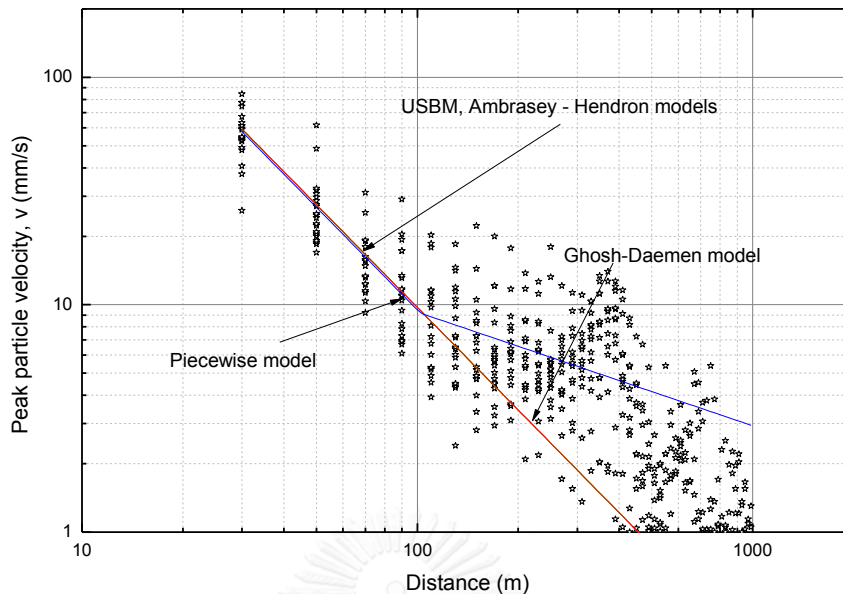


Figure 86 Comparison of prediction models for blasting in sandy ground

### 2.5.3. Rocky ground

Fitting results from selected prediction models are shown in Figure 87 and Table 56. From Table 56, the coefficients of determinations ( $R^2$ ) of all models are around 0.7. The ranking of models based on AIC, from the highest to the lowest, are USBM, Ambraseys and Hendron (1968), Ghosh and Daemen (1983) and the piecewise model, respectively. Since the  $R^2$  of all models are almost similar, the USBM which has the least numbers of parameters is given the highest rank by AIC.

Table 56 Comparison of prediction models for blasting in rocky ground

Fitting models		Fitting parameters				$R^2$
		$k$	$n$	$a$	$r_c$	
Prediction models						
1	USBM; $v = k \cdot (r/w^{0.5})^n$ ,	932	-1.5			0.740
2	Ambraseys and Hendron (1968); $v = k \cdot (r/w^{0.33})^n$	1264	-1.5			0.740
3	Ghosh and Daemen (1983); $v = k \cdot (r/w^{0.67})^n \cdot e^{-ar}$	1264	-1.5	0.0		0.740
Piecewise models						
4	$v = k_1 \cdot w^{0.5} \cdot r^{-1.5}$ , $r < r_c$	1032			-	0.740
	$v = k_2 \cdot w^{0.5} \cdot r^{-0.5}$ , $r > r_c$	-			-	

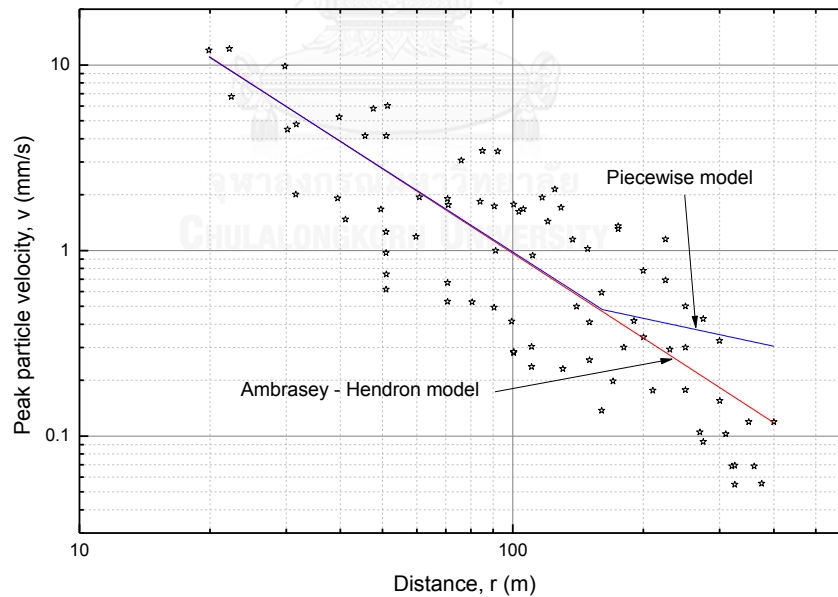


Figure 87 Comparison of prediction models for blasting in rocky ground

### 3. Vibratory rollers

#### 3.1. Comparison of vibrations in radial, transverse and vertical directions

Two test patterns were carried out for vibrations due to vibratory rollers. The arrangements of vibratory rollers and the geophone array are shown in Figure 88. A roller in the R pattern will run along the radial direction of geophones and the geophone array. For the T pattern, a roller will run perpendicular to the geophone array and parallel to the transverse direction of each geophone in the array.

Discussions in the following sections will use the results from site no. 1 (Sakon Nakorn) as examples. The data from all sites are provided in Appendix C.

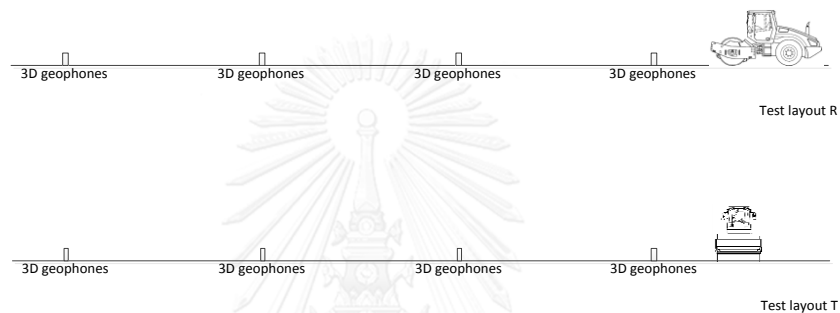


Figure 88 Test patterns for the study of vibrations due to vibratory rollers

#### 3.2. Attenuation characteristics in each ground type

##### 3.2.1. Results from test pattern R

Fitting analyses were carried out for determining the attenuation of PPV over distance. The data and fitting results are shown in Table 57 and Figure 90. Based on fitting results using Eq.(19), the optimum result occurred when the parameter  $a$  (which subject to a condition of non-negative value) was zero. Therefore, the influence of material damping was neglected in the further studies.

By comparing among models shown in Table 57, the best  $R^2$  was obtained when the  $n$  was equal to 0.5. Therefore, the vibrations seemed to be governed by surface waves. To investigate further, the trajectories of ground motion at various distances were plotted as shown in Table 59. The particle motions were also fitted with the typical trajectory of Rayleigh waves. Consequently, it was concluded that the ground vibrations were dominated by surface waves.

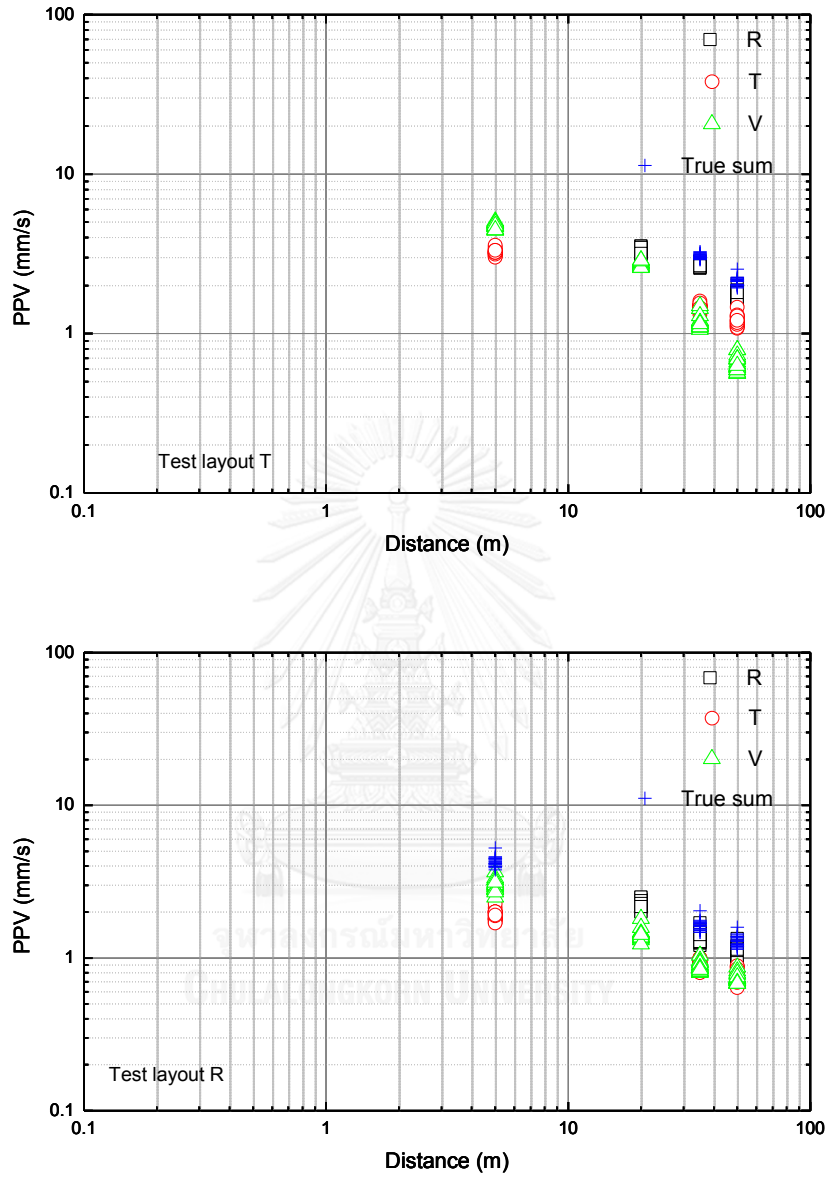


Figure 89 Comparisons between vibrations due to vibratory rollers in each direction

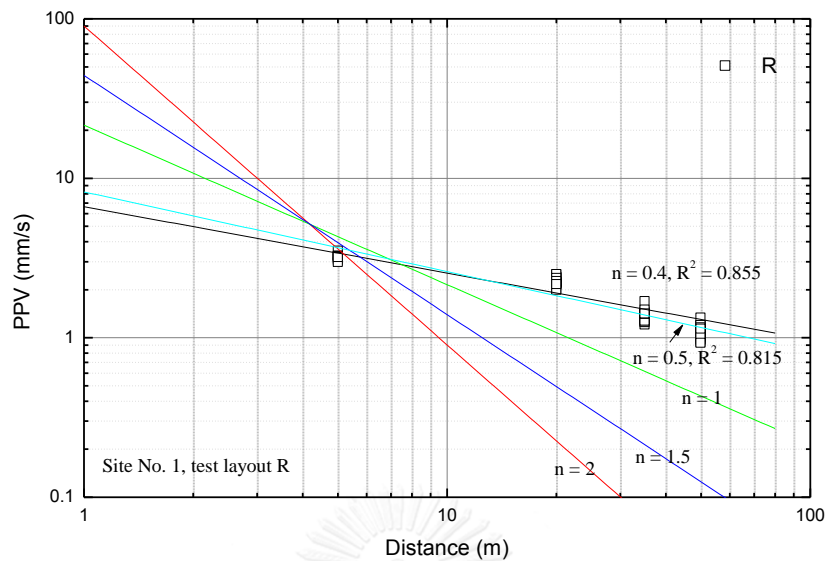


Figure 90 Attenuation of vibration of the layout R

Table 57 Results from fitting analyses for the measured data of layout R from site 1

Fitting models		Fitting parameters		$R^2$	Remarks
		$k$	$n$		
Conventional models					
1	$v = k \cdot r^{-n}$	7	0.4	0.855	
2	$v = k \cdot r^{-0.5}$	8		0.815	
3	$v = k \cdot r^{-1.0}$	22		-0.625	
4	$v = k \cdot r^{-1.5}$	44		-2.098	
5	$v = k \cdot r^{-2.0}$	90		-2.857	

### 3.2.2. Results from test pattern T

Fitting analyses were carried out for determining the attenuation of PPV over distance. The data and fitting results are shown in Table 58 and Figure 91. Based fitting results using Eq. (19), the optimum result occurred when the parameter  $a$  was zero. Therefore, the influence of material damping was neglected in the further studies.

By comparing among models shown in Table 58, the best  $R^2$  was obtained when the  $n$  was equal to 0.5. Therefore, the vibrations seemed to be governed by surface waves. To investigate further, the trajectories of ground motion at various distances were plotted as shown in Table 59. The particle motions were also fitted

with the typical trajectory of Rayleigh waves. Consequently, it was concluded that the ground vibrations were dominated by surface waves.

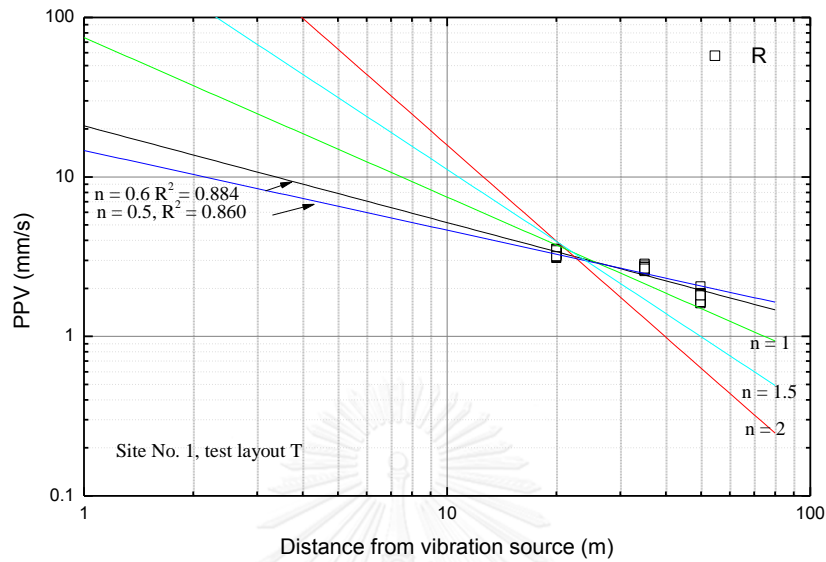
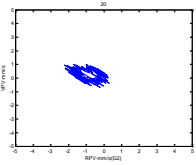
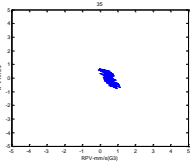
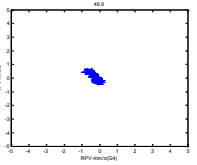
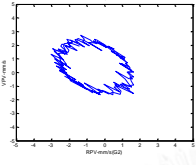
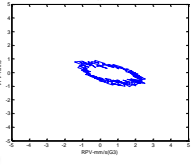
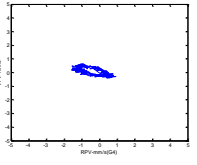


Figure 91 Attenuation of vibration of the layout T

Table 58 Results from fitting analyses for the measured data of layout T from site 1

Fitting models		Fitting parameters		$R^2$	Remarks
		$k$	$n$		
Conventional models					
1	$v = k \cdot r^{-n}$	21	0.6	0.884	
2	$v = k \cdot r^{-0.5}$	15		0.860	
3	$v = k \cdot r^{-1.0}$	75		0.560	
4	$v = k \cdot r^{-1.5}$	352		-0.510	
5	$v = k \cdot r^{-2.0}$	1584		-1.815	

Table 59 Trajectories of ground motion due to a vibratory roller

Layout	10m-from source	18 m-from source	37m-from source
R			
T			

### 3.3. Variation of dominant frequency

According to the measured data, the dominant frequencies of pattern R and T were 24 Hz as show in Figure 92. It is noted that these values were lower than the declared specification of the machine (31Hz).

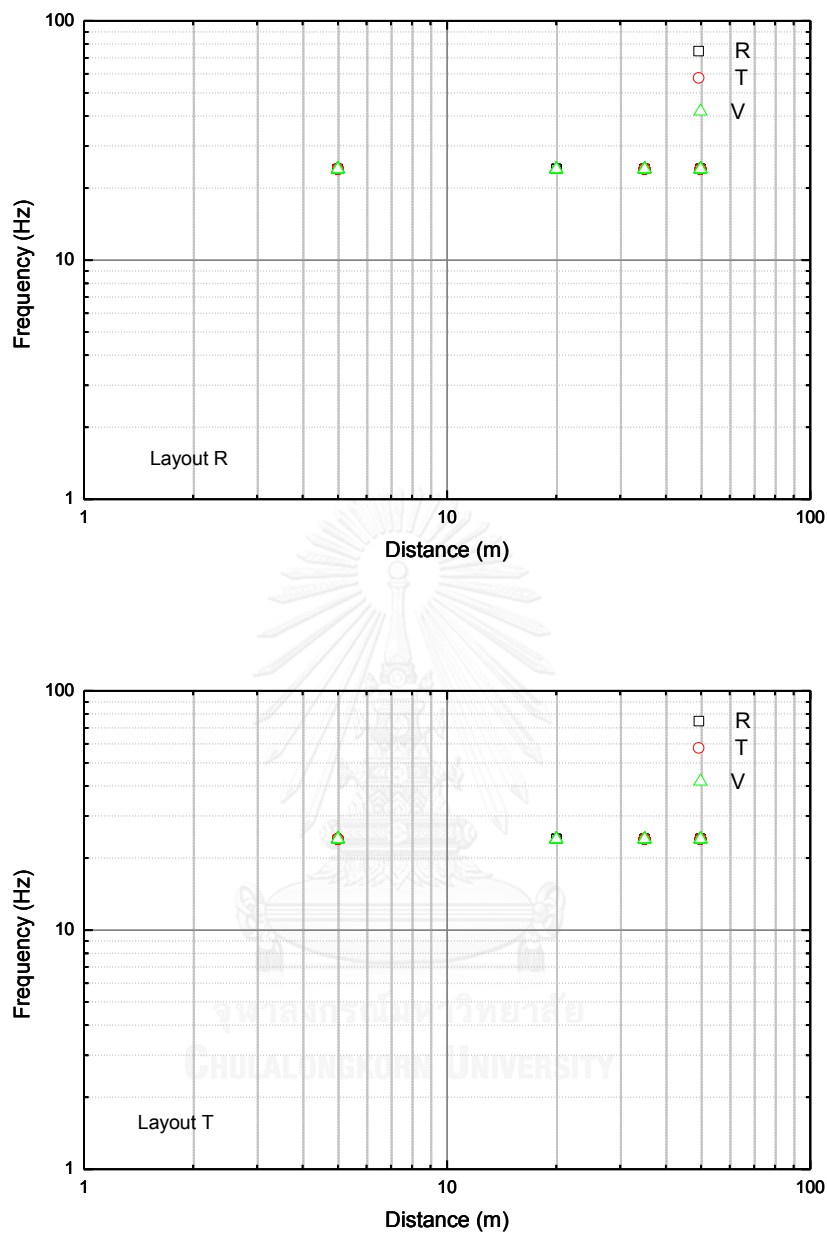


Figure 92 Dominant frequency of vibration due to rollers

### 3.4. Comparison with other prediction models

The measured data from layout T were fitted by the models proposed by Philipps G (2010), Achmus et al. (2004) and Hiller and Crabb (2000). Fitting results from selected prediction models are shown in Table 60 and Figure 93. The coefficients of determinations ( $R^2$ ) of all models in the literatures were less than 0.6. The best  $R^2$  was obtained from the model proposed by Achmus et al. Based on AIC scores, the ranking of models from the highest to the lowest are Hiller & Crabb, Achmus et al. and Philipps, respectively.



Fitting analyses and ACI test were carried out for determining the best prediction model over distance for top soil of sandy ground. The measured data from layout T were fitted by the simply prediction model such as, Philipps G (2010), Achmus et al. (2004) and Hiller and Crabb (2000). The data and fitting results are shown in Figure 93 and Table 60. From the fitting of 1<sup>st</sup> and 2<sup>nd</sup> in Table 60, the coefficients of determinations ( $R^2$ ) are more than 0.5. The 1<sup>st</sup> model shows the highest  $R^2$  of 0.866.

Table 60 Results from model fitting analyses for top soil of sandy ground

Fitting models		Fitting parameters				$R^2$
		$k$	$m$	$A$	$l$	
Prediction models						
1	Philipps G (2010); $v = 1.1 \cdot (w^{0.5} / r^{0.7})$	-				-
2	Achmus et al. (2004); $v = k \cdot (w^{0.5} / r)$	17				0.559
3	Hiller and Crabb (2000); $v = k \cdot m^{0.5} \cdot (A / (r + l))^{1.5}$	300	1	1.20	1.60	-0.308

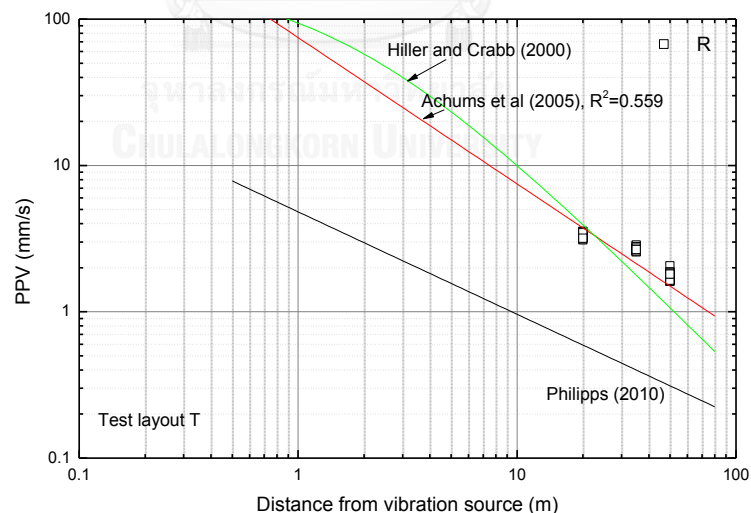


Figure 93 the prediction models fitting for layout T

### 3.5. The influence of roller weight

Based on Eq.(19), the magnitude of vibration near to its source ( $r = 1$  m) is controlled by the parameter  $\hat{k}$ . From a theoretical point of view, the energy of

vibration is proportional to the square of the amplitude of a wave. Since the energy of vibration is proportional to the roller weight, the prediction model could be reformulated as Eq.(25).

$$v = \sqrt{w} \cdot k^* \cdot r^{-n} \quad (25)$$

where  $w$  = operating weight (tons)

$k^*$  =  $\frac{\hat{k}}{\sqrt{w}}$  = fitting parameter

$r$  = distance from vibration source (m)

$n$  = geometric damping

The parameter  $k^*$  reflects the influences from remaining unconsidered factors, such as the energy loss, the stiffness of the ground, and so on. The fitting results using Eq. (25) are shown in Table 61. The  $R^2$  of most of the cases were higher than 0.7 and came out to be sufficient for practical purposes.

### 3.6. Frequency content and comparison with DIN 4150's guideline

According to the reason that mentions earlier, to adopt the aforementioned guideline, it was interesting to know the variation of dominant frequency over distance such as the ones shown in Figure 92.

Figure 92 showed that the dominant frequency of sandy ground were lower than operating frequencies around 80 %.

The measured data of each site were compared to DIN 4150's guideline for residential building. The results show that the setback distance were less than 5.4 m and 6.9 m from the vibration source for flat ground and incline ground respectively. The results of each sites show in Table 61.

Table 61 Summary of fitting analyses for vibration due to vibratory rollers

Site	Location	Ground condition	Vibration frequency (Hz)	Roller weight (tons)	Test pattern	Direction of the largest vibration	Dominant frequency (Hz)	Attenuation			$R^2$	$k^*$
								Direction	$k$	Geometric damping, $n$		
1	Sakon Nakorn province	Horizontal surface	31	19.2	R	R	24	R	8	0.5	0.815	1.8
								T	5	0.5	0.497	1.1
								V	6.4	0.5	0.947	1.5
					T	R	24	R	14.6	0.5	0.86	3.3
								T	7.5	0.5	0.96	1.7
								V	10	0.5	0.88	2.3
			R		V	20	R	N/A	N/A	N/A	N/A	
							T	14.7	0.5	0.91	3.4	
							V	16.6	0.5	0.847	3.8	
			T		R	20	R	14.7	0.5	0.86	3.4	
							T	N/A	N/A	N/A	N/A	
							V	7.1	0.5	0.9	1.6	
2	Nong Kai province	Inclined surface	28	10.6	R	R	22, 26	R	384	2	0.967	117.9
								T	328	2	0.983	100.7
								V	16.7	1	0.782	5.1
					T	R	26	R	16.4	1	0.97	5.0
								T	14.2	1	0.985	4.4
								V	8.9	1	0.98	2.7

Table 62 Setback distances of vibration due to vibratory rollers

Site	Location	Ground condition	Vibration frequency (Hz)	Roller weight (tons)	Test pattern	Direction of the largest vibration	Dominant Frequency (Hz)	Attenuation			DIN 4150 Limiting values (mm)	Setback distances
								Direction	$k$	Geometric damping, $n$		
1	Sakon Nakorn province	Horizontal surface	31	19.2	R	R	24	R	9.0	0.5	8.5	1.1
								T	4.9	0.5	8.8	0.3
								V	6.9	0.5	8.5	0.7
					T	R	24	R	15.3	0.5	8.5	3.2
								T	8.0	0.5	8.5	0.9
								V	11.4	0.5	8.5	1.8
			R		V	20	R	N/A	N/A	7.5	N/A	
							T	15.0	0.5	7.5	4.0	
							V	17.4	0.5	7.5	5.4	
			T		R	20	R	13.5	0.5	7.5	3.2	
							T	N/A	N/A	7.5	N/A	
							V	7.9	0.5	7.5	1.1	
2	Nong Kai province	Incline surface	28	10.6	R	R	22, 26	R	384.6	2	8	6.9
								T	329.8	2	8	6.4
								V	17.3	1	8	2.2
					T	R	26	R	17.0	1	9	1.9
								T	14.6	1	9	1.6
								V	9.2	1	9	1.0

### 3.7. Result summary

The results from the study of ground vibrations due to vibratory rollers can be summarized as follows;

- In this study, flat ground and incline ground can be seen in site no. 1 and 2 respectively.

- The largest ground vibration occurred in radial direction. The vibrations from tests under pattern T were slightly higher than the ones under pattern R.
- When the ground surface was horizontal, the vibrations were dominated by surface waves. For the inclined ground surface, the vibrations were dominated by body waves.
- Dominant frequencies were almost equal to the operating frequencies of the rollers.



## CHAPTER V

### CONCLUSIONS

Pile driving, blasting and vibratory rollers are sources of ground vibrations which can cause damages in buildings. Damages from these activities can be avoided or minimized if the magnitude of ground vibration along the propagating distance can be accurately predicted.

Field measurements of ground vibration were carried out in this study from eight pile driving sites, eight petroleum exploration sites and two vibratory compaction sites in Thailand. The study areas were grouped into three geology conditions, namely; sandy ground, clayey ground and rocky ground.

For pile driving equipments, drop hammers were used in seven sites and a hydraulic hammer was used in the eighth site. For blasting, the vibrations were generated by emulsion explosives buried and packed in boreholes at depths of 9 ~ 23 m. The explosives weighted 1 to 4 kg and had the length-to-diameter ratios of 6 ~ 25. For vibratory compaction, the vibrations were generated by 10.6 and 19.2 ton rollers which operated under frequencies of 26, 28 and 31 Hz.

The result from this study reflects domestic ground conditions and work practices in Thailand and should be useful for preparing vibration mitigation and monitoring plans.

Based on the results in this study, the conclusions can be made as follows;

#### **Pile driving**

1. Vibrations in clayey and sandy grounds were dominated by body waves over the distance of 0.6-1.9 times of pile penetration depth.
2. The vibrations were dominated by surface waves when the distance was greater than 1.3-1.9 times of pile penetration depth.
3. The vibrations were proportional to the stiffness of the grounds at pile tip and also proportional to the energy of driving equipments.
4. Based on the results in this study, vibration at a distance can be estimated by

$$v = \sqrt{\frac{w}{N_{SPT}}} \cdot k^* \cdot r^{-n}$$

where  $k^*$  = fitting parameter,  $n$  = geometric damping,  $w = mgh$  = input energy,  $N_{SPT}$  = Uncorrected SPT-N value,  $r$  = distance from vibration source (m),  $m$  = weight of hammer (kg),  $g$  = Acceleration of earth's gravity,  $h$  = drop height (m)

*Summary of parameter  $k^*$  for pile driving*

Zone	$W_h/W_p$	$k^*$	$n$	Distance
Near field	<1	2.8-8.0	1.5	r = 0.6 ~ 1.9 times of pile penetration depth
	>1	1.0-1.4	1.0	
Far field	all	0.2-0.4	0.5	r > 1.3 ~ 1.9 times of pile penetration depth

Remark:  $W_h$ ,  $W_p$  are weights of hammer and pile, respectively.

5. According to DIN 4150 and the proposed formula (approximately at 80% confidential level), the setback distance when driving a pile in dense sand with  $W_h/W_p > 1.0$  was around 1.6 times of pile penetration depth. The setback distance when driving a pile in stiff clay was 1.0 times of pile penetration depth for  $W_h/W_p > 1.0$  and 1.1 times of pile penetration depth for  $W_h/W_p < 1.0$ .

### **Blasting**

1. Vibrations in clayey and sandy ground were dominated by the vertical component. On the contrary, the peak particle velocity occurred in random directions in rocky ground. Therefore, it is recommended to consider the velocity vector instead of one-directional velocity for the later ground type.
2. The attenuation of vibration can be described by setting the geometric damping parameter to 1.5 for the near zone and to 0.5 for the far field. This characteristic conformed to the condition of body waves generated by an impulsive point source and Rayleigh waves generated by harmonic point source, respectively. The latter could be occurred if the ground vibrated under its natural mode of vibration.
3. Vibration velocity at a distance can be determined from equations shown below. It is noted that equations on the left most column will only give the best estimate of the mean value. Therefore, it is recommended to add the predicted normalized velocity ( $\bar{v}$ ) by a constant of 1. By doing this, the modified value will be approximately at 80% one-side upper prediction level provided that  $r > r_c$ .

Fitting models	Ground type	Fitting parameters			$R^2$
		$k_1$	$k_2$	$r_c$	
$\bar{v} = k_1 \cdot r^{-1.5}, r < r_c$	Clayey	5007	64	78	0.875
$\bar{v} = k_2 \cdot r^{-0.5}, r > r_c$	Sandy	4355	42	102	0.874
where $\bar{v} = v / \sqrt{w}$	Rocky	981	6	161	0.743

where  $r$  = distance from vibration source (m),  $r_c$  = the distance at the boundary between near and far zones (m),  $w$  = weight of explosive (kg),  $v$  = ground vibration (mm/s).

- Observed data shows no significant correlation between the dominant frequency and distance. On the contrary, the dominant frequency seemed to be related with ground condition. The dominant frequencies of vibration were around 17 Hz in dry sandy ground, 42 Hz in saturated sandy ground, 49 Hz in saturated clayey ground and 31~ 45 Hz in rocky ground. The presence of ground water could increase the dominant frequency significantly.
- Using the proposed formula (approximately at 80% prediction level) and DIN 4150's guideline, the setback distances between residential buildings and a 2-kg explosive were found to be 53, 149 and 221 m for rocky, sandy and clayey grounds, respectively.

### Vibratory rollers

- Vibrations in sandy ground were strongest in radial direction. Vibrations propagating from left and right sides of a roller were greater than the ones from the front and rear sides.
- Under flat ground condition, the attenuation of vibrations fitted with the geometric damping coefficient of 0.5. This behavior conformed to the condition of surface waves generated by a harmonic source. For vibrations over inclined ground, the geometric damping coefficient of 2.0 was obtained from the back analysis of field measurements.
- Based on the results in this study, vibration due to vibratory roller in sandy ground can be estimated by

$$v = \sqrt{w} \cdot k^* \cdot r^{-0.5} \text{ for flat surface}$$

$$v = \sqrt{w} \cdot k^* \cdot r^{-2} \text{ for inclined surface}$$



where  $w$  is the roller weight (tons),  $r$  is the distance from the vibration source (m),  $k^*$  is a fitting parameter; 1.1-4 for flat surface and 2.8-5.3 for inclined surface.

4. Using the proposed formula (approximately at 80% prediction level) and DIN 4150's guideline, the setback distances for residential buildings for sandy ground were found to be 5.4, 6.9 m for flat surface ( $n = 0.5$ ) and inclined surface ( $n = 2$ ) respectively.



## REFERENCES



Achmus, M., J. Kaiser and F. Wörden (2004). "Bauwerksschütterungen durch Tiefbauarbeiten." Bericht 20.

Ambraseys, N. and A. Hendron (1968). *Dynamic Behaviour of Rock Masses. Rock Mechanics in Engineering Practice*. Stagg, F., Zienkiewicz, OC, John Wiley & Sons, New York.

Amick, H. and M. Gendreau (2000). *Construction vibrations and their impact on vibration-sensitive facilities*. ASCE Construction Congress.

Athanasopoulos, G. A. and P. C. Pelekis (2000). "Ground vibrations from sheetpile driving in urban environment: measurements, analysis and effects on buildings and occupants." Soil Dynamics and Earthquake Engineering **19**(5): 371-387.

Attewell, P. and I. Farmer (1973). "Attenuation of ground vibrations from pile driving." Ground Engineering **6**(4): 26-29.

Attewell, P., A. Selby and L. O'Donnell (1992). "Estimation of ground vibration from driven piling based on statistical analyses of recorded data." Geotechnical & Geological Engineering **10**(1): 41-59.

Auersch, L. and S. Said (2010). "Attenuation of ground vibrations due to different technical sources." Earthquake Engineering and Engineering Vibration **9**(3): 337-344.

Bornitz, G. (1931). "Expansion of Heavy Drilling Producing Groud Motion in the Deep." Journal of Springer, Berlin.

Brenner, R. and S. Viranuvut (1977). Measurement and prediction of vibrations generated by drop hammer piling in Bangkok subsoils. Proceedings of the Fifth Southeast Asian Conference on Soil Engineering.

Clough, G. W. and J.-L. Chameau (1980). "Measured effects of vibratory sheetpile driving." Journal of the Geotechnical Engineering Division **106**(10): 1081-1099.

Deckner, F. (2013). "Ground vibrations due to pile and sheet pile driving: influencing factors, predictions and measurements."

Dowding, C. H. (1985). Blast vibration monitoring and control, Prentice-Hall Englewood Cliffs.

Dowding, C. H. (1996). Construction vibrations, Prentice Hall Upper Saddle River, NJ.

Dowding, C. H. and C. Dowding (1996). Construction vibrations, Prentice Hall Upper Saddle River, NJ.

German Standard, D. "4150-3.(1999)." *Structural Vibration–Part 3: Effects of vibration on structures*.

Ghosh, A. and J. J. Daemen (1983). A simple new blast vibration predictor (based on wave propagation laws). The 24th US Symposium on Rock Mechanics (USRMS), American Rock Mechanics Association.

Heckman, W. S. and D. J. Hagerty (1978). "Vibrations associated with pile driving." Journal of the Construction Division **104**(4): 385-394.

Hendron, A. (1978). *Engineering of rock blasting on civil projects: Structural and Geotechnical Mechanics* (Englewood Cliffs, NJ: Prentice-Hall, 1977), P242–277. *International Journal of Rock Mechanics and Mining Sciences & Geomechanics Abstracts*, Pergamon.

Hiller, D. and G. Crabb (2000). "ROUNDBORNE VIBRATION CAUSED BY MECHANISED CONSTRUCTION WORKS." TRL REPORT 429.

Kim, D.-S. and J.-S. Lee (2000). "Propagation and attenuation characteristics of various ground vibrations." Soil Dynamics and Earthquake Engineering **19**(2): 115-126.

Kopp, J. W. and D. E. Siskind (1986). Effects of millisecond-delay intervals on vibration and airblast from surface coal mine blasting, US Department of the Interior, Bureau of Mines.

Martin, D. J. (1980). "Ground vibrations from impact pile driving during road construction."

Massarsch, K. (1993). Man-made vibrations and solutions. Third international conference on case histories in geotechnical engineering (1993: June 1-4; St. Louis, Missouri), Missouri S&T (formerly the University of Missouri--Rolla).

Massarsch, K. (2004). "Vibrations caused by pile driving." Summer and Fall Featured Articles, Deep Foundation Institute Magazine, Hawthorne.

Massarsch, K. and B. Fellenius (2008). Ground vibrations induced by impact pile driving. Proceedings of the 6th international conference on case histories in geotechnical engineering. Arlington.

Massarsch, K., C. Madshus and A. Bodare (1995). Engineering vibrations and solutions. Proceedings: Third International Conference on Recent Advances in Geotechnical Earthquake Engineering and Soil Dynamics. St. Louis, MO.

Massarsch, K. R. (2002). Ground Vibrations Caused by Soil Compaction, Wave 2002. Proceedings, International Workshop.

Nicholls, H. R., C. F. Johnson and W. I. Duvall (1971). Blasting vibrations and their effects on structures, Bureau of Mines, Denver, CO (USA). Denver Mining Research Center.

Peterie, S. L., R. D. Miller and J. Ivanov (2014). "Seismology and Its Applications in Kansas."

Philipps G, S. F., Wieck J (2010). "Die vorsorgliche Beweissicherung im Bauwesen: Reihe begründet von Günter Zimmermann.

Fraunhofer IRB Verlag."

Pistol, J., F. Kopf, D. Adam, S. Villwock and W. Völkel (2013). "Ambient vibration of oscillating and vibrating rollers."

Rachpech, V., P. Bunnaul, P. Julapong and T. Walthongthanawut (2014). "Local ground parameters of blasting vibration models for different geological structures at Mae Moh lignite mine, Thailand." Songklanakarin Journal of Science & Technology **36**(1).

Rai, R. and T. Singh (2004). "A new predictor for ground vibration prediction and its comparison with other predictors." Indian journal of engineering and materials sciences **11**: 178-184.

Richart, F. E., J. R. Hall and R. D. Woods (1970). "Vibrations of soils and foundations."

Siskind, D. E., M. S. Stagg, J. W. Kopp and C. Dowding (1980). Structure response and damage produced by ground vibration from surface mine blasting, Bureau of Mines, Twin Cities, MN (USA). Twin Cities Research Center; Northwestern Univ., Evanston, IL (USA).

Svinkin, M. (1999). Prediction and calculation of construction vibrations. DFI 24th Annual members' conference, decades of technology—advancing into the future.

Svinkin, M. (2008). Soil and structure vibrations from construction and industrial sources. OSP8, Proceedings of the Sixth International Conference on Case Histories in Geotechnical Engineering, OmniPress, Arlington, Virginia.

Svinkin, M., B. Roth, W. Hannen, S. Niyama and J. Beim (2000). The effect of pile impedance on energy transfer to pile and ground vibrations. Proceedings of the Sixth International Conference on the Application of Stress-Wave Theory to Piles.

Svinkin, M. R. (2004). SOME UNCERTAINTIES IN HIGH-STRAIN DYNAMIC PILE TESTING.

Tangchawal, S. (2000). "Assessment on Rock Blasting Impacts."

Tangchawal, S. (2006). "Planning and evaluation for quarries: case histories in Thailand."

Tripathy, G. R. and I. D. Gupta (2002). "Prediction of Ground Vibrations due to Construction Blasts in Different Types of Rock." Rock Mechanics and Rock Engineering **35**(3): 195-204.

Uysal, Ö., E. Arpaz and M. Berber (2007). "Studies on the effect of burden width on blast-induced vibration in open-pit mines." Environmental Geology **53**(3): 643-650.

Verruijt, A. (2010). An introduction to soil dynamics, Springer Science & Business Media.

Wiss, J. F. (1967). "Damage effects of pile driving vibration." Highway Research Record(155).

Wiss, J. F. (1981). "Construction vibrations: state-of-the-art." Journal of the Geotechnical Engineering Division **107**(2): 167-181.

Woods, R. D. and L. P. Jedele (1985). Energy—Attenuation Relationships from Construction Vibrations. Vibration problems in geotechnical engineering, ASCE.

Woods, R. D., National Cooperative Highway Research Program. and National Research Council (U.S.). Transportation Research Board. (1997). Dynamic effects of pile installations on adjacent structures. Washington, D.C., National Academy Press.

# APPENDIX A

## Source properties Blasting



TENAGA KIMIA SENDIRIAN BERHAD (26191 A)

### TECHNICAL DATA SHEET

**PRODUCT:** EMULSION HIGH EXPLOSIVE (CARTRIDGED)  
**BRAND:** EMULEX<sup>®</sup>  
**SERIES:** EMULEX<sup>®</sup> 700  
**SIZE (mm):** 60

#### Product Specification

Grade / Series	Density (g/cc)	Detonation Velocity (m/s) <sup>1</sup>	Explosion Energy (MJ/kg) <sup>2</sup>	Bulk Strength (% Rel ANFO)	Water Resistance	Cap Sensitive	Fume Class
Emulex <sup>®</sup> 700	1.15 - 1.20	5,000 - 5,500	3.00	117	Excellent	Standard seismic detonator	1

<sup>1</sup> VOD of product is dependent on product properties and diameter design.  
<sup>2</sup> Energy value is calculated using a special design program. Calculation based on thermodynamic properties.

#### Shelf Life

TK cartridge emulsion products have a recommended shelf life of 1 year when stored in a clean, dry, cool and well-ventilated magazine.

#### Sleep Time

TK cartridge emulsion products' sleep time will be subjected to the recommended sleep time of the blasting agents or initiation systems that are used.

#### Temperature Requirement

TK cartridge emulsion products functioned well in temperatures ranging from 0° to 50° C.



#### Package Specification

Grade / Series	Dimension Size (mm)	Type of Cartridge	Cartridge Weight (Approx. kg)	Case Weight (Approx. kg)
Emulex <sup>®</sup> 700	60 x 180	ABS canister	0.5	20
	60 x 354	ABS canister	0.10	16

#### Disclaimer

**Administration & Sales Office**  
 Address: No. 8, Jalan SS 22/21, Damansara Jaya,  
 47400 Petaling Jaya, Selangor  
 Tel: +60-3-7729 7494  
 Fax: +60-3-7729 8383  
 E-mail: [sales@tenagakimia.com](mailto:sales@tenagakimia.com)

**Factory**  
 Address: Lot 5065, 48100 Batu Arang,  
 Selangor, Malaysia  
 Tel: +60-3-6035 2801  
 Fax: +60-3-6035 2802  
 E-mail: [plant@tenagakimia.com](mailto:plant@tenagakimia.com)

Website: <http://www.tenagakimia.com>

Explosion technical data sheet ([http://www.tenagakimia.com/Products\\_seismic.asp](http://www.tenagakimia.com/Products_seismic.asp))

# Roller compactor

## Bomag BW 219

### Technical Data

Shipping dimensions in m <sup>3</sup>	without ROPS	with ROPS
BW 219 DH-4i	33,353	44,053
BW 219 PDH-4i	33,353	44,053

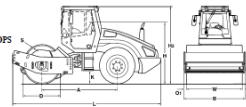
#### Standard Equipment

- BOMAG ECOMODE
- Anti Slip Control (ASC)
- Warning, information and operation displays with LCD
- Hydraulic travel and vibration drive
- Hydraulic articulated steering
- Articulated joints lock
- Rear axle with twin spring accumulator brakes
- No-Spin differential lock
- Warning horn
- Single lever control for travel and vibration
- Shock-mounted swivel seat, adjustable in height and length (Cabin)
- Contact scrapers (DHL/Plastic)
- Scrapers (DHL/Steel)
- Emergency STOP
- Noise insulation
- Backup warning system

#### Optional Equipment

- \* ROPS/FOPS cabin with seat belts
- Working lights front/rear
- ROPS with safety belt
- Radio (Bluetooth)
- Rotary beacon
- Indicator and hazard lights
- Contact scrapers (DHL/Steel)
- BOMAG Link-Meter (BLM)
- TERDAMETER 811/Meter
- BOMAG Documentation system
- Special painting
- Environmentally compliant hydraulic oil
- Air condition
- Sun roof
- Slidable seat (DSH)
- Puffing equipment kit
- Backup warning buzzer with broadcast technology
- Rearview camera
- Protective ventilation system

\* Standard delivery with CE conformity (valid within European Union)



Dimensions in mm	A	B	D	H	H1	K	L	Q1	S	W
BW 219 DH-4i	3255	2300	1400	2288	3022	450	6338	85	40	2130
BW 219 PDH-4i	3255	2300	1500	2288	3022	450	6338	85	35	2130

#### Technical Data

	BOMAG BW 219 DH-4i	BOMAG BW 219 PDH-4i
<b>Weight</b>		
Operating weight (C/C) w. ROPS-cabin	19,200	19,450
Asks load, drum C/C	13,500	13,150
Asks load, wheels C/C	6,300	6,300
Static linear load C/C	60,6	60,6
<b>Dimensions</b>		
Working width	2,130	2,130
Track radius, inner	3,890	3,890
<b>Driving Characteristics</b>		
Speed	0 - 13,0	0 - 13,0
Max. gradability without/vibr.	58/53	60/58
<b>Drive</b>		
Engine manufacturer	Deutz	Deutz
Type	TCD 6.1 L 6	TCD 6.1 L 6
Emission stage	Stage 3	Stage 3
Cooling	Liquid	Liquid
Number of cylinders	6	6
Performance ISO 9446	150,0	150,0
Performance SAE J 1995	201,0	201,0
Speed	min-1	2,200
Fuel	diesel	diesel
Electric equipment	V	12
Drive system	hydraul.	hydraul.
Drum driven	standard	standard
<b>Drums and Tyres</b>		
Number of pad feet	150	137
Area of one pad foot	cm <sup>2</sup>	100
Height of pad foot	mm	23,1-26/12PR
Tyre size		23,1-26/12PR
<b>Brakes</b>		
Service brake	hydraul.	hydraul.
Parking brake	hydromec.	hydromec.
<b>Steering</b>		
Steering system	oscill.artic.	oscill.artic.
Steering method	hydraul.	hydraul.
Steering, oscillating angle +/-	grad	35/12
<b>Exciter system</b>		
Drive system	hydraul.	hydraul.
Frequency (1)	Hz	26
Frequency (2)	Hz	31
Amplitude	mm	2,101,20
Centrifugal force	kN	220/240
Centrifugal force	t	33,3/24,5
<b>Capacities</b>		
Fuel	l	340,0

Tolerances according to ISO 9001. Machines may be driven with options.



Bomag technical data sheet (<http://www.bomag.com/world/en/products/soil-compaction/Single-Drum-Rollers-16-to-26-tons/BW+219+DH-4i:-4.html>)



**DRUM TYPES & WIDTH**




84"
SV505D-1
SV505T-1

**APPLICATIONS:**

- Medium-to-High Compaction Soil Jobs
- Wide Variety of Soils and Rockfill
- Highway and Airport Subgrades and Subbases
- Embankments
- Dams and Reservoirs
- Large Commercial and Industrial Tracts

**FEATURES & BENEFITS:**

- High Centrifugal Force Outputs
- Superior Shock Isolation Systems
- Dual Amplitude – Dual Frequency
- Choice of Drum Configurations
- Drum and Axle Drives for Traction
- Heavy-Duty Center Hitch Design
- ROPS and Seat Belts Standard
- Three Braking Choices
- Economical to Own and Operate

**SPECIFICATIONS:**

	SV505D-1	SV505T-1	
<b>DRUM</b>	Type	Smooth	Padfoot
	Size (WD)	84x63 in 2133x1600 mm	84x63 in 2133x1600 mm
<b>OPERATING</b>	Weight	23,525 lbs 10,670 kg	24,220 lbs 11,030 kg
	Credibility	62%	62%
<b>VIBRATION</b>	Frequency	2,200 rpm/1,850 rpm 37 Hz/29 Hz	2,200 rpm/1,850 rpm 37 Hz/29 Hz
	Centrifugal Forces	38,580 lbs/50,710 lbs 172 kN/225 kW	41,890 lbs/55,120 lbs 186 kN/245 kW
	Nominal Amplitude	04 in/10 mm 0.02 mm/2.0 mm	04 in/10 mm 0.02 mm/2.0 mm
	<b>ENGINE</b>	Cummins (Tier 3) USB4.5	Cummins (Tier 3) USB4.5
Make & Model			
	Horsepower	130 Hp @ 2300 rpm 97 kW @ 2300 min <sup>-1</sup>	130 Hp @ 2300 rpm 97 kW @ 2300 min <sup>-1</sup>
<b>BRAKING</b>	Hydraulic Service Brake + SAHR + Combined Footbrake		



FOR MORE INFORMATION, PLEASE SEE DRUM CONFIGURATION EXPLANATION ON PAGE 6.

Sakai SV 505 technical data sheet



## APPENDIX B

### SOIL PROFILE and SITE CONDITIONS

**Pile driving**

**Sandy ground**

*Site 3 Bangsan, Chon Buri*

KASEMDESIGN AND CONSULTANT CO., LTD. 180/61 - 62, 95 Sukawat Modern Condominium, 7th Floor, Sukawat Rd., Ratturana, Bangkok 10140 Tel. (66) 818 - 0881 - 1 Fax. (66) 818 - 1349 Website: www.kasemdesign.com E-mail: kacon@kasemdesign.com														
SUMMARY OF TEST RESULT														
Project : <b>ที่ 16 ลอด คอนโดมิเนียม</b>														
Location : <b>ตำบลบางสน อำเภอเมืองจันทบุรี จังหวัดจันทบุรี</b>										Boring : <b>BH - 3</b>				
Sample No.	DEPTH. m.		PHYSICAL PROPERTIES			ATTEBERG LIMITS			Soil Class.	ENGINEERING PROPERTIES				
	FROM	TO	W <sub>n</sub> %	γ g/cc	% passing #4 #200	LL %	PL %	PI %		S <sub>u</sub> ton/m <sup>2</sup>	S <sub>w</sub> ton/m <sup>2</sup>	Q <sub>u</sub> 100mm	N blows/m	V <sub>s</sub> 100m <sup>2</sup>
ST 1	0.50	0.95	7.56		73.98 24.53			NP	SM				18	
ST 2	1.50	1.95	22.73		100.00 38.52			NP	SM				10	
ST 3	2.50	2.95	21.13		97.86 42.31			NP	SM				7	
ST 4	3.50	3.95	25.03		100.00 31.67			NP	SM				3	
ST 5	5.00	5.45	33.90		100.00 41.52			NP	SM				3	
ST 6	6.50	6.95	21.05			31.00	27.14	3.86	ML				4	
ST 7	8.00	8.45	15.11			31.00	25.00	6.00	CL-ML				5	
ST 8	9.50	9.95	27.09			35.20	17.14	18.06	CL				7	
ST 9	11.00	11.45	26.60			55.50	21.43	34.07	CL				30	
SS 10	12.50	12.95	25.79			34.20	15.48	18.72	CL				19	
SS 11	14.00	14.45	20.79		100.00 30.16			NP	SM				26	
SS 12	15.50	15.95	14.94	2.04						10.41			36	
SS 13	17.00	17.45	14.78		100.00 25.70			NP	SM				47	
SS 14	18.50	18.95	13.95		100.00 31.70			NP	SM				84	
SS 15	20.00	20.45											50 /3 *	
PHYSICAL PROPERTIES			ATTEBERG LIMITS					ENGINEERING PROPERTIES						
W <sub>n</sub> =	Natural Water Content		LL =	Liquid Limit		S <sub>u</sub> =	Un drained Shear Strength							
γ =	Bulk Unit Weight		PL =	Plastic Limit		S <sub>w</sub> =	Remolded Shear Strength							
G =	Specific Gravity		PI =	Plasticity Index		V <sub>s</sub> =	Vane Shear Strength							
			SL =	Shrinkage Limit		N =	Standard Penetration Number							

KASEMDESIGN AND CONSULTANT CO., LTD.															
180/61 - 62, 95 Sukasawat Modern Condoview, 7th Floor, Sukasawat Rd., Ratburana, Bangkok 10140															
Tel. (02) 818 - 0881 - 2 Fax. (02) 818 - 1369 Website: www.kasemdesigns.com E-mail: kacom@kasemdesigns.com															
SUMMARY OF TEST RESULT															
Project : ที่ 10 ซอยคลองโคกขาม															
Location : ตำบลถนนสุขุมวิท อำเภอเมืองจันทบุรี จังหวัดจันทบุรี															
Boring : BH - 1															
Sample No.	DEPTH. m.		PHYSICAL PROPERTIES				ATTEBERG LIMITS			Soil Class	ENGINEERING PROPERTIES				
	FROM	TO	W <sub>n</sub> %	γ g/cc	% passing #4	% #200	LL %	PL %	PI %		S <sub>u</sub> ton/m <sup>2</sup>	S <sub>u</sub> ton/m <sup>2</sup>	Q <sub>p</sub> ton/m <sup>2</sup>	N blows/ft	V <sub>s</sub> ton/m <sup>2</sup>
ST 1	1.00	1.45	15.20		68.50	22.87			NP	SM				15	
ST 2	2.00	2.45	20.97		93.05	25.84			NP	SM				14	
ST 3	3.00	3.45	21.05		98.65	32.48			NP	SM				8	
ST 4	4.50	4.95	23.80		98.14	36.92			NP	SM				2	
ST 5	6.00	6.45	23.22		100.00	32.72			NP	SM				4	
ST 6	7.50	7.95	23.42				38.00	23.67	16.33	CL				5	
ST 7	9.00	9.45	26.95		87.58	25.47			NP	SM				35	
ST 8	10.50	10.95	13.29	2.11			42.10	18.20	23.90	CL	9.40			62	
ST 9	12.00	12.45	22.20				42.20	18.33	23.87	CL				22	
SS 10	13.50	13.95	24.81		98.11	24.60			NP	SM				21	
SS 11	15.00	15.45	22.89		100.00	37.50			NP	SM				25	
SS 12	16.50	16.95	15.42				31.35	20.10	11.25	CL				29	
SS 13	18.00	18.45	20.51	1.37			28.90	18.57	10.33	CL	15.13			43	
SS 14	19.50	19.95	14.64				35.75	20.50	15.25	CL				56	
PHYSICAL PROPERTIES			ATTEBERG LIMITS						ENGINEERING PROPERTIES						
W <sub>n</sub> =	Natural Water Content		LL = Liquid Limit						S <sub>u</sub> = Undrained Shear Strength						
g =	Bulk Unit Weight		PL = Plastic Limit						S <sub>u</sub> = Remolded Shear Strength						
G =	Specific Gravity		PI = Plasticity Index						V <sub>s</sub> = Vane Shear Strength						
			SL = Shrinkage Limit						N = Standard Penetration Number						

Pile 3-2

KASEMDESIGN AND CONSULTANT CO., LTD.															
180/61 - 62, 95 Sukasawat Modern Condoview, 7th Floor, Sukasawat Rd., Ratburana, Bangkok 10140															
Tel. (02) 818 - 0881 - 2 Fax. (02) 818 - 1369 Website: www.kasemdesigns.com E-mail: kacom@kasemdesigns.com															
SUMMARY OF TEST RESULT															
Project : ที่ 10 ซอยคลองโคกขาม															
Location : ตำบลถนนสุขุมวิท อำเภอเมืองจันทบุรี จังหวัดจันทบุรี															
Boring : BH - 2															
Sample No.	DEPTH. m.		PHYSICAL PROPERTIES				ATTEBERG LIMITS			Soil Class	ENGINEERING PROPERTIES				
	FROM	TO	W <sub>n</sub> %	γ g/cc	% passing #4	% #200	LL %	PL %	PI %		S <sub>u</sub> ton/m <sup>2</sup>	S <sub>u</sub> ton/m <sup>2</sup>	Q <sub>p</sub> ton/m <sup>2</sup>	N blows/ft	V <sub>s</sub> ton/m <sup>2</sup>
ST 1	1.00	1.45	16.92		54.88	16.21			NP	SM				16	
ST 2	2.00	2.45	24.12		100.00	33.62			NP	SM				9	
ST 3	3.00	3.45	25.57		100.00	63.17								5	
ST 4	4.00	4.45	29.82		70.70	37.50			NP	SM				2	
ST 5	5.50	5.95	44.92				55.56	40.00	15.56	ML				6	
ST 6	7.00	7.45	21.37				37.90	28.33	9.57	ML				11	
ST 7	8.50	8.95	20.15				27.45	18.33	9.12	CL				30	
ST 8	10.00	10.45	30.21	1.87			28.50	17.50	11.00	CL	2.63			15	
ST 9	11.50	11.95	20.32	1.90			30.20	18.50	11.70	CL	2.62			17	
SS 10	13.00	13.45	26.68											18	
SS 11	14.50	14.95	22.93											25	
SS 12	16.00	16.45	14.86				21.50	18.33	3.17	CL-ML				27	
SS 13	17.50	17.95	14.87	2.14							14.72			45	
SS 14	19.00	19.45	12.47	2.11							12.46			66	
SS 15	20.50	20.95												50 / 2 "	
PHYSICAL PROPERTIES			ATTEBERG LIMITS						ENGINEERING PROPERTIES						
W <sub>n</sub> =	Natural Water Content		LL = Liquid Limit						S <sub>u</sub> = Undrained Shear Strength						
g =	Bulk Unit Weight		PL = Plastic Limit						S <sub>u</sub> = Remolded Shear Strength						
G =	Specific Gravity		PI = Plasticity Index						V <sub>s</sub> = Vane Shear Strength						
			SL = Shrinkage Limit						N = Standard Penetration Number						

Pile 3-3

Soil profile



Site condition



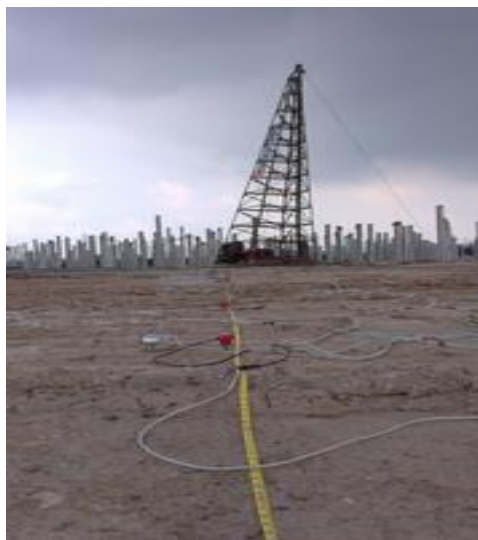
**Clayey ground**

Site 4 Bangna

BORING LOG									
PROJECT		BORING NO.		Ground elev.		DEPTH (m)		OBS. GWL. (m)	
LOCATION		BH-5		0.000 m.		30.45 m.		-0.35 m.	
INSPECTOR		START DATE		FINISHED DATE		SPT-N		PL-Wn-LL	
S. Jitwattana		21-06-55		21-06-55		B / FT		[---O---]	
SOIL DESCRIPTION	DEPTH (m)	SPT-N	B / FT	PL-Wn-LL	Su	$\gamma_1$	t/m <sup>3</sup>	SAMPLING METHOD	RECOVERY
TOP SOIL	0								
VERY SOFT TO SOFT CLAY, DARK GREY. (CH)	1							ST 1	
	2			110		0.87			
	3			118		0.62			
	4							ST 2	
	5			80		0.94			
	6							ST 3	
	7			88		1.27			
	8			88		1.10			
	9							ST 4	
	10			79		1.63			
	11			76		1.86			
SOFT TO MEDIUM CLAY, DARK GREY. (CH)	12			60		2.58			
	13							ST 8	
	14			61		2.34			
	15							ST 9	
	16			54		2.61			
	17			56		2.77			
VERY STIFF CLAY, GREY. (CH)	18							ST 10	
	19			21		3.0			
VERY STIFF SANDY CLAY, GREY. (CL)	20							SS 1	
	21			24		2.10			

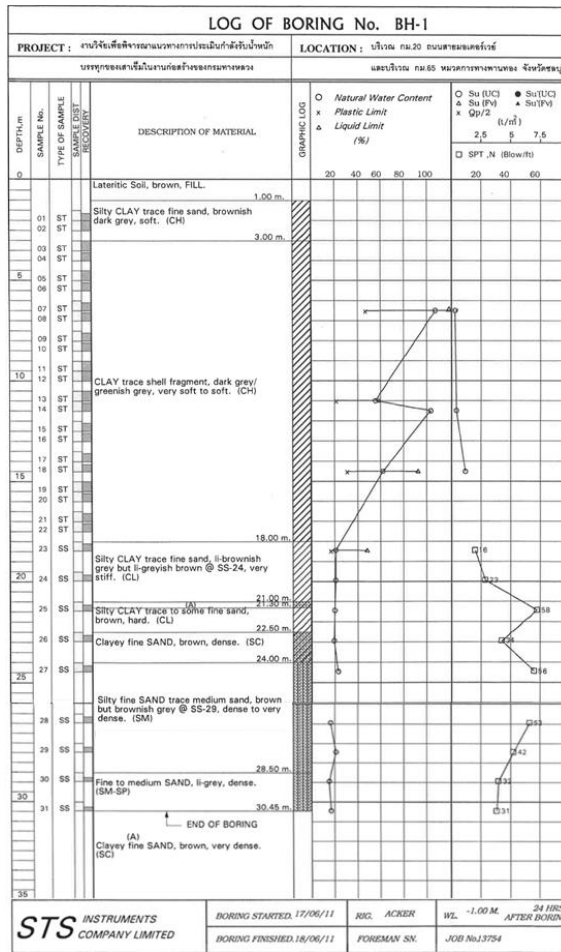
ABBREVIATIONS :  
 ST = Undisturbed Sample      LL = Liquid Limit       $\gamma_1$  = Total Unit Weight  
 SS = Split Spoon Sample      PL = Plastic Limit      SPT = Standard penetration Test  
 Wn = Natural Water Content      Su = Undrained Shear Strength

Soil profile



Site condition

Site 5, KM20

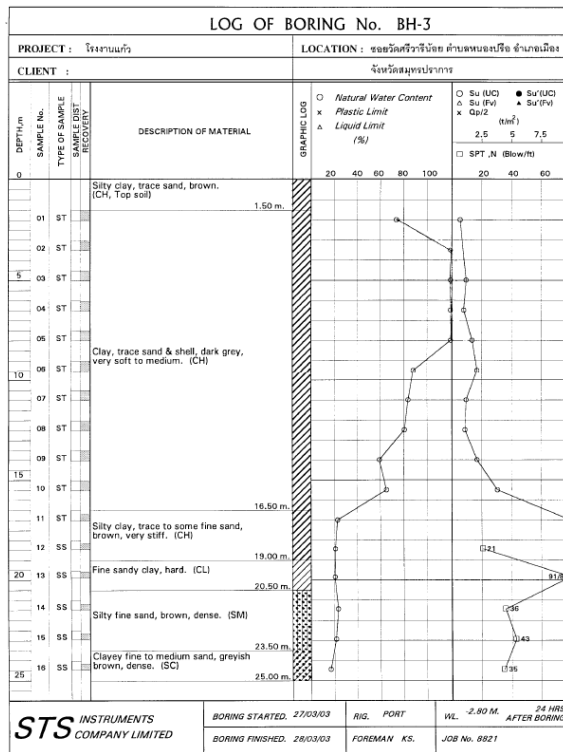


Soil profile

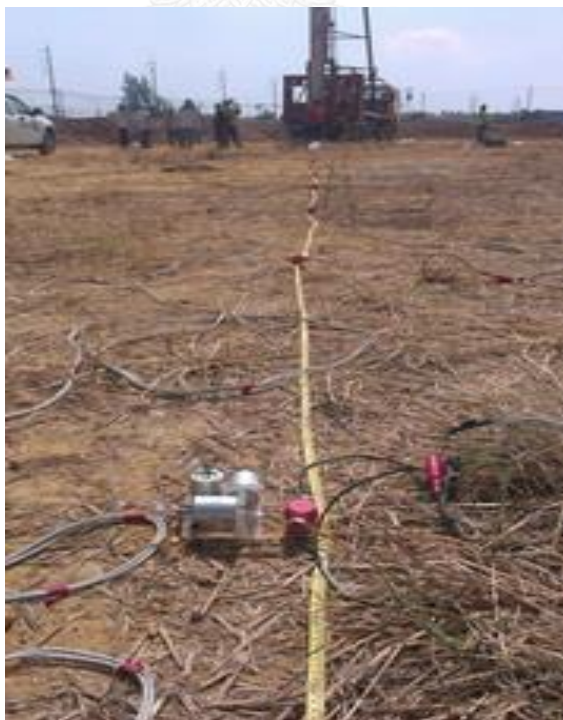


Site condition

Site 6, King power



Soil profile



Site condition



Site 7, MRT

BORING LOG.									
PROJECT: <small>WEI SHANG LIAO EXTENSION PROJECT CONTRACT NO. 100012</small>				BORING NO. BH-8		Ground elev. 0.000 m.			
LOCATION: <small>中正路與復興路 - 車站附近</small>				DEPTH (m) 50.00 m.		OBS. GWL (m) -0.80 m.			
INSPECTOR: <small>王明</small>				START DATE 16-4-55		FINISHED DATE 17-4-55			
SOIL DESCRIPTION	DEPTH (m)	GRAPHIC LOG.	METHOD	SAMPLING RECOVERY	SPT-N B / FT	PL-Wn-LL  ---○---	Su kN/m <sup>2</sup>	γ <sub>t</sub> kN/m <sup>3</sup>	
TOP SOIL.	0								
	1								
	2		ST 1						
	3		ST 2						
	4		ST 2		86	○	1.42	1.56	○
	5		ST 3		78	○	1.78	1.57	○
	6		ST 4						
	7		ST 4						
SOFT CLAY, DARK GREY.	8		ST 5		82	○	1.56	1.56	○
	9		ST 6		75	○	1.93	1.60	○
	10		ST 6						
	11		ST 7		80	○	1.52	1.54	○
	12		ST 8		72	○	2.05	1.62	○
	13		ST 8						
	14		ST 9		78	○	1.66	1.54	○
	15		ST 10						
(CH)	17		ST 11						
	18		SS 1		10	○		1.93	○
STIFF TO VERY STIFF CLAY, BROWNISH GREY.	19		SS 2		32	○			
	20		SS 2		18	○		1.88	○
(CH)	21								

ABBREVIATIONS :  
 ST = Undisturbed Sample    LL = Liquid Limit    γ<sub>t</sub> = Total Unit Weight  
 SS = Split Spoon Sample    PL = Plastic Limit    SPT = Standard penetration Test  
 Wn = Natural Water Content    Su = Undrained Shear Strength

Soil profile



Site condition

Site 9, Praram 5

STS INSTRUMENTS COMPANY LIMITED																			
SUMMARY OF TEST RESULTS																			
PROJECT THE CITY WESTIN 5 - วิทยาเขต 2										LOCATION วัดจำปา ถนนนครินทร์ จังหวัดนนทบุรี									
DATE 10/03/10			BORING No. BH-1			JOB No. 13052			BY PT		OBSERVED W.L. -0.80 M.								
SAMPLE No.	DEPTH M.		WATER CONTENT %	ATTERBERG LIMIT %			WET UNIT WEIGHT $\gamma_{wet}$	SIEVE ANALYSIS % FINER				CLASSIFICATION	UNDRAINED SHEAR STRENGTH, $0/m^2$						
	FROM	TO		LL.	PL.	PI.		No. 3/8"	No. 4	No. 10	No. 40		No. 200	UNCONFINED SHEAR		FIELD VANE SHEAR		UU TEST	POCKET PENETRATION
ST-01	1.50	2.00	92.80				1.50					CH	0.70					1.3	
ST-02	3.00	3.50	101.40				1.45					CH	0.70					1.3	
ST-03	4.50	5.00	77.30				1.55					CH	1.40					1.3	
ST-04	6.00	6.50	79.90				1.55					CH	1.20					1.3	
ST-05	7.50	8.00	58.90				1.69					CH	2.30					1.3	
ST-06	9.00	9.50	81.40				1.56					CH	2.30					1.3	
ST-07	10.50	11.00	86.90				1.50					CH	2.00					1.3	
ST-08	12.00	12.50	29.70				1.97					CH	4.50					10.0	
SS-09	13.50	13.95	27.40	48.90	21.10	27.40	1.98					CL						10.0	11
SS-10	15.00	15.45	22.60				2.00					CH						12.5	14
SS-11	16.50	16.95	28.50				1.92					CH	11.10					12.5	18
SS-12	18.00	18.45	21.40									CL						11.3	20
SS-13	19.50	19.95	17.00				2.14					CH	22.20					22.5+	43
SS-14	21.00	21.45	14.80				2.21					CH						22.5+	51
SS-15	22.50	22.95	25.00				1.94					CH						22.5+	35
SS-16	24.00	24.45	21.50							100	98	18	SM						56
SS-17	25.50	25.95	24.40										SM						52
SS-18	27.00	27.45	21.90										SM						67
SS-19	28.50	28.95	20.80							100	99	97	20	SM					48
SS-20	30.00	30.45	14.80										SM						49

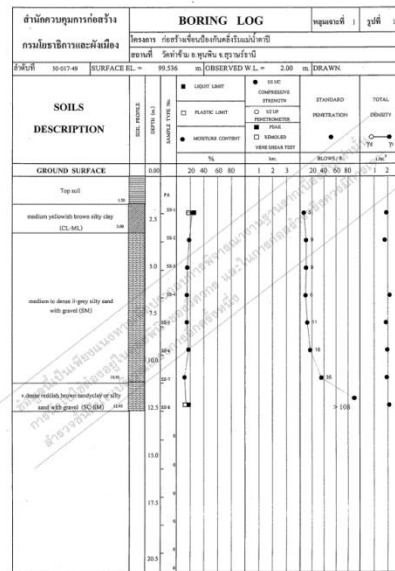
Soil properties



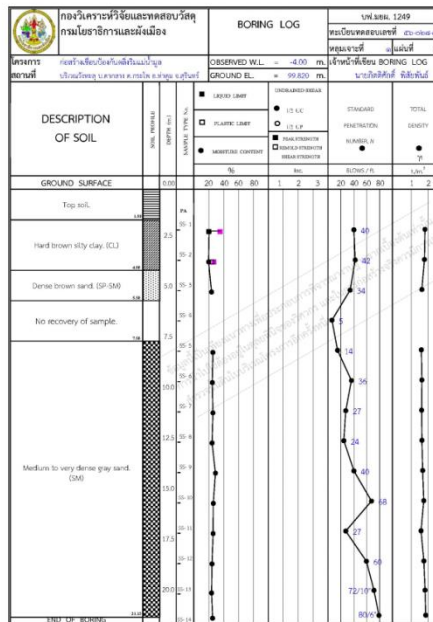
Site condition



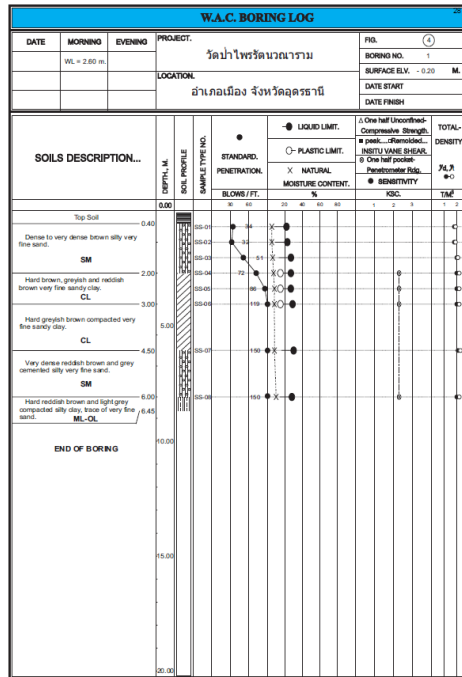
**Blasting**



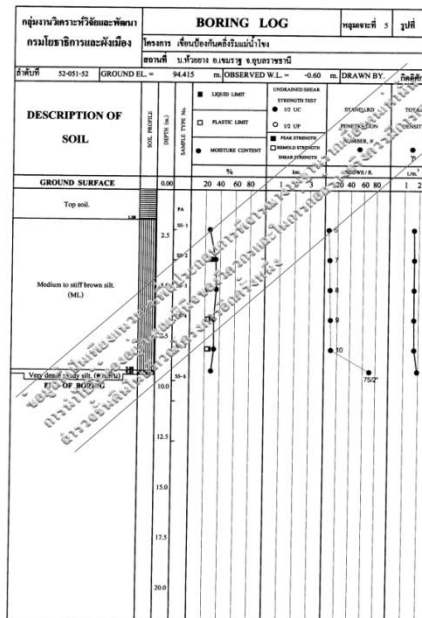
Blasting sites No. 2 (Surat Thani province)



Blasting sites No. 4 (Surin province)



Blasting sites No. 6 (Udon Thani province)

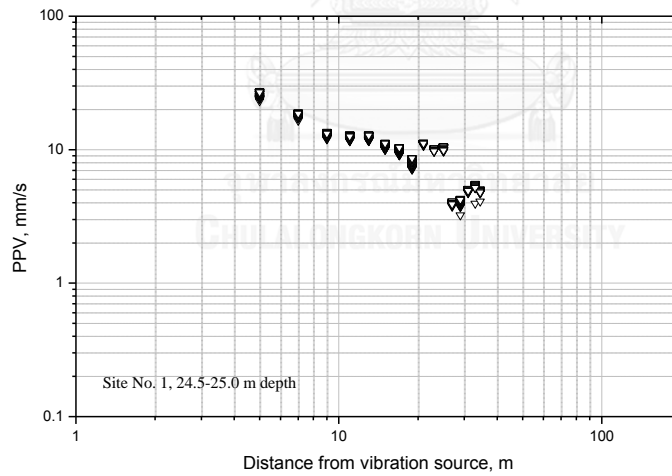
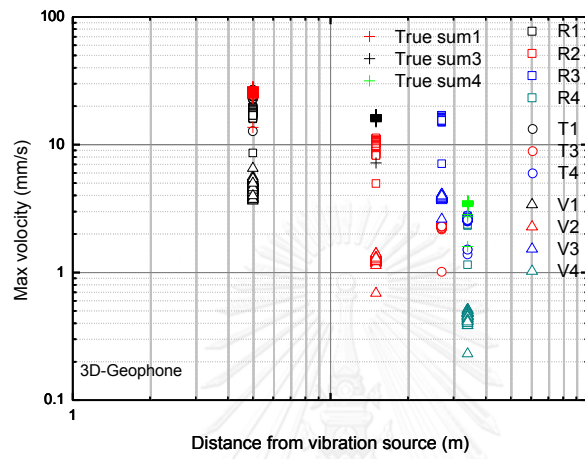


Blasting sites No. 7 (Ubon Rachathani province)

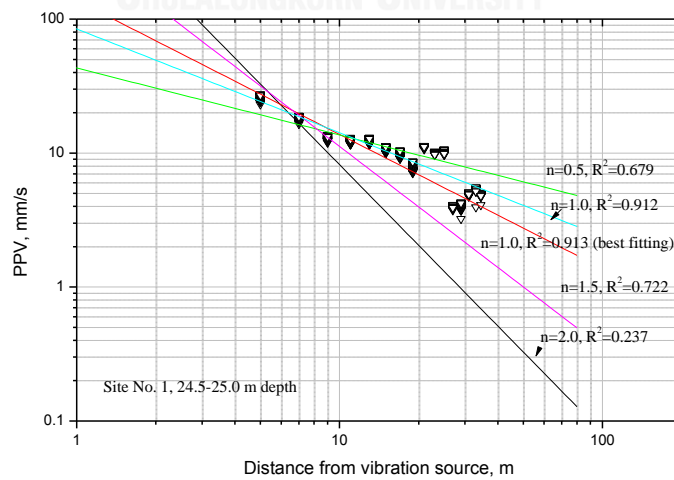
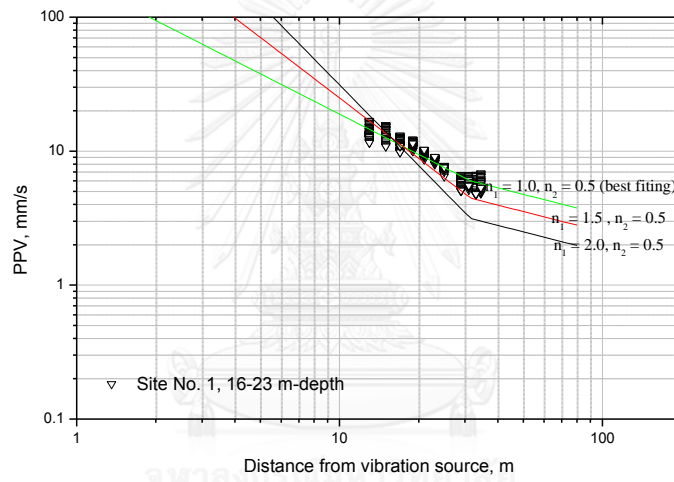
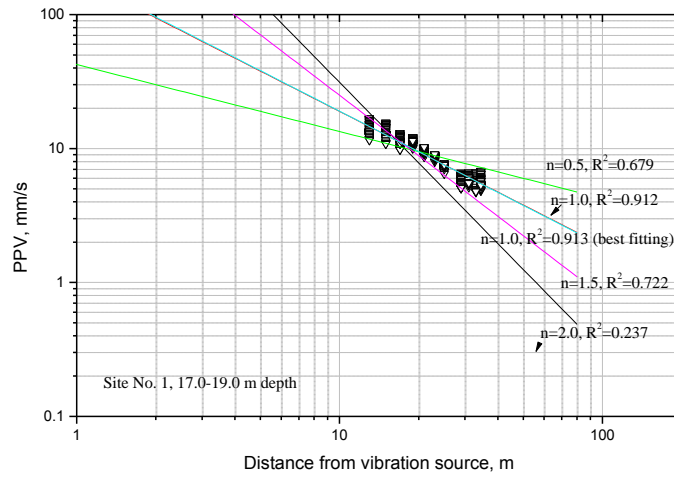
## APPENDIX C

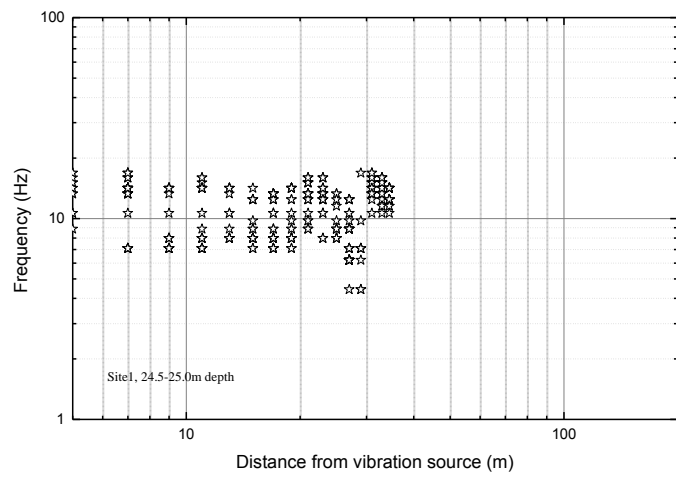
### Pile driving

#### Site No.1 (Scott)



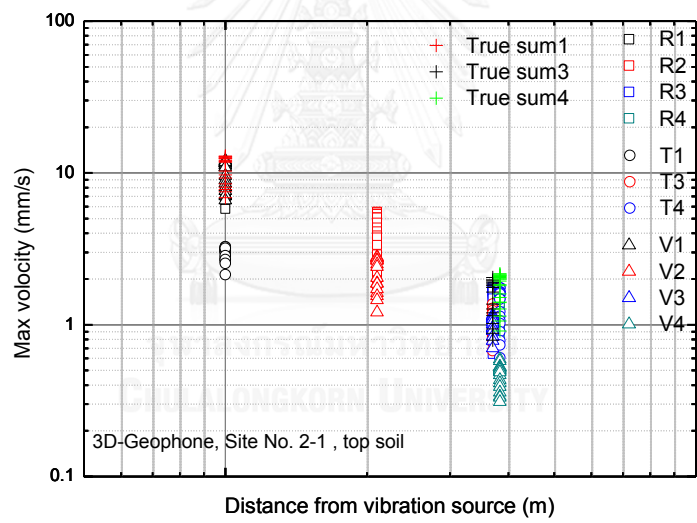


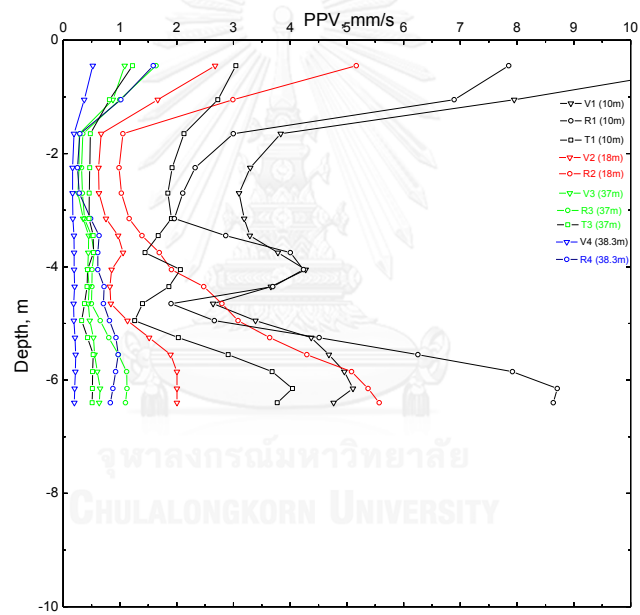
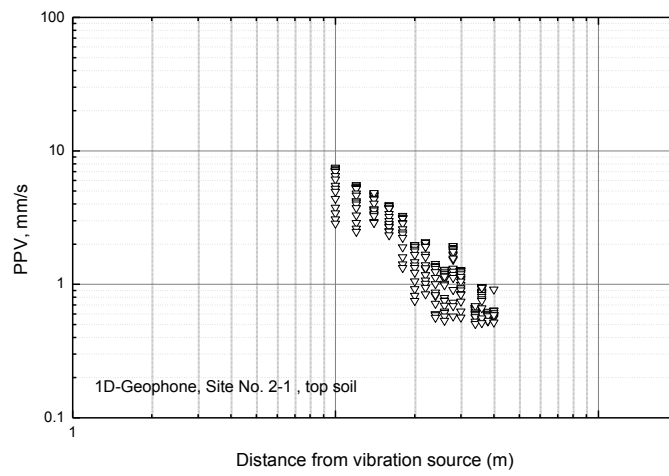


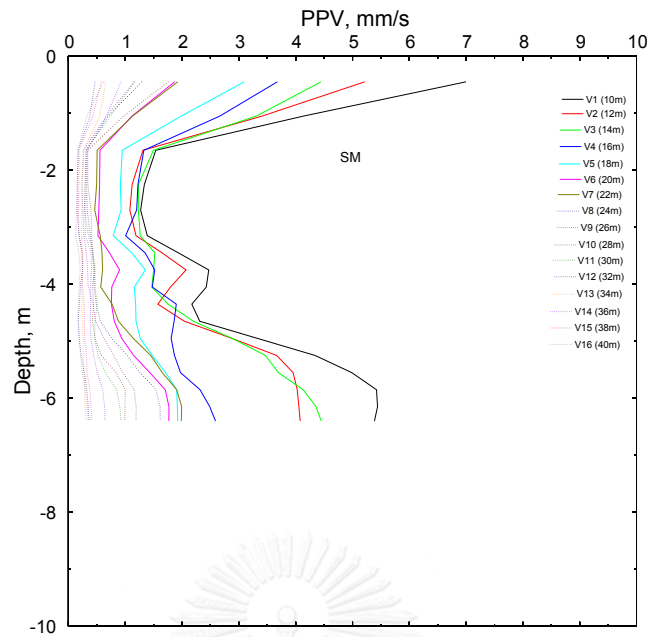


Site No. 2 (KM65)

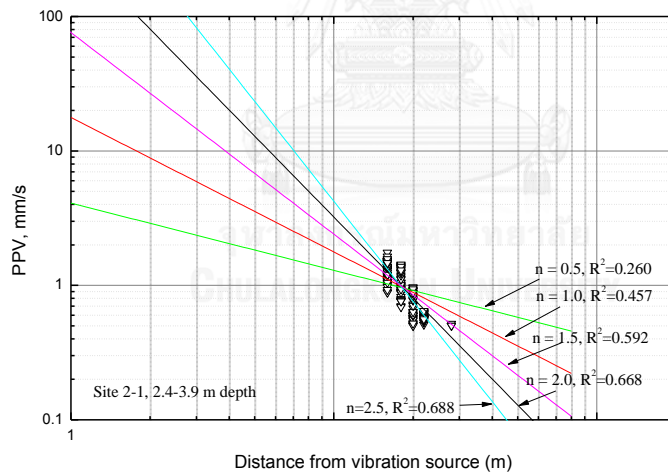
Pile 0.4x0.4x15 m



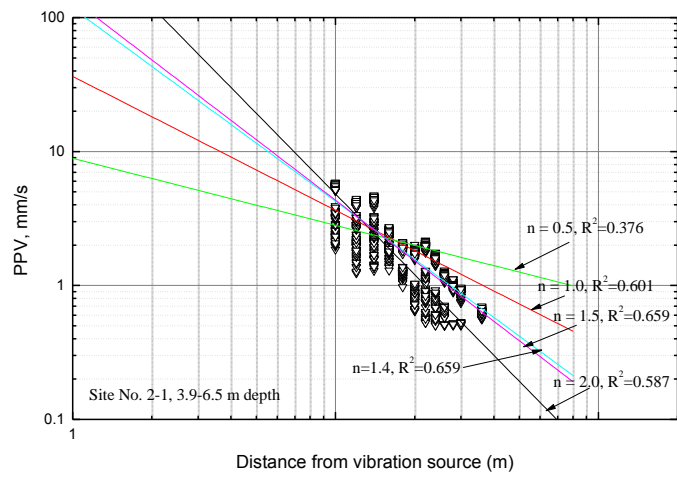




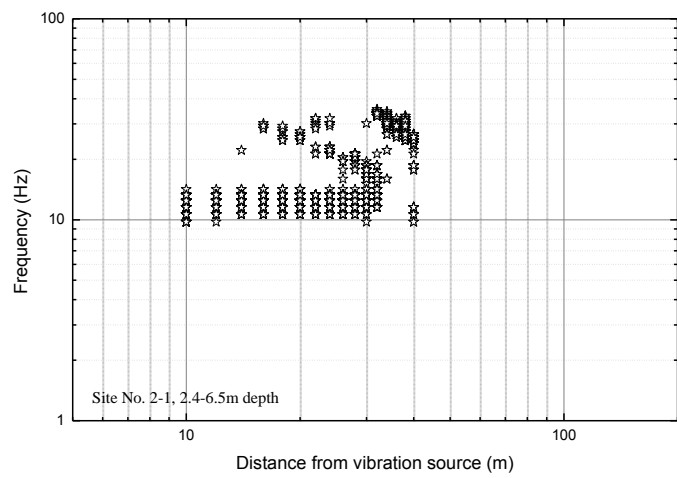
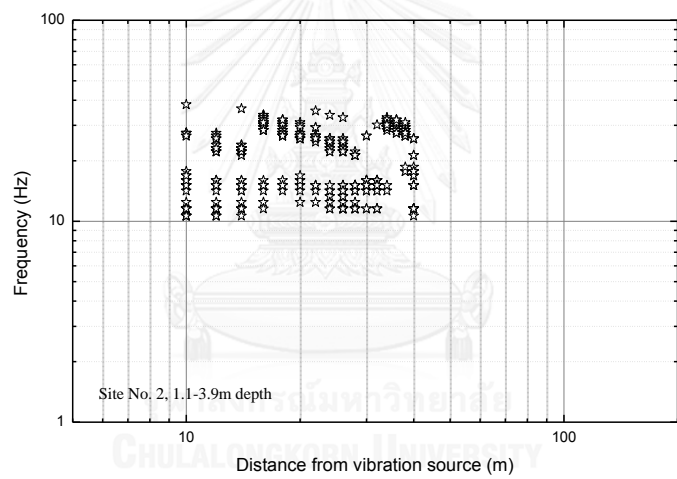
Attenuation characteristic



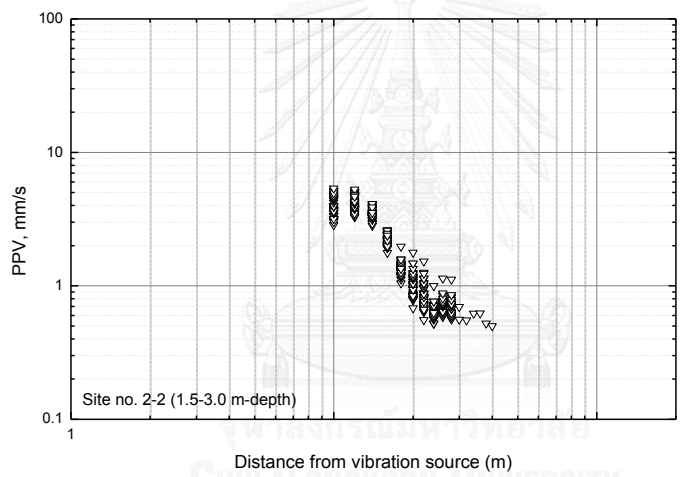
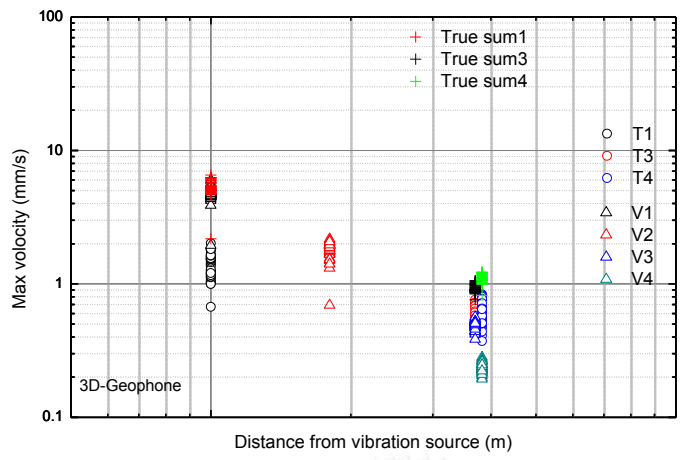


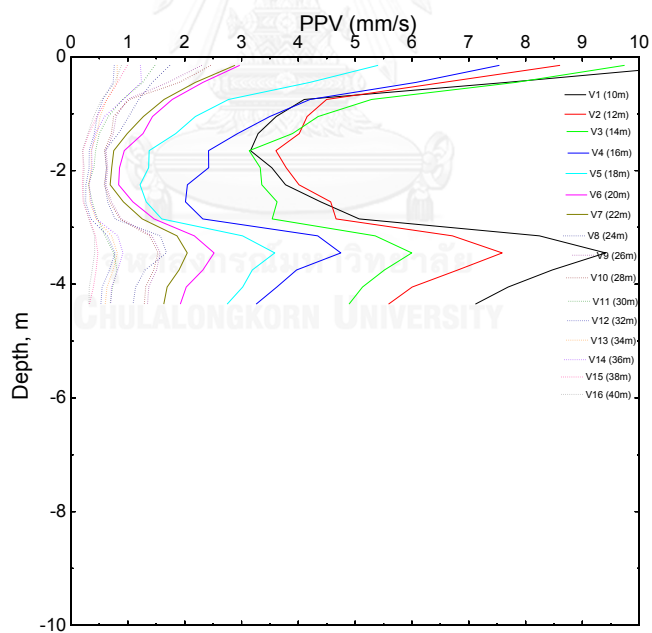
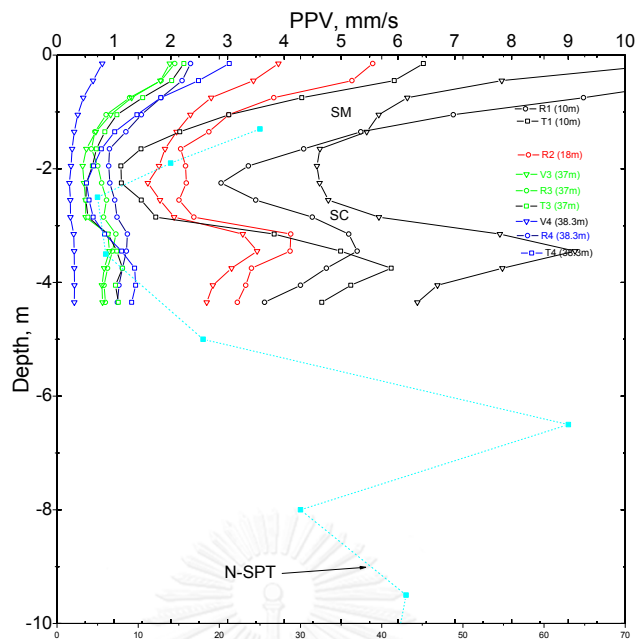


Frequencies in each depths

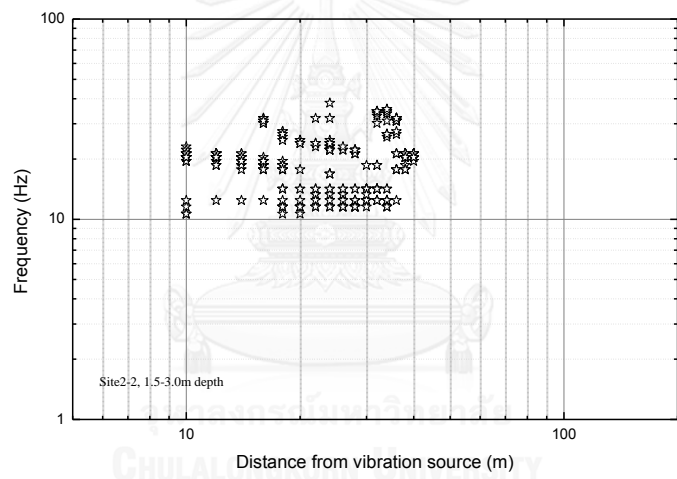
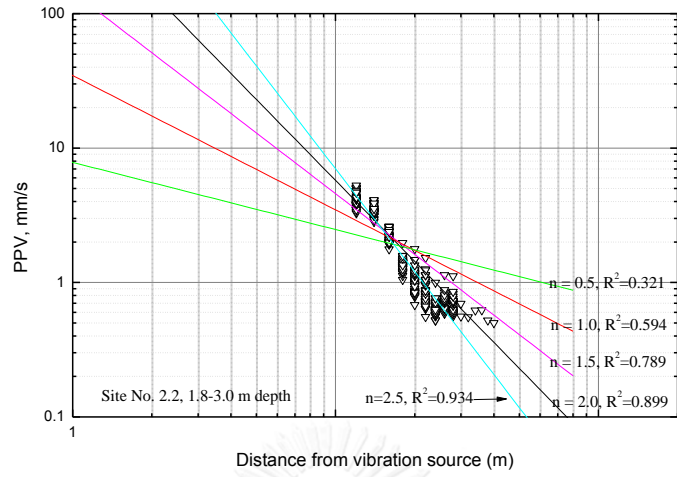


*Pile 0.6x0.6x15 m*



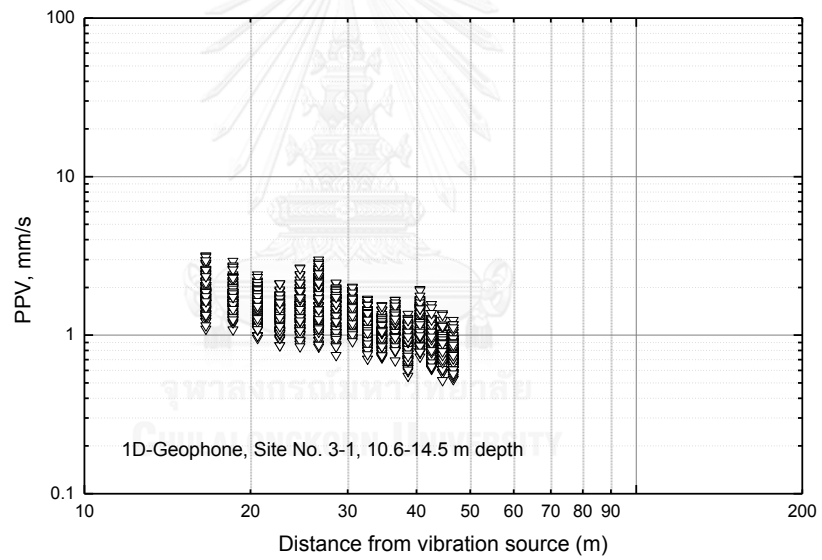
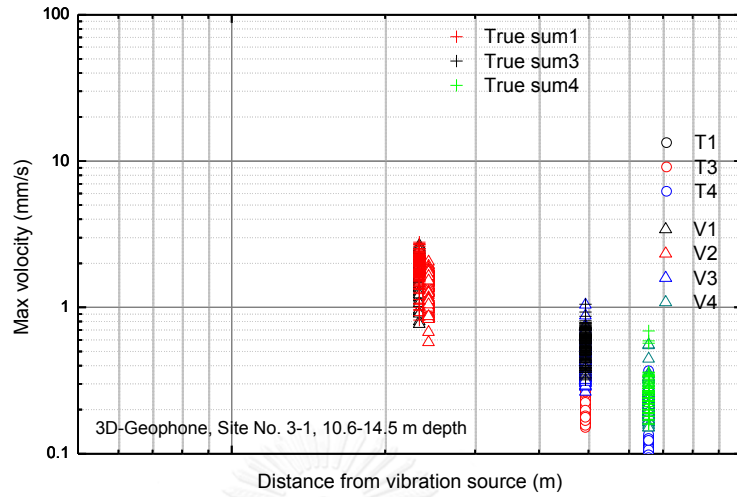


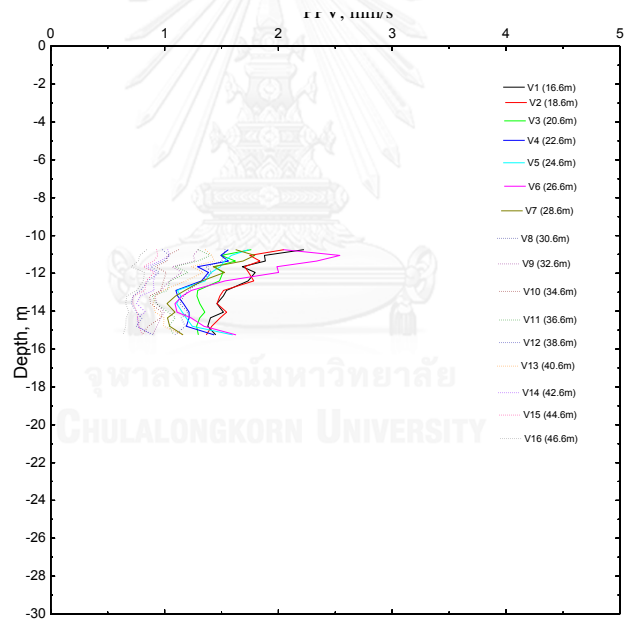
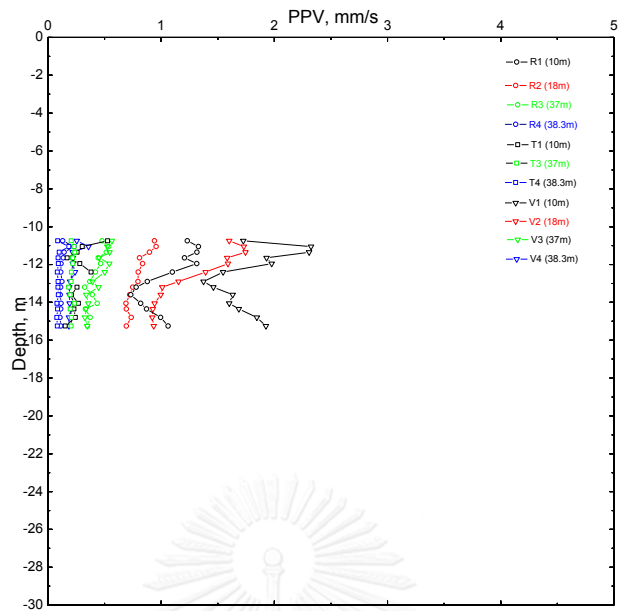
Attenuation characteristic



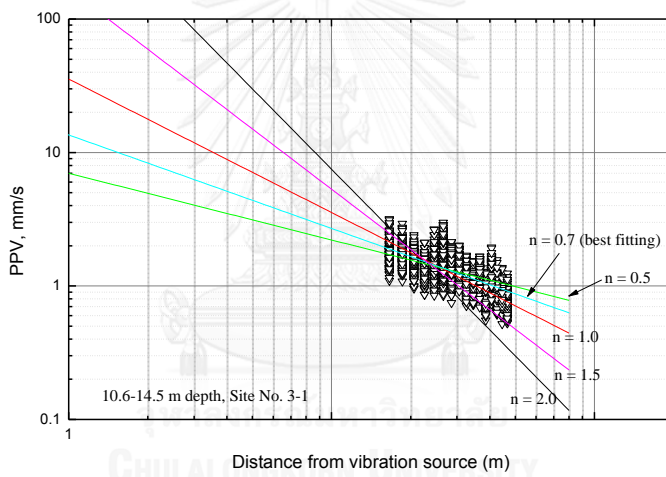
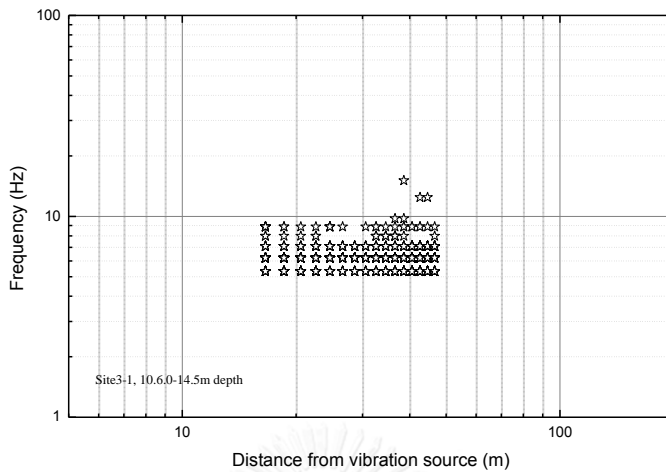
Site No.3 (Chanburi, Bangsan)

Pile No.1

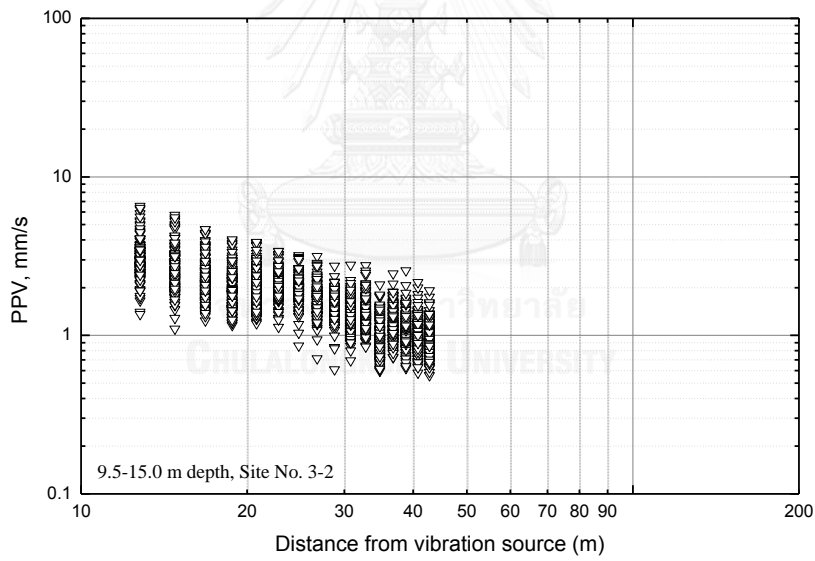
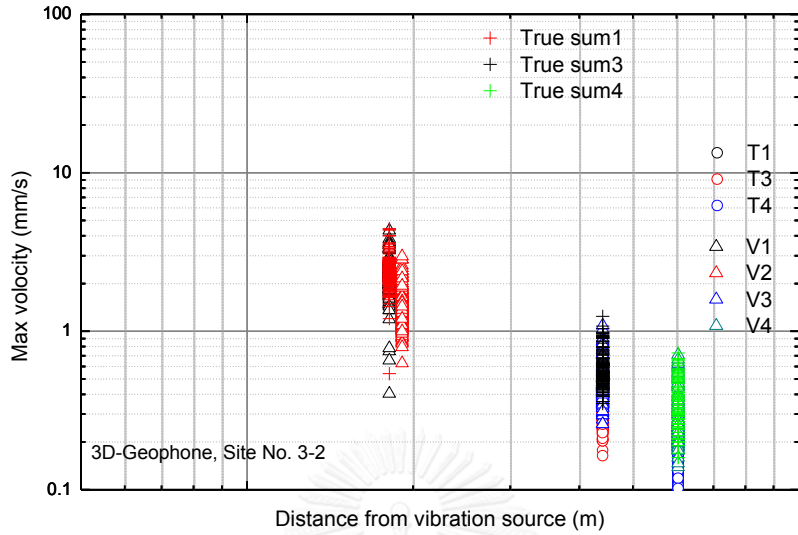




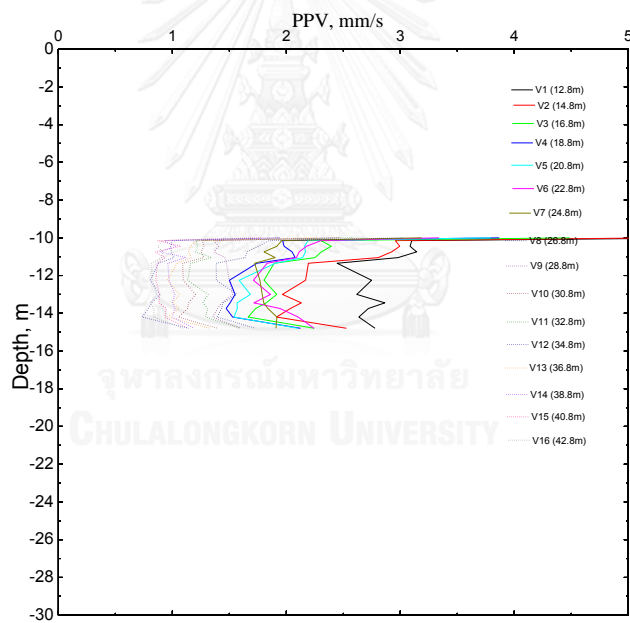
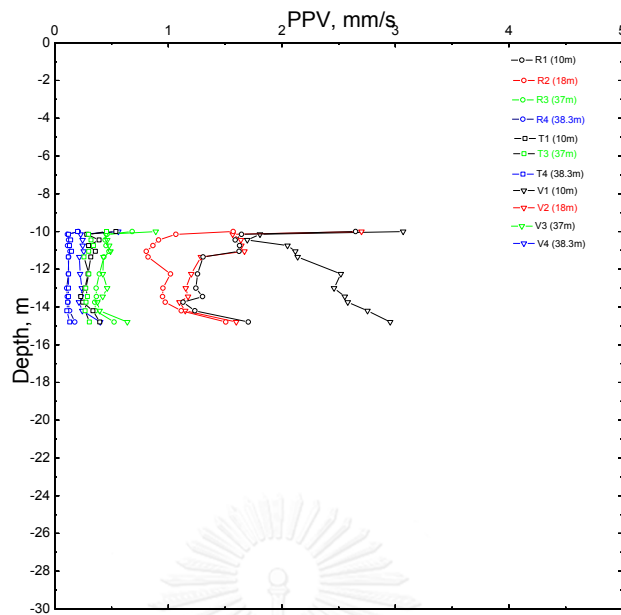
Attenuation characteristic



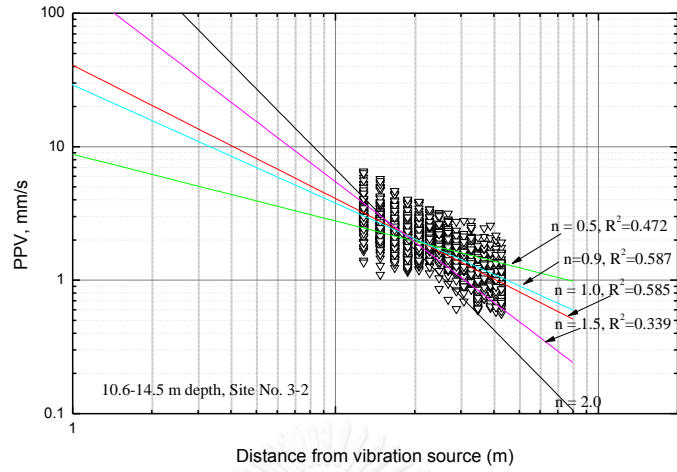
Pile No. 2



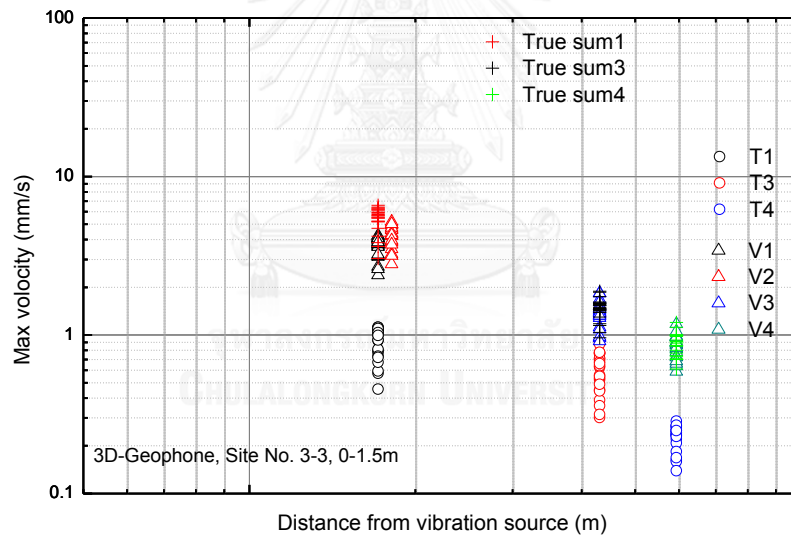


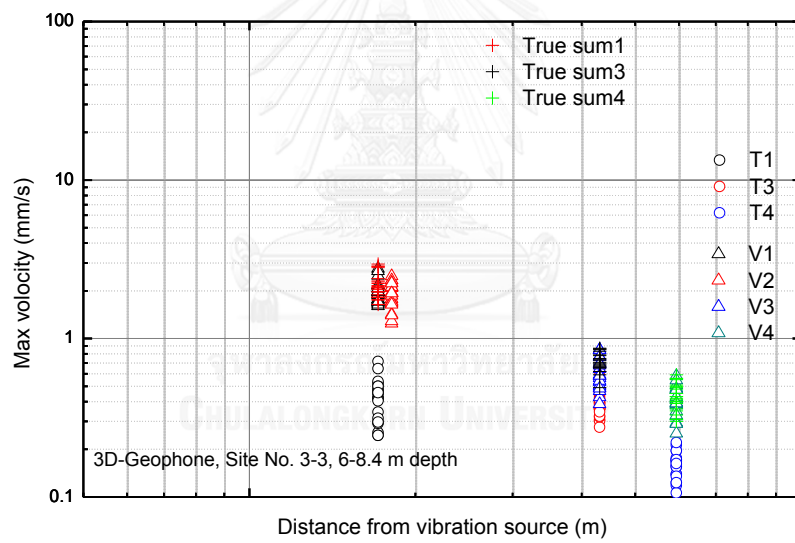
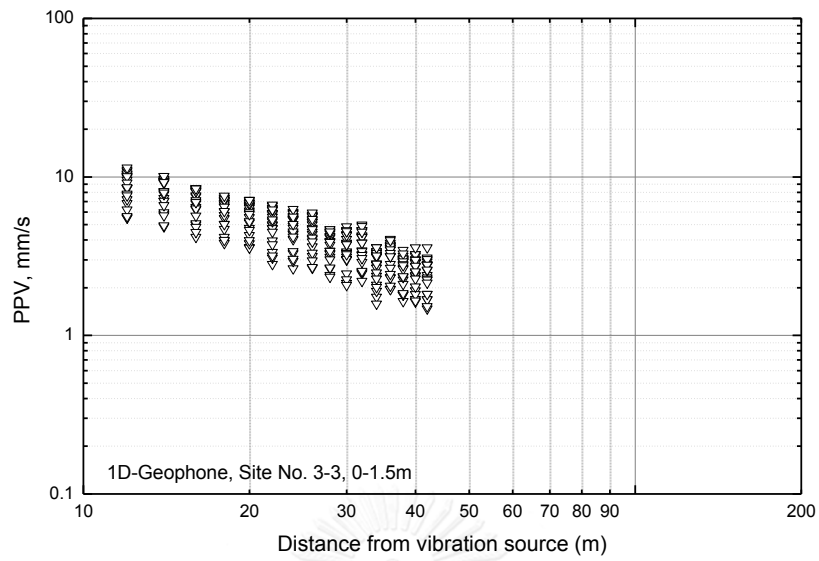


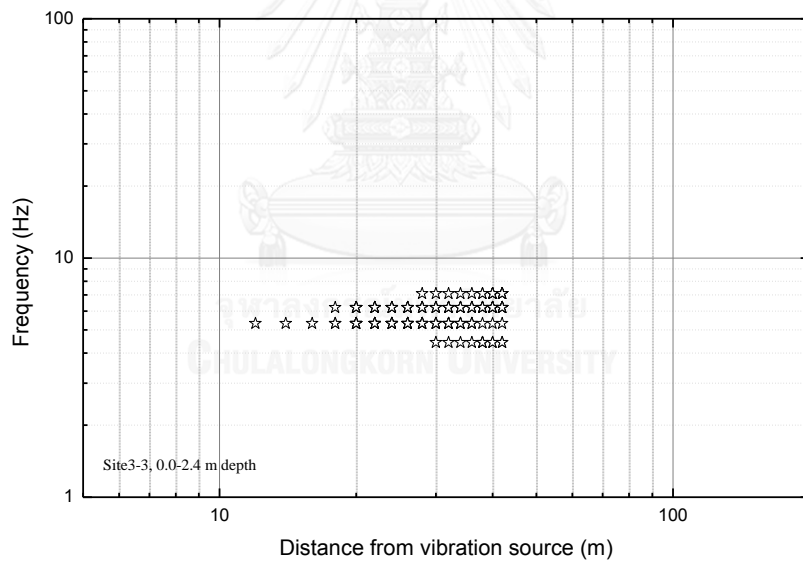
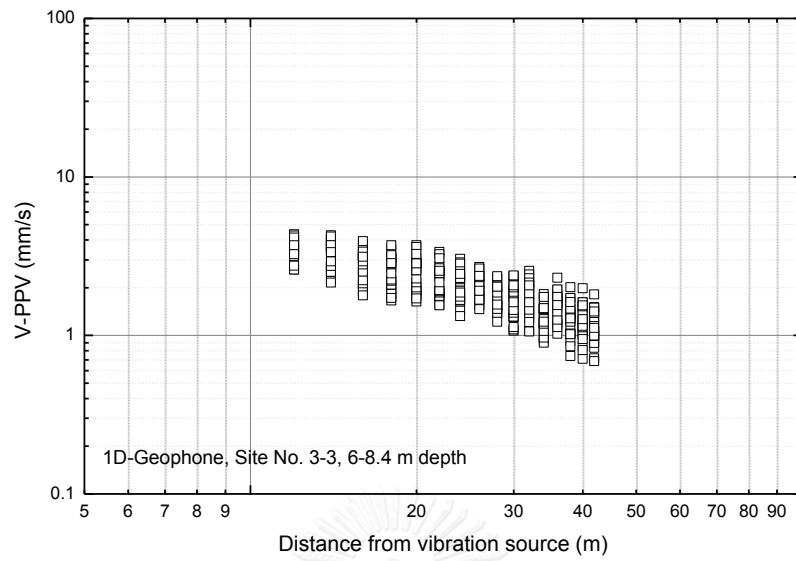
Attenuation characteristic



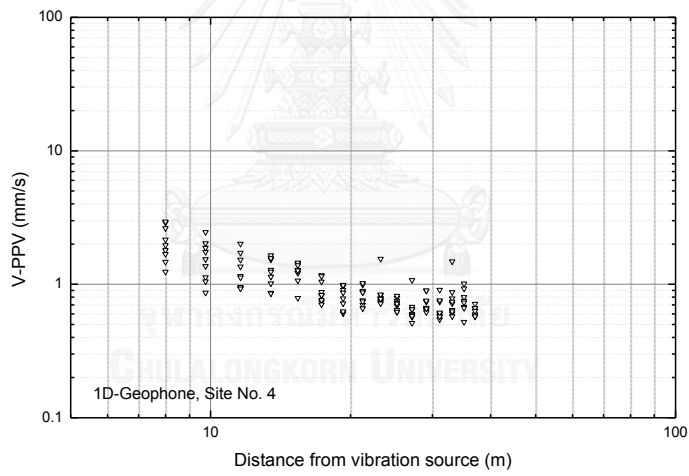
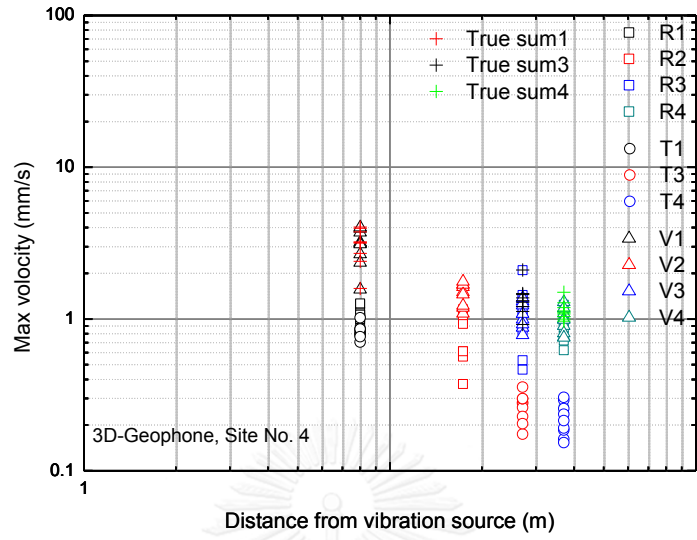
Pile No. 3

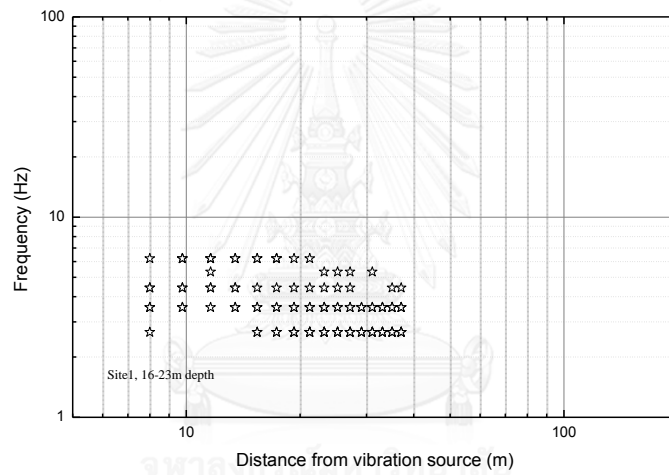
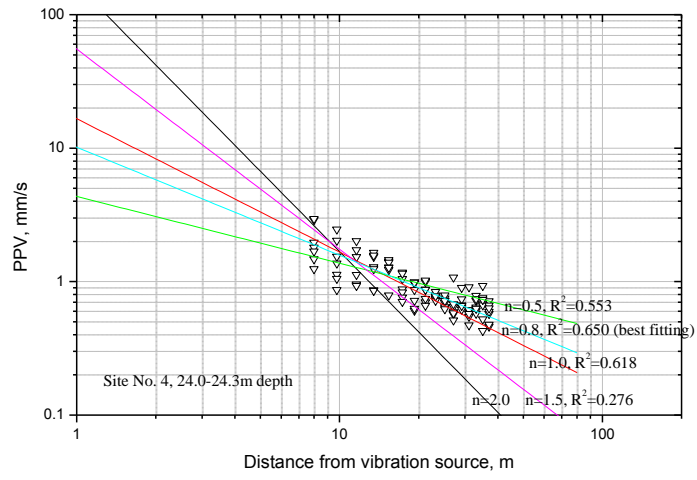




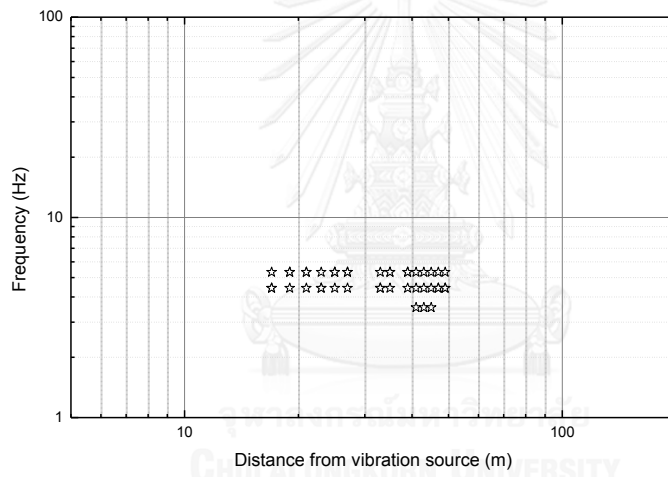
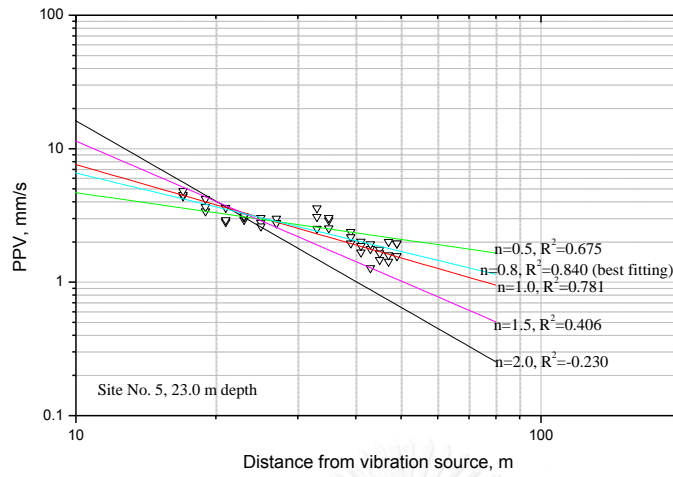


Site No. 4 (Bangna)

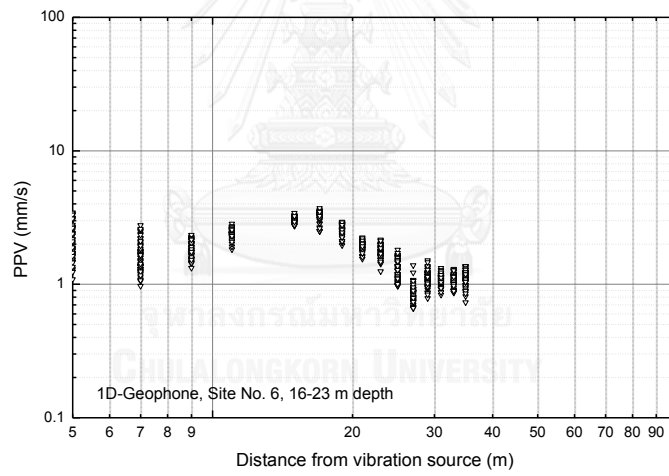
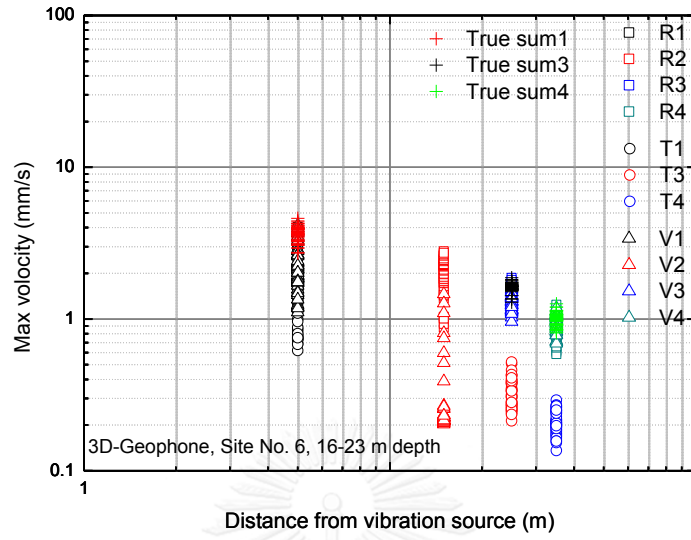




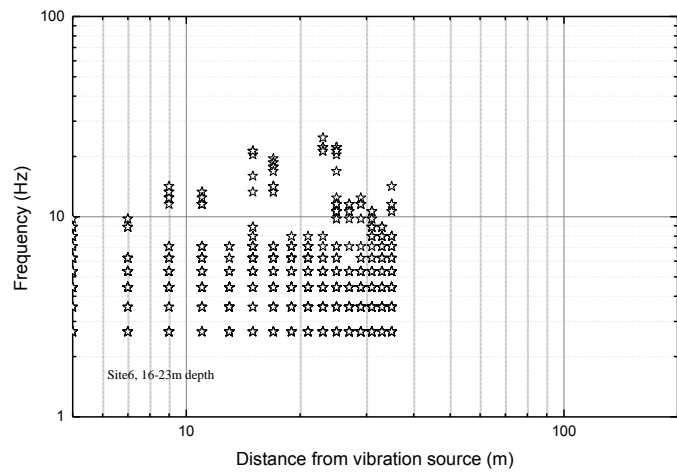
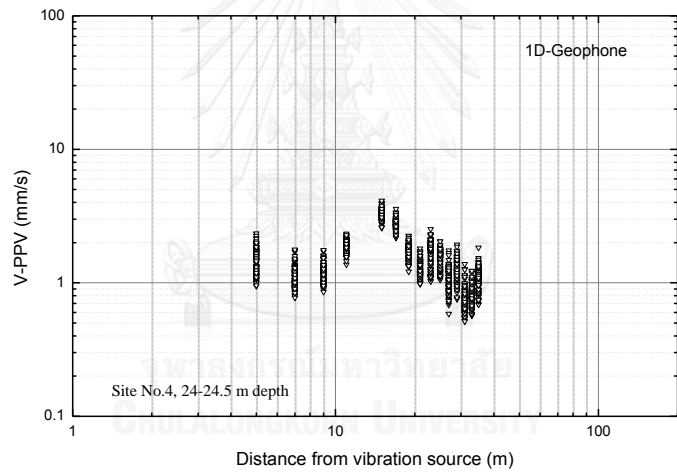
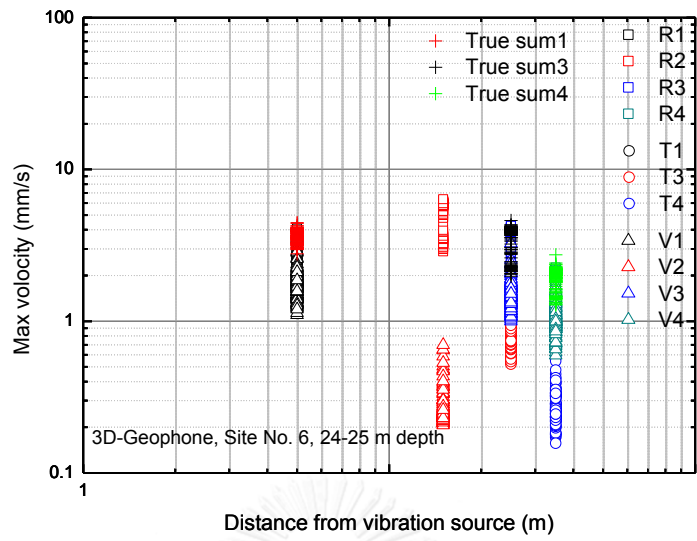
Site No. 5 (KM25)

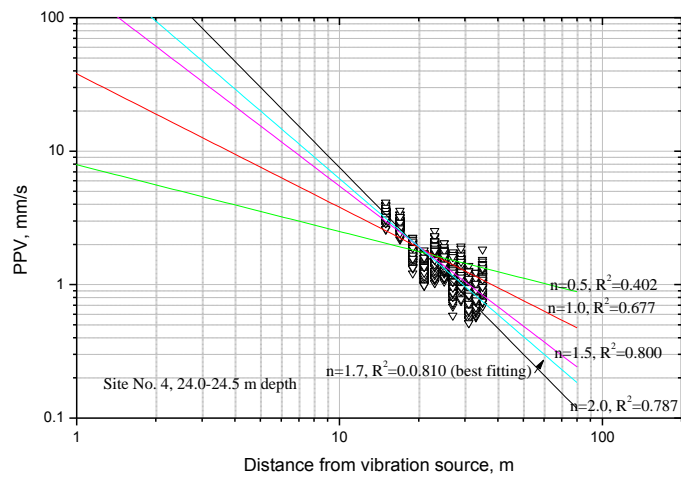


Site No. 6 (Kingpower)



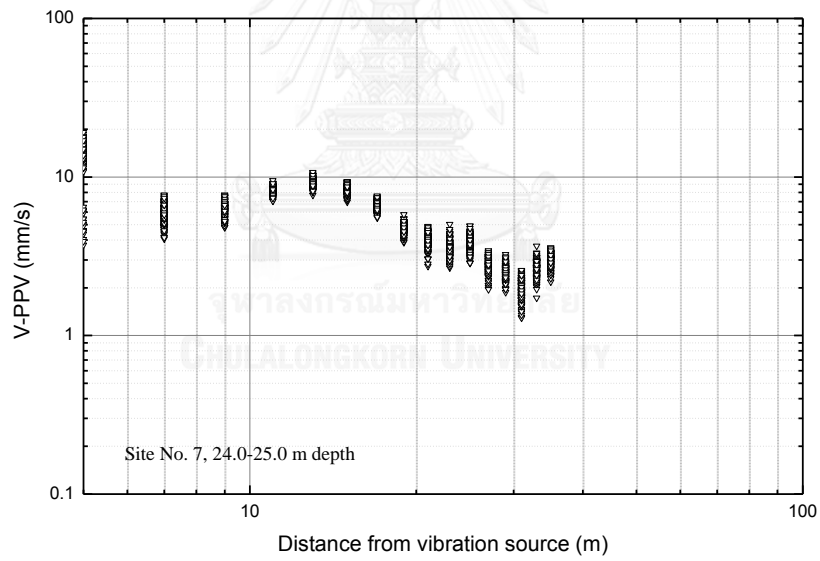
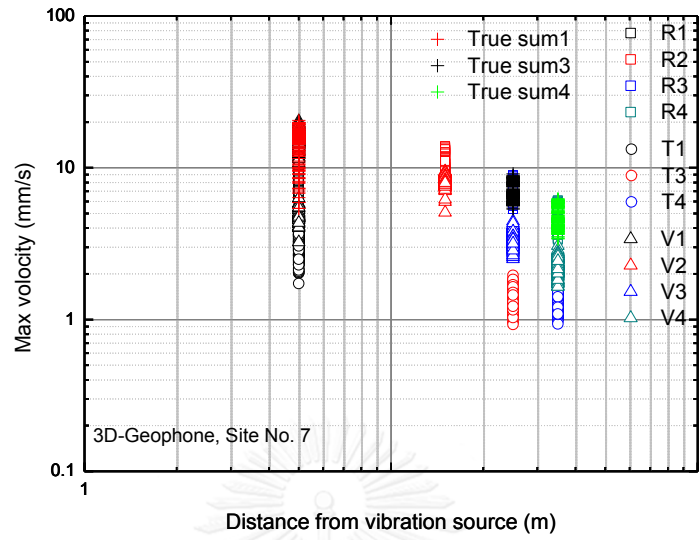




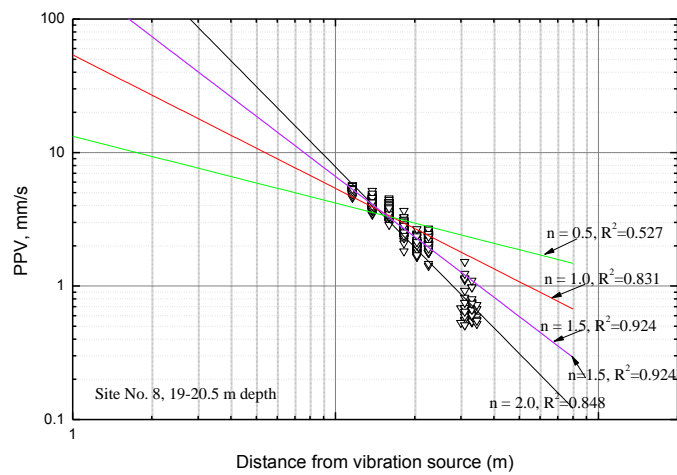
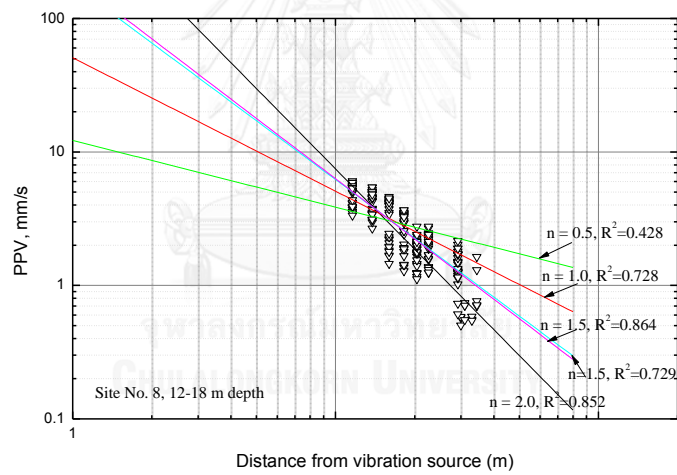
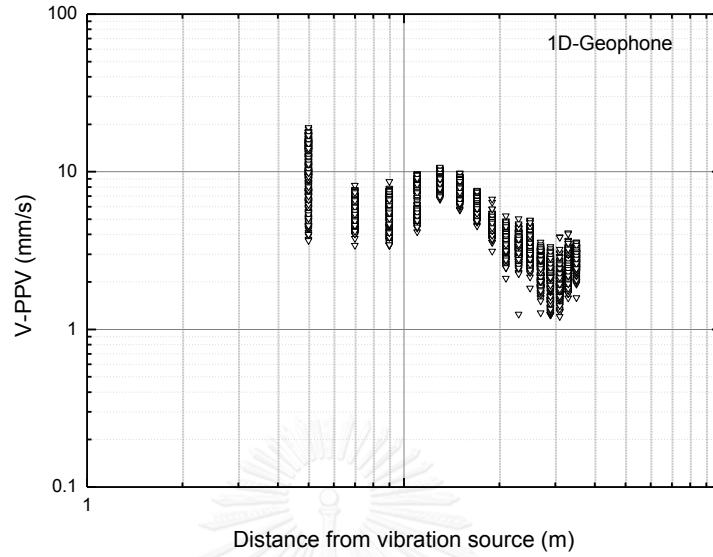


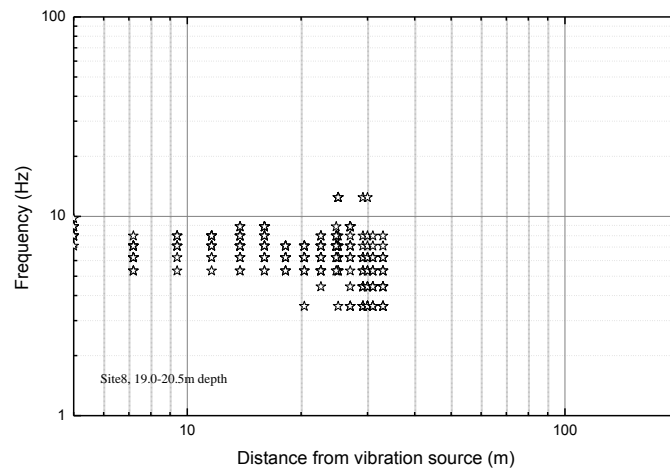
Site No.	Depth (m)	Fitting models		Fitting parameters			R <sup>2</sup>	Remarks
				k	n	a		
		Conventional models						
6	20.0-23.0 (N=46)	1	$v = k \cdot r^{-n}$	305	1.7		0.810	
		2	$v = k \cdot r^{-0.5}$	8			0.403	
		3	$v = k \cdot r^{-1.0}$	38			0.677	
		4	$v = k \cdot r^{-1.5}$	173			0.801	
		5	$v = k \cdot r^{-2.0}$	753			0.788	

Site No. 7 MRT



Site No. 8, Praram 5





**Blasting ground vibration**

**Clayey ground**

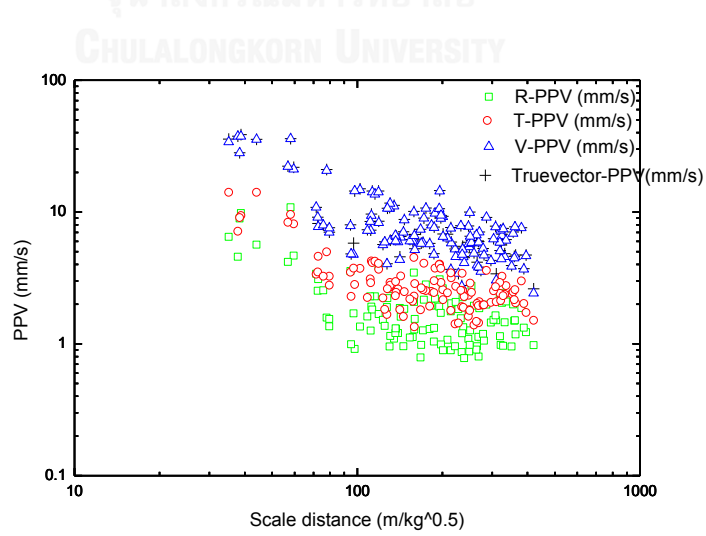
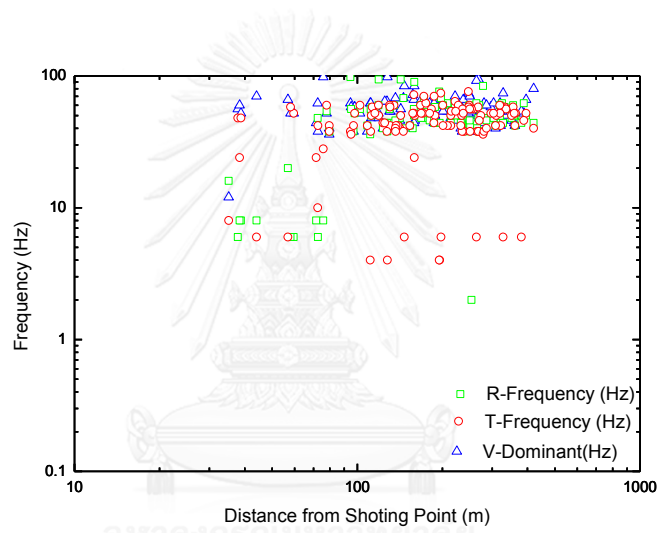
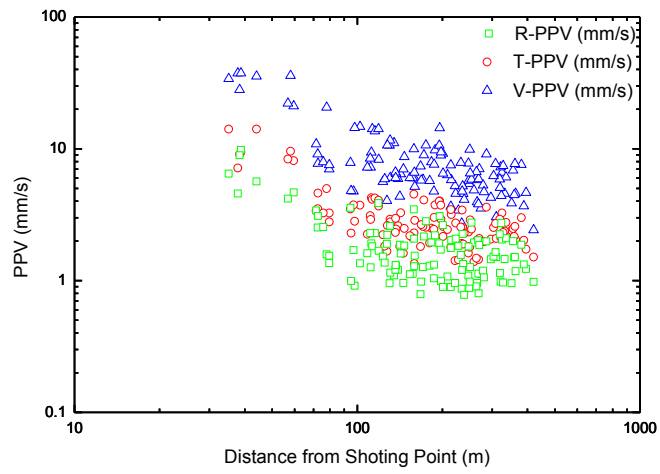
**Supan Buri province**

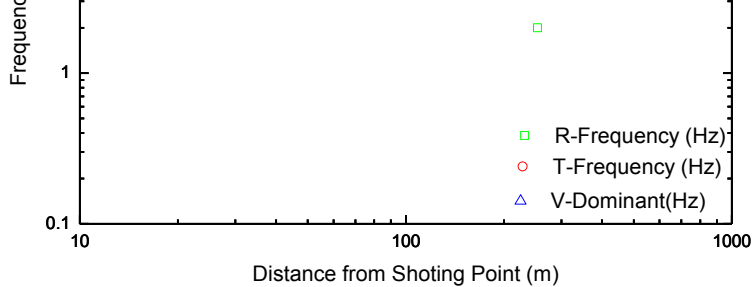
**1<sup>st</sup> Supan Buri province**

*Site condition*

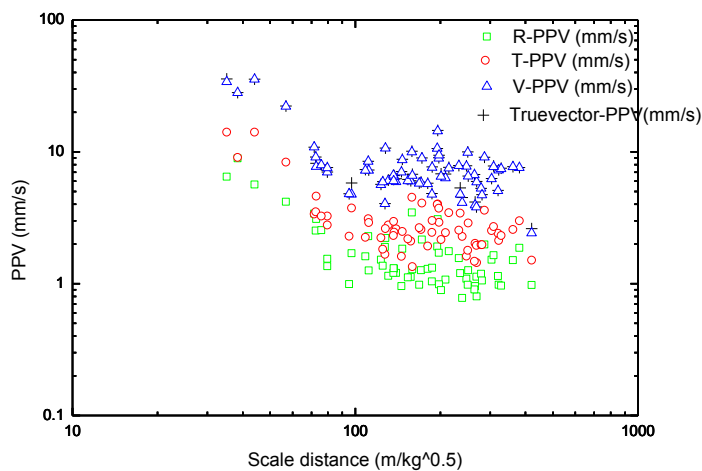
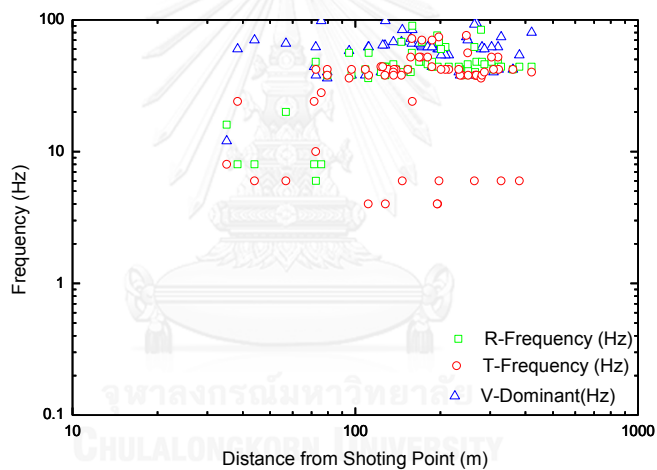
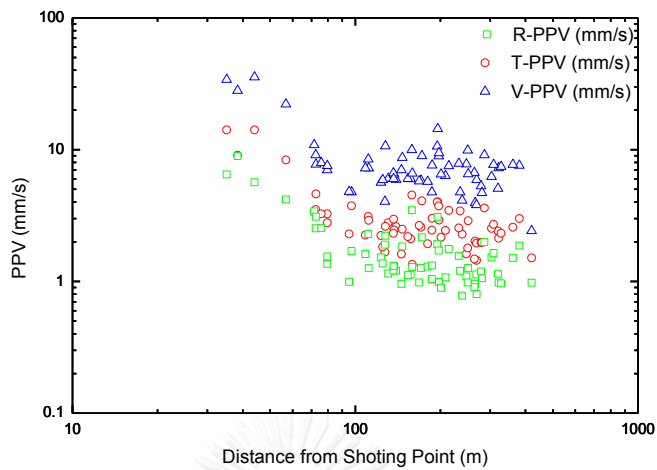


*The results of study*





2<sup>nd</sup> Supan Buri province



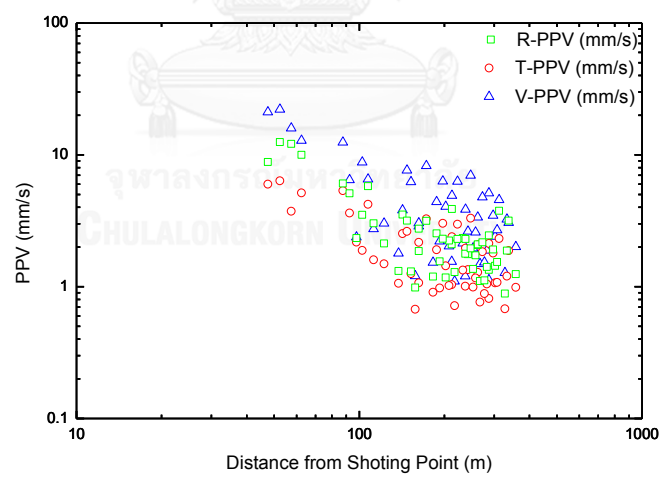
**Sandy ground**

Surat Thani province

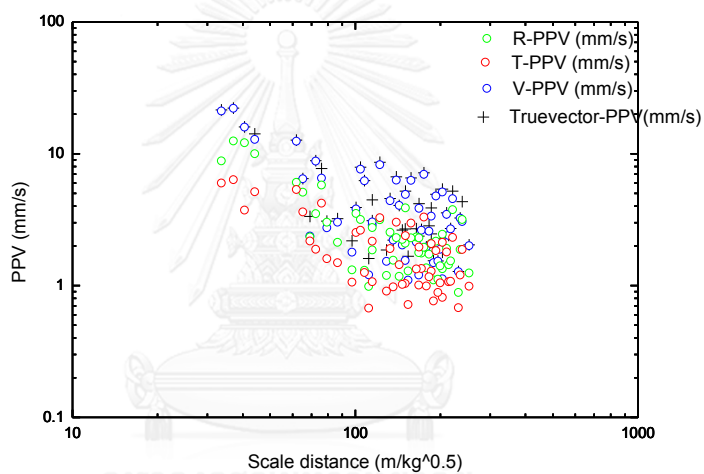
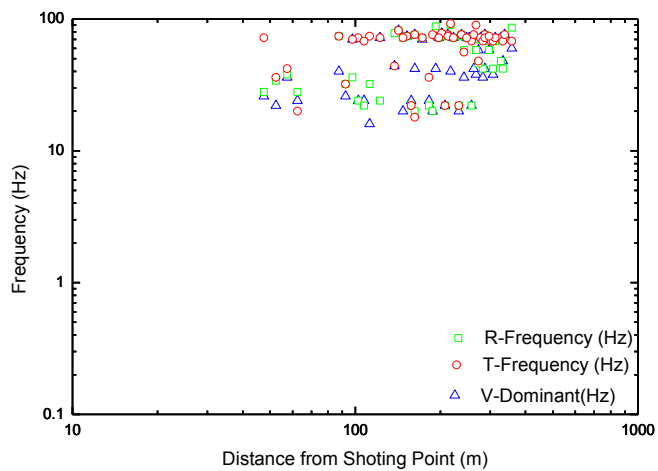
1<sup>st</sup> Surat Thani province (2kg)*Site condition*

Before

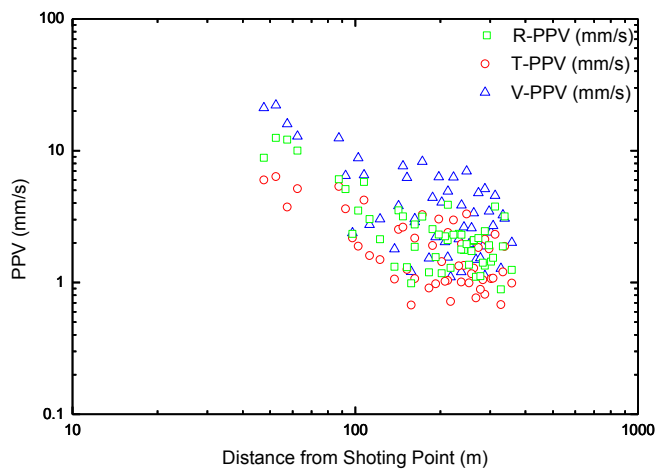
After

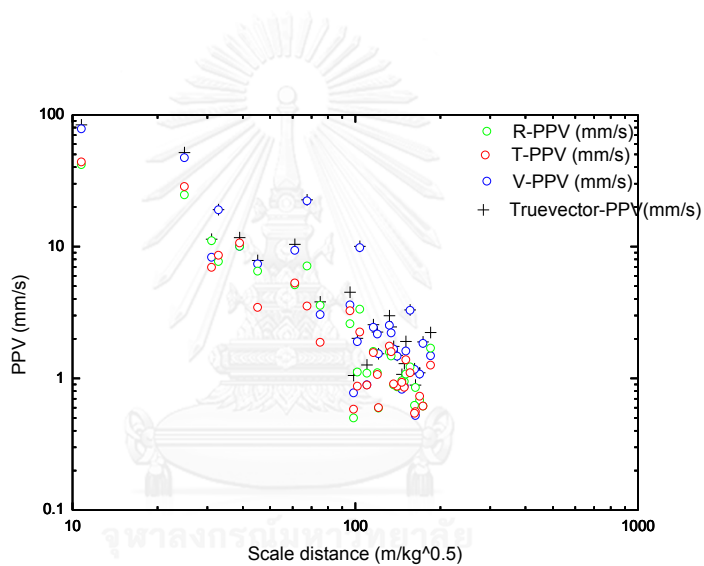
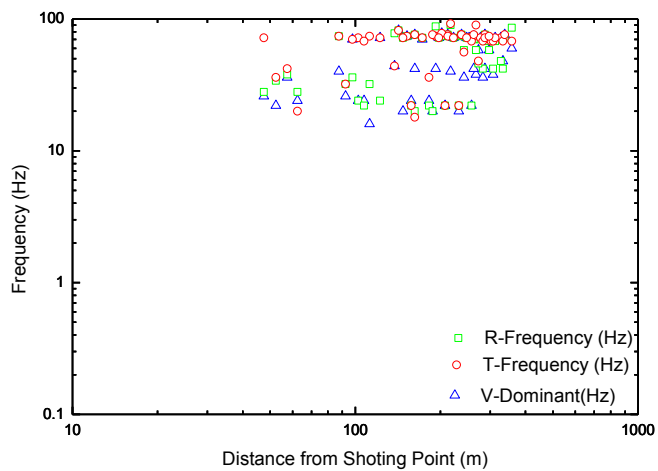
*The results of study*



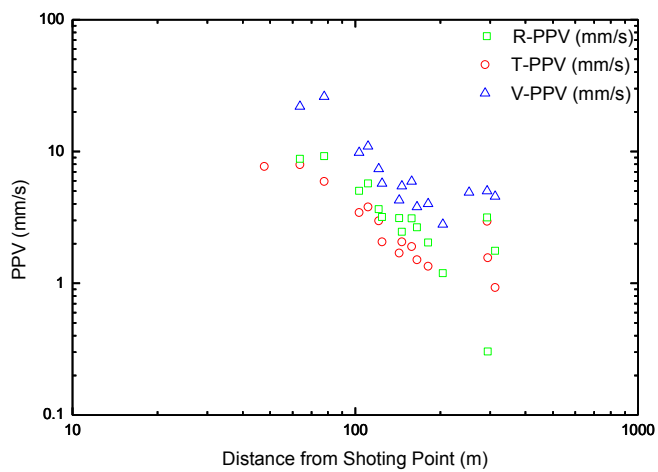


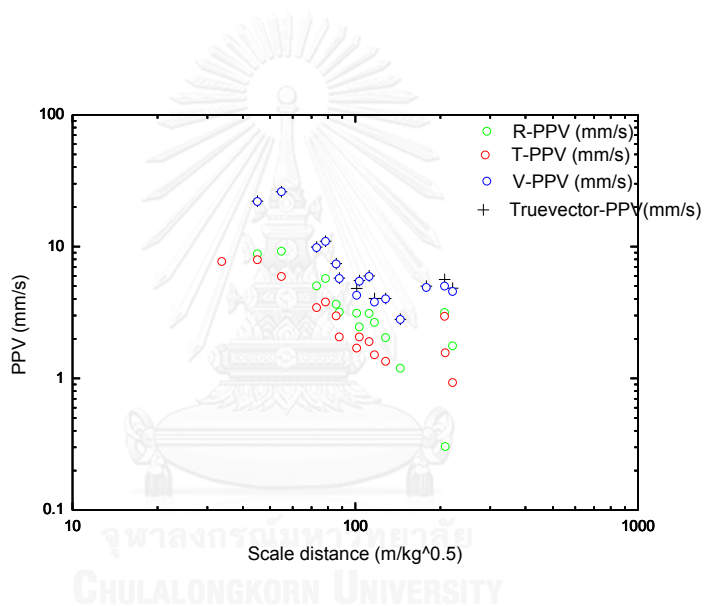
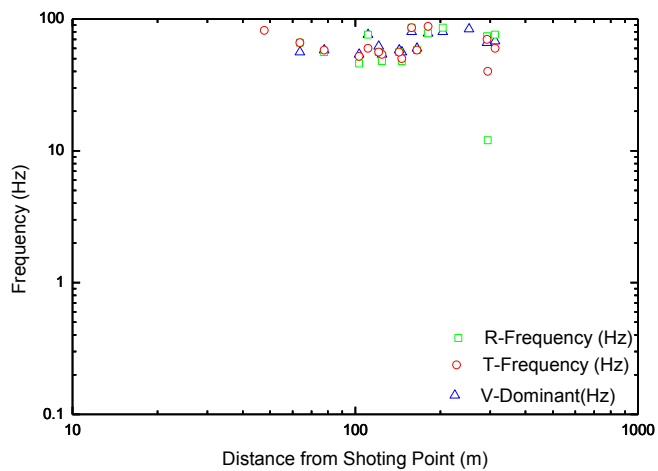
2<sup>nd</sup> Surat Thani province (2kg)



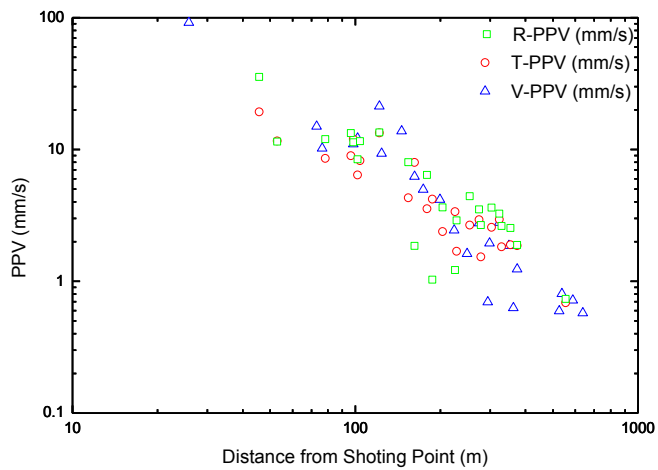


3<sup>rd</sup> Surat Thani province (2kg)





4th Surat Thani province (2kg)



Buri Rum province (3kg)

1<sup>st</sup> Buri Rum province (3kg)

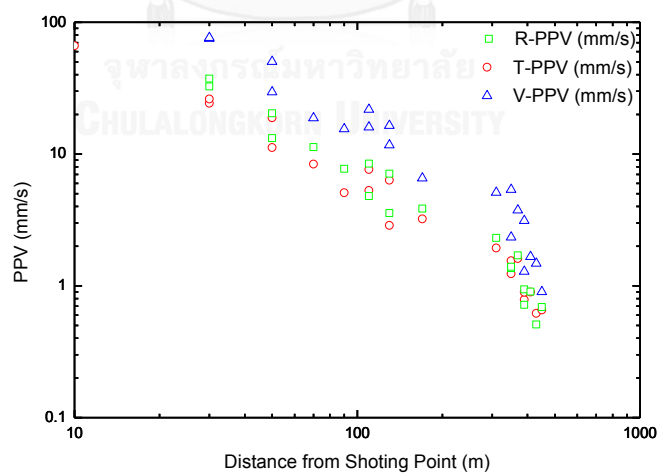
*Site condition*

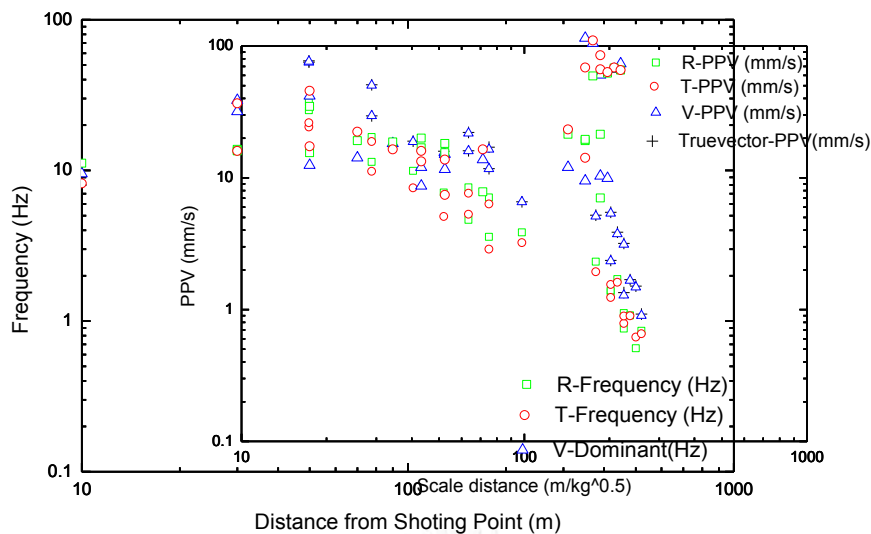


Before

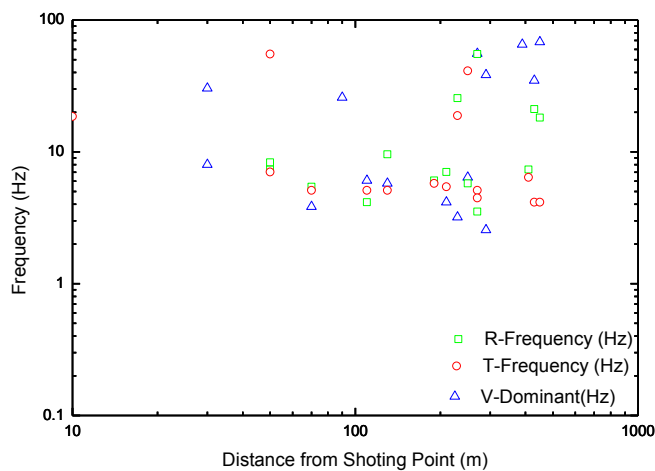
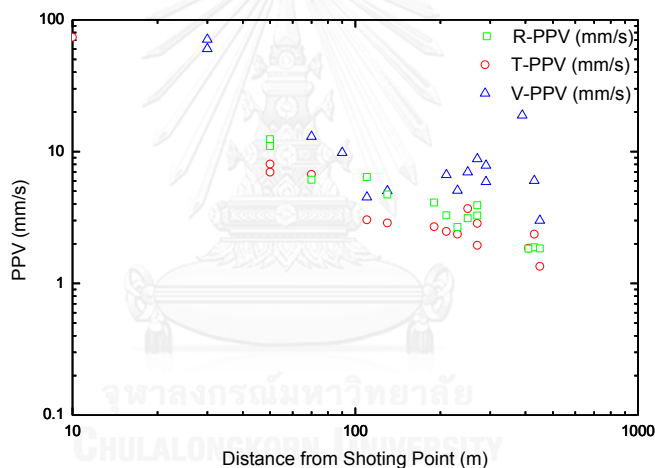
After

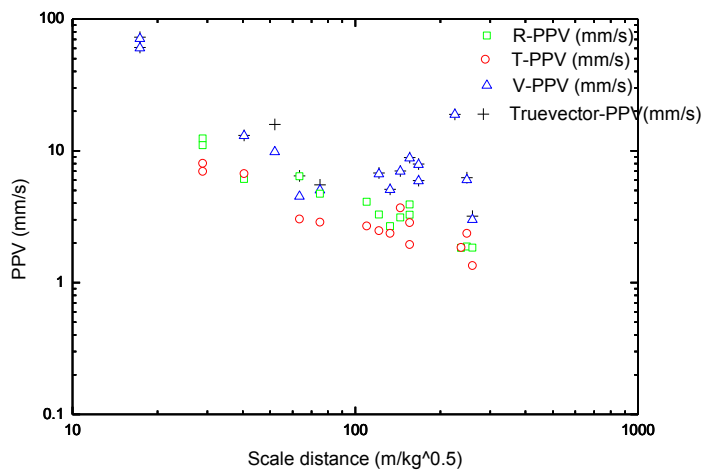
*The results of study*



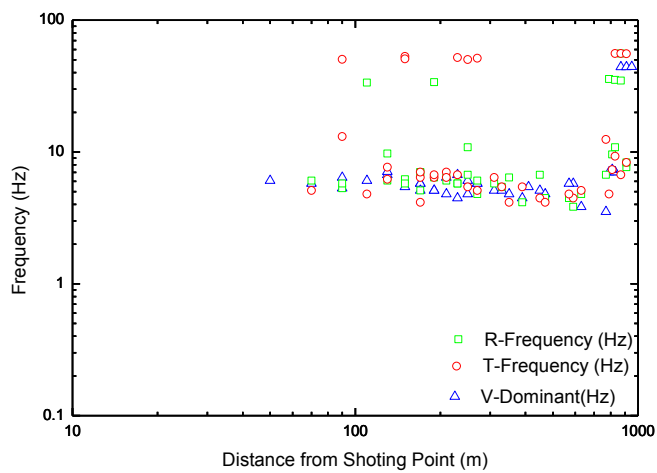
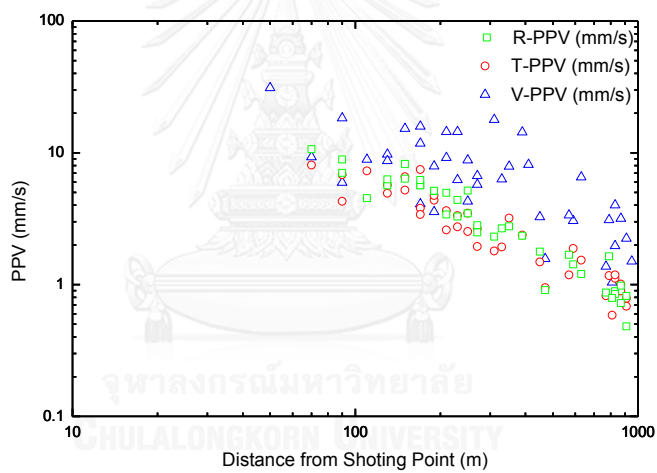


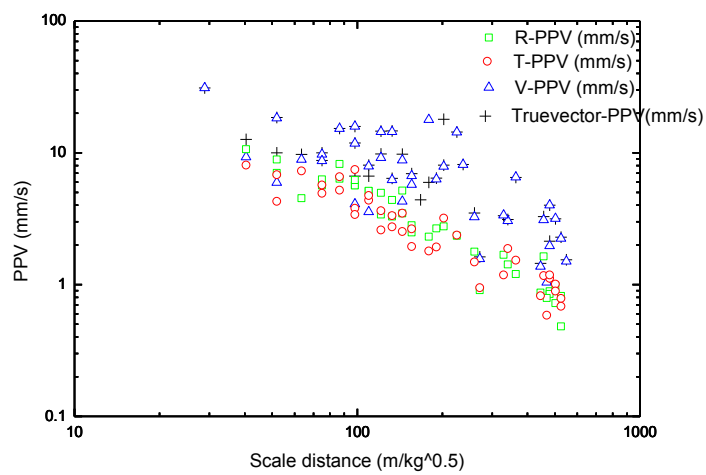
2<sup>nd</sup> Buri Rum province (3kg)





3<sup>rd</sup> Buri Rum province (3kg)





Su Rin Province (4kg)

1<sup>st</sup> Su Rin Province (4kg)

*Site condition*

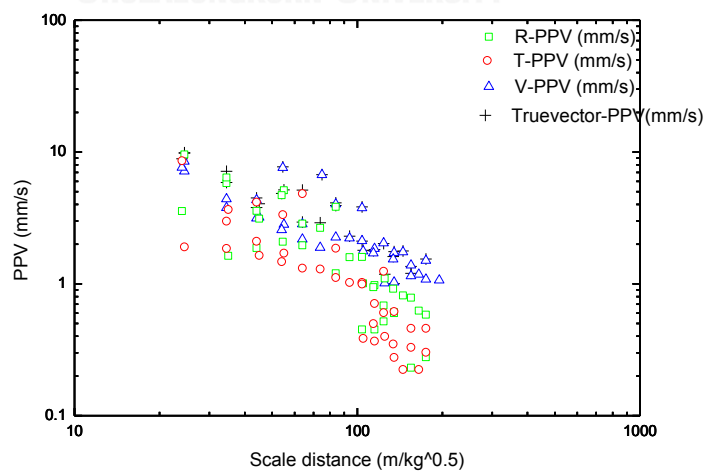
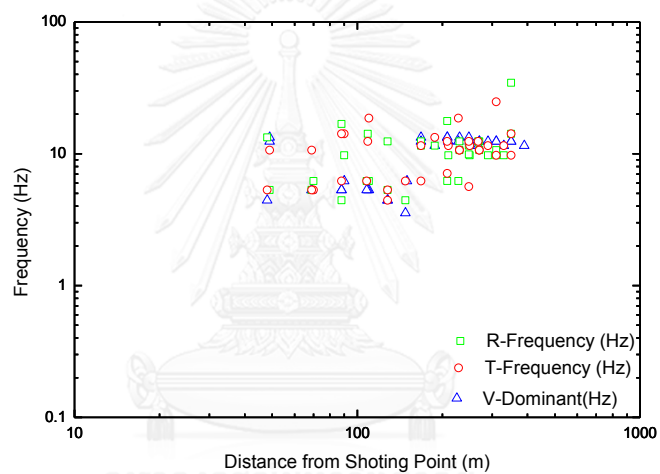
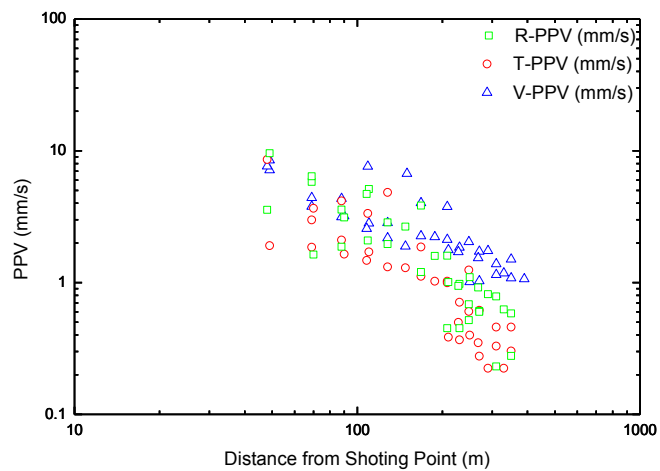


Before



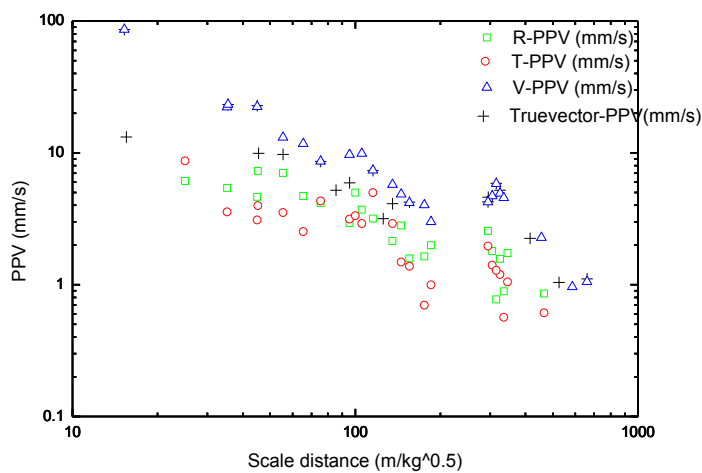
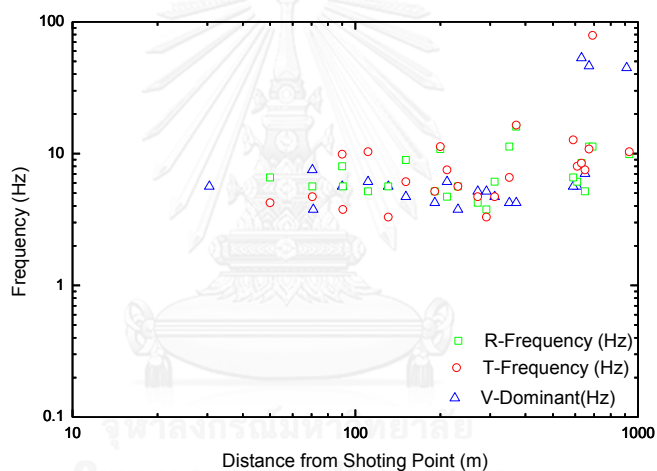
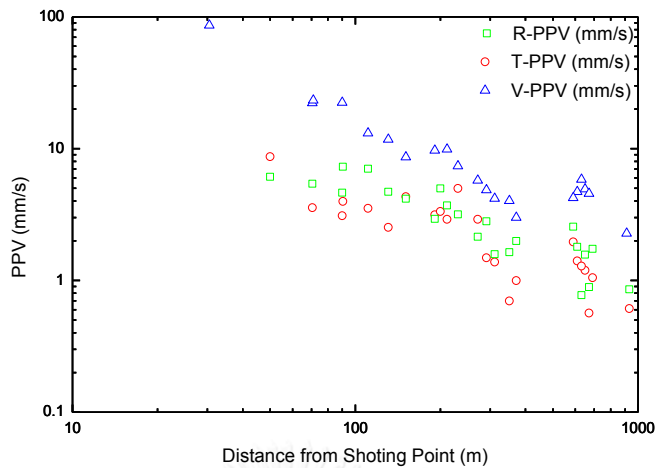
After

*The results of study*

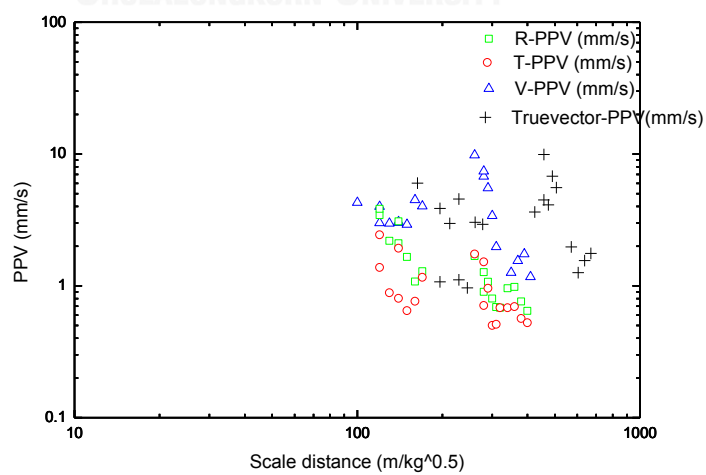
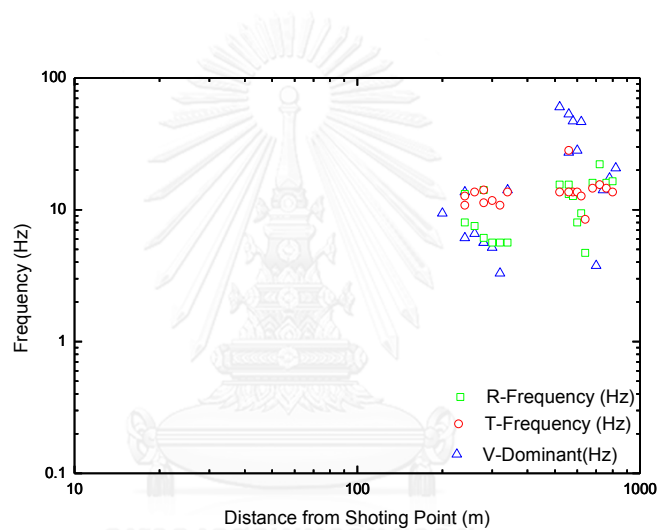
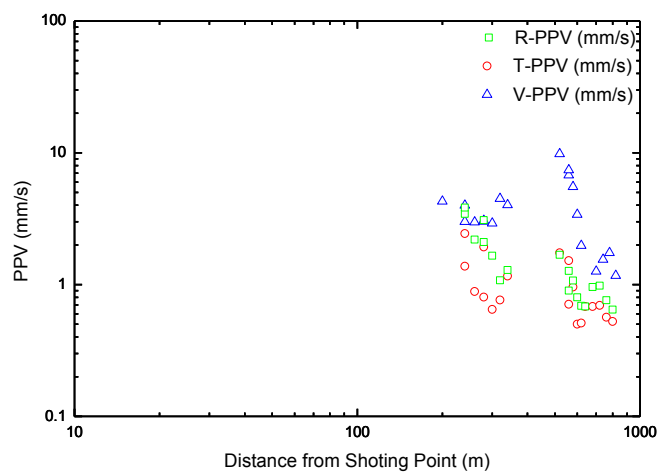




2<sup>nd</sup> Su Rin Province (4kg)



3<sup>rd</sup> Su Rin Province (4kg)



## Rocky ground

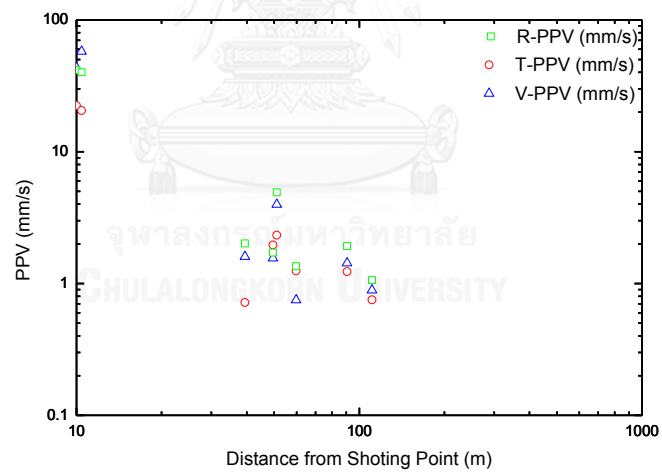
Kala Sin province

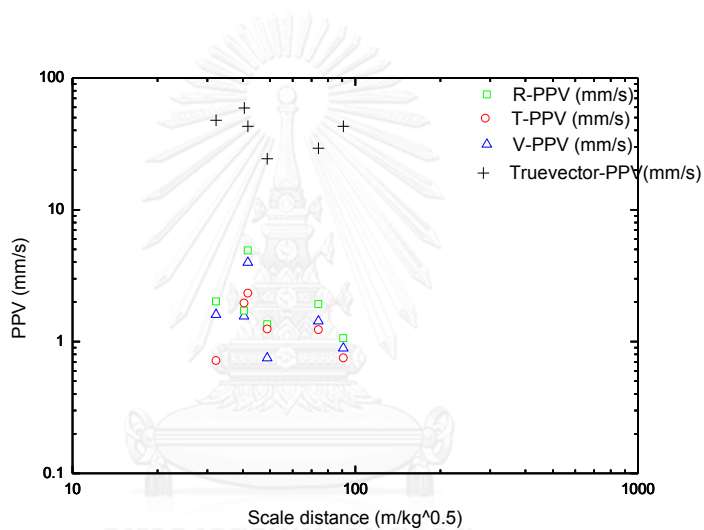
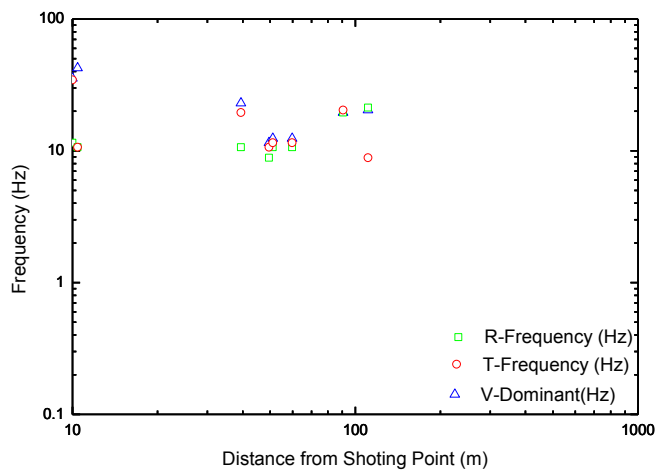
1<sup>st</sup> Kala Sin province

*Site condition*

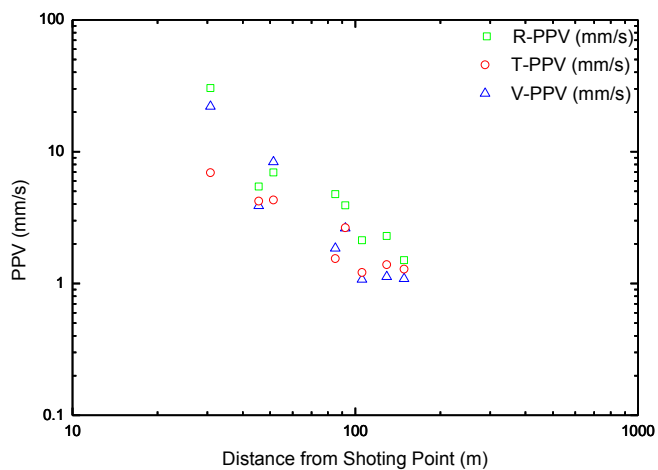


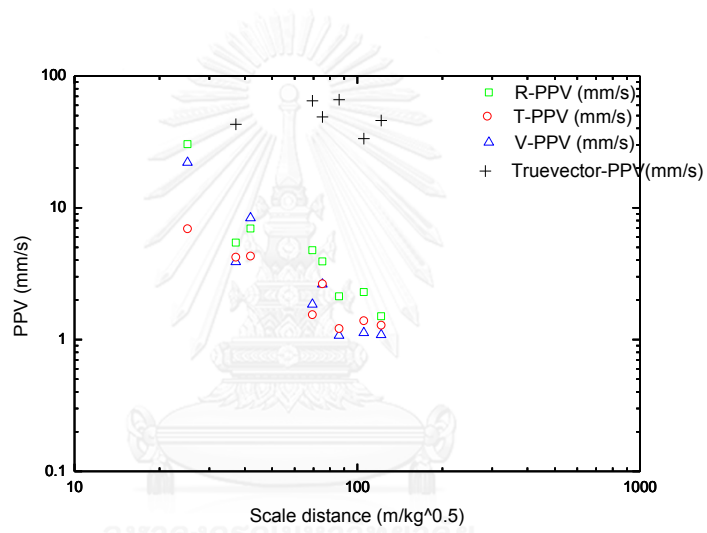
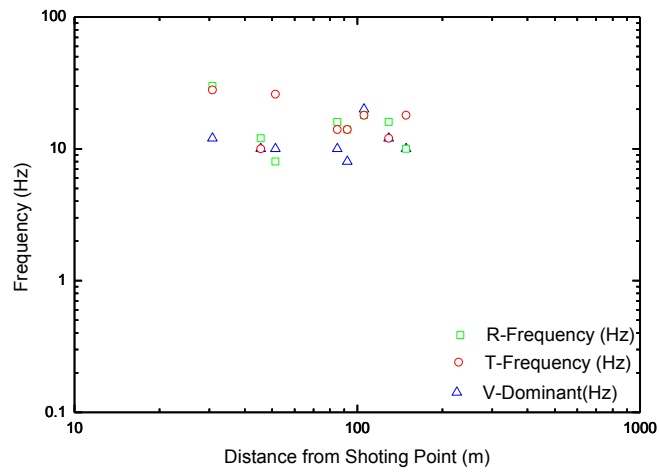
*The results of study*



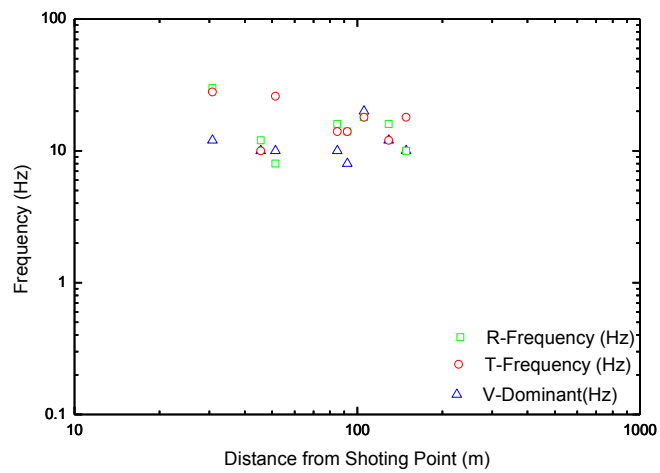


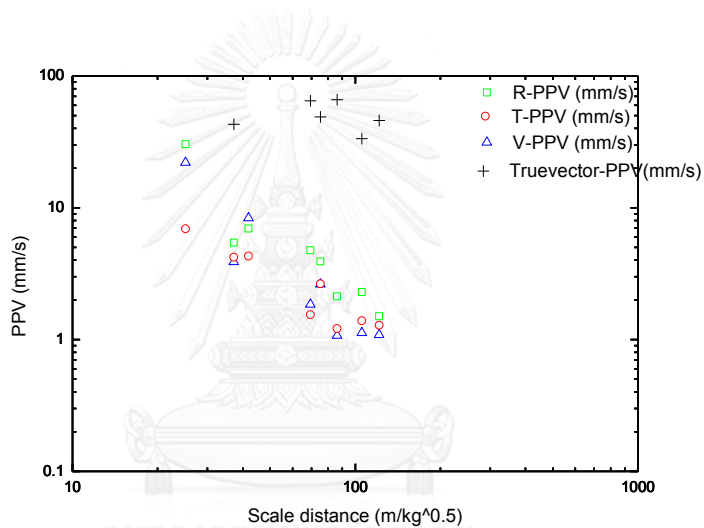
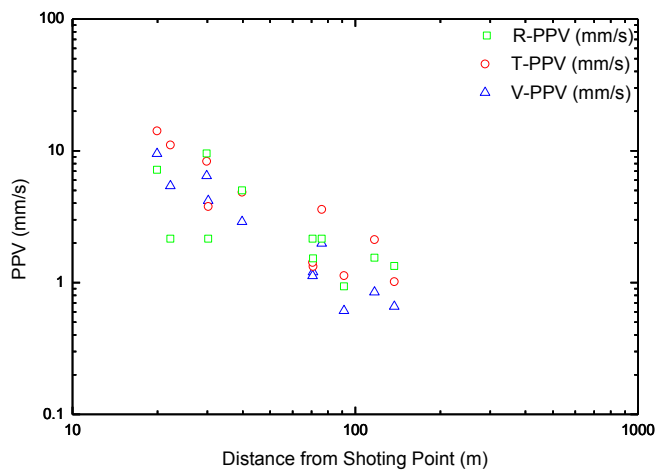
2<sup>nd</sup> Kala Sin province





3<sup>rd</sup> Kala Sin Province KALONGKORN UNIVERSITY



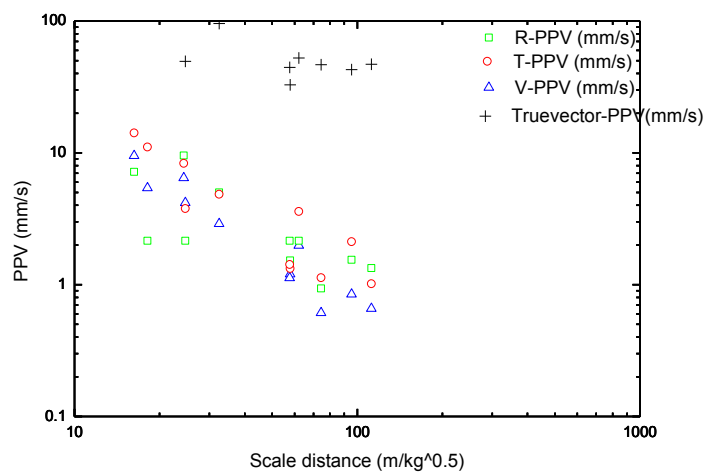
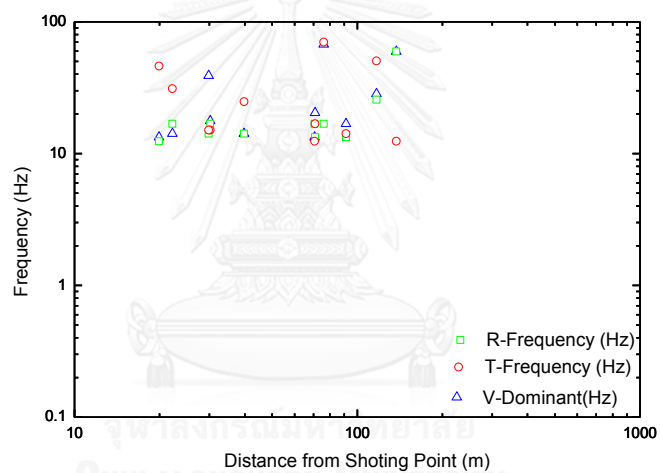
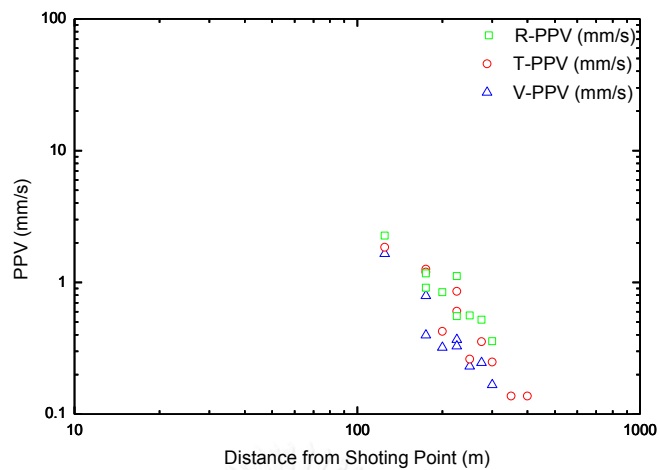


Udon Thani province

*Site condition*



*results of study*



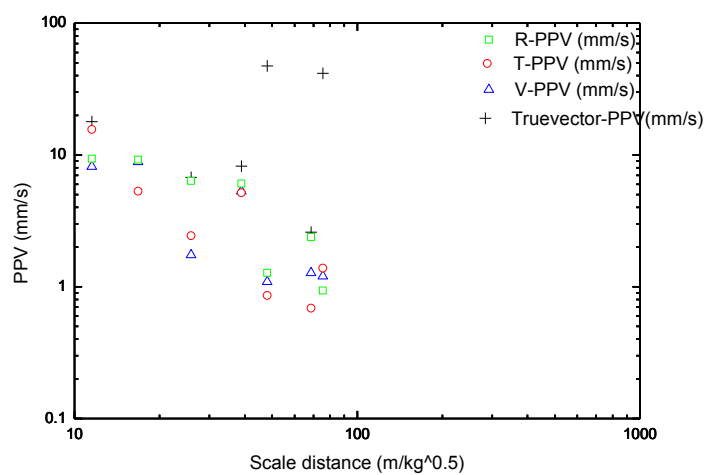
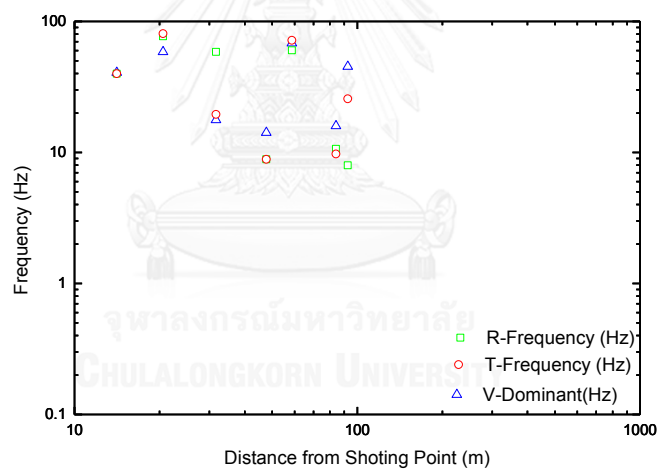
Ubon Ratcha Thani province

1<sup>st</sup> Ubon Ratcha Thani province

*Site condition*

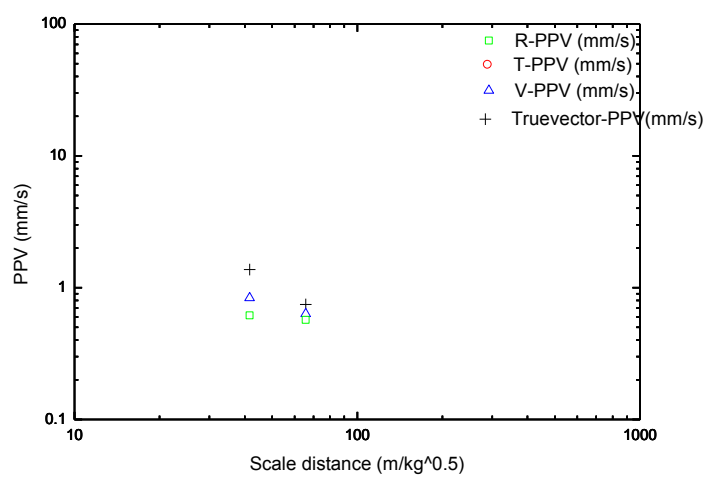
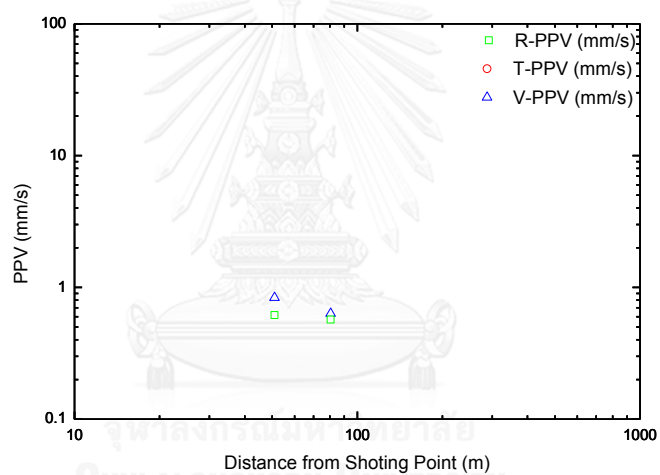
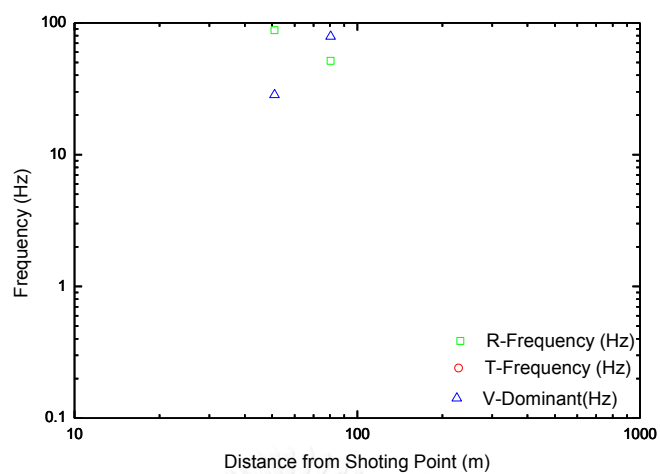


*The results of study*





2<sup>nd</sup> Ubon Ratcha Thani province



## Roller compactor

### Site 1 (Sakon Nakorn province)

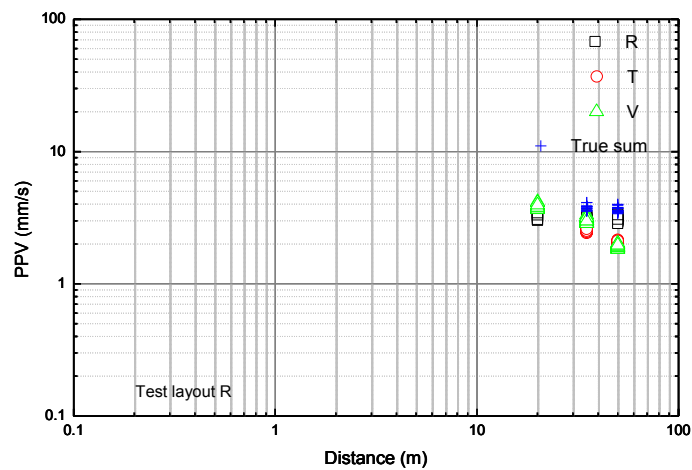
#### *Site condition*



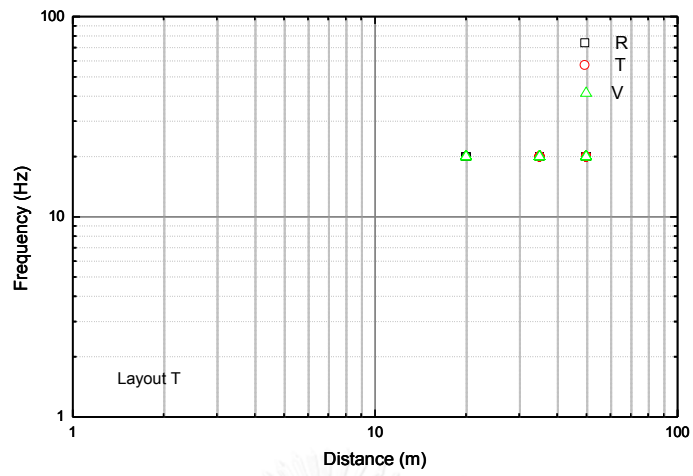
The vibration source; Single drum vibratory roller, BOMAG BW 219DH  
 Vibration frequency; 31/26 Hz

#### *The results of study*

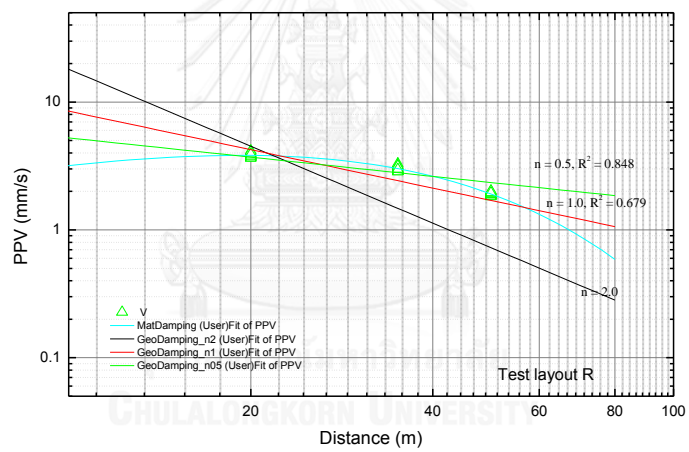
26 Hz



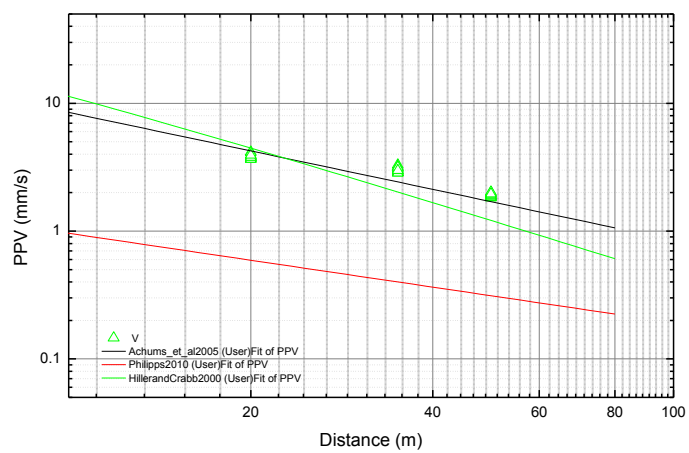
Vibration in each direction for the layout R



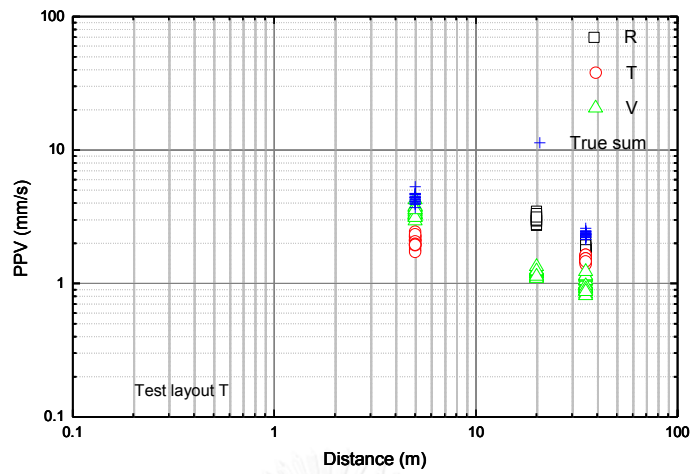
Dominant frequencies in each direction of the layout R



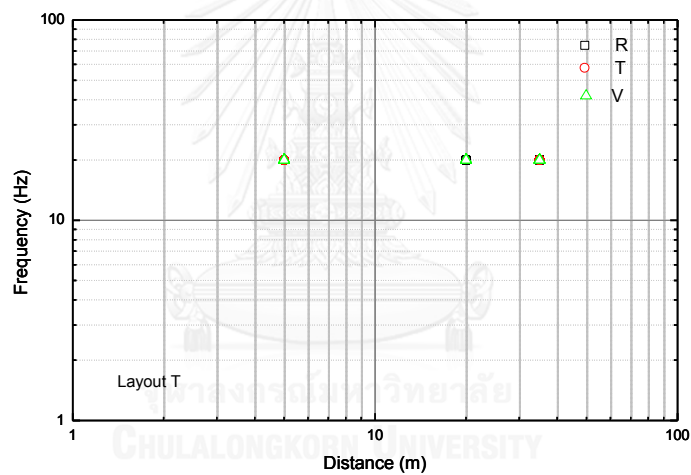
Attenuation of vibration of the layout R



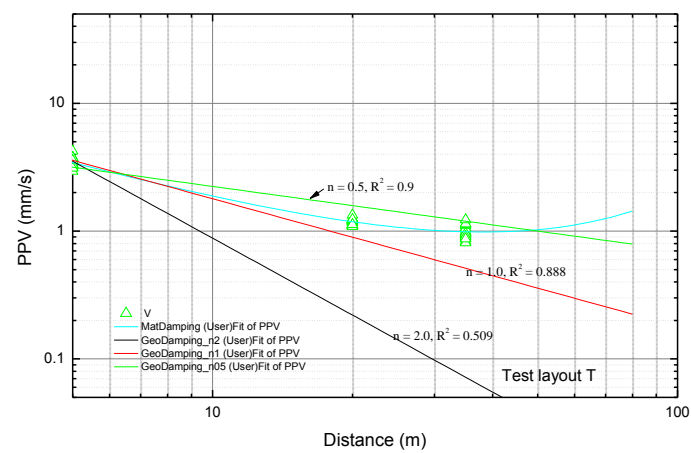
The prediction models fitting of the layout R



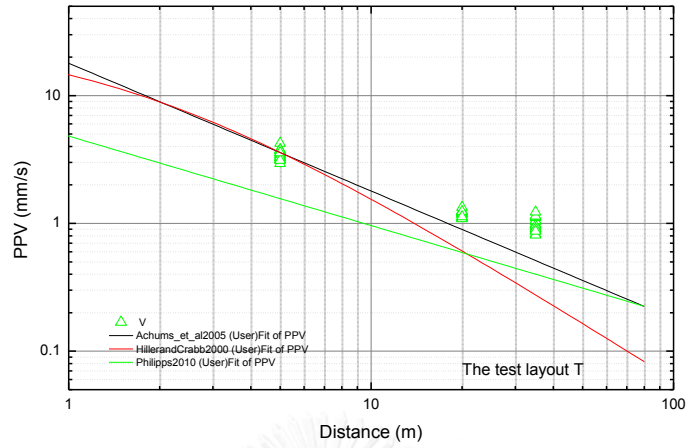
Vibration in each direction of the layout T



Dominant frequencies in each direction of the layout T



### Attenuation of vibration of the layout T



### The prediction models fitting of the layout T

#### Site 2 (Nong kai province)

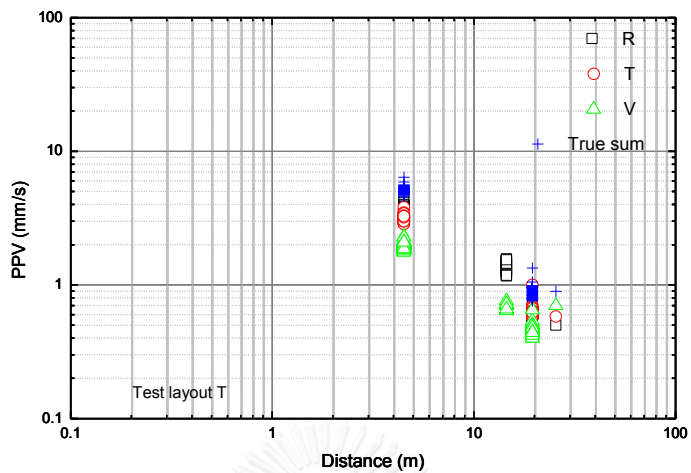
#### *Site condition*



The vibration source; Sakai SV505D

Vibration frequency; 28 Hz

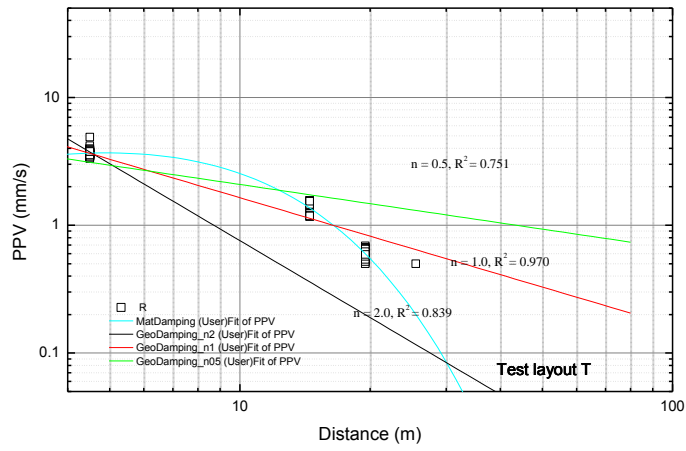
*Results of study*



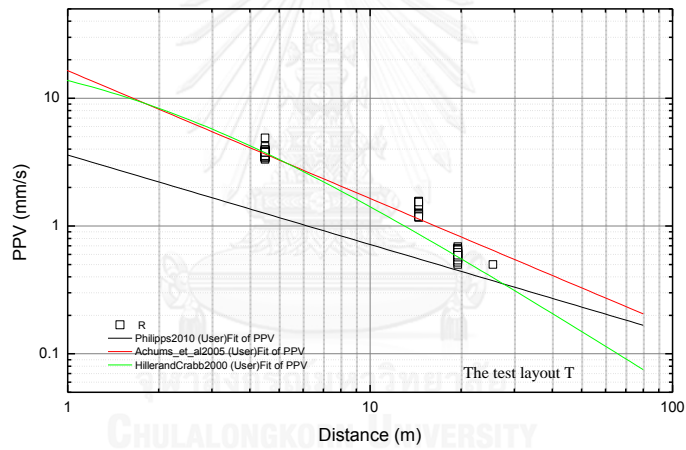
Vibration in each direction of the layout T



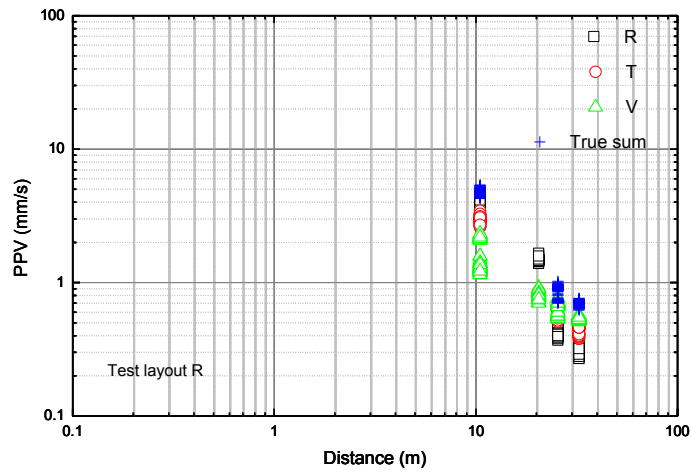
Vibration in each direction of the layout T



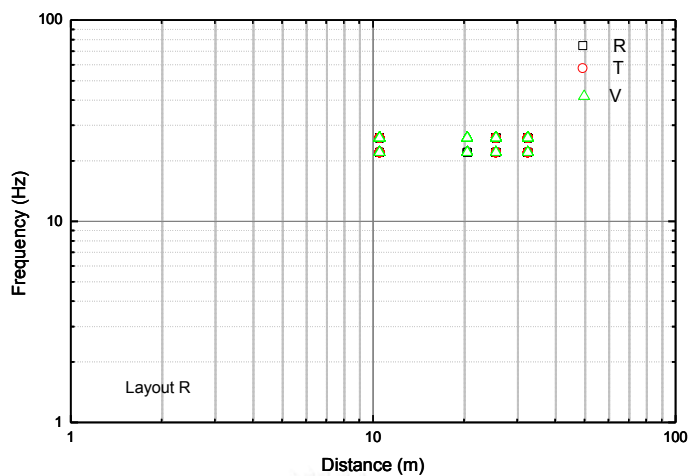
Attenuation of vibration of the layout T



The prediction models fitting of the layout T



Vibration in each direction of the layout R



Dominant frequencies in each direction of the layout R







